1-1-2010

Functional studies of microRNAs involved with ATRA induced differentiation of neuroblastoma cells

Niamh Foley
Royal College of Surgeons in Ireland

Functional studies of microRNAs involved with ATRA induced differentiation of neuroblastoma cells

RCSI

A Thesis submitted to The Royal College of Surgeons for the Degree of Doctor of Philosophy
By

Niamh Foley
Department of Cancer Genetics,
The Royal College of Surgeons,
123 St. Stephens Green,
Dublin 2,
Ireland.

August 2010

Under the supervision of Professor Raymond Stallings
Co-supervisor: Dr. Isabella Bray

Declaration

I declare that this thesis, which I submit to RCSI for examination in consideration of the award of a higher degree of Doctor of Philosophy, is my own personal effort. Where any of the content presented is the result of input or data from a related collaborative research programme this is duly acknowledged in the text such that it is possible to ascertain how much of the work is my own. I have not already obtained a degree in RCSI or elsewhere on the basis of this work. Furthermore, I took reasonable care to ensure that the work is original, and, to the best of my knowledge, does not breach copyright law, and has not been taken from other sources except where such work has been cited and acknowledged within the text.

Signed _____

Student Number 07212542

Date 13th August 2010

The work carried out in this thesis was kindly supported by
The Children's Medical and Research Foundation
Our Lady's Children's Hospital,
Crumlin

Table of Contents

List of Figures

Chapter 1

Chapter 2

Chapter 3

Chapter 4

Chapter 5

Chapter 6

List of tables

Chapter 2

Chapter 4

Summary

MicroRNA dysregulation has been widely reported in many cancers, including neuroblastoma, an often fatal paediatric cancer originating from precursor cells of the sympathetic nervous system. MiRNAs function as negative regulators of post-transcriptional gene expression, and can have oncogenic or tumour suppressor functions.

Here, we describe a large number of miRNAs that have altered expression in All-Trans Retinoic Acid (ATRA) induced differentiation of neuroblastoma cell lines. Differentiation status is associated with good prognosis in neuroblastoma, suggesting these ATRA-sensitive miRNAs play an essential mechanistic role in neuroblastoma pathogenesis. The aim of our study was to elucidate the functional role of ATRA-sensitive miRNAs, and their contribution to neuroblastoma outcome and disease. Forced over or under-expression of miR-184, miR-10a, miR-10b, miR-152 and miR-196a was accomplished in a variety of neuroblastoma cell lines, allowing us to determine the biological effects of each individual miRNA. The phenotypic effects included morphological differentiation, increased apoptosis, decreased cell proliferation, invasiveness, anchorage-independent cell growth, along with alterations in DNA methylation patterns and profound changes in mRNA transcript levels. mRNA targets were identified for miR-184 (*AKT2*), miR-10 (*NCOR2*) and miR-152 (*DNMT1*), allowing us to further define the mechanism by which each miRNA alters the cellular phenotype.

In conclusion, this study describes a detailed functional analysis of five ATRA-induced miRNAs. We identified miRNAs that play functional roles in

apoptosis, DNA methylation and differentiation in neuroblastoma cancer cells and demonstrated the relevance of these miRNAs to clinical parameters in neuroblastoma primary tumours. It is also proposed that these miRNAs could be of some value in potential miRNA-mediated therapeutics given their anti-proliferative effects on cells in vitro.

Abbreviations

AGO	Argonaute
AKT2	Akt Murine Thymoma Viral Oncogene Homolog 2
ALK	Anaplastic lymphoma kinase
AMP	Ampicillin
ANS	Autonomic Nervous System
ATRA	All Trans Retinoic Acid
AURKA	Aurora Kinase A
BSA	Bovine Serum Albumin
CCM2	Cerebral Cavernoous Malformation 2
CDS	Coding Sequence
C Elegans	Caernorhabiditis Elegans
CHD5	Chromodomain Helicase DNA Binding Protein 5
ChIP	Chromatin Immunoprecipitation
ChIP- Chip	Chromatin Immunoprecipitation on Microarray "Chip"
CLL	Chronic Lymphocytic Leukemia
CML	Chronic Myeloid Leukemia
CMV	Cytomegalovirus
CO2	Carbon Dioxide
COG	Children's Oncology Group
CRC	Colorectal Cancer
CT	Computed Tomography
CT	Cycle Threshold
DA	Dopamine
DEPC	Diethyl Pyrocarbonate
DMSO	Dimethyl Sulfoxide
DNA	Deoxyribonucleic acid
DNMT	DNA Methyltransferase
DOX	Doxycycline
dsRNA	Double Stranded RNA

dsRBD	dsRNA Binding Domain
ECL	Enhanced Chemiluminescence
EFS	Event Free Survival
ETOH	Ethanol
FACs	Fluorescent Activating Cell Sorting
FDR	False Discovery Rate
FISH	Fluorescence In-Situ Hybridisation
FITC	Fluorescein Isothiocyanate
FCS	Fetal Calf Serum
GFP	Green Fluorescent Protein
GFR	Growth Factor Reduced
GO	Gene Ontology
HDAC	Histone Deacetylase
HOX Genes	Homeobox Genes
Hrs	Hours
HVA	Homovanillic Acid
IDRFs	Image Defined Risk Factors
INRG	International Neuroblastoma Risk Group
INRGSS	International Neuroblastoma Risk Group Staging System
INSS	International Staging System
KIF1Bß	Kinesin Family Member 1B ß
LB	Lysogeny Broth
LOH	Loss of Heterozygosity
MDR	Multi Drug Resistance
µl	Microlitres
µm	Micromolar
Mins	Minutes
miR	microRNA
MKI	Mitosis Karyorrhexis Index
MNA	MYCN Amplification
MRI	Magnetic Resonance Imaging

mRNA	Messenger Ribonucleic Acid
MRP	Multi Drug Resistance Protein
MUT	Mutated
MYCN	Myelocytomatosis Viral Related Oncogene
NB	Neuroblastoma
NC	Negative Control
NCOR2	Nuclear Co Repressor 2
NGF	Neurotrophin Growth Factor
NIH	National Institute of Health
nM	Nano Molar
NRAS	Neuroblastoma RAS
NRQ	Normalised Relative Quantification
NT	Nucleotides
Oligos	Oligonucleotides
OS	Overall Survival
PBS	Phosphate buffered saline
PCR	Polymerase Chain reaction
PHOX2B	Paired Like Homeobox 2b
PI	Propidium Iodide
PI3K	Phosphatidylinositol 3 Kinase
ρmol	Pico Molar
PIP3	Phosphatidylinositol 3,4,5 triphosphate
qPCR	Quantitative Polymerase Chain Reaction
RA	Retinoic Acid
RAR	Retinoic Acid Receptor
RARE	Retinoic Acid Receptor Element
RIIID	Rnase III Domain
RISC	RNA Induced Silencing Complex
RNA	Ribonucleic Acid
RPMs	Repetitions Per Minute
RQ	Relative Quantification

RT	Reverse Transcription
RTqPCR	Reverse Transcription Quantitative Polymerase Chain Reaction
SCC	Squamous Cell Carcinoma
SDN	Small RNA Degrading Nuclease
SDS	Sodium Dodecyl Sulfate
Secs	Seconds
siRNAs	Small interfering RNAs
SNS	Sympathetic Nervous System
SRO	Smallest Region of Overlap
TBS	Tris Buffered Saline
TLDA	Taqman Low Density Arrays
TPA	12 O tetradeconoyl phorbol 13 acetate
TrkA	Neurotrophic Tyrosine Kinase, Receptor, Type 1
UTR	Untranslated Region
V/V	Volume to Volume
VMA	Vanillymandelic Acid
XPO5	Exportin 5

Acknowledgments

First and foremost I wish to thank my supervisor Professor Ray Stallings, for all the hard work, support and encouragement. Ray not only are you super super intelligent and an inspiration, you are a great person to work both for and with and I feel so lucky you choose me to work with you and thank you for making me so welcome as part of your team.

To Dr. Isabella Bray, my co-supervisor, Bella you have been amazing, I would not have got through this without you. You have been a wonderful source of comfort, knowledge, advice and help, not only that but you have reminded me to eat when I forgot, you have been my shoulder to cry on, brought me coffee, drink, chocolate or cake, whatever and whenever was required…I have never met anyone who is so selfless and giving and I hope you realise what an incredibly strong person you are. For everything you have done thank you! Above all this, you are a true friend and I hope that no matter where we end up we will always be friends.

All the Cancer Genetics Group both in RCSI and our extended family in Crumlin, with whom I worked everyday you are an amazing group to be part of.
Special thanks to Leah, the other "Dollybird" you have been my buddy in crime and a great source of fun, laughter, stories, hot chocolates, chats, dancing, karaokee and much more!. Disco Derek, you are nearly there too – can you believe it! It only seemed like yesterday we started. Thank you so much for your friendship, I can't wait to come visit you in the US of A! Dr Kenneth Bryan, "the statistical and computer genius" and Dr. Patrick Buckley "Daddy", thanks for all the help, advice and of course friendship. To Suzanne, thanks for everything all the knowledge and help you gave me along the way, the fun and friendship…and of course for getting pregnant so I could use your desk nice big desk to write up!! To Dr. Jacqui Ryan, Dr. Karen Watters, Dr. Amanda Tivnan, Sudip and Raquel thanks so much for everything!

My deepest love and gratitude goes to my Dad, you are an inspiration to all of us…if it was not for you I would not have got to where I am today, I love you so much and I am delighted for you and your new found happiness, you deserved it so much.
To the rest of my family…. Trish (Welcome to the clan…we are delighted to have you), Kevin, Ian and Michael, thanks for being the best brothers ever and I love you all so much. To the in-laws Vicky and Maedhb thanks for looking after my boys! To "Bump", I can't wait to meet you and love you already!

To all my friends especially, my closest friends Rach, Mel and Ails your friendship means so much to me and thanks for the fun, laughs and most of all being around when I needed you!

To Jeff, I promise now that the insanity ends and you can have fun Niamh back! Seriously you have been my strength for the last few years, you listened while I moaned, you cheered me up when I was blue, hugged me when I cried, and loved me when I needed it most. You bring out the very best in me and I love you so much.

Lastly to my Mum, you are the inspiration behind every piece of work in this thesis and every word on each page. Your strength and resilience against this horrific disease has pushed me every step of the way. I love and miss you so much and my only wish is that you could be here now to share this moment with me.

To Mum, this is for you.....

Chapter 1

Introduction

Chapter 1

Introduction

1.1 Neuroblastoma

1.1.1 Neuroblastoma: an overview

Neuroblastoma (NB) is a highly malignant pediatric cancer of the sympathetic nervous system (SNS). Although the exact means by which neuroblastoma cancer cells are formed remains unclear, it is however well established that the oncogenic cells of neuroblastoma tumours are derived from precursor or immature cells of the sympathetic nervous system (1). Neuroblastoma has a relatively low incident level (with incidence rates ranging between 6-10 children per million (2, 3), however it has a high death rate with approximately 15% of all childhood cancer deaths being attributed to neuroblastoma (4). The annual mortality rate is 10 per million children in the 0 to 4 year-old age group, and 4 per million in the 4 to 9 year old age group (4).

Neuroblastoma is a very interesting cancer in that it displays profound genetic heterogeneity and results in strikingly different outcomes across tumour subtypes. This wide and varied outcome ranges from the ability of the tumour to spontaneously regress without therapy (develop into a benign ganglioneuroma), to rapid tumour progression and death due to disease. This heterogeneity in clinical behaviour is poorly understood and in order to combat the disease we need to fully elucidate its pathogenesis.

Despite current guidelines for the subdivision of patients into various treatment groups, NB currently remains an elusive cancer to researchers. There is no known definite

cause, resulting in patients being subjected to multimodal treatment regimens that often have suboptimal outcome. The inability to find the optimum treatment has resulted in this continuously high mortality rate. This thesis examines what is known about neuroblastoma to date and investigates the role of microRNAs as potential tumour suppressors in this astoundingly heterogeneous neoplasm.

1.1.2 Origins of neuroblastoma

Neuroblastoma are extracranial solid tumours originating from altered development of neural crest embryonic cells (5). The neural crest is the transient component of the ectoderm formed during the third/fourth week of embryonic development. The neural crest is located between the neural tube and the epidermis of an embryo during neural tube formation (6) (Figure 1.1). Neural crest cells quickly migrate and differentiate during or shortly after neuration, an embryonic event marked by neural tube closure. The migration from the neural tube and differentiation into the different definitive cell types is controlled by a variety of gene signaling pathways (7), all of which are essential for precise development to occur. Genes involved include those of the WNT, FGF and BMP signaling pathways and other transcription factors such as neoglin and c-Myc. The neural crest is an essential component in development and gives rise to cells of the autonomic nervous system (ANS); some skeletal elements, tendons and smooth muscle; chondrocytes, osteocytes, melanocytes, chromaffin cells, and supporting cells and hormone producing cells in certain organs (8). It has been reported that neuroblastoma originates specifically from the postganglionic sympathetic progenitor cells which arise from the neural crest (1, 9).

Neuroblastoma is largely thought to be a spontaneous cancer; however initial reports estimated that approximately 22% of cases occur as a result of an inherited mutation (10, 11). More recent studies examining larger cohorts have revised this percentage and estimate that incidence of familial inherited neuroblastoma are approximately 5% (12-14). Both germline gene mutations and chromosomal aberrations which are related to familial neuroblastoma have been reported. Two such examples associated with familial cases of neuroblastoma include mutations of the anaplastic lymphoma kinase gene (ALK) (15) and the homeodomain transcription factor paired-like homeobox 2b gene (PHOX2B) (16, 17). A large scale genomic study by Altura *et al.*, (2007) (18) also identified a number of chromosomal abnormalities common to familial neuroblastoma tumours, including aberrations at 3p24-pter, 10p12-13, 10q25-qter, 16q12-22, and 20q13.3-qter.

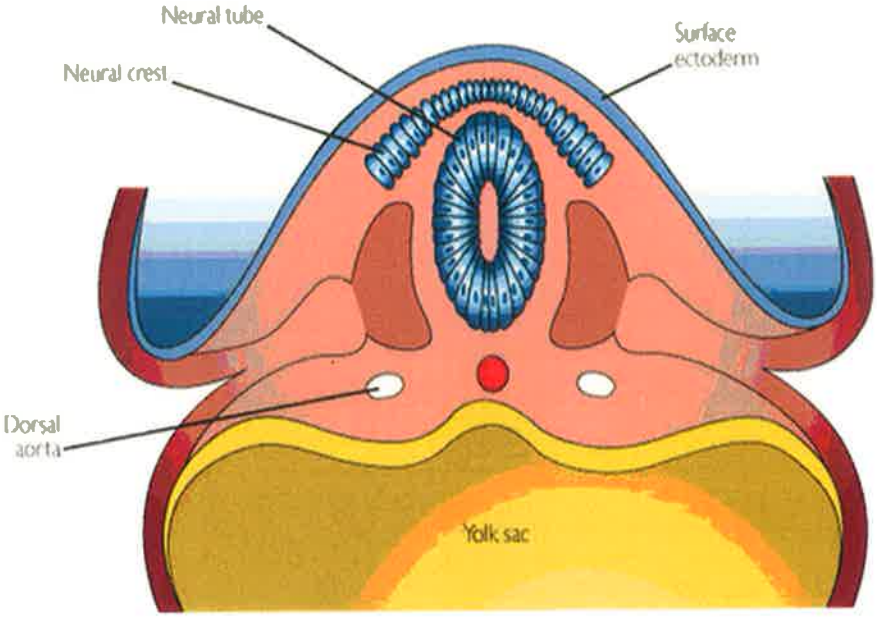

Moore and Persaud, 2003, (19)

Figure 1.1. Origins of the neural crest cells. Schematic diagram illustrating the neural tube and neural crest before neural tube closure in embryonic development.

1.1.3 Location and clinical manifestation of neuroblastoma

Neuroblastoma usually presents with an array of different symptoms either just after birth or early in childhood. Clinical manifestations are varied, often making diagnosis difficult. Common symptoms include abdominal mass, fever, weight loss, anemia and bone pain, other more unusual symptoms have been reported such as diarrhea, polymyoclonia opscolonus and erythrocyte abnormalities (20). Neuroblastoma tumours can develop anywhere in the sympathetic nervous system, however most often the tumour is located in the adrenal medulla (approximately 40% of cases). Other primary sites include the chest, abdomen and pelvis (21).

1.1.4 INSS Neuroblastoma tumour staging

Early and accurate identification of tumour subtypes and the subsequent behaviour of a tumour is essential in the determination of efficient and refined therapies. The need for accurate diagnosis is especially evident in cases where it may not be necessary for any therapy to be given at all, where a "wait and see" policy can be operated.

A number of clinical and biological factors are considered in the identification of tumour subtypes. The international neuroblastoma staging system (INSS) was set up in 1988 by Garrett Brodeur (22), and revised again in 1993 (23) with the aim of integrating worldwide clinical and laboratory studies, to identify consensus criteria for the diagnosis of neuroblastoma. This system classified neuroblastoma tumours into 5 stages, stages 1 to 4 and stage 4S. This tumour staging takes into account clinical and biological factors of neuroblastoma and is an essential part of the tumour classification process.

1.1.4.1 Stage 1 tumours

Stage 1 tumours are localized tumours; the cancer has not spread from the primary site. These tumours are operable and surgery alone can in many cases remove the whole tumour. This stage requires the least treatment and has a highly favorable outlook.

1.1.4.2 Stage 2 tumours

Stage 2 tumours can be subdivided into two groups. In the first sub-group, stage 2A, the tumours tend to be localized to one area. However, complete removal by surgery may be impossible or prove difficult. Stage 2B tumours are in most cases removable by surgery; however the cancer cells have also been detected in nearby lymph nodes.

1.1.4.3 Stage 3 tumours

There are a number of different categories of stage 3 tumours. Some tumours may be surgically removed, of these some may have infiltrated across the mid-line of the body and may or may not also have regional lymph node involvement. The stage 3 tumour may be located on just one side of the body but cancer cells have been detected in the lymph nodes on the far side. Lastly, stage 3 tumours may also be located across the midline and display bilateral lymph node involvement.

1.1.4.4 Stage 4 tumours

This is the highest risk patient subtype, where the tumour has spread to distant lymph nodes, the skin and other organs and areas of the body. Stage 3 and 4 patients whose tumor is classified as biologically favourable (based on histopathology, age at diagnosis and genetic profile) receive minor therapy. High risk patients (biologically unfavorable Stage 3 or Stage 4 infants or Stage 4 patients age > 1 year) receive surgery and intensive chemotherapy (24). Overall survival rate is approximately 80%, however tumours at stage 4 of disease have only a ~20% survival rate (4).

1.1.4.5 Stage 4S tumours

Stage 4S tumours display metastasis to skin, liver and possibly bone marrow. These tumours are easily resectable and are usually seen only in children under the age of 1. These tumours in most cases can spontaneously regress from a previously undifferentiated stage to a completely benign cellular appearance without any therapeutic intervention (25).

1.1.5 Histopathology of neuroblastoma – The Shimada System

Incorporated into the staging processes is the classification of the tumours according to tissue histopathology. Histopathological examination is based on the morphological features of a tumour which allows its categorization into one of a number of subtypes. This method of classification was established in 1984 by Shimada. Many aspects of the original classification method are still in place today, though modifications have been made over the years (26). The tumour classifications are based on clinical and biological observations in neuroblastoma tumours. These include the degree of cellular

differentiation divided into three categories (undifferentiated, poorly differentiated and differentiating); mitotic karyorrhectic index (MKI), which reflects the level of mitotic and karyorrhectic activity occurring (this is also divided into three categories low, medium and high); the presence or absence of schwannian stromal cells and age at diagnosis. Undifferentiated neuroblastoma histology is extremely different to that of the differentiated sub-group. These undifferentiated cells are small, round cells, dense, highly fibrotic and bunched together tightly in groups. Differentiated cells are spread out with neurite like processes and larger cytoplasms (Figure 1.2). Fundamentally the Shimada classification system is the most widely used technique for determining the histopathological subtype of a tumour and has been proven to be independently prognostic in multivariate analysis (26, 27). One drawback of histopathological analysis is that although advances in imaging technology have contributed to further aid in tumour classification, a biopsy or resection must be carried out for accurate histopathological diagnosis to be assessed.

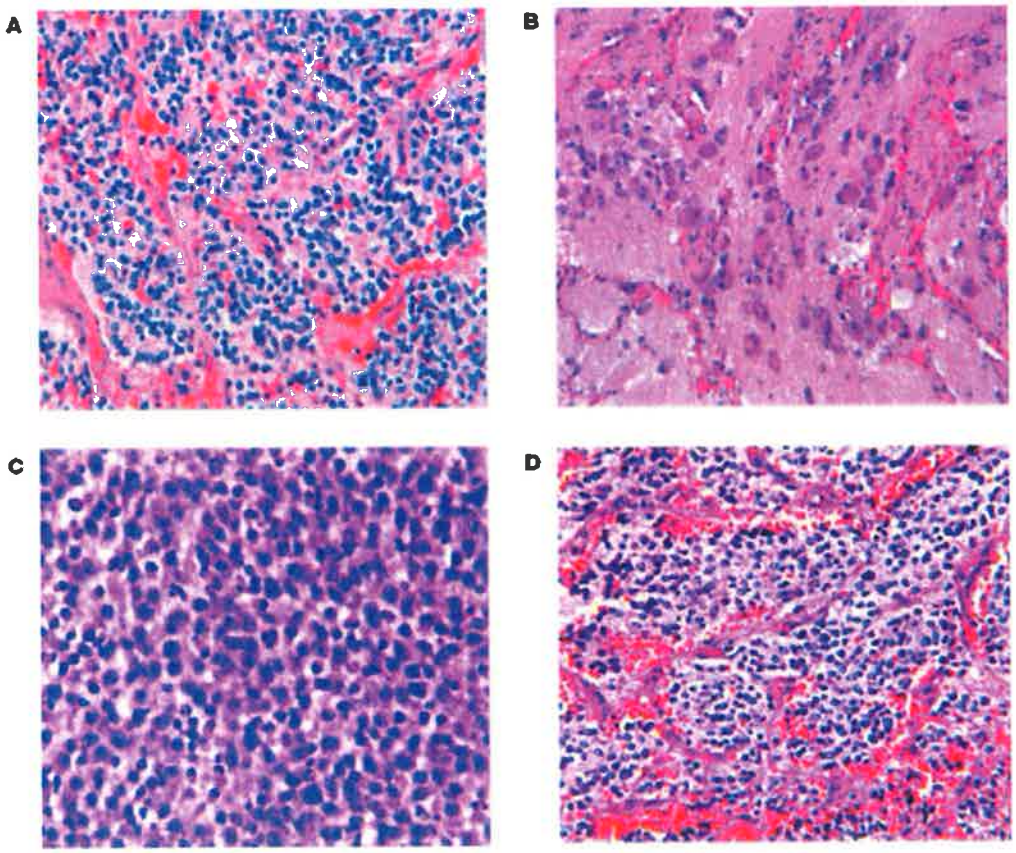

Shimada and Nakagawa, (2006) (28)

Figure 1.2. Neuroblastoma histopathology Microscopic Features of 4 neuroblastoma tumours. (A) Case 1. Neuroblastoma (Schwannian stroma-poor), poorly differentiated subtype with a low mitosis-karyorrhectic index (MKI), diagnosed at 4 months of age (favourable histology). (B) Case 2. Neuroblastoma (Schwannian stroma-poor), differentiating subtype with a low MKI, diagnosed at 3 years and 2 months of age (favourable histology). (C) Case 3. Neuroblastoma (Schwannian stroma-poor), undifferentiated subtype with a high MKI, diagnosed at 1 year and 4 months of age (unfavourable histology). (D) Case 4. Neuroblastoma (Schwannian stroma-poor), poorly differentiated subtype with a low MKI, diagnosed at 4 years and 8 months of age (unfavourable histology).

1.1.6 Age

Age is highly predictive of overall and event free survival in neuroblastoma. The older a child is at diagnosis the greater the likelihood of a poor prognostic outcome (29). The age cut offs for prognosis have been highly debated over the years. The international neuroblastoma risk group (INRG) (Section 1.1.15) identified the need for greater division within the staging groups of neuroblastoma based on age, for example, previously all stage 4 tumours regardless of MYCN status (see Section 1.1.8) were classified as high risk regardless of age (30). However, recent research has shown that age is the most powerful predictor of overall and event free survival in stage four neuroblastomas, with a survival rate of 63% in children under 18 months and 23% survival rate for children over 18 months. It has also proved to be successful in categorizing the lower risk stage 2 and stage 3 patients (29).

Age used concurrently with MYCN status provides an even more powerful diagnostic tool than MYCN status taken alone. For example children >1 year but <18 months without *MYCN* amplification (MNA) have a good chance of event free survival and do not need to be subjected to the same intense therapy currently assigned to high risk MNA patients of the same age (31). The current consensus for categorizing poor outcome patients based on age is all children diagnosed over the age of 15 months. This age cut-off was first determined by COG (Children's Oncology Group) in 2005 (32) and was validated by the INRG in a review of prognostic factors by Cohn *et al.*, in 2009 (29). Cohn *et al.* included all patients greater than 18 months with large "unresectable" tumours into the high risk classification. The INRG also found that children of age 18 months and older with non-*MYCN* amplification and stage 2/3 poorly or undifferentiated tumours had a

lower chance of survival than those with differentiating tumours. Age has been associated with a number of other neuroblastoma biological characteristics, such as degree of differentiation, DNA index, 11q status and MYCN levels.

1.1.7 DNA index (Ploidy)

DNA ploidy refers to the number of copies of a given chromosome in the tumour cells. DNA copy number alterations are widely reported in neuroblastoma (33-37). Tumours exhibiting whole chromosomal gains and losses (near triplod/hyperdiploid), without amplifications, segmental deletions or insertions are in many cases associated with more favourable subtypes and lower stage of disease in neuroblastoma (3, 37-40). Tumour cells which display DNA diploid status, but demonstrate frequent segmental gains, losses and amplifications are highly associated with advanced stage disease and unfavorable outcome (37, 41-44).

A recent study by Michels *et al.*, (39) demonstrated that neuroblastoma tumours could be clustered based on chromosomal aberrations by using high resolution aCGH to map chromosomal aberrations in 75 tumours and 29 cell lines. One group of predominantly young patients with extremely favourable outcome showed overrepresentation for whole chromosome gains and losses with little or no structural alterations (near triploid). Chromosomal gains and losses reported in this group included gain of chromosome 17 (seen in 90% of tumours in this cluster), 7 (80%), 6 (46%) and 18 (40%), and losses of chromosome 14 (73%), 10 (73%), 9 (60%), 3 (50%), 11 (47%) and 4 (43%). This difference between whole chromosomal gains/losses and segmental gains/losses across risk groups is clearly evident in Figure 1.3, from a study by

Vendesompele *et al.*, (1998), which determined patients categorized as high risk display a greater number of segmental losses and gains than those with better prognosis.

DNA ploidy is a significant prognostic factor in neuroblastoma subtyping along with stage 4 tumours and normal MYCN copy number. Tumours from infants display fewer if any segmental chromosomal abnormalities, when compared to older patients. This vast difference in the level of DNA copy number alterations is thought to contribute to the reason why younger patients have better survival probability than children diagnosed at an older age.

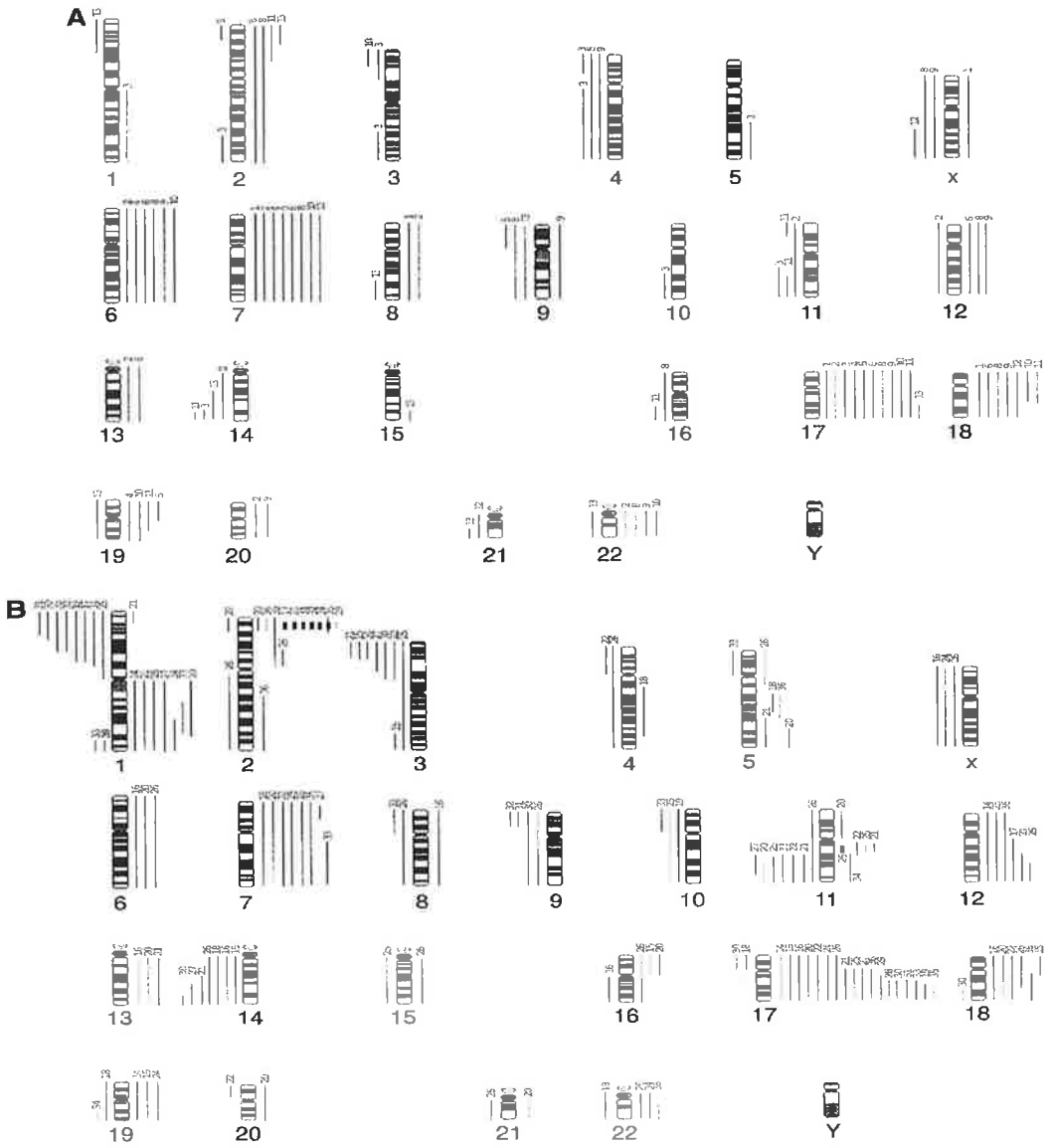

Vandesompele *et al.*, 1998, (45)

Figure 1.3. DNA copy number alterations in low risk versus high risk neuroblastoma tumours. These diagrams represent the alterations in DNA copy numbers as demonstrated by a cohort of 36 neuroblastoma tumours profiled using comparative genomic hybridization. Lines to the left of a chromosome ideogram demonstrate an underrepresentation or deletion and lines on the right demonstrate amplification or gain. Figure A represents tumours categories as low risk stage 1, 2 and 4s and Figure B represents the high risk subgroup (stage 3 and stage 4 tumours).

1.1.8 *MYCN* amplification

MYCN (myelocytomatosis viral related oncogene), is a member of the MYC family of helix-loop-helix transcription factors. Amplification of *MYCN* is seen in approximately 20 – 25% of neuroblastoma tumours. Established as the single most important prognostic factor in neuroblastoma patients (46). *MYCN* amplification is associated in most cases with advance stage of disease, rapid tumour progression and poor prognosis (4, 47). *MYCN* levels are also highly associated with other factors of poor survival in NB and correlate significantly with advanced disease stage. Children with metastatic disease and diploid *MYCN* status have an event free survival (EFS) of 93%, where as those with MNA have an EFS of 10% (48). This poor survival rate occurs despite the fact that these children undergo multimodal, high intensity chemotherapy regimens. This indicates that current therapeutics are not sufficient for this category of patient.

Shimada *et al.*, have previously demonstrated an inverse association between *MYCN* levels and the degree of tissue differentiation. It was also noted that *MYCN* amplification was associated with higher MKI activities suggesting that *MYCN* amplified tumours proliferate at a high rate (49, 50). So strong is the effect of *MYCN* amplification on neuroblastoma that over-expression of MYCN alone has been demonstrated to be sufficient to induce neuroblastoma in a mouse model (51). Despite this, MYCN status cannot predict all cases of poor survival and over 70% of neuroblastomas do not display *MYCN* amplification. A large number of *MYCN* single copy tumours demonstrate high rates of unchecked proliferation, resistance to treatment and poor OFS and EFS (43). There is no doubt that MYCN is an essential clinical factor which is of major prognostic significance in neuroblastoma, however the existence of such large numbers of poor

survival cases in which the tumours display *MYCN* single copy indicated a need for alternative classification methods.

1.1.9 Chromosome 1p deletions

Loss of heterozygosity at a polymorphic locus on chromosome 1p36 was identified as a genetic feature of a large number of neuroblastomas, with deletion of 1p seen in between 30-35% of neuroblastoma tumours. This deletion has been demonstrated in a number of studies to be associated with tumour stage and *MYCN* amplification (52-56). Although 1p deletion correlates with *MYCN* amplification it has also been established as an independent predictor of poor event free survival (57). Deletion on chromosome 1p is also predictive of worse event free survival in the lower and intermediate risk categories of patients (41).

Interestingly a number of publications have reported differences in the size and location of the region of DNA deletion on 1p in MNA tumours versus unamplified tumours. These reports provide evidence that the deletions of 1p in MNA amplified tumours are larger and encompass a more proximal region than those in *MYCN* single copy tumours (58, 59). This suggests that tumours harbouring deletions on 1p should be viewed as two different tumour sub-groups, dependent on MYCN status, for the purpose of identification of potential tumour suppressor candidates using SROs (smallest region of overlap). The association of 1p loss with poor survival would suggest there may be a number of tumour suppressor genes located on 1p. In keeping with this observation, Caron *et al.*, (2001) (59) identified two distinct regions of 1p deletion. The location of these loci

was dependent on the MYCN status of the tumour, with the deletion of one locus in the MNA tumours (1p36.1) and another (1p36.2-3) in single copy tumours.

Although a large number of genes have been mapped to regions of deletion on chromosome 1p, two genes have been proposed as potential tumour suppressors in neuroblastoma. These are *CHD5* (1p36.31) and *KIF1Bβ* (1p36.2). CHD5 was first identified by Thompson *et al.*, (2003) (60) and is a member of the chromodomain superfamily of proteins which contains a chromatin organizing modulator domain. This group established that *CHD5* was mapped to a region of 1p which is commonly deleted in some neuroblastomas and other cancer types. Furthermore, this study demonstrated that *CHD5* was preferentially expressed in the nervous system and was undetectable in other tissues. In addition *CHD5* levels were inversely correlated with 1p deletions, *MYCN* amplification, advanced stage of disease and unfavourable histology in 137 NB tumour samples. Okawa *et al.*, (2007) (61) mapped 23 genes to the SRO in a number of neuroblastoma samples. Of the 23 genes identified, *CHD5* was chosen as an interesting candidate for further study. This group used a cohort of 101 neuroblastoma tumours and confirmed that *CHD5* was associated with overall and event free survival in both univariate and multi-variate analysis. They further verified that over-expression of *CHD5* abrogated colony forming ability and tumour growth in NFL and IMR5 cells both *in vivo* and *in vitro*. Despite the fact that only one of the alleles encoding *CHD5* was deleted (61), there was little or no detectable levels found in neuroblastoma cell lines and unfavourable neuroblastoma samples. Fujita *et al.*, (2008) (62) proposed a two-hit theory to explain this reduced expression of *CHD5*, by demonstrating the existence of strong levels of methylation at the *CHD5* promoter on the remaining allele.

KIF1Bß is a member of the kinesin superfamily of proteins and is located in a region of chromosome 1p36.2 commonly deleted in neuroblastoma and other cancers. *KIF1Bß* is a haplo-insufficient gene deleted from one allele in neuroblastoma (63). Up-regulation of this gene in neuroblastoma cells resulted in a reduction in cell growth, and the induction of p53 dependent apoptosis. SiRNA knock-down of *KIF1Bß* in HELA cells not harbouring any deletions on 1p and endogenously expressing *KIF1Bß* resulted in significant increase in cell growth. Transplantation of immortalized mouse mammary gland cells transfected with the anti-sense RNA to *KIF1Bß* into nude mouse resulted in the tumour formation. Schlisio *et al.*, in 2008, (64) demonstrated using *Egl1N3* (a prolyl hydroxylase down stream effector of developmental apoptotic pathways) knockout mice, that *KIF1Bß* acts down stream of this pathway and is essential for apoptosis to occur.

1.1.10 Aberrations of chromosome 11q

Although MNA is the single most powerful predictor of survival in neuroblastoma, it cannot determine survival probability and outcome in all cases. MNA is seen in ~20% of NB cases and 1p deletions seen in only ~30-35% (65, 66). The degree of overlap between 1p deletions and MNA in tumours leads to the theory that alternative oncogenic mechanisms must be in place in the other ~70% of NB tumours.

One such mechanism is the hemizygous loss of a large region on chromosome 11q. Deletion of 11q is commonly found in neuroblastoma and usually occurs on the long arm of the chromosome (67). One of the most predictive segmental deletions on chromosome 11q is the loss of one allele at a polymorphic locus on 11q23. The first comprehensive study on 11q allelic status confirmed 44% of the NB tumours studied had 11q23 loss of

heterozygosity (LOH) (68). Constitutional rearrangements of 11q have also been observed (69). 11q status has been associated with age and older children (2.5 – 7 years) show the greatest level of aberration of this chromosome (70). The most interesting discovery was that although associated with poor overall and event free survival, 11q deletions are inversely correlated to *MYCN* amplification in a large number of studies (41, 70-73). 11q deletions have been highly associated with poor survival in single copy *MYCN* tumours (71) and as a result this genetic aberration is now used as diagnostic marker in non-MNA neuroblastomas (29). When taken together *MYCN* amplification and 11q- account for greater than 70% of all high stage 4 tumours (39, 40, 74). In 2009, aberrations of chromosome 11q were added to the pre-treatment risk classification categories (29).

Although predominantly inversely correlated with *MYCN* amplification, Spitz *et al.*, (2006), discovered a small subset of tumours (n=13) in their cohort of 611 NB tumours that displayed both an 11q aberration and MNA. These tumours displayed worse clinical outcome than those with MNA alone (70). Of these 13 patients, 11 experienced a relapse and nine died.

The key to further understanding the means by which deletion of chromosome 11q contributes to overall survival is to identify tumour suppressors located in the region of deletion. Different size deletions of chromosome 11q have been identified and the advent of more accurate technology has allowed the identification of the commonly deleted SORs across tumours cohorts. This mechanism allows the identification of the exact functional region of deletion and the identification of potential candidate tumour suppressor genes that may be harbored in this region. One such gene is *CADM1*, which transcribes a cellular adhesion protein, involved in neural cell development (75). A putative tumour suppressor,

CADM1 maps to chromosome 11q2 and is commonly deleted in NB. *CADM1* expression is inversely associated with advanced stage disease and poor survival (39, 76). Over-expression of *CADM1* reduces neuroblastoma cell viability in culture (76).

1.1.11 Aberrations of chromosome 17

Unbalanced rearrangement of chromosome 17q is another significant genetic alteration reported in a large number of neuroblastomas. This rearrangement was first identified by Fred Gilbert in 1984 (77) and is now recognized as the one of the most frequent genetic abnormalities in neuroblastoma (42). A number of alterations of chromosome 17 have been described. The two most commonly reported are the gain of the distal arm of 17q21 and whole chromosome 17 gain (near triploidy). Three separate groups demonstrated a translocation of 1p to 17q (78-80), others reported 17q translocations to chromosomes 3, 5, 6, 11, 19, 20 and 33 (80, 81). In 1997 Lastowska *et al.*, (82) determined using fluorescence in-situ hybridization (FISH), that chromosome 1p was the most common site of translocation for 17q, with the second most frequent site being 11q13. Tumours with loss of 11q harbour a large number of segmental aberrations (83), one of these, the gain of 17q genetic aberration, is seen in approximately 90% of 11q- NB tumours (84).

There are conflicting views on the exact association of chromosome 17 aberrations with NB outcome and risk factors. Caron *et al.*, (1995) reported 17q gain in 38% of neuroblastoma tumours (85). Latawaska *et al.*, (82) demonstrated that approximately 75% of their tumours displayed overrepresentation of chromosome 17 material, be it whole or part gain. Plantaz *et al.*, (1997) (86) established that gain of chromosome 17 material

(either whole or partial chromosomal gain) is the most common chromosomal abnormality in neuroblastoma, found in 72% of their tumour cohort. This study also identified an association between 17q gain, 1p loss and/or 11q loss and advanced stage disease. Bown *et al.*, (1999) (42) demonstrated using univariate analysis that gain of 17q was statistically associated with poor survival, *MYCN* amplification and 1p deletion. This study also reported that no tumour showed *MYCN* amplification without either deletion of 1p or gain of 17q. Furthermore, they concluded that 17q gain was the most powerful prognostic factor in neuroblastoma. A follow up study by the same group in 2001 using a larger tumour cohort reiterated that 17q was associated with advanced stage of disease, patient age, 1p deletion and *MYCN* amplification. In addition the group claimed that unbalanced gain of 17q21 was an extremely important indication of poor overall survival (OS) in neuroblastoma and recommended that it become priority that this genomic alteration be used as diagnostic marker alongside MYCN status and 1p deletion at the time of tumour categorization (87). Brinkschmidt *et al.*, (88) demonstrated similar results in a smaller tumour set.

Two groups, Spitz *et al.*, (2003) and Buckley *et al.*, (2010) contradict these studies associating 17q gain with poor survival. Spitz *et al.* (89) examined the use of 17q as a prognostic indicator in neuroblastoma. This study confirmed that 17q gain occurred in 61% of 193 investigated tumours, and that this gain correlated with stage 4, 1p loss, 3p loss, 11q loss, *MYCN* amplification and age. However, analysis of tumours lacking MNA and 11q loss found no association of 17q with survival. Buckley *et al.*, (83) also demonstrated using a large tumour cohort that unbalanced gain of 17q is not individually predictive of OS or EFS. Although Buckley *et al.* demonstrated that 17q was not predictive of outcome in 11q-

tumours a recent study has found a role for 17q gain in tumour categorization. This study (90) identified 17q gain as a predictor of worse overall survival in a subset of tumours that did not display 11q- or *MYCN* amplification. Therefore, whether an independent prognostic factor, or merely a modifying factor 17q gain may be of significant use in categorizing tumours that fall outside the scope of existing prognostic factors such as MNA or 11q deletions.

1.1.12 Loss of chromosome 3p

Hemizygous loss of genomic material from chromosome 3p in neuroblastoma was first reported in 1997 by Hallstensson *et al.*, (91). Spitz *et al.*, (2006) (92), demonstrated that genomic alterations at chromosome 3p occurred in 18% of tumours studied (15% deletion and 3% imbalances). There were a greater number of 3p deletions in tumours categorized as stage four disease when compared to all other stages of disease. The stage four tumours displayed 17 deletions of 3p and 3 imbalances on 3p in a group of 54 stage 4 tumours. Furthermore, Spitz and colleagues demonstrated that deletions on chromosome 3p could discriminate stage four tumours, where incidence of 3p deletion was lower in stage 4 tumours which experienced no relapse event.

Loss of chromosome 3p has been reported to be highly associated with 11q deletions (73, 93, 94) and patients with both 3p loss and 11q loss have a higher median age at diagnosis than patients with MNA (45, 67, 93). Deletions on 3p have also been associated with 17q gain (45), this is in keeping with the previously discussed association between 11q loss and 17q gain. Although associated with overall and event free survival (67, 68, 92) in univariate analysis, there is no evidence to prove that loss of 3p can act as

an independent predictor of prognosis. Loss of 11q with concurrent 3p loss may however provide a means of greater definition within categories of high risk patients without *MYCN* amplification (67, 93).

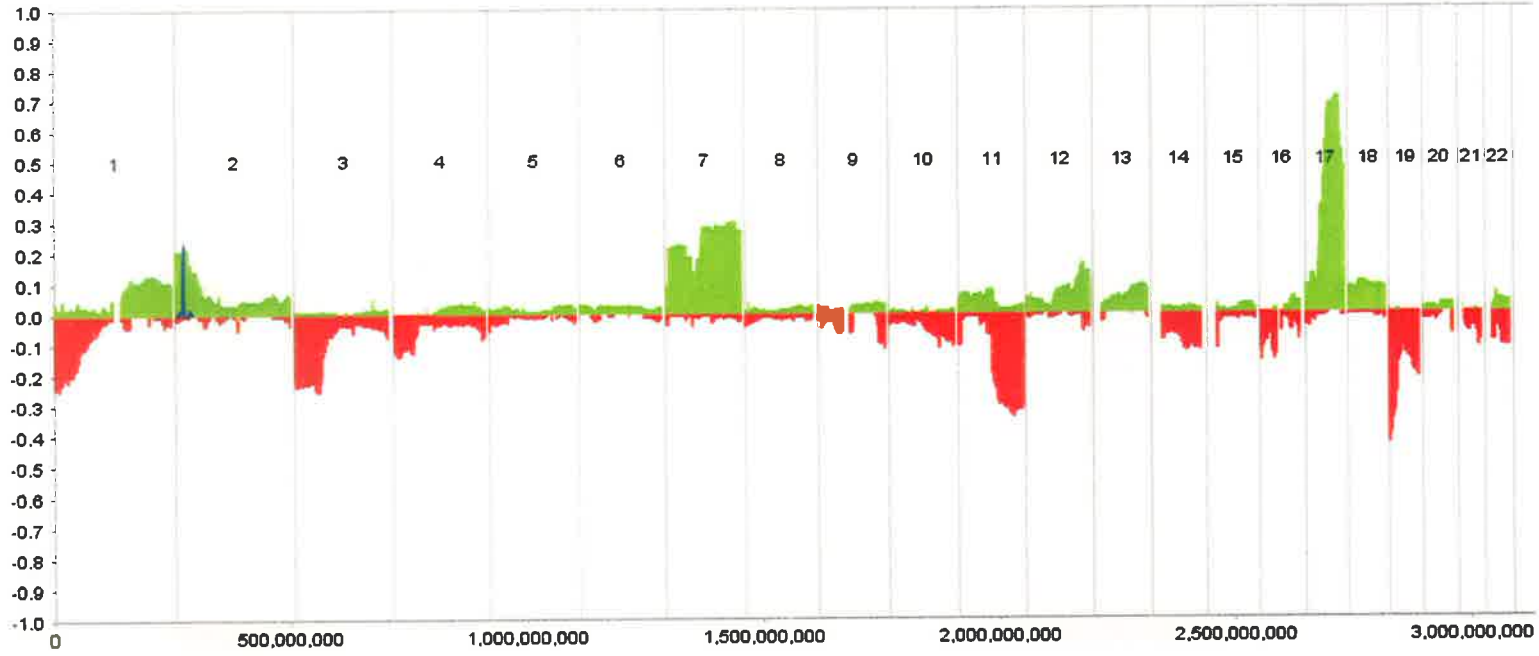

Buckley *et al.*, 2010, (83)

Figure 1.4 DNA copy number alterations from 160 primary neuroblastoma tumours across the genome. Regions of hemizygous loss (displayed in red bar) and hemizygous gains (displayed in green bar) are plotted for each autosome with the observed frequency (percent) of each aberration detected in the tumour series plotted on the Y-axis. The frequency of *MYCN* and *ALK* amplifications is also plotted (blue).

1.1.13 Urinary catecholamines

Catecholamines are hormones released by the adrenal gland, including dopamine, epinephrine, and norepinephrine. These hormones play an essential function in the body's response to stress. The use of urinary catecholamines are well established as biological markers in the detection of neuroblastoma (reviewed in Brodeur 2003 (4)). Homovanillic acid (HVA), vanillymandelic acid (VMA) and dopamine (DA) levels have all been associated with neuroblastoma diagnosis. The relationship between neuroblastoma stage, outcome and these hormonal markers has been examined in order to establish if they can provide further patient stratification. High VMA levels have been associated with favorable features of neuroblastoma including younger age, no *MYCN* amplification, no 1p deletion and disease stages 2 and 4S (95-98), whereas higher dopamine levels positively correlated with poor outcome, *MYCN* amplification, older age at diagnosis and 1p deletion (96, 98, 99). Patients with normal HVA levels have also been associated with better overall survival (98).

1.1.14 Genes of potential therapeutic benefit for neuroblastoma

1.1.14.1 Trk A: a tumour suppressor in neuroblastoma

TrkA is a tyrosine kinase transmembrane glycoprotein expressed during the development of the nervous system. Neurotrophin growth factor (NGF), a product known to induce differentiation in certain neuroblastoma cell lines, is an activating ligand of TrkA. TrkA is expressed at low levels in NB cells, and Nagawara *et al.*, (1994) (100) demonstrated an inverse relationship between levels of *MYCN* and *TrkA*. *TrkA* expression

has also been associated with low stage of disease and younger age at diagnosis (101, 102). In most patients younger than 1 year, high expression of *TrkA* correlates with a good prognosis, especially in patients with stages 1, 2, and 4S disease (103). Another member of this tyrosine kinase family, *TrkB* has been shown to have a positive correlation with *MYCN* levels and is associated with aggressive phenotype (104). *TrkA* over-expression is associated with cell growth arrest, increased apoptotic cell death and differentiation of NB cells in culture (104-107), implying these are the mechanism by which TrkA exerts its tumour suppressor functions in NB. Apoptosis as a tumour suppressor function of TrkA was validated by Lavoie *et al.*, (2005) (108) who verified that TrkA p53-induced dependent apoptosis in neuroblastoma cells. Another potential mechanism of TrkA-induced apoptosis was demonstrated by Harel and colleagues (2009) (109). This study identified CCM2 (cerebral cavernous malformation 2) as an interacting partner of TrkA, and demonstrated CCM2 binding to TrkA can induce phosphotyrosine kinase binding domain-mediated apoptosis. They also established, using a cohort of 478 tumours, that long-term survival positively correlated with the combined expression of *CCM2* and *TrkA*. Furthermore, this study determined that silencing of *CCM2* can rescue the apoptotic phenotype in NB cells.

1.1.14.2 Aurora Kinase A (AURKA): a potential therapeutic target for neuroblastoma

Aurora Kinase A (AURKA) has recently emerged as a potential therapeutic target in neuroblastoma. AURKA is a member of the serine/threonine family of Aurora proteins which play an active role in cell division, with responsibility for spindle formation during

cell division and protein translation (110). AURKA is now a well established oncogene which is over-expressed or amplified in a large number of cancers (reviewed in Carvajal, 2006 (111)). In neuroblastoma *AURKA* levels are high in *MYCN* amplified tumours and activation of MYCN in culture induces *AURKA* expression (112). AURKA has also been demonstrated to act as a potent stabilizer of MYCN. Otto *et al.*, (2009) (113), determined that shRNA degradation of *AURKA* resulted in down regulation of protein but not mRNA levels of *MYCN*, suggesting that AURKA regulation of MYCN occurs at a post transcriptional level. This study proposed that AURKA stabilizes MYCN by interfering with P13 kinase dependent, mitosis specific degradation of MYCN. This suggests that a positive feedback mechanism is in place by which MYCN enhances Aurora Kinase A levels, which in turn stabilize MYCN.

Previous studies using MYCN as a therapeutic target by reducing its ability to dimerize have been inconclusive; however recent studies have examined potential mechanisms of destabilizing MYCN. Because AURKA can stabilize MYCN it may prove to be a means by which destabilization of MYCN may be achieved. An inhibitor of *AURKA*, MCN8237, which has been hugely successful in adult cancer clinical trials has now been fast tracked to a neuroblastoma pediatric clinical trial by the Childrens Oncology Group after anti-tumourigenic activity both *in vivo* and *in vitro* in neuroblastoma was demonstrated (114).

1.1.15 The international neuroblastoma risk group

As described in detail here, there are a large number of biological and genetic factors associated with NB outcome and progression. In 1986 the International

Neuroblastoma Risk Group (INRG) was established to develop a more accurate method for using these factors for tumour classification and to ensure international consensus of classification methods. This group used a cohort of (8,800) tumours to identify the most significant factors determining tumour subtype, disease classification and subsequent mode of therapy for neuroblastoma patients. In the past, patient age and tumour stage were the main diagnostic factors considered. However with advances in technology and greater genetic understanding, a number of other factors are now considered essential in the processes of classification, disease outcome and determination of therapeutic regimens. The INRG has in place a classification protocol which details how accurate disease staging can be obtained. The staging protocol has changed over the years, so as to advance with scientific discovery, with its most recent report on staging published in 2009 (29). The INRG classification takes into consideration the clinical factors of age at diagnosis, disease stage, and the results of the Shimada method of histopathological classification, as well as the biologic factors of amplification status of the *MYCN* oncogene, DNA index >1 and 11q status.

Many countries have adopted the methods of clinical staging as recommended by the group; however there have been a number of difficulties with the staging protocol reported. One example of this is that to assign INSS criteria to a tumour surgical excision or a biopsy sample is needed. For tumours which have potential to spontaneously regress and a policy of "wait and see" is used, or for which surgery is not a safe option, it is impossible to properly categorize the tumour as no tumour sample is available for genetic, histopathological, or biological testing.

The advent of detailed imaging has helped address this lack of knowledge for un-resectable tumours. Imaging is extremely beneficial for a number of reasons, it is not highly invasive to the patient and it can be used to identify categories of tumours that may not need surgical intervention or tumours that it may be beneficial to treat with therapy before removal. Imaging is also an extremely strong technique from a clinical perspective because these images are reproducible across all patients and can be evaluated centrally in retrospective studies.

In 2005 the Siopen Group (Pediatric Oncology Europe Neuroblastoma Group) reported that examining tumours by imaging prior to resection and assigning these tumours surgical risk factors could determine the prospect of adverse surgical outcome. This group subsequently recommended using age, IDRFs (image defined risk factors) and *MYCN* status to risk categorize patients (115). In 2005 the INRG adopted the policy of pre-surgical screening using imaging (116), to determine image defined surgical risk factors (IDRFs), into their recommendations. Determination of image-defined risk factors takes into consideration location of the primary tumour, the sites (if any) of metastasis and determines the risk for surgical intervention. Simon *et al.*, 2008 (117) confirmed the usefulness of imaging in NB risk categorization, however this study concluded that IDRFs were not sufficient on their own to act as risk predictors.

In 2009 using recommendations ascertained from clinical data the INRG established a preoperative staging system to be used as a mechanism of classification using imaging before operative tissue data is available for categorization. This preoperative staging system is referred to as the International Neuroblastoma Risk Group Staging

System (INRGSS) and based on imaging disease stage is grouped into four categories as defined by Monclair *et al.*, 2009 (118).

- L1 - Localized tumour not involving vital structures as defined by the image defined risk factors. This tumour is confined to one body compartment.
- L2 - Loco-regional tumour with one or more image defined risk factor.
- M - Distant metastatic disease (except tumours defined as stage MS).
- MS - Metastatic disease in children younger than 18 months with metastasis confined to skin, liver or bone marrow.

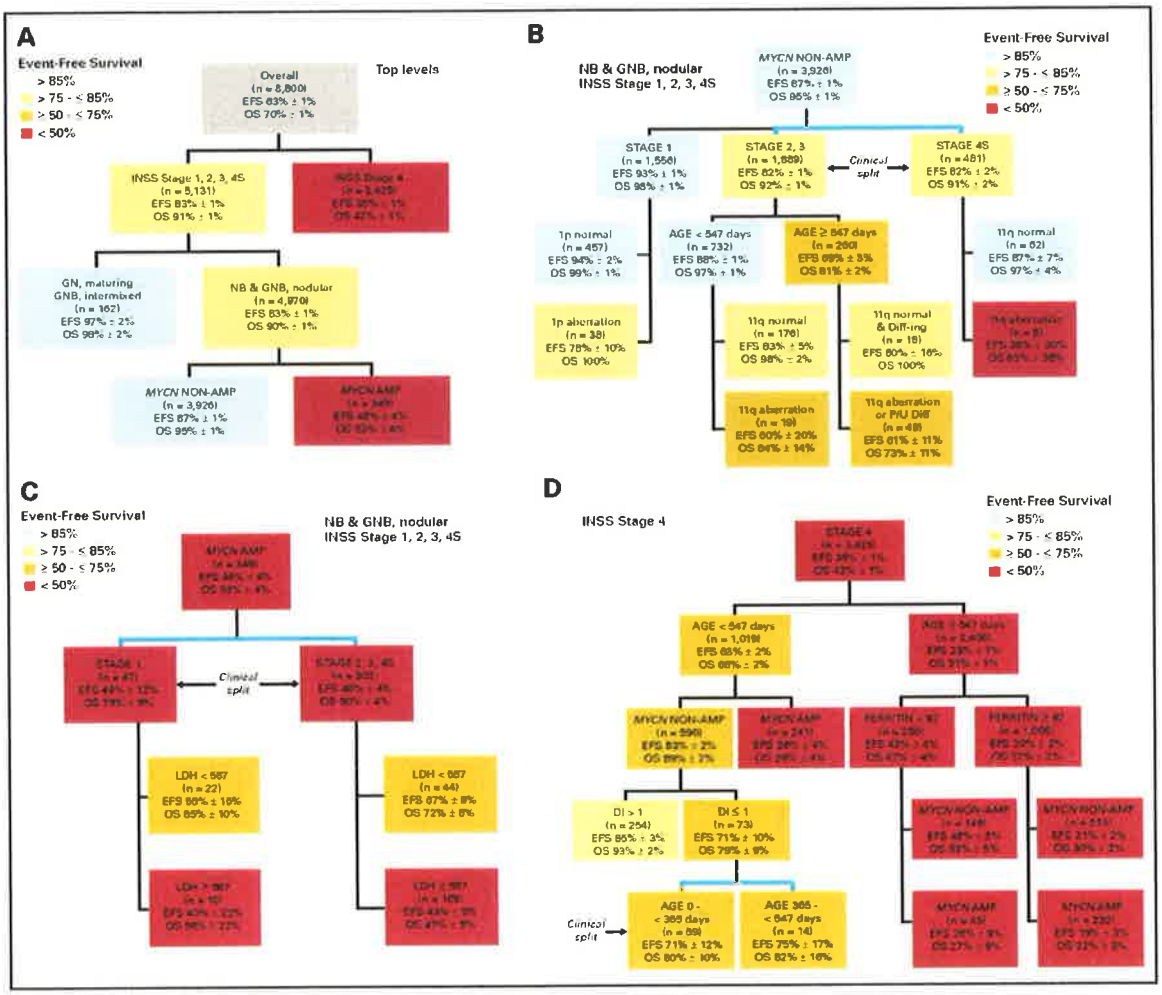

Cohn *et al.*, 2009 (29)

Figure 1.5. EFS regression analysis of the INRG cohort. This tree regression analysis categorizes factors significantly associated with survival in NB. The groups are divided into four trees, all samples as one group regardless of stage or MYCN status (A), INSS stage 1,2,3 and 4s non *MYCN* amplified (B) and *MYCN* amplified (C), and stage 4 tumours (D). Sub categories of survival are highlighted in different colours. EFS-Event free survival, OS-Overall survival, DI-DNA index, AMP-Amplified, NON-AMP-Non amplified, INRG-International neuroblastoma risk group, NB- Neuroblastoma, GNB – Ganglioneuroblastoma, GN – Ganglioneuroma, INSS International Neuroblastoma Staging System, LDH – Lactate dehydrogenase.

1.1.16 Current therapies assigned to neuroblastoma

There are a number of different courses of action taken in the treatment of neuroblastoma. As previously mentioned, this tumour displays a diverse clinical heterogeneity and as a result different tumour subtypes (depending on clinical stage and predicted outcome) require different handling in the clinical setting. The current methods of treatment as recommended by the Children's Oncology Group and the National Cancer Institute and published on the NIH National Cancer Institute website (www.cancer.gov) are dependent on the risk stratification of the tumour. Patients are divided into three groups low, medium and high risk patients. In many cases low stage tumours are initially just observed with no treatment carried out, or in some cases surgery alone is sufficient and no follow up drug regimen is required.

Criteria for implementation of the "wait and see" protocol include tumour localisation, age at diagnosis, absence of invasive growth, the levels of urinary catecholamines such as VMA and HVA (less than 50 μg/mg creatinine) and informed consent from the parents of the child (119). In most cases these tumours will spontaneously regress and the infant has been saved the trauma of drug therapy. In certain low risk patients surgery and chemotherapy will be assigned. Chemotherapy is however only administered to symptomatic low-risk patients. The current regimen for low risk patients includes low doses of cyclophosphamide, doxorubicin, and etoposide. Intermediate risk patients undergo surgery, followed by the same regimen of chemotherapy stated above. However, tumours in this subset that display unfavourable biology will receive a second cycle of chemotherapy versus patients with favourable biology. Neuroblastoma patients diagnosed with high risk disease face a far more intense and invasive therapeutic regimen.

This regimen includes extremely high doses of cyclophosphamide, doxorubicin, and etoposide but with the addition of cisplatin and isoflamide. After response to therapy, resection of the tumour is attempted and myeloablative chemotherapy and autologous stem cell transplantation performed. Radiation of residual tumour and original sites of metastases is often performed before, during, or after myeloablative therapy. After recovery, patients are treated with oral 13-*cis*-retinoic acid for 6 months. Both myeloablative therapy and retinoic acid improve outcome in patients categorized as high risk.

Despite the intensity of treatment, EFS remains low for high-risk patients and relapse is common. It is also evident that certain cases categorized as high risk may not require such intense treatment. This emphasizes the need for more precise categorisation of tumours within the high risk groups to determine more appropriate, tailored drug regimens. Existing multimodal therapies include treatment with a cocktail of drugs and invasive procedures. Despite this, the outlook for children in high risk categories remains extremely poor.

1.1.17 Spontaneous regression and the implications for neuroblastoma

Greater knowledge of the means by which some neuroblastoma tumours can undergo spontaneous regression, would contribute greatly to the knowledge of the molecular mechanisms underlying this cancer. In 1927 two doctors, Harvey Cushing and Burt Wolbach working in Boston performed investigative surgery on a child who had previously recovered from cancer. They reported the discovery of a mature ganglioneuroma in a lymph node. As ganglioneuromas are benign tumours which cannot

metastasize, it was hypothesised that what had been discovered was a metastatic NB tumour that had spontaneously regressed and differentiated to become a benign gangioneuroma (120). Since this paper first reported the ability of neuroblastoma to spontaneously regress, this has become a well published phenomenon. In fact neuroblastoma has the highest rate of spontaneous regression of any cancer type (121). It is estimated that spontaneous regression takes place in up to 54% of neuroblastoma patients, with overall survival in this group of patients being ~92% (122)

1.1.17.1 Differentiation

Differentiation is a major process in human development; it is the process by which an immature cell type develops into a mature functional cell. Neuroblastoma is believed to be derived from neural crest cells which at some point lose the ability to differentiate and fail to develop into a fully mature cell (1). By comparing marker gene expression in human SNS cells during various stages of embryonic and fetal development and the marker gene expression of neuroblastoma cells, Edsjo *et al.,* (123) confirmed that neuroblastoma cells share gene characteristics of immature neuronal cells, thus implying neuroblastoma cells are derived from precursors of immature cells of sympathetic ganglionic lineage (Figure 1.6). Neuroblastoma cells are typically undifferentiated, round and with small cytoplasms. This being said, many tumours contain a large number of differentiated cells with larger nucleus and cytoplasm. The differentiation status of the cells is related to a number of neuroblastoma prognostic factors: poorly differentiated cells are associated with poor survival, MNA, MKI and stage of disease (26, 49, 124). The degree of differentiation in neuroblastoma tumours is highly associated with disease outcome. Shimada *et al.,* (2001)

(124) reported OS to be 30% in undifferentiated tumours versus 61% in poorly differentiated tumours and 81.4% in differentiating tumours. Regardless of age undifferentiated tumours had poor overall survival, however the two differentiating sub-types showed OS and EFS were significantly better in children <5 years than those older.

Many doctors and researchers consider that understanding the mechanism by which certain neuroblastoma tumours differentiate and others do not could have major implications for outcome and therapy. It is evident from the literature that a number of pathways can induce differentiation in neuroblastoma; however certain tumours remain unresponsive to differentiation therapy. There are a number of agents that are well established to induce differentiation *in vivo* and *in-vitro* including retinoic acid and phorbolesters such as TPA (12-*O*-tetradeconoyl phorbol-13-acetate) and 13-cis-retinoic acid. As already mentioned, differentiation agents are currently used in the final stages of therapy. Induction of differentiation in neuroblastic tumours follows along the pattern of neuronal crest development (125) removing cells from their tumour-like cell type and pushing them towards their original pathway of development.

Further investigation of this phenomenon may aid in unlocking the processes involved in differentiation and the resistance of certain subtypes of neuroblastoma to this process. This information may subsequently provide insight needed to produce a novel and viable therapeutic for high risk neuroblastoma.

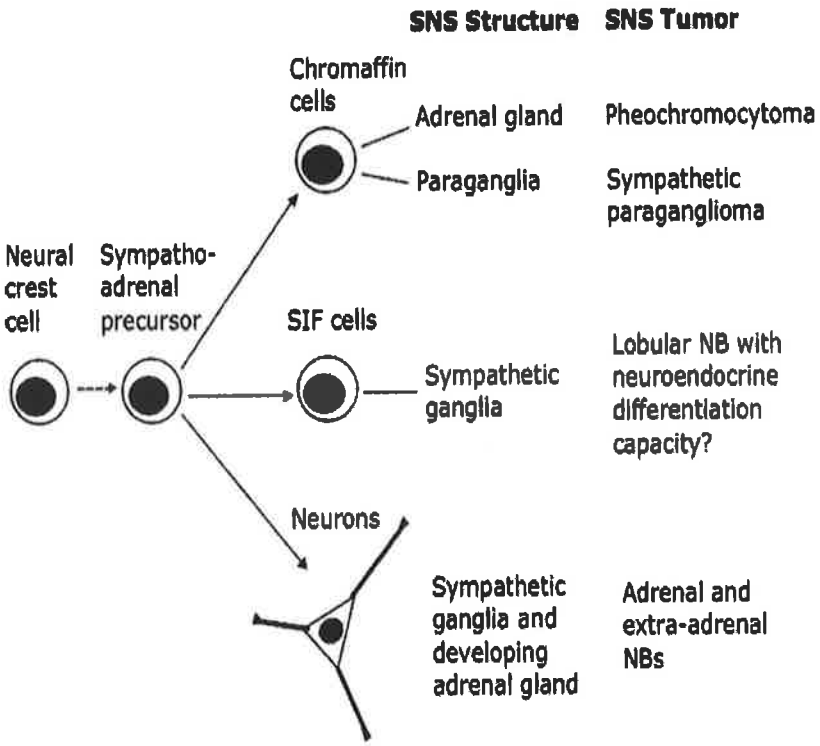

Edsjo, Holmquist and Pahlman 2007 (123)

Figure 1.6 Sympathetic Nervous System (SNS) cell lineages of neural crest origin and their derived tumour forms. Neuroblastoma cells are derived mainly from sympathetic ganglia and the developing adrenal gland neuronal lineage with the possibility that some originate from small intensely fluorescent (SIF) in origin to sympathetic ganglia.

1.2 MicroRNAs

1.2.1 Discovery and Identification

MicroRNAs are non-coding RNA sequences that have the ability to post-transcriptionally regulate gene expression. These sequences are non-coding in that they are transcribed from DNA but are not translated into protein. For many years non-coding RNAs were deemed redundant. MicroRNAs were first described as having a functional significance by Lee *et al.*, in 1993 (126), with the discovery of lin-4, a small non-coding RNA 22 nucleotides in length. This group observed lin-4 could initiate an RNA-RNA binding interaction through sequence complementarity with the 3'UTR (un-translated region) of lin-14 mRNA, and subsequently cause translational repression of the lin-14 protein. Degradation of lin-14 was concurrent with lin-4 up-regulation during development of *Caernorhabditis elegans.* The degradation of lin-14 is an essential mechanism in the control of developmental timing in *C-elegans* and the results suggested that this small non-coding RNA lin-4 was responsible for the process of this developmental dependant degradation.

With this initial finding, and the subsequent discovery seven years later of let-7, another non-coding sequence that played a similar role in developmental timing in *C-elegans*, it was largely assumed that these were unique sequences only expressed in the worm (127). This notion was however expelled with the discovery of conservation of let-7 regulation across many species (128). This discovery lead to the beginning of what can only be described as an explosion of a new field of scientific research: microRNA regulatory sequences and the functions these non-coding RNAs play in all processes of the cell.

Large scale identification of microRNAs became one of the first challenges in this field. In 2001, Lee and Ambros (129), used all information known about these microRNAs at the time, length ~22nts, location (non-coding sequences), high degree of conservation between orthologs in *C-elegans* and related species, and the fact these small non-coding microRNAs are processed from a larger stem-loop type sequence to develop a bioinformatics approach for the mining and identification of novel microRNAs. This study led to the identification of 15 gene sequences that were deemed to initially form stem-loop sequences of ~65 nucleotides in length, and then produce shorter sequences of ~22 nucleotides.

It became evident that these microRNAs were not only functioning in the mediation of developmental timing but also in the control of cellular function. We now know that approximately 3% of the genome encodes for microRNAs (130) and that these microRNAs have diverse patterns of differential tissue expression (131), indicating diverse functions across all systems. Many microRNAs are highly conserved suggesting an essential non-redundant role in cellular processes (132).

The active form are known as the mature microRNAs, defined as single-stranded RNAs of approximately 22 nucleotides in length that act on target mRNAs to cause translational repression through a variety of different processes. Since the discovery of microRNAs numerous studies have revealed key regulatory roles in a number of physiological pathways including developmental timing, cell survival, cell death and cell differentiation (132, 133).

1.2.2 MicroRNA transcription

MicroRNAs are transcribed in the nucleus as primary (pri-) microRNA stem-loop transcripts (134), which can be up to several thousand base-pairs in length. These stem-loop transcripts include 5'caps and a 3' poly (A) tail (135, 136). RNA Polymerase II (Pol II) was the first enzyme identified as being responsible for microRNA transcription. This was demonstrated using both a knockout of Pol II and chromatin immunoprecipitation (CHIP) experiments for Pol II (137). Pol II binding to the promoters of miR-23a, miR-27a and miR-24-2 confirmed microRNAs were being transcribed primarily by RNA polymerase II (137). At the outset it was thought that it was just Pol II that could transcribe these small non coding RNAs. This presumption was made because many microRNA are several kilobases in length and contain repetitions of more than four U's within their sequence, and multiples in a sequence are known to terminate the activity of the DNA polymerase, RNA Pol III.

In 2006 Borchet *et al.*, (138) screened 500 base-pairs up- and down-stream of all known microRNA for repetitive elements. This study identified ~50 microRNAs located within repetitive elements and most interestingly showed a miR polycistronic cluster on chromosome 19 from which MicroRNAs and ALU repeats accounted for over 60% of the 100-Kbp region. Most of these ALU repetitions in this cluster contained Pol III promoter elements. Validation experiments were carried out for a number of microRNAs in this cluster; miR-515-1, miR-517a, miR-517c and miR-519a-1 were all identified as being transcribed by Pol III. Further computational analyses suggested other miRNAs within this cluster, and other human miRNAs with upstream ALU-, tRNA- or MWIR polymerase III promoter elements, may be similarly transcribed. Although Pol II is still thought to be the

predominate enzyme responsible for transcription, the different mechanisms of actions of these two regulatory elements widens the regulatory potential for microRNAs and the subsequent downstream RNA target of these pathways.

Although many microRNA have been discovered, few microRNA promoter regions have been identified. MicroRNAs can be defined by their location either within genes (intronic) or between genes (intergenic). Location of the microRNA transcript is paramount in order to determine the mechanism by which it is transcribed. Intergenic microRNAs are controlled by individual promoter elements, for many of which the location of the promoter is not yet defined. In most cases, intronic microRNA transcription is controlled by the promoter element of the host gene. A recent study by Monteys *et al.*, (139) however, demonstrated that microRNA transcription can occur independently of the host promoter. This paper predicted that transcription of ~35% of the intronic microRNAs can be controlled by either the host gene promoter or an independent promoter; adding another layer of complexity to the already diverse regulatory mechanism of microRNAs. The mechanism of bi-promoter activation was validated experimentally using miR-128-2, resolving previous reports suggesting expression of certain intronic microRNAs did not correlate with their host gene.

Regulation of microRNAs remains complex, poorly understood process and until fully understood we will not be able to fully appreciate the contribution these microRNA play in all physiological functions.

1.2.3 Pri-microRNA cleavage

The next step in the microRNA processing pathway is the pri-miRNA cleavage in the nucleus to produce a much shorter pre-microRNA (of approximately 70 nt in length). Cleavage is carried out by a complex which contains the RNase III enzyme Drosha (RNASEN) (140) and the double stranded RNA binding domain protein DGCR8 (DiGeorge Critical Region 8) (141). A study by Lee *et al.*, (2003) demonstrated using RNA interference that both elements of this complex, Drosha and DGRC8, are essential for microRNA processing. Knock-down of either resulted in the accumulation of unprocessed Pri-miRs and a reduction in Pre-miRNA and functionally mature microRNAs (140).

Drosha is a class II RNase protein which means it contains two binding domains (RNase III domains) and one double stranded RNA binding domain (dsRBD) (142). Han *et al.*, (143) carried out site-directed mutagenesis to determine the Drosha protein domains functionally required for microRNA processing. Deletion of the n-terminal region did not affect microRNA processing, but mutations of the middle region (the two RIIIDs and the dsRBD) inactivated microRNA processing. Drosha/DGCR8 mediates cleavage at both ends of the hairpin structure through the two RNAse III domains. Each one binds to the 3' and 5' strand of the pri-miR respectively to produce the shorter pre-miRNA. Cleavage of the 5' strand by RNIIIDb results in a 2nt overhang at the 3' end. DGRC8 contains two double stranded RNA binding domains, although known to be essential in this biogenesis pathway its exact role is not fully understood. One suggested role for DGCR8 was that it may be essential for ensuring the correct orientation of the microRNA into the cleavage complex; however this theory has not yet been validated experimentally (143). Whereas

other reports have suggested that it guides Drosha to the exact site of cleavage (144, 145). This Drosha/DGCR8 mechanism for processing the pre-microRNAs is highly conserved across species (144, 145)

1.2.4 Mirtrons

Not all microRNAs undergo Drosha processing in the nucleus to produce pre-microRNAs. Other forms of intronic microRNAs exist. These microRNA are transcribed directly as short introns, which bypass the Drosha processing complex and are transported by Exportin 5 (XPO5) into cytoplasm. These microRNAs are known as mirtrons. The Drosha processed Pre-miR contains a region of nucleotides referred to as the "lower stem" by which the microRNA is recognised by Drosha (144, 145). Mirtrons do not have this region and therefore are not recognised by Drosha. Mirtrons are cleaved by means of splicing machinery. A mechanism demonstrated by two groups, Ruby *et al.*, (2007) and Okamara *et al.*, (2007). Okamara *et al.* showed that by inserting G's for C's in the 5' splice sites of two functional mirtrons, the hairpin or mature ~22 nucleotide sequence was not produced. After splicing of the sequence to produce a hair-pin fold it undergoes lariat-debranching, this process was confirmed by the knock-down of the lariat enzyme Ldbr which inhibits production of the mature product. After splicing and debranching the pathway then merges with the conventional microRNA processing pathway at the export step, where mirtrons are also transported to the cytoplasm using Exportin5 (XPO5). Knock-down of XPO5 in Droshphilia by Okamura *et al.*, (2007), showed a 60-80% reduction in the mirtron hairpins and mature products. After cleavage the mirtrons retain a stem-loop structure similar to that of the drosha processed microRNA and can go on to be

processed by Dicer (146). Although microRNA processing can produce the final mature sequence from either the 5' or 3' arm of the stem loop, mirtrons predominately select for 3' origin mature sequences (147).

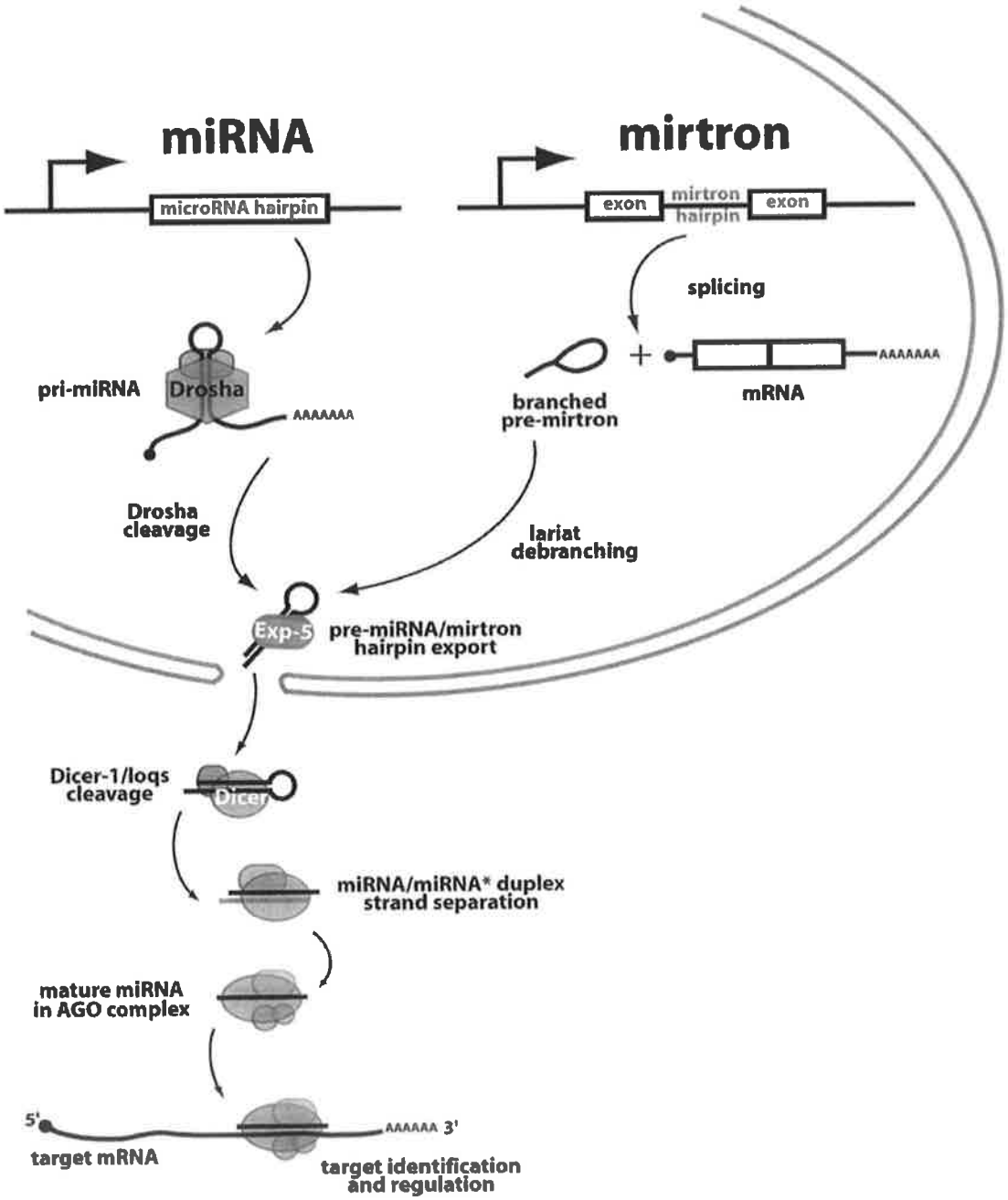

Okamara *et al.*, 2007 (146)

Figure 1.7. Mirtron processing. Mirtrons are microRNAs which are transcribed from intronic regions of genes, bypass the Drosha cleavage step and are instead cleaved by splicing machinery of the cell. Except for Drosha bypass introns follow the same pathway of development as Drosha processed miRNAs.

1.2.5 Transport of pre-miRNA into the cytoplasm

Transport of the pr5-miRNA from the nucleus into the cytoplasm for further processing is facilitated by XPO5. Before the transport machinery for microRNAs had been established XPO5 had already been validated as the nuclear shuttle for VA1, a non-coding RNA (148, 149). Due to the structural similarities of the terminal mini-helix of >14bp bearing a 5' and 3' overhang between VA1 and microRNAs it was hypothesised by Yi *et al.*, (2003) (150) that these non-coding RNAs may share similar mechanisms of nuclear export. This group went on to validate this theory by showing knock-down of *XPO5* led to no changes in the abundance of the pri- or pre-miRNA, but a significant decrease in the levels of the mature miRNA (using total miRNA). A clear reduction in the levels of both pre-miR and mature miRNA in the cytoplasm was also observed, suggesting the pre-miR sequence never leaves the nucleus.

XPO5 transport is dependant on a RanGTP energy gradient as a source of energy for microRNA coupling and transport. The product can bind to XPO5 in the presence of high energy levels in the nuclear envelope and then both the product and RAN are released by GTP hydrolysis in the cytoplasm (151, 152). XPO5 recognises a 2-nt overhang on the 3' end of the pre-miRNA and exports the pre-miRNA into the cytoplasm by this RNA-GTP dependant mechanism (153).

Further work determined that unlike VA1, which required a greater than a 14nt over-hang, microRNAs required a mini-helix with greater than 16bp over-hang for binding, an 18bp over-hang for high affinity binding and that although a 2nt 3' over-hang is optimum for miR-XPO5 binding, minor changes are tolerated. Interestingly, this study also demonstrated that mutations in the pre-miRNA binding sequence which resulted in

reduced XPO5 affinity also resulted in reduced steady state levels of pre-miR in transfected cells. This suggests that XPO5 may also play a role in protecting pre-miRs from degradation in the nucleus (154). This theory was validated by Okada *et al.*, (2009) (155) who demonstrated using x-ray structure modeling that XPO5 surrounds the microRNA to protect it during export out of the nucleus, (Figure 1.8).

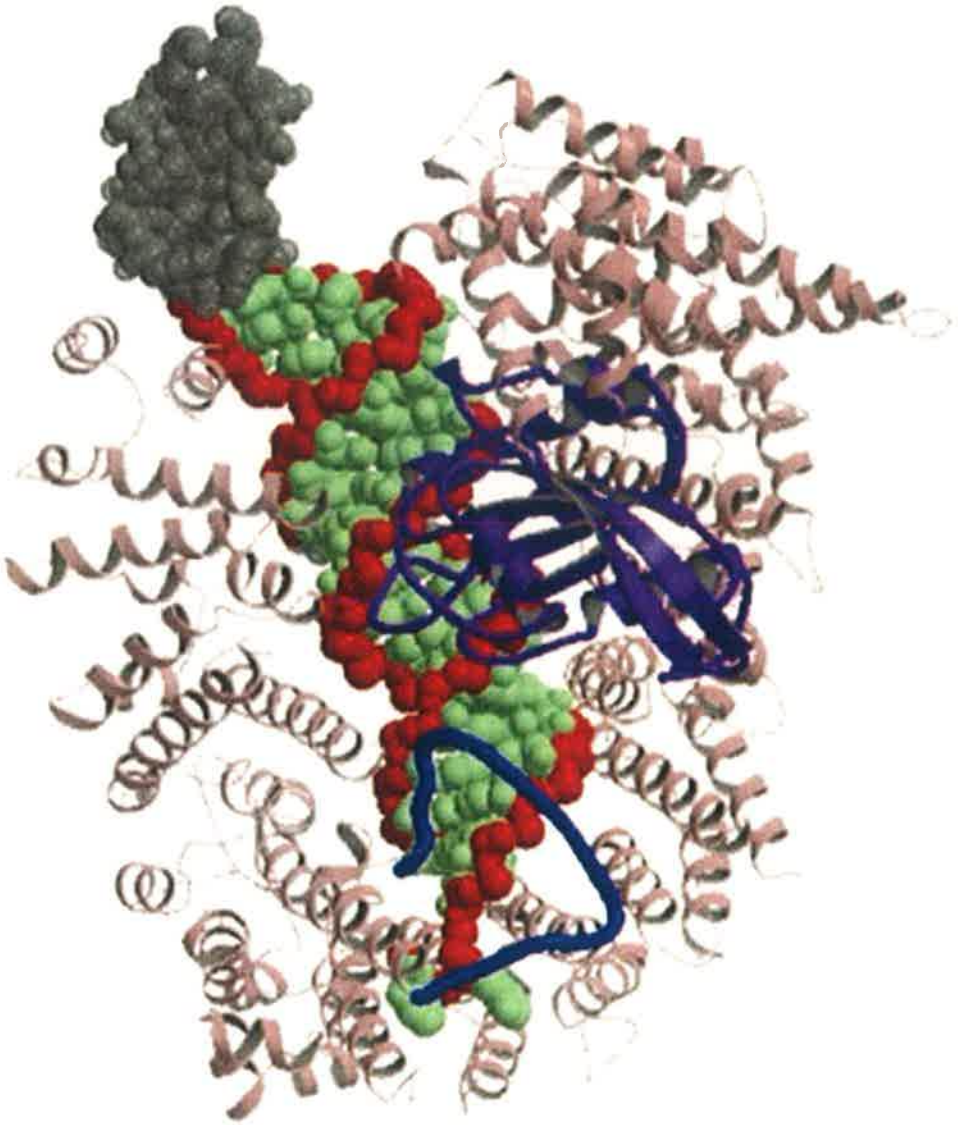

Okada *et al.*, 2009 (155)

Figure 1.8. Crystallised structure of a microRNA bound to Exportin5. This diagram is a crystal model of Exportin5 (pink) with human pre-miRNA-30a (red and green) bound and ready for transport. The purple schematic is the bound RanGTP.

1.2.6 Processing by Dicer

MicroRNAs when exported out of the nucleus by XPO5 are not yet in their mature functional form. These microRNAs need to undergo further cleavage to become the small mature miRNAs which are responsible for inhibition of transcription and translation throughout the genome. Dicer is a highly conserved member of the superfamily RNase III nucleases which was first discovered to play a role in the RNAi pathway by Bernstein et *al.*, (2001). This study produced evidence that Dicer is primarily responsible for the cleavage of double stranded RNA in *C-elegans*. They also demonstrated that the human homolog of Dicer was capable of generating ~22nt RNAs from the dsRNA substrates, suggesting these structurally similar proteins may share some distinct biochemical functions (156). Grishok *et al.*, (2001) (157) demonstrated lin-14 and let-7 were also processed in the same manner and that Dicer cleaved the loop off the stem-loop resulting in a dsRNA sequence of ~22nts in length. This was the first step in the elucidation of the processing of microRNAs by Dicer.

Further studies revealed Dicer interacts with two other proteins, PACT (protein activator of PKR) (158) and TRBP (a double stranded RNA binding protein) (159) in the cytoplasm, and although these proteins are not directly needed for Dicer processing of the microRNA, it is believed that they may contribute to Dicer stability, and are responsible for RISC loading after cleavage (RISC loading complex).

Dicer contains a helicase domain, dsRNA (double stranded RNA) binding domains, two RNase type III domains and a PAZ domain (160, 161). Although there are two isoforms of Dicer the microRNA processing by Dicer is carried out predominately by Dicer-1 and not Dicer-2 (162). This is also true for the cleavage of the mirtrons (146).

After cleavage by Dicer, it is believed that this multi-protein complex with the double stranded RNA attached binds to a member of the Argonaute family of proteins (AGO 1-4). The double stranded RNA is then released from Dicer/TRBP/PACT complex and loaded on to the RISC complex (reviewed by Kim, 2009 (163)). The exact mechanism of how this transfer is carried out is not fully understood.

Either one of the strands from the dsRNA sequence has potential to act as a mature microRNA, however the RISC (RNA induced silencing complex) complex chooses to preferentially uptake one of these strands (the 'guide' strand) over the other (the 'passenger' strand), based on thermodynamic stability (164).

1.2.7 Strand selection by RISC

The RISC complex modulates the effects of RNA interference, for both siRNAs and microRNAs (163). The microRNA guides the RISC complex to the target mRNA, which in turn destroys the target protein either by degradation of the mRNA or inhibition of mRNA translation. The RISC initially contains the whole double stranded molecule. Selection of the active 'guide' strand is chosen based on the thermodynamic properties of the two 5' termini. Khvorova *et al.*, (2003) (164) established that the RISC complex preferentially takes up the strand with lower internal stability at the 2-4nt on the 5' end. This strand is retained in the RISC and the other strand is removed resulting in the active RISC complex being formed (Figure 1.9). These results were further validated *in vivo* by Schwarz *et al.*, in 2003 (165).

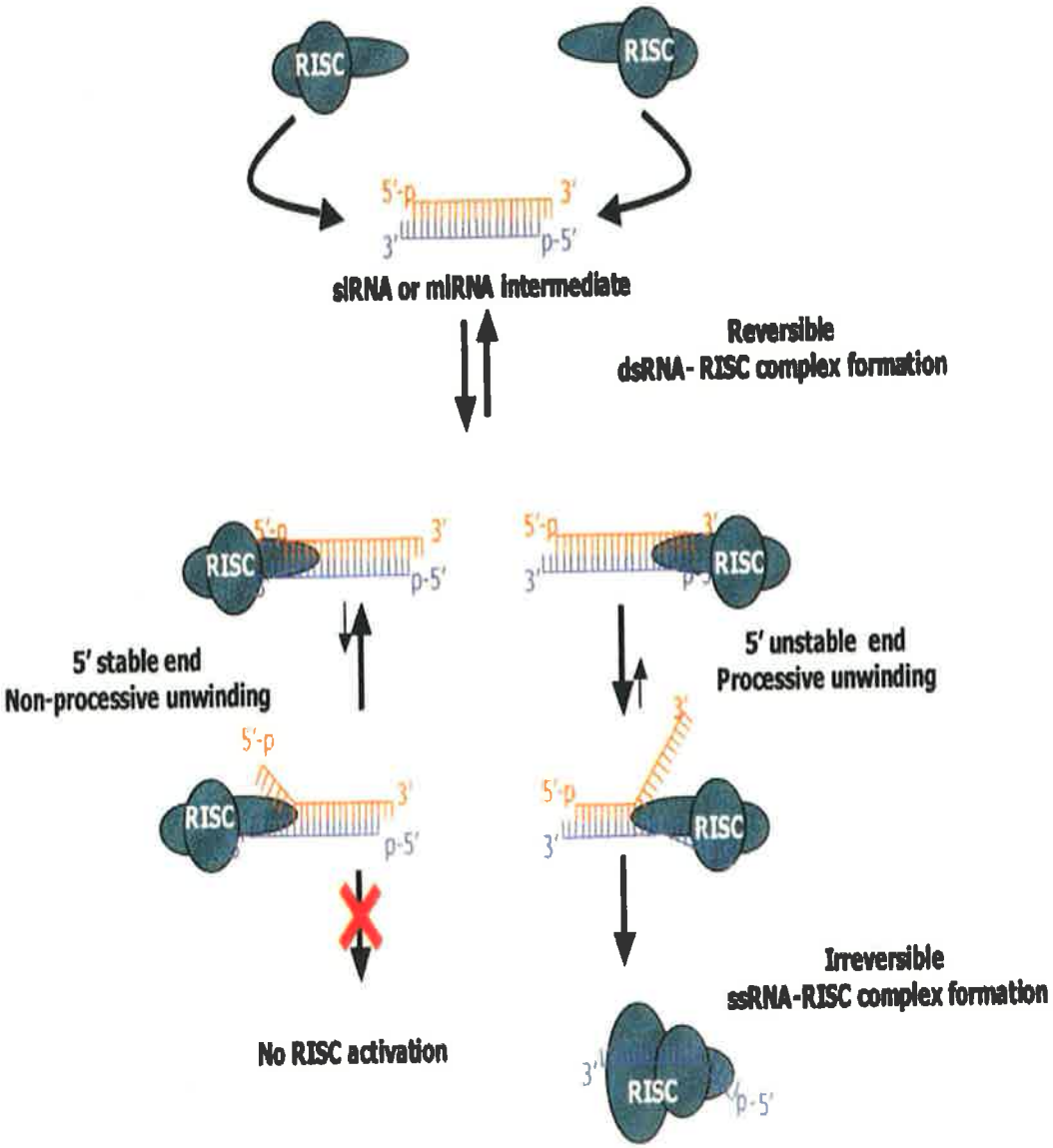

Khvorova *et al.*, 2003 (164)

Figure 1.9. Determination of miRNA strand uptake by the RISC complex. Thermodynamic stability of the 5' end of each strand of the microRNA duplex determines which strand will be taken up and used by RISC and which strand will be removed.

1.2.8 The composition and mechanism of action of the RISC complex

It is well established that the mature microRNA is incorporated into the RISC complex, which is made up of a ribonucleotideprotein assembly. This complex is diverse in its functions and plays a part in a variety of RNA silencing pathways. Although it is established as the mechanism by which regulatory RNAs exert their functions, the actions of the RISC complex is not very well annotated or understood. The main components of the miRNA-RISC complex are members of the Argonaute family of proteins (AGO 1-4) and the single stranded guide sequence. The Argonaute family of proteins are highly conserved across species, functioning as effectors of the RNAi pathways. AGO2 is the only member of the Argonaute family that has been reported to function in the siRNA-RISC pathway (131). However it is established that all four AGO family member proteins are functionally active in miRNA-mRNA repression in mammals (166-168). The argonaute proteins are characterised by two binding domains, PAZ and PIWI (169). Liu *et al.*, 2004 (131) demonstrated using site directed mutations that the PIWI domain was essential for RNA cleavage by AGO2. Two mutations in this region of the protein resulted in a continued ability of the protein to bind its siRNA but an inability for the complex to cleave the target protein. This is the basic method by which this complex functions; however the detailed intricate mechanism is not yet understood.

When the passenger strand of the miRNA is removed from the RISC complex, RISC becomes active (164, 170). The complex is then guided towards its target mRNA sequence, where it exerts its actions and protein expression is prevented. Although it is known that the primary responsibility of the microRNA is the recognition and binding of the RISC complex to the RNA target sequence by means of sequence complementarity

(171), the exact mechanism by which the RISC-microRNA complex locates its target sequence is unclear.

Once the complex is bound to the target it is then the responsibility of the Argonaute protein to initiate RNA degradation, destabilisation or protein translation inhibition (172). Both the sequence homology and the member of the Argonaute protein in the complex contribute to which mechanism of gene silencing then ensue. The PIWI region of the AGO2 complex is the component of the RISC complex believed to have the ability to result in the "slicer" activity and RNA degradation (173, 174), whereas the other members of the family of AGO proteins can only function via protein translation repression.

The level of complementarity of binding is also thought to contribute to the subsequent action of the RISC complex. MicroRNA target sequence degradation can still occur even in the presence of incomplete base pairing with its target sequence, allowing each microRNA to target a large number of different mRNA. With such a broad range of potential targets, each microRNA has the potential for immense regulatory functions. It has been estimated that approximately 30% of the genes of the human genome are under regulation by microRNAs (175).

The current gold standard means for miRNA target identification involves the use of algorithms, which take into account a number of known components of binding. One of the most published theories is that the greater the level of homology between the "seed" region (nucleotides 2-8) at the 5' end of the microRNA and the target sequence of the mRNA the greater the chance that RNA degradation will occur. Mismatches and bulges in the seed region are also believed to greatly affect the level of repression.

This field is rapidly evolving and we know now that microRNAs can also bind to the 5'UTR (176), within coding sequences of targets (177, 178) and can activate target sequences by binding to promoter regions resulting in activation of the transcript (179). It is essential that these target predication algorithms are updated continuously to account for such advances. Even if keeping abreast of advances in this field, these algorithms are not perfect, emphasising the need for lab-based target validation.

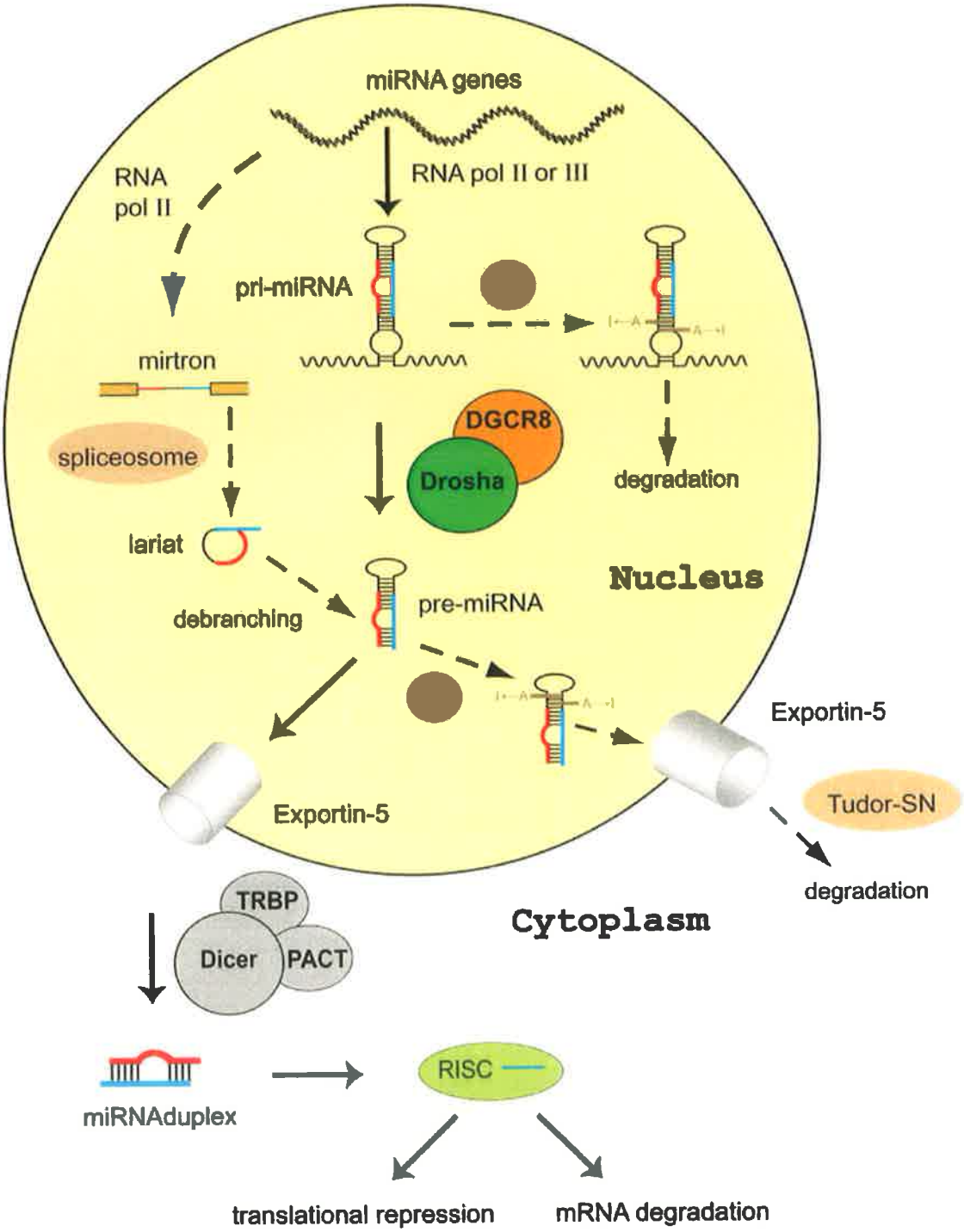

Faller and Guo, 2008 (180)

Figure 1.10 Overview of microRNA processing.

1.2.9 Current challenges in the field of microRNA biogenesis

1.2.9.1 MicroRNA discovery

It is predicted that there are thousands of microRNAs in the human genome; however it is evident that not all of these microRNAs have been discovered. There have been many methods used to examine experimentally microRNA levels including northern blots; microarray based profiling, in situ hybridisation and RTqPCR. However, studies based on all of the above mechanisms are limited to examining microRNAs that are currently known and annotated. Novel, unidentified microRNAs which may be of importance in disease are not being detected using these means of testing. With the advent of next generation genome wide deep sequencing it is hoped that this gap will soon be eradicated, allowing for more informed microRNA profiling of disease.

1.2.9.2 Multiple potential targets

Exact base pair complementarily leading to mRNA cleavage, has been reported in plant miRNA biology (181), but is less frequently observed in vertebrae. With gaps and bulges in alignment still resulting in binding and protein translational inhibition each microRNA has a vast number of predicted potential targets (reviewed by Calin and Croce, 2006 (182)). This imperfect binding of a microRNA to a target sequence creates many problems for accurate target identification. Currently there are a number of bioinformatic tools in use for predicting mRNA targets, each using slightly different algorithms. Many of these target prediction programmes are currently designed on the premise that binding occurs between the miRNA seed region which is positions 2-7 of the 5' end of the

microRNA and it a region in the 3'UTR of its target gene. The greater the base pair homology between the "seed" region of a microRNA (nucleotide 2-8) and its mRNA target, the greater the likelihood that the microRNA indeed targets the mRNA of interest. Some of these algorithms also take into account the conservation of the microRNA and its target across species, with the premise that if conserved, this sequence miRNA-RNA interaction may be functionally important.

1.2.9.3 Alternative binding locations

Until very recently it was believed that all microRNAs only bound to their target gene in its 3'UTR, resulting in the subsequent degradation of mRNA or inhibition of protein translation. This is still understood to be the primary and most efficient mechanism of action of the microRNAs (183) however; it is now known that microRNA binding to mRNA sequences is more complex than this. A number of groups have recently reported microRNA binding in other regions of the gene, including to the 5'UTR (176) and coding sequence sites (CDS) (184). An even more complex development has been the discovery that microRNAs can increase the levels of target mRNAs developing a novel role for microRNAs as activators of translation (178, 179, 185). Another level of complexity in microRNA binding discovered, is the ability of microRNAs to bind to conserved 5'TOP motifs, in the 5'UTR of target genes and result in translational enhancement. This has been validated using miR-10a (178).

Lee *et al.*, (2009) (176) reported the discovery of many endogenous motifs within the 5'UTRs specific to the 3' ends of miRNAs. This group determined that not only do microRNAs have the ability to bind to the 5'UTR of a gene, but they can simultaneously

bind the 3'UTR and the 5'UTR of a target gene resulting in greater gene inhibition than binding to the 3'UTR alone. This was validated for AXIN2 (Axin-related protein) which contains a miR-34a binding sites in both the 3'UTR and the 5'UTR. Using a vector which contained both binding regions they showed a greater reduction in luciferase activity than vectors containing each binding site individually. The same group in a later publication identified conserved uAUGs in the 5'UTR of these genes as the regions of microRNA binding. These uAUGs are conserved sequences which are found primarily in the 5'UTR and are known to act as translational regulators. This study combines both miRNAs and uAUGs which function together resulting in translation repression (186).

Forman *et al.*, (2008) (187) used a computational algorithm to identify microRNA binding regions within the coding sequences of genes. This computer algorithm searched for conserved sequence motifs within coding regions, in keeping with the previous theory that microRNAs preferentially bind to its target via sequence homology, searches were carried out for conserved motifs of 8bp in length. The top 15 scored motifs across the genome, displayed enrichment for binding sites of four microRNAs, let-7, miR-9, miR-125a and miR-153. They also confirmed that Dicer was a direct target of let-7, by CDS binding using a vector containing the gene coding sequence, without the 3'UTR.

These are just initial studies, examining alternative mechanisms of actions of microRNAs and it is clear that there is still a large amount of unanswered questions and undiscovered functions of microRNAs.

1.2.9.4 MicroRNAs re-entering the nucleus

It has been proposed that certain mRNAs are subject to RNA interference within the nucleus of the cell. A recent publication by Castanotta *et al.*, (188) demonstrated that CRM1, also known as XPO1, can shuttle mature pre-miRNAs from the cytoplasm back into the nucleus. This study also demonstrated that CRM1 interacts with members of the RISC complex, potentially leading to an even greater level of complexity. Previous reports that display that siRNAs can affect chromatin remodeling, and that they can also bind to promoters of genes (189) causing transcriptional silencing It was then considered possible that microRNAs may have a similar role to play, in transcriptional control within the nucleus.

Gonzalez *et al.*, (2008) (190) confirmed using miR-17-5p and miR-20a that microRNAs can cause transcriptional down-regulation by binding by its seed region to the gene promoter. Place *et al.*, (2008) (86) demonstrated that not only could microRNA binding to the promoter induce gene silencing but it can also enhance transcription. Using miR-373 as an example, this study demonstrated that a microRNA can induce the expression of genes by binding via sequence homology to a region within the promoter of a gene and activating transcription. This was experimentally validated by showing that miR-373 binds to the promoter region of e-cadherin and CSDC2 resulting in transcriptional activation of both genes.

1.2.11.2 Degradation of microRNAs

Precise maintenance of expression levels and appropriately timed degradation of microRNAs is essential in normal homeostasis (191-193). This is especially evident during

embryonic and nervous system development, where microRNAs are expressed at different levels during the various developmental stages (reviewed in Fineberg *et al.,* 2009 (194)). This indicates a requirement for not only the specific production of microRNAs, but also their precisely regulated degradation. As previously discussed XPO5 is believed to help protect microRNAs from degradation, however the mechanism by which degradation occurs is unclear. There is at present very little known about the processes involved in maintenance of microRNA homeostasis and the timed degradation that occurs during development. Ramachandran and Chen, (2008) (195) discussed one mechanism in which small RNA degrading nuclease (SDN) genes, cause degradation of mature miRNAs in *Arabidopsis.* Simultaneous knock-out of three SDN genes caused an increase in mature miRNA levels and a subsequent pleiotrophy of developmental defects. Although plant microRNAs are similar to mammalian microRNAs this mechanism of degradation is yet to be confirmed in a mammalian model. This paper also only deals with degradation of mature miRNAs, and as reported by Zeng *et al.*, (2004) degradation of the pre-miR before maturation can occur (154), though the mechanism is currently unknown. One mechanism of degradation of the microRNA precursors described is the degradation of the Let-7 family by Lin28/28b. This process which was described by Heo *et al.*, (196) demonstrates that Lin28/28b mediate the terminal uridylation of the let-7 precursors priming them for degradation. The means of this degradation was later demonstrated to be carried out by the terminal uridylyl transferase TUT4 (197, 198).

A large number of complexities which exist in the processes of microRNA biogenesis and function are not fully elucidated, resulting in a lack of understanding of the global effects on cellular homeostasis and disease.

1.2.10 MicroRNAs and cancer

Cancer is an intricate disease believed to originate primarily from genetic abnormalities both familial and acquired which lead to an alteration of normal cellular state. This leads to the loss of control of cell division and ability of cells to evade the immune system, resulting in initial tumour formation and eventually metastatic disease. It is evident that every cellular process is regulated in some means by microRNAs. With the pleiotrophic effects which microRNAs can have on the regulation of cell growth, cellular development, differentiation and apoptosis it is inevitable that dysfunction of these microRNAs would play a role in disease state.

Over 50% of microRNAs are transcribed from regions of the genome either deleted or amplified in at least one cancer, indicating differential expression of these microRNAs may contribute to the initiation or maintenance of disease state (199). The first association between microRNA levels and cancer was made with the discovery that miR-16 and miR-15 mapped to a region of genomic deletion in Chronic Lymphatic Leukemia (CLL). This deletion has been observed in over 50% of the cases (200) and both miR-15 and miR-16 were subsequently shown to be down regulated in CLL. Ectopic up-regulation of these microRNAs in CLL cells *in vitro* induced apoptosis. This was directly attributed to inhibition of the anti-apoptotic gene *BCL-2*, confirming the role of miR-15 and miR-16 as tumour suppressors in CLL (201).

Since this original discovery there has been an explosion in this area of research. There are now a large number of microRNAs which have been successfully identified as either tumour suppressors or oncogenes in various types of cancers. Cancers documentated with aberrant microRNA expression profiles include leukemia (200), pancreatic (202),

colon (203), thyroid (204), lung (205), breast (206) , testicular (207) and neuroblastoma (208) .

1.2.11 MicroRNAs and neuroblastoma

The exact mechanism by which microRNAs exert their action on the initiation, dissemination and progression of cancer is still not fully understood. However, it is evident that they play a substantial role in the pathogenesis of many forms cancer. More specifically dysregulation of microRNAs has been widely reported in neuroblastoma. Here we summarize the most recent and most remarkable discoveries relating to microRNAs in neuroblastoma, and discuss the potential uses for microRNAs in the processes of tumour categorisation, diagnosis and therapeutic regimens.

A number of large scale studies on microRNA dysregulation in neuroblastoma have been carried out. The first such study was performed by Chen and Stallings in 2007. This pioneering study examined the differential expression of a number of microRNAs across clinical subtypes of neuroblastoma tumours. Their most notable discovery was the identification of a large number of microRNAs which were down regulated in the subgroup of *MYCN* amplified tumours (208). A number of later studies have since followed up with similar results, and also demonstrated that certain microRNAs are up-regulated in the presence of *MYCN* amplification. Overall this confirms that the transcription factor MYCN exerts a regulatory control on a large group of microRNAs in neuroblastoma (209-211). The exact mechanism by which MYCN exerts a repressor or activator function on these microRNAs has yet to be fully elucidated.

One possible mechanism was proposed in a study by Murphy *et al*, in 2009. They identified using chromatin immunoprecipitation that MYCN binds to a large number of promoters and CpG islands throughout the genome in neuroblastoma, with higher levels of binding occurring in the *MYCN* amplified state. Although this study confirms MYCN binding in the vicinity of a large number of miRNA loci (212), validation that this is the mechanism by which MYCN exerts control of these microRNAs will not be possible until the exact promoter region of each microRNA is annotated.

Previous work from this lab identified miR-184 as a microRNA significantly down-regulated in MNA tumours and demonstrated that over-expression of miR-184 in neuroblastoma induced a reduction in cell viability as a result of increased levels of apoptosis (208). This thesis identifies *AKT2* as the mRNA target responsible for this tumour suppressor effect of miR-184 *in vitro* and proposes that MYCN contributes to tumourigenicity, in part, through suppression of miR-184, leading to increased levels of *AKT2*. Therefore it is evident that MYCN provides a tumourigenic effect, in part, by protecting *AKT2* mRNA from degradation by miR-184, permitting this important pro-survival pathway to remain functional in neuroblastoma.

MicroRNA 29a was identified as being under-expressed in MNA tumours (209). Xu *et al.*, (2009) found it to act as a tumour suppressor by directly targeting B7-H3, a cell surface immunomodulatory glycoprotein which contributes to the processes of immune escape by inhibiting cells of the immune system such as T cells and natural killer cells (213). This indicates that MYCN functions via this microRNA to protect the tumour from identification and subsequent degradation by the immune system.

Aberrant methylation is well documented in cancer (214-217) and in neuroblastoma (218-221). This study has discovered a role for miR-152, another microRNA also down regulated in *MYCN* amplified tumours (209) and up-regulated in All Trans Retinoic Acid (ATRA) treatment of SK-N-BE cells as having a role in the epigenetic control of neuroblastoma cells. Here we demonstrate that ectopic up-regulation of miR-152 results in the down regulation of the DNA methyltransferase protein *DNMT1*. DNMT1 is responsible for the maintenance of methylation across the genome (222). It has also been established that miR-26a and miR-26b, also regulated by MYCN and up-regulated in ATRA treatment of SH-SY5Y (223), are predicted to target *DNMT3b*. These results suggest that MYCN contributes to high levels of methylation in neuroblastoma by exerting control over microRNAs which can target proteins involved in the maintenance of methylation.

A number of MYCN activated oncogenic microRNAs have been identified as playing a role in the progression of neuroblastoma. Bray *et al.*, (2009), identified 14 microRNAs over expressed in the MNA state. Among the over-expressed microRNAs was the miR-17-5p-92 cluster (miR-17-5p, -18a, -19a, -20a and -92), over-expression of which, was associated with poor overall survival ($P<0.009$) in neuroblastoma tumours (209) and drug resistance in neuroblastoma (224). A later group further demonstrated correlation between expression of the 17-5p cluster and its host gene *MIRHG1,* a gene which is associated with poor overall survival in neuroblastoma (225). Schulte *et al.*, (2010) (211), demonstrated that although the 17-5p cluster is induced by MYCN, levels of this microRNA cluster was more significantly associated with poor survival than MNA. This may be due to the fact that this cluster can also be induced by *c-MYC* which is highly

expressed in a subset of *MYCN* single copy neuroblastomas with poor prognosis (226). Targets of this cluster that have been functionally validated include the p21 tumour suppressor gene *CDKN1A* (224) the pro-apoptotic gene *BIM* (224) and Clusterin (*CLU*) (227).

Another oncogenic microRNA over-expressed in the *MYCN* amplified state is miR-421, which in turn results in the down regulation of *ATM* (Ataxia-telangiectasia mutated) a serine/threonine kinase, which that plays a central role in the maintenance of genomic integrity by activating cell cycle checkpoints and promoting repair of DNA double-strand breaks (228).

Schulte *et al.*, (2010) related a number of microRNAs to levels of TrkA, a major determinate of positive overall survival in neuroblastoma (Section 1.1.14.1). This study demonstrated that 6 microRNAs were positively correlated and 3 negatively correlated with *TrkA* levels both *in vivo* and *in vitro*. Of interest, miR-542-5p, a microRNA which has been associated with positive survival in a number of studies (209-211), was positively correlated with *TrkA* expression and miR-92, a neuroblastoma oncomiR (229) was negatively associated with *TrkA* levels in the same study (211).

As previously discussed, neuroblastoma exhibits a large number of genomic aberrations and a number of studies have examined the impact of these aberrations on microRNA expression. Welch *et al.*, (2007) (230) demonstrated that tumours harbouring a 1p deletion expressed low levels of miR-34a. MiR-34a is located on chromosome 1p and Welch and colleagues demonstrated that ectopic over-expression of this microRNA induces apoptosis and impedes cell proliferation in neuroblastoma. A number of papers have now been published examining the oncogenic functions of miR-34a in

neuroblastoma. Targets of miR-34a have been identified and validated, the most notable of these with regards to neuroblastoma being *E2F3* and *MYCN*. Other targets identified include *BCL2*, *CCND1* and *CDK6* (208, 231-233). MiR-34c, another member of this microRNA family, maps to a region of genomic instability in neuroblastoma on chromosome 11q and has been shown to have anti-proliferative effects in neuroblastoma (231). This thesis also presents data that demonstrates that another member of the miR-34 family, miR-34b is not expressed in a large percentage of the neuroblastoma tumours and is highly up-regulated in response to ATRA treatment of neuroblastoma cells.

Bray *et al.*, (2009) (209) concluded that DNA copy number alterations account for approximately 10% of miRNAs dysregulated in NB and further established a relationship between prognostically significant imbalances and microRNA expression levels. This study used aCGH to compare genomic losses and gains to miRNA expression. A total of 51 miRNA loci exhibited significant ($P<0.05$) differences in mean expression between tumours exhibiting a copy number alteration versus those with diploid status. Although it is well established, that genomic aberrations contribute to disease pathogenesis in neuroblastoma, the link between genomic alterations and miRNA expression had not been previously made. Of particular interest was the discovery that miR-29c, was down regulated in MNA tumours, despite the fact that it maps to a region of gain on chromosome 1p, commonly gained in MNA tumours. This data indicates that the effects of genomic DNA copy number change can be abrogated by some alternative mechanism; in this case regulation by the MYCN oncogene.

1.2.12 MicroRNAs and differentiation in neuroblastoma

The regulation of cell fate from stem cells to the various mature cells is an essential process in development, maintenance and growth. The process of cellular differentiation is a tightly controlled mechanism in place to control cellular developmental timing and has a major role in this process of cell fate specification. Differentiation is central to the pathogenesis of neuroblastoma as tumor cells are immature neural crest cells which have lost the ability to differentiate into mature neuronal cell types. Histopathological examination of tissue samples has demonstrated that NB tumours cells, with a greater degree of differentiation are associated with a better clinical outcome and degree of differentiation and has also been negatively correlated with MYCN status (49).

Under normal conditions MYCN is required for the proliferation of neural cells and subsequent mitotic degradation of MYCN allows cell cycle exit of neural cells and concurrently the commencement of differentiation (234). It has been proposed that *MYCN* amplification and the inability for MYCN degradation to occur may contribute to the inability of neuroblastoma cells to differentiate resulting in unchecked proliferation. Though this may sometimes be the case, there are however many *MYCN* non-amplified cell lines that do not respond to differentiation therapy suggesting this is not the only mechanism preventing differentiation of NB cells.

Differentiation and the regulation of neural stem cell fate is a tightly controlled by many processes (reviewed by Qu *et al.* (235)), and failure of any of the pathways involved may contribute to neuroblastoma pathogenesis. MicroRNAs are both specifically and highly expressed in the nervous system especially during development (reviewed by Li *et al.*, 2010 (236)), suggesting that these small non-coding RNAs may play a significant role

in neuronal development and cell fate specification. Elucidation of microRNA involvement in cell fate and differentiation will aid in our understanding of the underlying mechanisms that contribute to NB pathogenesis.

Two early studies demonstrated that microRNA profiles are significantly altered following induction of differentiation in neuroblastoma cells (208, 223). It has also been established that the down regulation of the transcription factor MYCN is an immediate effect of ATRA-induced differentiation in *MYCN* amplified cells (237). Therefore it' is not surprising that a number of MYCN-regulated microRNAs are altered in response to retinoic acid.

As previously discussed a number of the MYCN regulated microRNAs have been demonstrated to be down regulated after ATRA treatment. Loven *et al.,* (2010) (238) established that MYCN induced microRNAs miR-18a and 19a, target the estrogen receptor alpha 1 (ESR1) resulting in the inability of neuroblastoma cells to undergo differentiation. Subsequent inhibition of miR-18a resulted in differentiation of neuroblastoma cells as measured by extensive neurite outgrowth. The oncogenic MYCN enhanced 17-92 cluster was also shown to be down regulated in retinoic acid treated neuroblastoma cells and consequently a number of the tumour suppressor targets of these microRNAs were up-regulated (239).

As discussed in Section 1.1.16, retinoic acid treatment is a part of the therapeutic regimen in certain neuroblastoma patients. As a differentiation agent, retinoic acid is less toxicity than conventional cancer treatments. Unlike chemotherapy, which fundamentally works by inducing death of the tumourgeneic cells, differentiation therapy works by inducing tumour cells to resume the process of maturation. Although differentiation

therapy does not destroy the cancer cells, it restricts proliferation, allowing the application of more conventional methods to eradicate the malignant cells. A number of tumour suppressor microRNAs which may contribute to this process have also been identified through differentiation studies of neuroblastoma cells *in vitro* in the present study.

Laneve *et al.*, (2007) (223) examined the functional effects of the ectopic up-regulation of three ATRA-induced microRNAs: miR-9, miR-125a and miR-125b in neuroblastoma cells. When up-regulated in these cells all three microRNAs induced a reduction in cell proliferation and anti-sense knockdown of all three was able to counteract the slow down effect that retinoic acid has on cell growth. The truncated form of the neurotrophin receptor tropomyosin-related kinase C (t-TRKc) was validated as a common target to all three. A further study showed that ectopic over-expression of miR-125b contributed to induced neurite outgrowth (240). Laneve *et al.* (241) have more recently published a paper demonstrating that miR-9 is suppressed in undifferentiated cells by binding of RE1 silencing transcription factor (REST) to its promoter.

Chen *et al.* (2010) (242), reported that two more ATRA-altered microRNAs, miR-7 and miR-124, contribute to a differentiated phenotype. MiR-7 which is down regulated in SH-SY5Y cells in response to ATRA reduces the ability of these cells to undergo ATRA-induced differentiation when ectopically over-expressed *in vitro*. This results suggests that down-regulation of miR-7 is essential for the induction of retinoic acid-induced differentiation to occur. This study also identifies that ectopic expression of ATRA-induced miR-124 *in vitro*, results in an increase in neurite outgrowth. MiR-128 is another microRNA which has been demonstrated to be up-regulated in ATRA-treated

neuroblastoma cells and ectopic over-expression of this microRNA lead to reduced cell motility and invasiveness through the down-regulation of target mRNAs, *DCX* and *Reelin*.

It is evident therefore that altered expression of microRNAs contribute to the differentiation-induced phenotype. This remains a highly complex and poorly understood process and further understanding of microRNA function neuronal cell development and differentiation is required to obtain the overall picture.

1.2.13 MicroRNAs as therapeutic targets and diagnostic markers

MicroRNAs can potentially target a large number of mRNA sequences. Because of relaxed complementarity requirements in animals, the use of microRNAs as therapeutic targets may prove unpredictable due to off-target binding effects. Despite this concern many microRNA have proved to be highly successful in animal models for disease treatment (243-245).

The idea behind the use of microRNAs as therapeutic molecules is the loss of function theory. This works on the premise that if a microRNA is deleted in a tumour, its removal is contributing to the carcinogenic phenotype and replacing it will activate tumour suppressing pathways. With the advent of specific targeted delivery mechanisms such as adenoviruses (246) and nano-particles (247) we may in time hone the ability to use microRNAs as therapeutics.

The use of anti-sense molecules for targeting oncogenic or disease causing microRNAs has great potential for the future of disease treatments. An inhibitor of microRNA miR-122 is currently being used in human clinical trials for the treatment of the

Hepatitis C virus. This clinical trial came about as this inhibitor of miR-122 demonstrated major success in preventing the replication of this virus in chimpanzees (248).

Several studies have reported the use of miRNA profiles as potential diagnostic/prognostic signatures in cancer. Colorectal cancer is a difficult cancer to diagnose with highly invasive tests required to confirm diagnosis. Recent work has shown that endogenous plasma miRNAs exist in a form that is resistant to plasma RNase activity (249). The same study showed high correlation between miRNA levels in plasma and serum, indicating that both were suitable for investigations of miRNAs as blood-based biomarkers. More specifically, the up-regulation of certain miRNA has been reported in colorectal cancer (250), and expression patterns of microRNAs are systematically altered in colon adenocarcinomas (251). One study has demonstrated a similar pattern of differential expression of microRNAs in plasma and tumour of colorectal cancer patients (252). CRC was the first cancer to be used as a model for the detection of tumour-related microRNAs in the serum, and this research paves the way for a sensitive, rapid and minimally invasive blood test for CRC and other cancers.

1.2.14 Use of microRNAs in tumour classification

It is evident from a number of studies that microRNAs are potential prognostic markers in neuroblastoma. As previously discussed, further classification of neuroblastoma tumours is essential, not only to determine prognosis but also for the selection of appropriate therapy. As neuroblastoma is a pediatric cancer, it is imperative that we consider the effects of harsh therapeutics on patient well-being and future development. For example, most patients with high stage tumours receive intensive multi-drug treatment.

There is evidence however, that microRNAs expression signatures have the potential to refine patient stratification prior to therapy.

Buckley *et al.* (83) demonstrated using a previously published miR-signature (209) that 11q- tumours could be split into two distinct sub groups with significantly different clinical outcome. They determined that these sub-groups also differed in the number of segmental genomic imbalances (83), which is consistent with recent reports showing the overall pattern of genomic imbalances is highly predictive of clinical outcome in neuroblastoma (253, 254). As 11q- tumours are usually considered high risk, improved stratification of this subgroup will allow for better treatment selection by detecting patients who require a less intense therapeutic regimen from those still in need of more intense and invasive intervention.

1.3 Aims and significance of this study

Large scale profiling studies have indentified differential expression of microRNA across neuroblastoma subtypes. The dysregulation of these microRNAs can be associated with clinical parameters such as expression of known oncogenes and tumour suppressors, stage, age, differentiation status and genomic imbalances. This knowledge is now contributing to more accurate categorisation and diagnosis, as well as potential novel therapeutic applications for this disease.

Treatment regimens for high risk neuroblastomas involve intensive, multi-modal chemotherapy, often resulting in only short-term effects. In order to improve treatment we need a better understanding of the molecular characteristics controlling pathogenesis and progression.

Neuroblastoma cells can be induced to undergo differentiation *in vitro* when treated with ATRA, and are often used as a model system to study biochemical pathways and disease pathogenesis. The aim of this study is to further elucidate the role of microRNAs in neuroblastoma pathogenesis by performing a detailed functional analysis of microRNAs responsive to ATRA treatment.

Chapter 2.0

Materials and Methods

Chapter 2

Materials and Methods

2.1 Preparation for cell culture

2.1.1 Water

Ultrapure water was used in the preparation of all media and 1x solutions. Pre-treatment, involving activated carbon, pre-filtration and anti-scaling was first carried out. The water was then purified by a reverse osmosis system (Millipore Milli-RO 10 Plus, Elgastat (UHP)). This system is designed to produce purified water from a suitable municipal water supply. The system utilises a semi-permeable reverse osmosis membrane to remove contaminants from the feed water. This results in water which is low in organic salts, organic matter, colloids and bacteria with a standard of 12-18 MΩ/cm resistance.

2.1.2 Glassware

Solutions pertaining to cell culture and maintenance were prepared and stored in sterile glass bottles. Bottles (and lids) and all other glassware used for any cell-related work were prepared as follows; all glassware and lids were soaked in a 2% (v/v) solution of RBS-25 (AGB Scientific) for at least 1 hour. This is a de-proteinising agent which removes proteinaceous material from the bottles. Following scrubbing and several rinses in tap water, the bottles were washed twice by machine (Miele G7783 washer/disinfecter) using Neodisher GK detergent and sterilised by autoclaving. Waste

bottles containing spent medium from cells were autoclaved, rinsed in tap water and treated as above.

2.1.3 Sterilisation

Water, glassware and all thermostable solutions were sterilised by autoclaving at 121°C for 20min under 15 p.s.i. pressure. Thermolabile solutions were filtered through a 0.22μm sterile filter (Millipore, millex-gv, SLGV-025BS). Low protein-binding filters were used for all protein-containing solutions. Acrodisc (Pall Gelman Laboratory, C4187) 0.8/0.2μm filters were used for non-serum/protein solutions.

2.2 Routine management of cell lines

2.2.1 Safety precautions

All routine cell culture work was carried out in a class II down-flow re-circulating laminar flow cabinet (NuAire Biological Cabinet). Any work which involved toxic compounds was carried out in a cytoguard (Gelman). Strict aseptic techniques were adhered to at all times. Both laminar flow cabinets and cytoguards were swabbed with 70% ethanol (ETOH) before and after use, as were all items used in the experiment. Each cell line was assigned specific media and waste bottles and only one cell line was manipulated at a time in the cabinet which was allowed to clear for 15min between different cell lines. The cabinet itself was cleaned each week with industrial detergents (Virkon, Antec. International; TEGO, T.H.Goldschmidt Ltd.), and then wiped down with 70% ETOH, as were the incubators. A separate laboratory coat was kept for aseptic work and sterile nitrile gloves (Fisher, FB6921) were worn at all times during cell work.

2.2.2 Cell lines

All cell lines used throughout this study originated from neuroblastoma patients. The cell lines used, their sources and their basal media requirements are listed in Table 2.1. Lines were maintained in 25cm^2 flasks (Fisher, TKV-123-011R), 75cm^2 flasks (Fisher, TKV-123-031L) or 175cm^2 flasks (Fisher, TKT-130220Q) at 37°C and fed every two days. Cells were routinely cultured in antibiotic to prevent contamination of experiments with bacteria; the antibiotic used was alternated between Pencillin/Streptomycin and Gentamicin every 2 months to avoid resistant strains of bacteria

Table 2.1. Cell lines used in study

Cells lines, the source of origin and the basal media required for culture.

Cell Line	Source	Media*
SKNAS	ATCC	EMEM
KELLY	ECCC	RPMI
SKNBE	ATCC	MEM and F12
SH-SY5Y	ATCC	MEM and F12
SHEP-TET21	Dr. Jason Shohet	RPMI

ATCC = American Tissue Culture Collection
ECCC = European Collection of Cell Culture
*All media was supplemented with 10% FBS and 2mM L- Glutamine, MEM and F12 also contained Non Essential Amino Acids.

2.2.3 Subculture of adherent lines

During routine sub-culturing or harvesting of adherent lines, cells were removed from their flasks by enzymatic detachment. Following aspiration of waste medium, cells were rinsed with pre-warmed PBS (Phosphate buffered saline) made up using 1 PBS tablet (Sigma, P4417) in every 100mls (37°C). The purpose of this was to remove/inhibit any naturally occurring trypsin inhibitor which would be present in residual serum. Fresh trypsin/EDTA (Biosciences, 25300-054) was then pipetted onto the cells (2.5ml/25cm^2 flask, 7ml/75cm^2 flask or 10ml/175 cm^2 flask) and the flasks incubated at 37°C until the cells were seen to have detached (5 min). The trypsin was deactivated by addition of an equal volume of growth medium (i.e. containing 5% serum). The entire cell suspension was transferred to a 15ml or 50ml tube (Fisher Scientific CFT-420-075L, CFT-645-010C) and centrifuged at 1,200 rpm for 3 min. The resulting cell pellet was re-suspended in pre-warmed (37°C) fresh growth medium, counted (Section 2.2.4) and used to re-seed a flask at the required cell density or to set up a given assay.

2.2.4 Cell counting

1 Cell counting and viability determinations

2 Samples were trypsinised (Section 2.2.3) and transferred to a 15ml tube (Fisher Scientific CFT-420-075L) then centrifuged at 1,200 rpm for 3 min. The resulting pellet was re-suspended in 1ml of pre-warmed (37°C) fresh growth medium, from which 10µl was taken and loaded onto a haemocytometer (Neubauer).

3 Cells in the 16 squares of the four outer corner grids of the chamber were counted microscopically. An average number per corner was calculated with

the dilution factor being taken into account and final cell numbers were multiplied by 10^4 to determine the number of cells per ml. The volume occupied by the sample in the chamber is 0.1cm x 0.1cm x 0.01cm i.e. $0.0001cm^3$ (therefore cell number x 10^4 is equivalent to cells per ml).

2.2.5 Freezing cell stocks

To allow long term storage of cell stocks, cells were frozen and cryo-preserved in liquid nitrogen at temperatures below –180°C. Once frozen properly, such stocks should last indefinitely.

1. Cells to be frozen were harvested in the log phase of growth (i.e. actively growing and approximately 50 - 70% confluent) and counted as described in Section 2.2.4.
2. Pelleted cells were re-suspended in freezing media consisting of DMSO/serum (1:9, v/v) (Sigma, D2650). This solution was slowly added drop wise to the cell suspension to give a final concentration of at least $5x10^6$ cells/ml. (This step was very important, as DMSO is toxic to cells. Adding DMSO slowly gives the cells time to adjust to the DMSO and prevent cell lysis occurring).
3. The suspension was aliquoted into cryovials (Fisher, CRY-100-021F) which were quickly placed in the vapour phase of liquid nitrogen containers (approximately -80°C). After 2.5 to 3.5 h, the cryovials were lowered down into the liquid nitrogen where they were stored until required.

2.2.6 Cell thawing

Due to the sensitivity of cells, thawing must be carried out quickly but carefully ensuring cells are acclimatised gradually to 37°C.

1. Immediately prior to the removal of a cryovial from the liquid nitrogen stores for thawing, a sterile universal tube containing growth medium was prepared for the rapid transfer and dilution of thawed cells to reduce their exposure time to the DMSO freezing solution which is toxic at room temperature.
2. The cryovial was removed and thawed in the water bath.
3. When almost fully thawed, the DMSO-cell suspension was quickly transferred to the media-containing universal.
4. The suspension was centrifuged at 1,200 rpm. for 3 min, the DMSO-containing supernatant removed, and the pellet re-suspended in fresh growth medium.
5. Thawed cells were then placed into 25cm^2 tissue culture flasks with 7mls of the appropriate type of medium and allowed to attach overnight.
6. After 24 h, the cells were re-fed with fresh medium to remove any residual traces of DMSO.

2.2.7 Mycoplasma analysis

Mycoplasma has long been recognised as common contaminants of cells in continuous culture. To prevent interference with experimental results mycoplasma examinations were carried out routinely (at least every 3 months) on all cell lines used in this study.

2.2.7.1 Mycoplasma testing procedure

For this procedure, MycoAlert® Mycoplasma Detection Kit (Lonza, Rockland USA) was used. MycoAlert® causes the lysis of mycoplasma. The MycoAlert® substrate then reacts with mycoplasmic enzymes catalysing the conversion of ADP to ATP.

1 600µl of MycoAlert® Assay buffer was added to the vial of MycoAlert® Reagent and mixed gently. This was then left to equilibrate at room temperature for 15minto ensure complete rehydration.

2 600µl of MycoAlert® Assay buffer was added to the vial of MycoAlert® substrate and mixed gently. This was then left to equilibrate at room temperature for 15minto ensure complete rehydration.

3 Media was removed from a confluent flask of cells and transferred into 15ml tube and centrifuged at 1,500rpm for 5 min.

4 100µl of supernatant culture media was transferred to a luminometer tube for use in the procedure.

5 The luminometer was programmed to take a 1 second integrated reading.

6 100µl of MycoAlert® reagent was added to each sample and allowed incubate at room temperature for 5 min.

7 Samples were then placed in the luminometer and read (Reading 1)

8 100µl of MycoAlert® Substrate was added to each sample and was left to incubate for 10 min.

9 Samples were placed in luminometer and read (Reading 2)

10 The ratio reading of reading 2/reading 1 was calculated. Cells infected with Mycoplasma will routinely produce results ratio greater than 1.

11 Any samples with a result of borderline 1 were retested again after 24 h.

2.3 Specialised techniques in cell culture

2.3.1 Assessment of cell numbers - acid phosphatase assay

1 Cells were plated in a 96 well plate (Fisher, TKT-521-110p). Following the incubation period, determined by the given experiment media was removed from the plates.

2 Each well on the plate was washed with 100µl PBS. This was removed and 100µl of freshly prepared phosphatase substrate (10mM p-nitrophenol phosphate (Sigma 104-0) in 0.1M sodium acetate (Sigma, S8625), 0.1% triton X-100 (BDH, 30632), pH 5.5) was added to each well. The plates were wrapped in tinfoil and incubated in the dark at 37°C for 2 h.

3 The enzymatic reaction was stopped by the addition of 50µl of 1M NaOH to each well.

4 The plate was read in a dual beam plate reader at 405nm with a reference wavelength of 620 nm.

2.3.2 Assessment of apoptosis

2.3.2.1 Caspase 3/7 activity

Apoptosis was measured using the Caspase Glo®3/7 assay (Promega G8091). This is a luminescent assay that measures caspase 3 and caspase 7 activities. Cells for this assay were set up in a 96 well white walled luminometer plate (Perkin Elmer). Cells were assayed 72h after set-up. Caspase-Glo® Buffer was added to the Caspase-Glo® Substrate and 100µl of reagent added to each well. The plate was then mixed and incubated at room temperature for 2 h. Luciferase activity was recorded using a Wallac plate reader (Perkin Elmer) and the background read (a well containing just media) was

deducted from the experimental sample. The level of luminescence observed was proportional to the level of caspase activity.

2.3.2.2 Annexin V staining

Annexin V staining was used as a means of validating caspase assay results.

1 Cells were plated in a 6 well plate (Fisher, TKT-520-090B) and incubated for 72hr. Media was removed from the cells, transferred to a 15ml tube and centrifuged at 8,000rpm for 3 min. This was done to ensure retention of apoptotic cells in the media. The excess media was removed leaving the cell pellet in the tube.

2 Attached cells were detached using trypsin. An equal amount of culture media was added and the cells were transferred into the 15ml tube containing the pellet from step 1 and centrifuged gently at 500rpm. Media was removed and discarded.

3 The pellet was re-suspended and washed X 3 in 1% bovine serum albumin (BSA).

4 Apoptosis was measured using the FITC (Fluorescein Isothiocyanate) Annexin V Apoptosis Detection Kit I (BD Biosciences 556547). This kit functions by detecting apoptotic cells via staining with propidium iodide (PI) dye and Annexin V FITC labeled antibody.

5 Cells were re-suspended in 1X binding buffer at a concentration of $1X10^6$.

6 100µl of cells was placed in a 15ml tube.

7 5µl of FITC stain and 5µl of PI stain was added to each sample. A non-stained control, a FITC only control and a PI only control were used for calibration. Cells were vortexed gently and left in the dark at room temperature for 15min.

8 400µl of 1 X binding buffer was added to each sample.

9 Each sample was then run on the BD Facs Aria and analysed for apoptosis. FITC/PI positive cells were considered to be either undergoing or to have undergone apoptosis.

2.3.3 All Trans Retinoic Acid (ATRA) treatment of cells

All-Trans Retinoic Acid stock solution of 5µm was made up in methanol. Stocks were stored at -20°C. Cells were sub-cultured as described in Section 2.2.3. As SK-N-BE neuroblastoma cells had previously been reported to be responsive to ATRA they were used for all ATRA experiments through out this thesis. Cells were plated at a cell concentration of $8X10^5$cells/ml), SK-N-BE cells were seeded in a T25 culture flask (5ml, final cell number $4X10^6$ cells and 6 well plates (1ml per final concentration of $8X10^5$cells Cells were allowed settle for one day, after this the media was replaced everyday with SK-N-BE culture media (Table 2.1) containing 5µmol of ATRA. Cells were harvested for protein and RNA at Day 0, Day 3 and Day 7.

2.3.4 SH-EP21N neuroblastoma cell line

The Tetracycline Controlled Transcriptional Activation (TET) system was originally developed in the University of Heidelberg by Professors Bujard and Gossen (255). This system of repressible expression allows reversible transcription in the presence of the antibiotic Tetracycline. The SHEP-Tet 21system cell line used in our experiments has been used in the past to detect transcriptional targets of the neuroblastoma oncogene MYCN (256). This cell line uses the Tet-off system and therefore expresses high levels of MYCN in the untreated state. Cells were cultured for approximately two weeks in media made up with tetracycline free fetal bovine serum

in order to normalise levels of MYCN. The cells were then treated with a final of concentration of 50ng/ml of Doxycycline (Dox), a derivative of tetracycline, in order to turn off MYCN expression. This process was validated using Taqman RTqPCR and western blotting (Section 3.1.2).

2.3.5 Invasion assay

2.3.5.1 Preparation of invasion chambers

Invasion assays were carried out using BD BioCoat™ Growth Factor Reduced (GFR) MATRIGEL™ Invasion Chambers (BD Biosciences, 354483). Inserts were rehydrated as specified by manufacturer's protocol. Cell suspensions were prepared in culture media containing 5% Foetal Calf Serum (FCS) at a concentration of $1X10^6$ cells /ml. 500µl of media containing the same concentration of was added to the well of the BD Falcon™ TC Companion Plate. 100µl of cell suspension was then added into the insert. The invasion assays were then incubated for 48h at 37°C, 5% CO_2 atmosphere.

2.3.5.2 Removal of non-invading cells

After incubation, the non-invading cells were removed from the upper surface of the membrane. The inner side of the insert was wiped with a wet swab (PBS soaked not UHP) while the outer side of the insert was stained with 0.25% crystal violet for 10 and then rinsed in UHP and allowed to dry. Inserts were then viewed under the microscope.

2.3.5.3 Counting of invading cells

Cell counting was facilitated by photographing the membrane using an inverted microscope. The cells were observed at 200X magnification. Cells in the central fields of duplicate membranes were counted and an average count calculated from 10 counts per chamber. Data was expressed as the percentage invasion through the GFR Matrigel^{TM} matrix membrane relative to the migration through the control membrane.

2.3.6 Soft agar assay - colony forming efficiency

A sterile 1% agarose solution (1g of agar in 100ml of ultra pure water) was melted immediately prior to use and plated on a 10cm^2 petri dish until the plate was completely covered. 1.5X10^6 cells in 10mls of culture media was added to the plate. Media was replaced every 4-5 days, for 21 days. Colonies were stained with 0.1% crystal violet. Plates were photographed; colonies were counted in replicate studies and counts normalized to the negative scrambled control.

2.4 MiRNA and siRNA transfection optimisation

2.4.1 Optimisation for a 96-well plate

In order to determine the optimal conditions for miRNA and siRNA transfection in 96-well plates, transfections with a siRNA against kinesin (Ambion Inc., 16704) was carried out for each cell line. Kinesin is a motor protein which is involved in mitotic cell division, knocking out kinesin causes a termination in cell division and hence the level of cessation is representative of the transfection efficiency. Cell suspensions were prepared at 1x10^4, 2.5x10^4, 5x10^4, 5x10^4, 1x10^5, 2.5x10^5 and 5x10^5 cells per ml. Solutions of negative control siRNA (Ambion Inc., AM4636) and

kinesin siRNAs at a final concentration of 10nM were prepared in optiMEM (Gibco™, 31985). NeoFX solutions at a range of concentrations (from 1µl to 6µl) were prepared in optiMEM in duplicate and incubated at room temperature for 10 min. After incubation either the negative control or kinesin siRNA solution was added to each NeoFX concentration. These solutions were mixed well and incubated for a further 10min at room temperature. Replicates of 10µl of the siRNA/neoFX solutions were added to a 96-well plate. The cell suspensions were added to each plate at a final cell concentration of $1x10^3$, $2.5x10^3$ and $5x10^3$ cells per well. The plates were mixed gently and incubated at 37°C for 24h. After 24h, the transfection mixture was removed from the cells and the plates were fed with fresh medium.

The plates were assayed for changes in proliferation at 72h using the acid phosphatase assay (Section 2.3.1). Optimal conditions for transfection were determined as the combination of conditions that gave the greatest reduction in cell number after kinesin siRNA transfection and also the least cell death in the presence of transfection reagent. The optimised conditions for the cell lines are shown in Table 2.2.

Table 2.2. Optimised conditions for miRNA/siRNA transfection in 96-well plates

Cell line	Seeding density per ml	Volume NeoFX per well (µl)
Kelly	$3*10^4$	0.5µl
SKNAS	$3*10^4$	0.5µl
SKNBE	$5*10^5$	0.5µl

2.4.2 Optimization for a 6-well plate

To determine the optimal conditions for miRNA/siRNA transfection in 6-well plates, an optimisation with a siRNA for GAPDH (Ambion Inc., AM4605) was carried

result was validated using the acid phosphatase assay (Section 2.3.1) in a 96 well plate following optimal transfection conditions as described in Section 2.4.1.

2.4.4 Invasion effects of miRNA transfection

Transfections were carried out in 6-well plates using optimised conditions described in Section 2.4.2. 48h after transfection cells were used in invasion assays (Section 2.3.5).

2.4.5 Effects of miRNA transfection on colony forming ability of cells

Transfections for soft agar were carried out in a 6 well plate using optimised conditions as described in Section 2.4.2. After 24h the cells were trypsinised and set up in a soft agar assay as described in Section 2.3.6.

Table 2.4 MiRNA Pre-miRs and Anti-miRs used in this study

Target name	Ambion IDs
Negative Control 1	AM171110
miRNA-184	PM10207
miRNA-10a	PM10787
miRNA-10b	PM11108
miRNA-152	PM12269
miRNA-196a	PM10068
Anti-miR Negative Control 1	AM17010
Anti-miR 184	AM10207
Anti-miR 10a	AM10787
Anti-miR 10b	AM11108
Anti-miR 152	AM12269
Anti-miR 196a	AM10068

Table 2.5. SiRNAs used in this study

Target name	Ambion IDs
AKT2	S1215
AKT2	S1216
AKT2	S1217
NCOR2	S18467
NCOR2	S18468
NCOR2	S18469
siRNA Negative Control	AM4611

2.5 Plasmid DNA manipulation

Plasmid vectors were used for expression of both miRNAs and protein coding genes in cell systems. Vector Maps of all plasmids are listed in Appendix 1. PcDNA3-AKT2 was a kind gift from Prof. Joe Testa (Fox Chase Cancer Centre, Philadelphia).

Table 2.6. Expression plasmids used in this study

Plasmid	Supplier	Catalogue No.
pcDNA6.2–GW/EmGFP	Invitrogen	V4930001
pcDNA6.2–GW/EmGFP Negative Control	Invitrogen	V4930001
pMIR-REPORT™ miRNA Expression Vector	Ambion	AM5795
pMIR-REPORT™ miRNA β-Gal Control Vector	Ambion	AM5795
pcDNA-3_AKT2	Prof Joe Testa	N/A
psiCHECK™-2 Vector	Promega	C8021

2.5.1 Cloning of the miR-184 stem-loop

The stem loop precursor sequence of miR-184 was cloned into the pcDNA6.2-GW/EmGFP expression vector (BLOCK-iT Pol II miR RNAi Expression Vector kit, Invitrogen) to generate a miR-184 stem-loop expressing plasmid. This is a linearised Cytomegalovirus (CMV) driven vector, which is designed to facilitate unproblematic cloning of microRNA expressing oligonucleotides (oligos) 3' of the promoter. Oligonucleotides were designed which encode the sense and antisense strands of the pre-miR184 stem loop sequence (Figure 2.1). These oligonucleotides were designed to include the appropriate 5' and 3' (bold and red) overhangs to facilitate cloning into the linearised pcDNA6.2-GW/EmGFP vector (supplied within the BLOCK-iT kit, Invitrogen).

(a) Pre-miR184 Sense strand:

TGCTGCCAGTCACGTCCCCTTATCACTTTTCCAGCCAGCTTTGTGACTGTAA

GTGTTGGCAGGAGAACTGATAAGGGTAGGTGATTGA

(b) Pre-miR184 Antisense strand:

CCTGTCAATCACCTACCCTTATCAGTTCTCCTGCCAACACTTACAGTCACAA

AGCTGGCTGGAAAAGTGATAAGGGGACGTGACTGGC

Figure 2.1 Oligos for the pcDNA6.2-GW/EmGFP-miR-184 stem-loop vector. The stem loop precursor sequence of miR-184 was cloned into the pcDNA6.2-GW/EmGFP expression vector (BLOCK-iT Pol II miR RNAi Expression Vector kit, Invitrogen) Oligonucleotides were designed which encode the sense and antisense strands of the pre-miR184 stem loop sequence (Figure 2.1). These oligonucleotides were designed to include the appropriate 5' and 3' (bold and red) overhangs to facilitate cloning into the linearised pcDNA6.2-GW/EmGFP vector.

2.5.2 Cloning of pMIR-REPORT™ luciferase reporter vector

The pMIR-REPORT™ luciferase reporter vector (Ambion) was used as the backbone in the miR-184-AKT2 target experiments. A 76nt long region of the 3'UTR of *AKT2* containing the predicted miR-184 binding site (underlined and in pink) was designed with ligation sites appropriate for the pMIR REPORT™ vector (SPE1 5' on the sense strand, shown underlined and green, and HIND III 5' on the anti-sense strand, not shown). These oligos were synthesised by Sigma. A cut site unique to this sequence (B1pI, underlined and blue) and not in the multiple cloning site of the vector was also introduced into this sequence; to be used to determine efficient oligo insertion into the plasmid. A negative control vector was also designed; three mutations (lower case and yellow) were introduced into the seed region of miR-184 binding site of this sequence. The rest of the insert remained exactly as described above.

(a) Insert miR-184 target sequence

5'CTAGTCCTCTGTGTGCGATGTTGTTATCTGACAGTTCTCCGTCCCTACTGG

CCTTTCTCCTCGTCTTCGCTCAGCA 3'

(b) Insert miR-184 mutated target sequence

5'CTAGTCCTCTGTGTGCGATGTTGTTATCTGACAGTTCTtCaaCCCTACTGGC

CTTTCTCCTCGTCTTCGCTCAGCA 3'

Figure 2.2 Oligos for miR-184 binding site in the 3'UTR of *AKT2*. (a)The 3'UTR of *AKT2* containing the predicted miR-184 binding site (underlined and in pink) containing ligation sites appropriate for the pMIR REPORT™ vector (SPE1 5' on the sense strand, shown underlined and green, and HIND III 5' on the anti-sense strand, not shown). These oligos were contained a cut site unique to this sequence (B1pI, underlined and blue) and not in the multiple cloning site of the vector to be used to determine efficient oligo insertion into the plasmid. (b) A negative control vector was also designed; three mutations (lower case and yellow).

2.5.3 Annealing of oligonucleotides

Oligonucleotides were re-suspended at the same molar concentration in annealing buffer (Table 2.7). Equal amounts of complimentary oligos were added together in a 1.5ml eppendorf tube and incubated at 95°C for 5 min, after which the heat block containing the samples was removed from the apparatus and allowed to cool to room temperature (or at least 30°C) for 1hr. 2µl of each single strand (+5µl loading dye) and 10µl annealed product (+5µl loading dye) were run on a 1% agarose gel, to ensure ligation had occurred, as seen for miR-184 stem-loop annealed oligos (Figure 2.3).

Figure 2.3 Annealed miR-184 oligos for pcDNA6.2 Vector. This image demonstrates efficient annealing of oligo strands occurred (lane 3).

Table 2.7. Recipe for annealing buffer

Component	Volume
Tris, pH 7.5–8.0	10Mm
NaCl	50Mm
EDTA	1mM

2.5.4 Restriction enzyme digestion

All restriction digests were carried out using fast restriction enzymes from Fermentas. All components (Table 2.8) were mixed together in an eppendorf. The samples were mixed gently, centrifuged and then incubate at 37°C in a heat block or water thermostat for 5 min.

Table 2.8. Restriction digest

Component	Volume (µls)
Purified Vector DNA	2
Buffer	2
Enzyme 1 (e.g. Hind III)	1
Enzyme 2 (e.g. Spe1)	1
dH20	4

2.5.4.1 Confirmation of digestion

The pMIR-REPORT™ Vector was cut using Spe1 and HindIII and the sample was then run on a 1% agrose gel, to ensure that the cut had occurred. The higher weight band (size 6408kb) representing the MCS-excised, was then extracted from the gel. DNA was purified using the Qiagex II Gel Extraction Kit (Qiagen, 20021) as described in Section 2.5.5. This step was taken to ensure that the region of the multiple cloning site was removed completely preventing re-ligation to the vector in future experimental steps.

2.5.5 Qiagen Gel Extraction

Using a clean sharp scalpel the DNA band was excised from the gel and placed in a clean 1.5ml eppendorf tube. The gel extract was weighed and then solubilised by addition of 3 volumes of QX1 buffer to 1 volume of gel (e.g. 300µl of buffer to 100mg of gel extract). This buffer has a high salt content which causes disruption of the agarose and the subsequent disassociation of DNA binding proteins from the DNA fragments. The sample was vortexed for 30secs and then incubated at 50°C for 10min. During the incubation period the sample was vortexed every 2min to ensure adequate

mixing. After the incubation period the sample was centrifuged for thirty seconds and the supernatant discarded. The pellet was then washed to ensure removal of all salt contaminants. The sample was washed and re-suspended by vortexing in 500µl of buffer PE. The sample was centrifuged for 30secs, the supernatant removed and the wash step repeated. The pellet was then air dried for 10-15min or it turned white in colour. The DNA was eluted in 20µl of 10mM Tris-cl ph8.5, centrifuged for 30 seconds. The supernatant containing the purified DNA was placed in a separate tube, quantified using the Nanodrop and stored at -80°C until required for further use.

2.5.6 Ligation of annealed oligonucleotides into vector

The annealed oligos were ligated into the vector downstream of the luciferase gene. Ligation was carried out using the recipe below (Table 2.9). A negative control with dH_20 instead of insert DNA was also included. Various ligations were carried out to determine the optimum insert to vector ratio. A 2:1 ratio was determined optimal. All components of the ligation were added together in a tube and vortexed lightly and ligation was carried out overnight at room temperature. After incubation the samples were heated at 75°C for 5min to stop the reaction.

Table 2.9. Ligation recipe

Component	Volume (µls)
DNA Annealed Insert (400ng/µl)	2
Vector (200ng/µl)	2
10x Ligation Buffer	1
T4 Ligase	1
dH20	4

2.5.7 Restriction enzyme digestion of plasmid DNA

5µl of each isolated plasmid sample was electrophoresed on a 2% agarose gel to check for degradation. A restriction digestion was then carried out to confirm orientation of the insert, using the insert specific cut site. All digestions were carried out using the recipe as outlined in Table 2.8, using just one cut enzyme and increasing the amount of H_20 accordingly.

The samples were run on a 1% agarose gel, together with 3µl loading dye. From the banding patterns observed, the orientation of the insert was correctly discerned. From this information, samples were selected for large-scale plasmid preparation.

2.5.8 PsiCHECK2 vector cloning

For all luciferase experiments carried out using the psiCHECK™-2 vector all inserts for each gene containing the microRNA target sequence of interest or the microRNA mutated target sequence were designed in house. The oligo designs and the vector were sent to MWG who synthesized the oligos, generating the plasmid-oligo construct. For this vector large sections of the 3'UTR of the gene of interest containing the microRNA target sites were used. These sequences and the mutated sequences can be found in Appendix 2.

2.6 Microbiology

2.6.1 Transformation of bacteria

50µl of competent One Shot® E.coli bacterial competent cell suspension (Invitrogen, C4040-10) was mixed with 20ng DNA and placed on ice for 30min. After incubation the mixture was heat-shocked at 42°C for 45 sec and then placed on ice for 2 min. Then 250µl of pre-warmed (37°C) S.O.C media (Sigma, S1797) was added to the

competent cell suspension and incubated at 37°C for 1hr. 50µl and 100µl of this suspension was spread on ampicillin (AMP) (Sigma A6140) selecting agar plates (Table 2.10), and incubated overnight at 37°C.

Single colonies, which grew on these selecting plates, were further streaked onto another selecting plate and allowed to grow overnight at 37°C.

Table 2.10 LB (Lysogeny broth)/agar recipe

Component	Supplier	Catalogue no.
1 litre H_2O	NA	NA
10g Bacto-tryptone	Sigma	93697
5g yeast extract	Sigma	Y1625
10g NaCl	Sigma	S3014
*15g agar	Sigma	05038

*For LB Broth, agar is not added

2.6.2 Large scale plasmid preparation

A single colony was picked from a freshly streaked selective plate (2.6.2.1) and used to inoculate a starter culture of 2-5ml LB medium containing 50µg/ml AMP. The culture was incubated at 37°C with vigorous shaking (~300rpm) for ~8h. A 2ml sample of this suspension was added to 200mls of LB AMP (50µg/ml) and left to grow for 12-16hwith vigorous shaking. The bacterial cells were harvested by centrifugation at 6000 x g for 15min at 4°C.

Plasmid DNA was then extracted (Section 2.9) using the QIAGEN ® Endofree Plasmid Purification Kit (Qiagen, 12362). DNA concentration was determined by measuring using the Nanodrop at OD_{260nm}.

2.6.3 Transfection of mammalian cells with exogenous DNA

2.6.3.1 Optimisation of plasmid transfection protocol

Prior to experimental transfections involving the various DNA fragments (into the different cell lines), transfection protocols was first optimised for each of the parameters involved. The target cell line was trypsinised in the usual fashion (Section 2.2.3) and set up in the appropriate plate (i.e. 96/24/6-well plate) at several different cell concentrations, which were arbitrarily chosen. Following incubation overnight at 37°C, the cells were transfected according to the transfection protocol. Throughout this thesis all DNA plasmid transfections were carried out using the transfection reagent Lipofectaimine 2000. Only the volumes of transfectant and concentration of DNA were altered to ascertain the most efficient combination. Cells were transfected either in the presence of serum overnight or for fourhin the absence of serum, both at 37°C.

2.6.3.2 Transfection of DNA plasmids

One day prior to transfections, the cells were seeded from a single suspension into a 6 well plates at $5x10^5$ cells per well. On the day of the transfection the plasmid to be transfected was diluted to the appropriate concentration as determined from optimisation experiments and displayed in Table 2.11, in 250µl of optimem. In a separate eppendorf the appropriate concentration of lipofectamine (Table 2.11) was diluted in 250µl of optimem and left at room temperature for 15min. Both solutions were then combined allowed to incubate at room temperature for a further 30min. Just before the incubation time is complete the cells were prepared for transfection. The cells were first examined under the microscope to ensure at least 80% confluency. The media was then removed from the cells and replaced with 2mls of the cell line

appropriate antibiotic free media. Once the 30 minute transfection incubation was complete 500µl of transfection mix was then added to the plate cells in a drop wise fashion. The plate was swirled or placed on a rocker for 30 seconds to ensure complete mixing. The plate was incubated in at 37°C for four h, after which the media containing lipofectaimine was removed and replaced with normal media containing antibiotic.

Table 2.11. Optimal conditions for DNA plasmid transfection

Vector	Concentration of lipofectamine (6 well)	Concentration of vector (6 well)
pcDNA3-AKT2	4µl	1µg
pcDNA6.2-GW/EmGFP- miR-184	4µl	750ng
pMIR REPORT™	4µl	2µg
psiCHECK™-2 Vector	4µl	2µg
B-gal pMIR REPORT™ control	4µl	2µg

2.6.3.3 Estimation of transfection efficiency

MiR-184 plasmid contained a GFP tag and could be visualised using a fluorescence microscopy. For all other transient transfections, 6 well plates were transfected and taken down in sets of two (for RNA and protein samples) at 24, 48 and 72 h. RNA extraction was carried out as described in Section 2.8.2. This was followed by RTqPCR using the sequence specific RT primer for the miR or gene of interest to determine expression.

2.6.3.4 Co-transfection of reporter plasmid and miRNA

One day prior to transfections, the cells to be transfected were plated from a single cell suspension (Section 2.2.3) and seeded in a 6 well plate at $5X10^6$ cells per ml. On the day of transfection 2µg of plasmid and 30nM of miRNA (final concentration per well) were diluted in 250µl of optimem. In a separate eppendorf 4µl of Lipofectaimine 2000 (Invitrogen, 11668-019) was diluted in 250µl of optimem and left at room temperature for 5min. The suspension containing the plasmid DNA and the miRNA was then added to the suspension containing the Lipofectaimine 2000 and left to incubate at room temperature for 30min. This was subsequently added directly into the well already containing 2mls of the appropriate culture media.

2.6.4 Dual luciferase assays

2.6.4.1 The Dual-Glo® luciferase assay

The Dual-Glo® luciferase assay (Promega, E2920) was used to measure luciferase activity when normalisation was to be carried out to a second co-transfected vector. This assay was used for the pMIR-REPORT™ vector (Ambion) luciferase vector. The experimental DNA insert used in the pMIR-REPORT™ vector was that of the miR-184 target site in the 3'UTR of *AKT2*. The control for this experiment was the β-gal reporter vector supplied with the pMIR-REPORT™ vector.

The Dual-Glo® Luciferase Reagent can be added directly to cells in growth medium. This reagent induces cell lysis and acts as a substrate for firefly luciferase, producing a stable luminescent signal. Dual-Glo® Stop & Glo® Reagent was then added to quench the luminescence from the firefly reaction and provided a substrate for Renilla luciferase in the reaction.

2.6.4.2 The Dual-Luciferase® reporter assay

The Dual-Luciferase® reporter assay system (Promega, E1910) was used to simultaneously assay firefly and Renilla reporter luciferase activity. This was necessary when using the psiCHECK™-2 luciferase vector (Promega C8021) which contained both luciferase firefly (experimental) and Renilla (control) luciferins within the same vector. The experimental DNA inserts used in the psiCHECK™-2 Vector were the miR-10a and miR-10b target sites of *NCOR2*, the miR-152 target site of *DNMT1* and the miR-196a target sites of *NRAS*. This vector allows luciferase levels to be measured sequentially from a single sample. The firefly luciferase reporter was measured first by addition of Luciferase Assay Reagent II (LAR II). After quantifying the firefly luminescence, the reaction was then stopped, and the Renilla luciferase reaction was initiated by addition of Stop & Glo® Reagent to the same tube. All luciferase activity was read using a Wallac Plate Reader (Perkin Elmer).

2.7 Analytical techniques

2.7.1 Western blot analysis

2.7.1.1 Sample preparation

Cells were grown in flasks until they reached 80-90% confluency. They were then trypsinised and centrifuged at 1,000rpm for 5min. The pellet was washed in PBS and re-pelleted twice. The tube was inverted and drained of supernatant. Further treatment of the cell pellet depended on the type of extract required.

2.7.1.2 Lysis of cell pellet

Cell lysis was carried out using RIPA buffer (Sigma, R0278), 1% phosphatase inhibitor cocktail 1 (Sigma, P2850), 1% phosphatase inhibitor cocktail 2 (Sigma, P5726), protease inhibitor (0.04%) was added to the pellet (150µl pellet from T75, 50µl/T25, 25µl per well from a 6 well plate) and left rocking on ice for 30 min. (A 100X stock solution of protease inhibitors consisted of 400mM DTT (Sigma, D5545), 1mg/ml aprotonin (Sigma, A1153), 1mg/ml leupeptin (Sigma, L2884), 1mg/ml soybean trypsin inhibitor (Sigma, T9003), 1mg/ml pepstatin A (Sigma, P6425) and 1mg/ml benzamidine (Sigma, B6506). Whole cell extracts were aliquoted and stored at -80°C.

2.7.1.3 Quantification of protein

Protein levels were determined using the BCA protein kit (Pierce, 23225) (A series dilutions of BSA (Sigma, A9543) to be used as standards). This is highly sensitive and selective colorimetric detection of the cuprous cation (Cu^{1+}) by bicinchoninic acid. A stock solution of 25 mg/ml BSA was used to make a standard curve. Dilutions ranged from 0 mg/ml to 50 mg/ml.

The dye reagent was made up of 50 parts Solution 1 to 1 part Solution 2. 25µl of each standard and 25µl of experimental protein sample were plated out in duplicate on a 96 well plate. 200µl of the dye reagent was added to each sample. The plate was incubated for a period of 30min at 37°C. The OD_{562} was measured, against a reagent blank, using the Wallac luminometer. The concentration of the test samples was determined from the standard curve created from standard concentrations. From this, a relative volume for each protein sample was determined for loading onto the gels. Usually 10-30 µg protein per lane was loaded.

2.7.1.4 Gel electrophoresis

Proteins for western blot analysis were separated by SDS-polyacylamide gel electrophoresis (SDS-PAGE). Resolving and stacking gels were prepared as outlined in Table 2.12 and poured into clean 10cm x 8cm gel cassettes which consisted of 2 glass plates, separated by 0.75mm plastic spacers. The plates were cleaned by first rinsing in detergent, followed by tap water and finally UHP. After drying, the plates were wiped down in one direction using tissue paper soaked in 70% ETOH. The combs used were also cleaned in this way. After these had dried, the resolving gel was poured first and overlaid with 99% isoproponal (Sigma, I9516) and allowed to set for 1 hour at room temperature. The stacking gel was then poured and a comb was placed into the stacking gel in order to create wells for sample loading. Once set, the gels could be used immediately or wrapped in aluminium foil and stored at 4°C for 24 h.

1X running buffer (14.4g Glycine, 3.03g Tris and 1g Sodium dodecyl sulfate (SDS) in 1L) was added to the running apparatus before samples were loaded. The samples were heated to 95°C for 2min prior to loading. The samples were loaded onto the stacking gels, in equal amounts relative to the protein concentration of the sample. The loading buffer (Sigma, S-3401) was added directly at ½ volume to each of the test samples.10µl of a broad range or a high range molecular weight colour protein markers (Fermentas SM1845, SM1851) was included in each gel to detect protein size. The gels were run at 100V for approximately 1.5 h. When the bromophenol blue dye front was seen to have reached the end of the gels, electrophoresis was stopped.

Table 2.12. Preparation of electrophoresis gels

Components	Resolving gel (6%)	Resolving gel (10%)	Stacking gel
30% BIS Acrylamide (Sigma, A3449)	1.4 mls	2.38 mls	0.67 mls
Ultrapure water	3.64 mls	2.66 mls	2.7 mls
1.5M-Tris/HCl, pH 8.8	1.82 mls	1.82 mls	-
1.25M-Tris/HCl, pH 6.8	-	-	0.5 mls
10% SDS (L3771)	70 µls	70 µls	40 µls
10% Ammonium persulphate (Sigma, A3678)	70 µls	70 µls	40 µls
TEMED (Sigma, T9281)	5.6µls	8.4 µls	4 µls

2.7.1.5 Western blotting

Following electrophoresis, the acrylamide gels were equilibrated in transfer buffer (25mM Tris, 192mM Glycine (Sigma, G-7126) pH 8.3-8.5 without adjusting) for 5 min. Protein in gels were transferred onto Hybond ECL nitrocellulose membranes (GE Healthcare, RPN203D) by wet electroblotting in an electrophoretic transfer unit. A blotting sponge was placed on the plate of the wet transfer rig (BioRad, 1703914). Two sheets of mini trans-blot filter paper (BioRad, 1703932) were soaked in transfer buffer and placed on the sponge. The acrylamide gel was placed over the blotting paper. A piece of nitrocellulose membrane, cut to the same size of the gel, was prepared for transfer (soaked for 10sec in transfer buffer) and placed over the gel, making sure there

were no air bubbles. Two more sheets of pre-soaked filter paper were placed on top of the gel. Excess air was removed by rolling a plastic tube over the filter paper. Another transfer sponge was placed on top and the transfer rig closed. The proteins were transferred from the gel to the nitrocellulose at a current of 90V for 30-60min.

All incubation steps from now on, including the blocking step, were carried out on a revolving apparatus (Stovall, Bellydancer) to ensure even exposure of the blot to all reagents. The nitrocellulose membranes were blocked for 2hat room temperature with fresh filtered 5% non-fat dried milk (Cadburys, Marvel skimmed milk) in Tris-buffered saline (TBS) with 0.5% Tween (Sigma, P5927) pH 7.5. After blocking, the membranes were rinsed once in 1X TBS and incubated with 5 to 10 mls primary antibody in TBS with 0.5% Tween. The specific conditions for each antibody are outlined in Table 2.4.2 below. Bound antibody was detected using enhanced chemiluminescence (ECL).

Table 2.13 Primary antibodies used for western blot analysis

Antibody	Dilution/ Concentration	Supplier	Catalogue no.
AKT2 (R)*	1/500	Millipore	07-372
NCOR2 (R)	1/500	Abcam	ab2780
DNMT1 (R)	1/1000	Sigma	D4567
βIII Tubulin (R)	1/2000	Abcam	ab18207
GAP 43 (R)	1/500	Millipore	AB5220
NRAS (G)**	1/1000	Abcam	ab77392
MYCN (M)***	1/500	Santa Cruz	Sc-5993
B-Actin (M)***	1/2000	Abcam	ab6276
GAPDH (M)	1/3,000	Abcam	ab8245
α-Tubulin (M)***	1/1000	Abcam	ab7291

*R- Rabbit

**G- Goat

***M- Mouse

Table 2.14. Secondary antibodies used for western blot analysis

Antibody	Dilution/ Concentration	Supplier	Catalogue no.
Mouse	1/2000	Abcam	ab6728
Rabbit	1/2000	Abcam	ab6721
Goat	1/1000	Abcam	ab6741

2.7.1.6 Enhanced chemiluminescence detection

Protein bands were developed using the Western Lightening Plus ECL Enhanced Chemical Substrate (Perkin Elmer, NEL105001) according to the manufacturer's instructions. The blot was removed to a darkroom for all subsequent manipulations. A sheet of parafilm was flattened over a smooth surface, e.g. a glass plate, making sure all air bubbles were removed. The membrane was placed on the parafilm, and excess fluid removed. Equal volumes of detection reagents 1 and 2 were combined and used to completely cover the membrane. Charges on the parafilm ensured the fluid stayed on the membrane. The reagent was removed after one minute and the membrane wrapped in cling film.

The membrane was exposed to CL-X POSURE FILM (Thermo Scientific, PN34091) in an autoradiographic cassette for various times, depending on the signal (30s – 15 min). The autoradiographic film was then developed. The exposed film was developed for 5min in developer (Kodak, LX24, and diluted 1:6.5 in water). The film was briefly immersed in water and fixed (Kodak, FX-40, diluted 1:5 in water), for 5min. The film was transferred to water where it was rinsed and then air-dried.

2.7.2 Immunofluorescence

2.7.2.1 Fixation of cells

Cells were fixed using 4% paraformaldehyde (Sigma, P6148), made up in PBS. For fixation, medium was removed from 6-well plates; cells were rinsed 3 times with PBS and then incubated at room temperature for 25min in 500µl of 4% paraformaldehyde. The paraformaldehyde was removed from the cells, and they were washed X3 in PBS for 5min. Cells were permeabilised in 0.5% Triton X-100 (T8787) for 5 min. The cells were washed in PBS, 5min X3 times. Fixed cells were stored at 4°C in 500ul of PBS until ready for use.

2.7.2.2 Immunofluorescence procedure

Cell preparations (6-well tissue culture plates) previously fixed with paraformaldehyde and stored at 4°C (Section 2.7.2.1) were equilibrated to room temperature. Non-specific binding was blocked using 2.5% BSA in PBS for 30min at 37^{0}C.

The cells were incubated over night at 4^{0}C in 500µl of optimally diluted primary antibody (see Table 2.15 for dilutions) made up 2.0% BSA/PBS. Double staining, staining with two antibodies could be carried out simultaneously when the two different primary antibodies were mixed in BSA/PBS and added to the cells. The cells were rinsed in PBS/ 0.1% Tween (Sigma) for 5min X5. The appropriate secondary antibody(s) (Table 2.16) were diluted in PBS, added to samples and incubated in the dark at room temperature. The cells were then counterstained with a DAPI solution (Sigma, 32670) for 5 min. After staining, the cells were washed with 1ml PBS and examined microscopically

Table 2.15 Primary antibodies used for immunoflorescence staining

Antibody	Dilution/ concentration	Supplier	Catalogue no.
βIII Tubulin (R)*	1/200	Abcam	Ab18207

*Rabbit

Table 2.16 Secondary antibodies used for immunoflorescence staining

Antibody	Dilution/ concentration	Supplier	Catalogue no.
Alexa Flour 688 (A.M)*	1/500	Invitrogen	A-21088
Alexa Flour 488 (A.R)**	1/500	Invitrogen	A-11008

* Anti-mouse
**Anti-rabbit

2.7.2.3 Neurite outgrowth measurement using Cellomics

The stained cells were imaged in 6 well plates using Cellomics ArrayScan VTi instrument (Thermofisher) equipped with 10x PlanApo objective lens (NA 0.45), 120W Hg arc illumination source (EXFO) and a monochrome CCD camera (Hamamatsu Orca AG). Images of 49 fields of view were registered from each well with 1024x1024 pixel resolution (645nm pixel size). The fluorescence of DAPI (nuclei) was excited using 375 – 400nm light and collected in 425 – 460 band, whereas the fluorescence of Alexa 488 (whole cells) was excited using 470 – 490nm light and collected in 500 – 550 band.

The images of nuclear fluorescence were pre-processed using rank leveling (25 pixel window) for background subtraction. The nuclei, cell bodies and neurites were

2.8.2 RNA isolation

Total RNA/including small miRNAs was extracted from neuroblastoma tumour samples, cultured cell lines and plasmid-transfected cell lines, using the miRNeasy™ Kit (Qiagen 217004). The size of the flasks varied, but the method remained the same. The tumour samples were initially ground down using a mortar and pestle before proceeding to the lyses steps outlined below. Cultured cells were trypsinised and the pellet was washed twice with PBS.

The cells/tumours were lysed using 700µl of QIAzol™ (Qiagen). If lysis was incomplete the QIAshredder was used to further break up the sample. The following procedure is outlined in the protocol for miRNeasy™. The samples were allowed to stand for 5min at room temperature to allow complete dissociation of nucleoprotein complexes. 140µls of chloroform was added per 700µl of QIAzol™ used and the sample was shaken vigorously for 15 sec and allowed to stand for 3minat room temperature. The sample was centrifuged at 12,000 x g for 15min at 4°C in a microcentrifuge. This step separated the mixture into 2 phases with the RNA contained in the colourless upper aqueous layer. The aqueous layer was transferred to a new eppendorf and 525µls of 100% Ethanol was added and mixed thoroughly using a pipette. The ethanol is added to provide appropriate binding conditions for all RNA molecules. 700µl of the sample was then added into a miRNeasy mini spin column in a 2ml collection tube, the sample was then centrifuged at 10,000rpm for 15 seconds. The spin column, allows binding of RNA to the membrane, and phenol and other contaminants are washed away. The flow through was discarded. This was repeated with what remained of the sample. 700µl of Buffer RWT was added to the spin column, and centrifuged at 10,000rpm for 15secs. Flow through was again discarded. Next 500µl of Buffer RPE was added to the spin column and centrifuged at 10,000rpm, for 15secs. This step was repeated and the

sample was this time centrifuged for 2 min. The spin column was transferred to a new tube and an extra 1 minute spin was preformed to remove any residual wash buffer. The spin column was again transferred to a new tube and 30-50µl of DEPC water was added to the spin column and centrifuges at 10 000rpm for 1min.

2.8.2.1 RNA quantitation

RNA was quantified spectrophotometrically by Nanodrop using the following formula: OD_{260nm} x Dilution factor x 40 = µg/ml RNA

Before applying the RNA sample the pedestal was wiped down using a lint-free tissue dampened with UHP. 1µl of UHP was then loaded onto the lower measurement pedestal. The upper sample arm was then brought down so as to be in contact with the solution. "Nucleic acid" was selected on the Nanodrop software to read the samples. After the equipment was initialised the "blank" option was chosen, and after a straight line appeared on the screen the "measure" option was selected. A "blank" reading was taken between each sample measurement. The upper and lower pedestals were cleaned with a clean dry wipe between samples. When finished, the pedestal was cleaned with a wipe dampened with UHP followed by drying with a dry wipe.

An A_{260}/A_{280} ratio of 1.8-2 is indicative of pure RNA, although RNA with ratios from 1.7 – 2.1 were routinely observed and used in subsequent experiments. The yield of RNA from most lines of cultured cells is 100-200µg/ 90mm plate. In these studies 2-3µg RNA per $75cm^2$ flask was retrieved. RNA samples were diluted to 500 ng/ µl and stored at $-80^{o}C$

2.8.2.2 . Separating nuclear and cytoplasmic cell fractions

Nuclear and cytoplasmic fractionation was carried out using reagents from the Universal Magnetic Co-IP Kit (Active Motif, 54002). The cell pellet was resuspended in 500µl of Complete Hypotonic Buffer by pipetting up and down. This was incubated on ice for 15 min, after which 25µl of Detergent was added to the cells and mixed by pipetting up and down a number of times. Mix was then centrifuged for 30 seconds at 14,000g in a centrifuge pre-cooled to 4°C. The supernatant is retained as it contains the cytoplasmic fraction and the remaining pellet contains the nuclear fraction. RNA extraction of each section was then carried out as described in Section 2.8.2.

2.8.3 Reverse-Transcription Polymerase Chain Reaction (RT-PCR)

Reverse transcriptase (RT) reactions were set up on benches using micropipettes, which were specifically allocated to this work.

2.8.3.1 Reverse transcription of isolated RNA

To generate cDNA, from isolated RNA, the reagents in Table 2.17 were mixed in a PCR eppendorf (Eppendorf, 0030 121 023). The RT reaction was carried out on the Veriti® Thermal Cycle (Applied Biosystems) by incubating the eppendorfs at 37°C for 1 hour. The RT enzyme was inactivated by heating to 95°C for 5min. The cDNA was stored at -20°C until required for use in PCR reactions as outlined in Section 2.8.3.3.

Table 2.17. Reverse transcription to produce cDNA for gene expression

Reagent	Volume	Supplier	Catalogue no.
10X RT Buffer	2µl	Applied Biosystems	4319979
Multiscribe Transcriptase	1µl	Applied Biosystems	0904095
Random Primers	2µl	Applied Biosystems	N80801274367381
dNTP mix 100mM	1µl	Applied Biosystems	
RNase Inhibitor			0904095
Total RNA	1µl	Applied Biosystems	NA
DEPC Water	10µl (50ng/µl)	NA	NA
	3.2µl	NA	

2.8.3.2 Reverse transcription using microRNA specific primers

To generate cDNA from extracted RNA for the microRNAs of interest, the reagents in Table 2.18 were mixed in a PCR eppendorf. To form the sequence specific cDNA of the microRNA of interest, sequence specific reverse transcription primers were used. These primers are listed in Table 2.19. The solution was mixed and the RT carried out on the Veriti® Thermal Cycle (Applied Biosystems). The RT was carried out at 16°C for 30min, followed by incubation at 42°C for 30min. The RT enzyme was inactivated by heating to 85°C for 5min. The cDNA was stored at -20°C until required for use in PCR reactions as outlined in Section 2.8.3.3.

Table 2.18. MicroRNA specific reverse transcription

Reagent	Volume (µl)	Supplier	Catalogue no.
10X RT Buffer	1.5	Applied Biosystems	4319979
Multiscribe Transcriptase	1	Applied Biosystems	0904095
dNTP mix 100mM	0.15	Applied Biosystems	4367381
RNase Inhibitor			
Total RNA	0.19	Applied Biosystems	0904095
Nuclease free Water	10 (50ng/µl)	NA	NA
RT Primer for microRNA	0.16	NA	NA
	2	Applied Biosystems	Table 2.19

Table 2.19 MicroRNA specific RT primers

Primer Pair	Supplier	Assay Id.
miR-184	Applied Biosystems	00485
miR-152	Applied Biosystems	000475
miR-10a	Applied Biosystems	000387
miR-10b	Applied Biosystems	002218
miR-196a	Applied Biosystems	000495
RNU66	Applied Biosystems	01002

2.8.3.3 Polymerase chain reaction (PCR) amplification of cDNA

RNA was isolated (Section 2.8.2) from the cells and cDNA synthesised as per Section 2.8.3.1/2. The cDNA subsequently analysis for genes or microRNAs of interest by Polymerase Chain Reaction (PCR). A fast polymerase chain reaction (PCR) procedure was followed in this study. The FAST protocol was carried out on the Applied Biosystems 7900HT Fast System. Real time PCR analysis was preformed using the Applied Biosystems Assays Taqman® Fast PCR kits, using primer probes as outlined in Table 2.20. Experiments were preformed in triplicate, as per manufacturer's instructions. All reagents were aliquoted and stored at -20°C. All reactions were carried out on a PCR specific work bench. A typical PCR reaction was carried out by plating the reagents in Table 2.21 into a 96-well FAST plate. Samples were mixed by pipetting two or three times and PCR was carried out using cycles below.

Cycles for FAST PCR:

	95°C for 20 sec	-	denaturation
40 cycles:	95°C for 01 sec	-	denaturation
	60°C for 20 sec	-	annealing

Table 2.20. MicroRNA and gene specific PCR primers

Primer	Supplier	Assay Id.
AKT2	Applied Biosystems	Hs01086099_m1
MYCN	Applied Biosystems	Hs00232074_m1
RPLPO	Applied Biosystems	Hs99999902_m1
NCOR2	Applied Biosystems	Hs01549808_m1
DNMT1	Applied Biosystems	Hs00945899_m1
DNMT3A	Applied Biosystems	Hs00173377_m1
DNMT3B	Applied Biosystems	HS001171875_m1
NRAS	Applied Biosystems	Hs00986871_m1
βIII Tubulin	Applied Biosystems	Hs00964965_m1
GAP43	Applied Biosystems	Hs00967138_m1
miR-184	Applied Biosystems	000485
miR-10a	Applied Biosystems	000387
miR-10b	Applied Biosystems	002218
miR-196a	Applied Biosystems	000495
miR-152	Applied Biosystems	000475
RNU66	Applied Biosystems	01002

Table 2.21. FAST PCR reaction components

Reagent	Volume	Supplier	Catalogue no.
Taqman® Fast Universal Master Mix	5µl	Applied Biosystems	4352042
Taqman® microRNA or gene specific PCR Primer	0.5µl	Applied Biosystems	Table 2.20
DEPC Water	3.5µl	NA	NA
cDNA	1µl	NA	NA

2.8.3.4 Reverse Transcription of RNA for Taqman® Low Density micro-fluidic cards

RNA was reverse transcribed using the miRNA reverse transcription kit (Applied Biosystems). Cell line RNA was used in combination with the stem-loop Multiplex primer pools (Applied Biosystems), allowing reverse transcription of 48 different miRNA in each of 8 RT pools allowing simultaneous reverse transcription of 364 miRNAs including 8 endogenous controls. The Multiplex primer pools (Applied Biosystems) were used with RNA from treated and untreated SK-N-BE samples. The reverse transcription using the pools was then carried out as per Section 2.8.3.2.

2.8.3.5 PCR for Taqman® Low Density micro-fluidic cards

PCRs for taqman low density arrays were carried out with 100ng/ul of each sample specific cDNA pool as generated in Section 2.8.3.4, made up in Taqman® Fast Master Mix and H_20. 100µl of each sample was added to the corresponding pool fill port on the card. The card was sealed, centrifuged and then run on the 7900HT

2.8.3.5.1 Statistics and normalisation for Taqman® Low Density micro-fluidic cards

Prior to calculating relative expression values, mean normalization was carried out by subtracting the mean sample Ct (Cycle threshold) from the individual miRNA Ct values. The threshold line is the level of detection or the point at which a reaction reaches a fluorescent intensity above background. The threshold line is set in the exponential phase of the amplification for the most accurate reading. The PCR cycle at which the sample reaches this level is called the CT (Applied Biosystems Technical notes). Normalized relative quantification (NRQ) of miRNA was calculated with reference to the Ct max (maximum Ct value for an individual miRNA across all tumour samples) using: $NRQ = 2^{(Ctmax-Ct)}$. CT values greater than 35 were removed before analysis was carried out. As a CT value above 35 is seen to represent a single molecule template, all CT>35 were considered noise.

2.9 DNA extraction

DNA Extraction was carried out using the DNeasy® Blood and Tissue kit (Qiagen, 69506). The following procedure is outlined in the DNeasy® Blood and Tissue kit handbook. Cells were harvested as per Section 2.2.3; washed cells were then centrifuged to create a pellet which was then re-suspended in 200µl of PBS. 20µl proteinase K was then added to the sample, followed by 200µl of lysis buffer (Buffer AL), the sample was mixed thoroughly by vortexing. This solution was then incubated at 56°C for 10 min. Following incubation 200µl of (98-100%) ethanol was added and mixed carefully. The mix was then added to a DNeasy spin column in a 2ml collection tube and centrifuged at 8,000rpms for 1min. The flow through was discarded. The DNeasy spin column was placed in a fresh collection tube, 200µl of the first wash

buffer (Buffer AW1) was added and the sample was centrifuged at 8,000rpms for 1min again the flow through was discarded. The DNeasy spin column was placed in a new collection tube; 500µl of the second wash buffer (Buffer AW2) was added to the spin column and centrifuged for 2minat 14,000rpms. This high speed was used to ensure that the spin column is dried in this step. The spin column was then placed in a clean 1.5ml microcentrifuge tube, 200µl of elution buffer (Buffer AE) was added directly to the spin column and allowed incubate for 1 minute at room temperature. Elution was carried out by centrifugation at 8,000rpms for 1min.

2.10 Collection of tumour data

Tumour material was obtained from either the Children's Oncology Group Tumour Bank (n = 108), or the Tumour Bank at Our Lady's Children's Hospital, Dublin (n = 37). Patients were treated under either the U.S. neuroblastoma treatment protocol or the European treatment protocol between 1998 and 2004.

This work was approved by the Research Ethics Committee of the Royal College of Surgeons on 16th October 2007 (application No. REC241) and by the Research Ethics Committee of Our Lady's Children's Hospital on 5th August 2008 (application number GEN/70/07).

The tumour cohort came from patients with stage 4 (n = 74), stage 3 (n = 31) and stages 1, 2 and 4s (n = 40) disease (INSS). In total, 36 tumours had MYCN amplification (MNA) while 42 tumours had loss of 11q without MNA. MYCN amplification and loss of 11q were predictive of both poor EFS ($p<0.0001$) and OS ($p<0.0001$) in this set of 145 tumours (209).

2.11 Statistics/bioinformatics

2.11.1 Statistical analysis of neuroblastoma primary tumours

EFS time was calculated from the time of enrolment on the front-line or biological study until the time of the first occurrence of relapse, progressive disease, secondary malignancy, or death, or until the time of last contact if no event occurred. OS time was calculated until the time of death or until last contact. EFS and OS are presented as the estimate +/− the standard error.

2.11.2 Statistics

Statistics used for calculating p values depended on the sample set in question. Statistics for tumour information and larger data sets, for which uniform distribution was unclear, was calculated using Mann-Whitney non-parametric test. Students T test was used for all other smaller experimental sets. All experiments through out this study were carried out in triplicate unless otherwise stated. Error bars on all graphs are representative of standard deviation.

2.11.3 Identification of microRNA predicted targets

MicroRNA target prediction websites Target Scan Version 5.1 http://www.targetscan.org/ and Microcosom from EMBL-EBI http://www.ebi.ac.uk/ were used for identification of predicted microRNA targets of interest.

2.12 Microarray based profiling

2.12.1 Microarray profiling of ChIP-chip analysis of MYCN binding

ChIP assays were performed using the B8.4.B or NCMII-100 anti-MYCN antibodies according to the standard NimbleGen ChIP protocol. Cells were cross-linked with 1% formaldehyde solution for 10minon ice, centrifuged and rinsed with ice-cold PBS. Cell nuclei were isolated and sonicated to generate fragments of approximately 1kb in length. 2mg/ml was used per ChIP reaction. DNA was enriched by immunoprecipitation using 10µg of either antibody complexed to M-280 Sheep anti-Mouse Dynabeads (112-02D, Invitrogen). The formaldehyde crosslinks, protein and RNA was removed from the immunoprecipitated DNA sample through heat denaturing, proteinase K and RNase A treatments. A non-enriched sample of DNA was as input. ChIP and input DNA was fluorescently labeled using Kenow fragment (New England Biolabs M0212M) and Cy5/Cy3 random primers (TriLink BioTechnologies N46-0001-50 / N46-0002-50). The Cy5-ChIP and Cy3-input labeled DNA samples were then co-hybridized to a custom array which was designed to include tiled sequences of 50kb 5' and 20kb 3' of 528 miRNAs (Roche NimbleGen). Image files generated after scanning were analyzed using NimbleScan Software Version 2.4.

Sites of enrichment were identified using the normalised Log_2 ratios and the NimbleScan peak finding function. The in-built peak analysis algorithm detects significantly enriched regions that have at least 4 probes above a threshold value of log 2.0, identifies them as "peaks" and assigns a false discovery rate (FDR). An FDR value of 0.1 was used in the initial screening of peaks from individual experiments for both NCMII-100 and B84B antibodies. Peaks with an FDR less than 0.1 and which were only shared across ChIP reactions using both MYCN antibodies were filtered using an

in-house built java application. This produced a final set of consistently bound high confidence regions for each of the cell lines used in the study. This final set of high confidence peaks was subsequently used in further transcription factor binding site and Gene Ontology analysis.

2.12.2 Microarray gene expression profiling

Total RNA was extracted from SK-N-BE cells (untreated and ATRA-treated biological repeats, miR-10a, miR-10b, miR-196a, miR-152 and negative control transfected) using the QIAGEN RNeasy Mini Kit (Cat. No. 74101) as per Section 2.8.2, including DNase treatment to ensure complete removal of any genomic DNA. RNA integrity was confirmed with the Experion RNA StdSens Analysis Kit (BioRad 700-7103). The SuperScript Double-Stranded cDNA Synthesis Kit (Invitrogen 11917-020) was used to generate cDNA according to the manufacturer's protocol. Cy3 labeling of ds-cDNA was performed overnight using the NimbleGen One-Color DNA Labeling Kit (Roche NimbleGen, 05223555001). Four micrograms of Cy3-labelled ds-cDNA was hybridized to the *Homo Sapiens* 4 x 72K gene expression array (Roche NimbleGen), according to the manufacturer's protocol. Arrays were scanned on the Axon 4000B Scanner and images acquired using GenePix Pro 6.0. The mRNA expression data (scanned .tif images) were analysed using NimbleGens NimbleScan software version 2.4, which applies quantile normalization to the data (257). Quantile normalisation computes the mean over the empirical intensity distribution of all arrays. This mean distribution is then re-assigned to each of the arrays, effectively making the distribution of probe intensities for each array in a set of arrays the same. This allows comparison of results across multiple arrays. NimbleScan was then used to apply the Robust Multichip Average (RMA) algorithm as described by Irizarry *et al.*, (2003) to

generate Gene Calls which are the normalised gene expression values for each gene featured on the array (258).

2.12.3 Methylated DNA Immunopreciptiation (meDIP)

DNA was extracted as per Section 2.9. Four micrograms of sonicated DNA was incubated overnight with 10µg of anti-5' methyl-cytidine antibody (Eurogentec). MeDIP and input DNA was differentially labeled and hybridized to a CpG Island promoter plus array from Roche Nimblegen (Human Meth 385K Prom Plus CpG; 05543622001). Arrays were scanned as per Section 2.12.1. Based on the normalized $\log_2$ ratio data a one-sided Kolmogrov-Smirnov test (KS; using a sliding window of 750BP) was applied to identify probes which displayed significantly more positive distribution of intensity log-ratios than those on the rest of the microarray. The p-value score for each probe was displayed as -log10 from the windowed KS test around that probe. Identification of hypermethylated peaks was preformed by searching for at least two probes above a p-value minimum of 2, and peaks within 500Bp of each other were merged. Only peaks detected in duplicate experiments were used for further analysis.

Chapter 3

MiR-184: a tumour suppressor gene in neuroblastoma

Chapter 3

MiR-184: a tumour suppressor gene in neuroblastoma

3.1 The role of miR-184 in neuroblastoma

MiRNA expression profiling carried out by Chen and Stallings (208) and several other research groups (209, 210, 229) demonstrated that several miRNAs are differentially expressed in different genetic subtypes of neuroblastoma. In particular, *MYCN* amplified (MNA) compared to non-MNA tumours displayed a significant shift in miRNA expression. One such miRNA that was expressed at lower levels in the MNA tumours was miR-184. This microRNA was demonstrated to cause a decrease in cell proliferation and an increase in caspase mediated apoptosis when transiently-transfected into both MNA and non-MNA neuroblastoma (NB) cell lines. In this report we identify the molecular mechanism by which miR-184 exerts its negative effects on neuroblastoma cell survival. This involves the direct targeting of the 3'UTR of *AKT2* mRNA, a major downstream effector of the phosphatidylinositol 3-kinase (PI3K) pathway, an important pro-survival pathway in cancer (259). Thus, MYCN causes enhanced tumourgenicity, in part, through the repression of a miRNA that targets this important pro-survival gene, a novel association with neuroblastoma pathogenesis.

3.1.1 MiR-184 expression is inversely correlated to *MYCN* levels in neuroblastoma cell lines

Chen and Stallings 2007 (208) demonstrated that miR-184 was significantly down-regulated in MNA tumours. We examined this association between *MYCN* and miR-184 *in vitro* using four neuroblastoma cell lines. The following cell lines were chosen based on *MYCN* status, Kelly (MNA), SK-N-BE (MNA), SK-N-AS (*MYCN* single copy) and SH-SY5Y (*MYCN* single copy, *MYCN* over expressed). A RTqPCR screen of these cell lines for miR-184 expression revealed a much higher level of miR-184 in SK-N-AS cells compared to the other three cell lines (Figure 3.1).

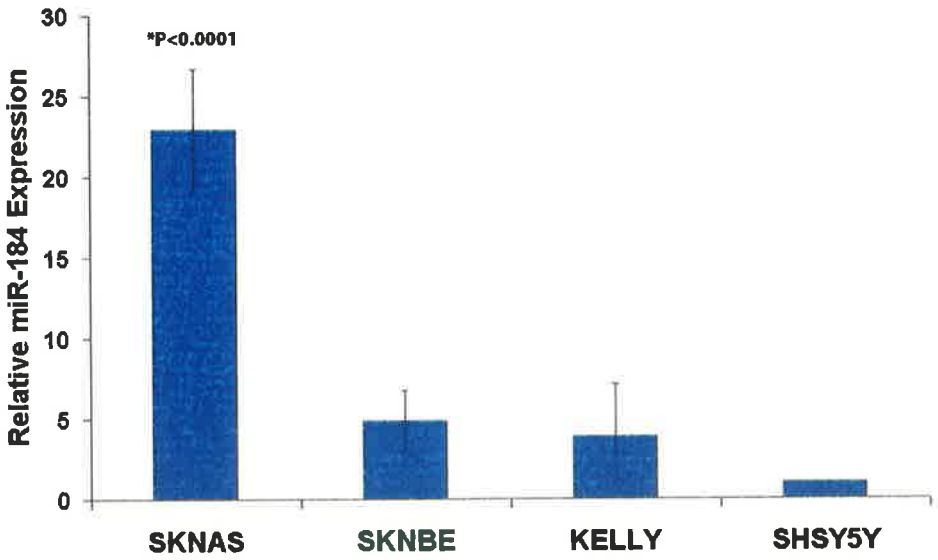

Figure 3.1. MiR-184 is expressed at a low level in cell lines expressing higher levels of *MYCN*. MiR-184 is significantly lower in cell lines expressing high *MYCN* levels, SK-N-BE (MNA), Kelly (MNA), SHSY5Y (*MYCN* over expressed) relative to SK-N-AS which is *MYCN* single copy. *P<0.0001 compared to SHSY5Y miR-184 levels.

3.1.2 MiR-184 is regulated by *MYCN*

Due to the fact that the original observation of miR-184 down regulation in MNA tumours was based on data generated from a limited set of tumours, 12 MNA tumours and 23 non-MNA tumours, we expanded the analysis to include 128 additional primary NB tumours (31 MNA and 97 non-MNA). As illustrated in Figure 3.2 a miR-184 is highly down-regulated in this larger independent set of MNA tumours relative to the other tumour subtypes ($P < 0.0001$). These results provide further evidence that MYCN may have a role to play in the regulation of miR-184 in neuroblastoma. To further evaluate this possibility in an experimental system where, we used the SH-EP21N neuroblastoma cell line which contains a repressible *MYCN* transgene, which allows the ectopic expression of *MYCN* to be reduced by the addition of Dox. As illustrated by RTqPCR (Figure 3.2 b) and western blotting (Figure 3.2c), addition of Dox to the SH-EP21N cell culture causes a dramatic reduction in *MYCN* mRNA and protein levels. *MYCN* depleted SH-EP21N cells display an 8-fold increase in miR-184 levels (Figure 3.2 d), providing further support that MYCN negatively regulates miR-184 expression. In addition MYCN chromatin immunoprecipitation to microarrays (ChIP-chip) identifying a MYCN binding site 2.7 kb up-stream of the predicted miR-184 transcriptional start site (Figure 3.3) in the *MNA* cell line Kelly and SH-EP21N untreated cells. Interestingly, the addition of Dox to the SH-EP21N cell line abolished MYCN binding which in turn is associated with a 8-fold increase in miR-184 expression (Figure 3.2 d).

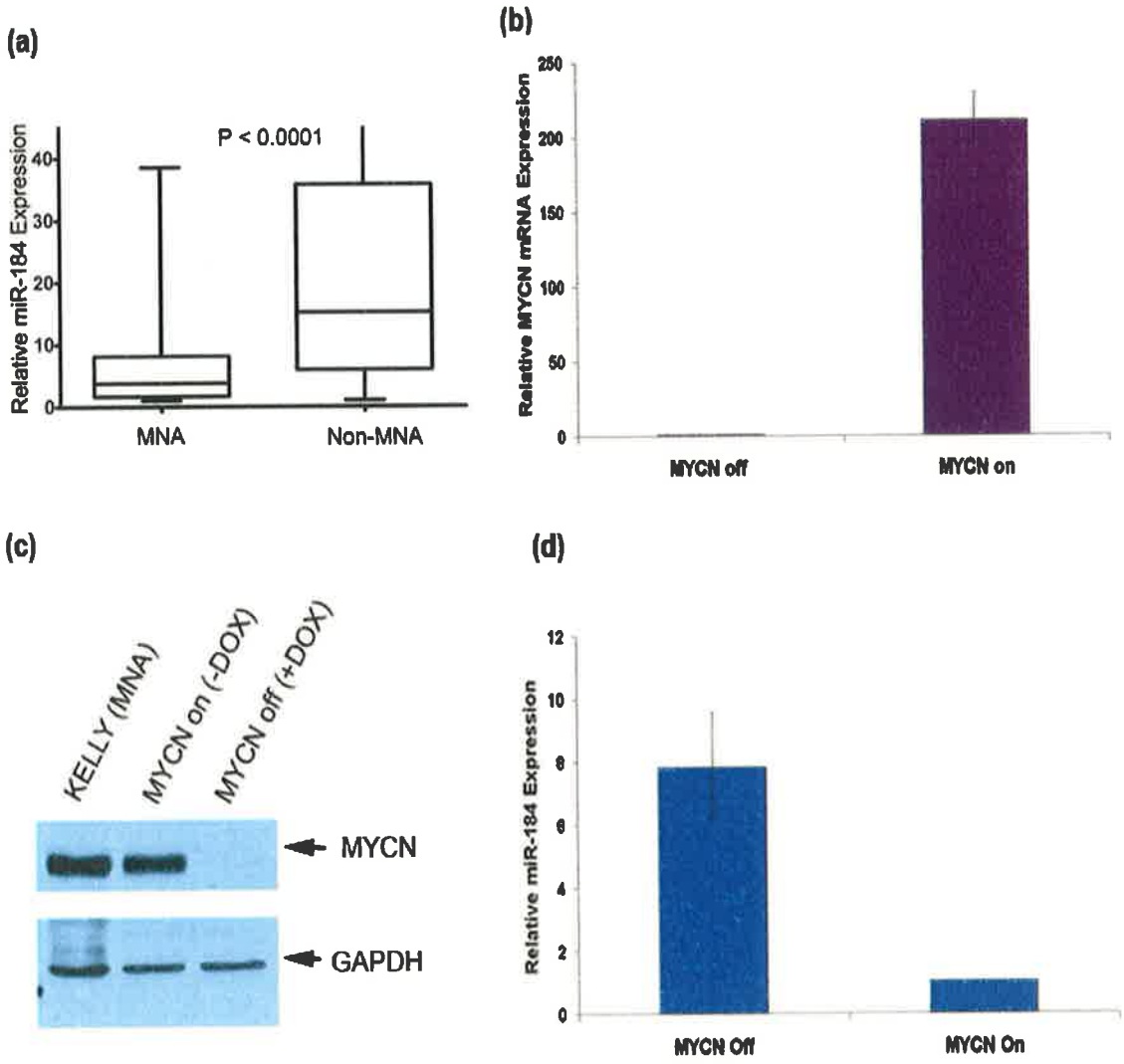

Figure 3.2. MiR-184 is regulated by MYCN. (a) MiR-184 is significantly lower in MNA tumours when compared to non-MNA tumours. *MYCN* levels are significantly down regulated at both (b) mRNA level and (c) protein level after addition of doxycycline to the SH-EP21N neuroblastoma cell line. (c) SH-EP21N *MYCN* levels are comparable to the MNA cell line Kelly before treatment with doxycycline. (d) MiR-184 is up-regulated ~8-fold when *MYCN* is suppressed in this model.

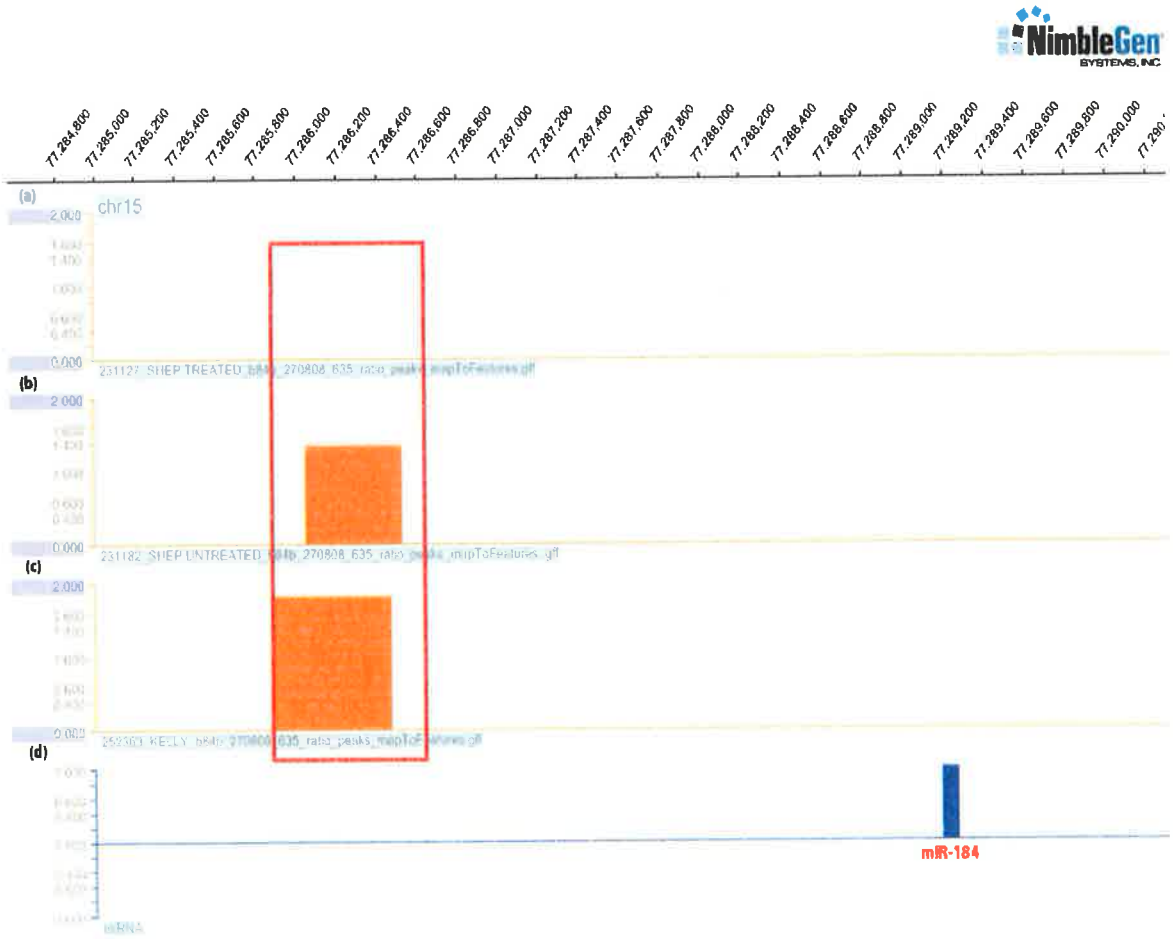

Figure 3.3. MiR-184 is potentially regulated by MYCN binding up-stream. Chip chromatin immunoprecipitation assay demonstrates an absence of MYCN binding (no orange peak) 5' of miR-184 in the (a) MYCN repressed state. MYCN binding is demonstrated (orange peaks) a 2.7 kb region 5' of the predicted miR-184 transcriptional start site, in *MYCN* amplified (b) SH-EP21N untreated and (c) Kelly cells.

3.1.3 Ectopic over expression and down-regulation of miR-184

There is much controversy surrounding the use of mature mimics in experiments due to the supra-physiological changes in miR levels following transfection.

In order to demonstrate that mature mimics yield similar results to ectopic up-regulated miRNAs at physiological levels, miR-184 was ectopically over expressed using both a synthetic mature miRNA and a plasmid expressing the stem loop precursor to miR-184 (pcDNA6.2-GW/EmGFP-miR-184) in both Kelly and SK-N-AS cells. The vector encoded for green fluorescent protein (GFP) allowing determination of adequate uptake of the vector by the cells. This resulted in a transfection efficiency of approximately 80% for both Kelly and SK-N-AS cells.

Cell lines were analysed by RTqPCR at 24, 48 and 72h to determine expression of miR-184. The mature miR-184 synthetic oligo was shown to increases levels of miR-184 by ~10,000-fold in Kelly cells (Figure 3.4 a), and ~1000-fold in SK-N-AS cells (Figure 3.4 b). Transfection of pcDNA6.2-GW/EmGFP-miR-184 into Kelly cells yielded between 6.5 to 15-fold ectopic up-regulation of mir-184 expression (Figure 3.5 a). Transfection pcDNA6.2-GW/EmGFP-miR-184 resulted in a 3.9 and 9-fold ectopic up-regulation in SK-N-AS cells (Figure 3.5 b). MiR-184 was inhibited by transfection with anti-miR-184. Knock down of miR-184 was carried out in both Kelly (Figure 3.6 a) and SK-N-AS (Figure 3.6 b) NB cell lines using chemically modified single stranded oligonucleotides designed to specifically bind to and inhibit miR-184.

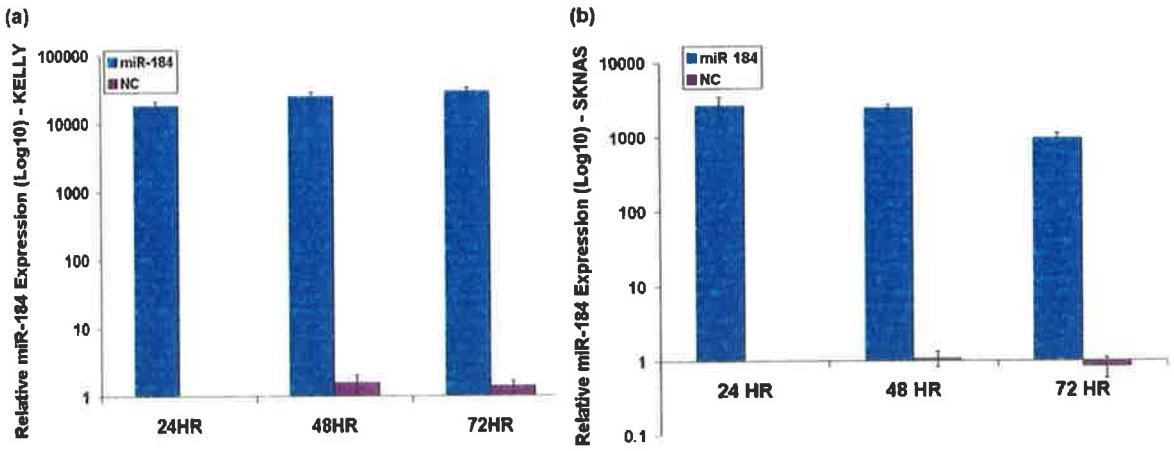

Figure 3.4. Fold change of miR-184 following transfection with mature mimic. Transfection of miR-184 mature mimic resulted in large increases in miR-184 levels in (a) Kelly and (b) SK-N-AS cells. Values are normalised relative to the scrambled oligonucleotide control (NC).

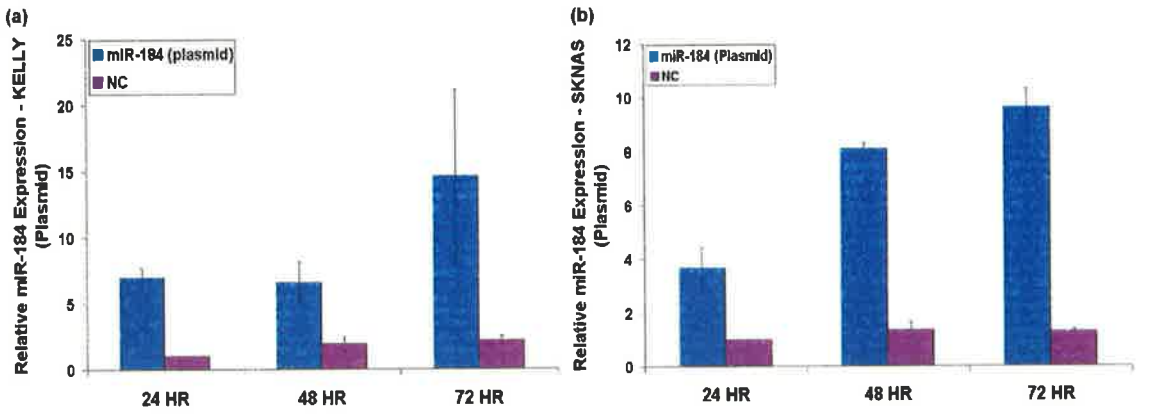

Figure 3.5. Fold change of miR-184 following transfection with pcDNA6.2-GW/EmGFP-miR-184. Transfection of pcDNA6.2-GW/EmGFP-miR-184 showed a ~6.5-15-fold increase of miR-184 in (a) Kelly cells and ~3.9-9-fold increase in (b) SK-N-AS cells relative to cells transfected with the pcDNA6.2-GW/EmGFP negative control vector.

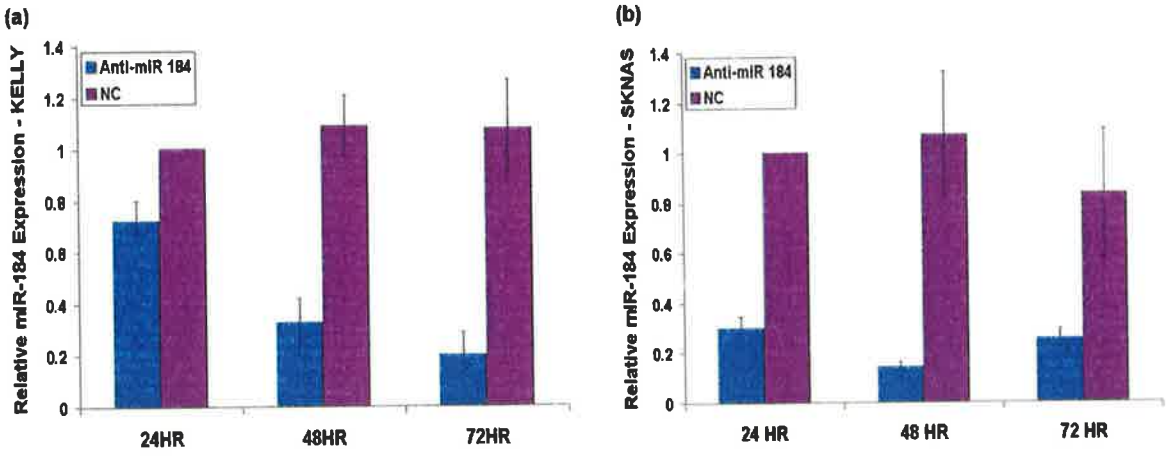

Figure 3.6. Fold change of miR-184 following transfection with an anti-miR-184 oligonucleotide. The anti-miR to miR-184 showed significant knockdown of endogenous miR-184 expression levels in both (a) Kelly and (b) SK-N-AS relative to a scrambled oligonucleotide control (NC).

3.1.4 Effect of ectopic over-expression of miR-184 on cell numbers

Both the synthetic mature miR-184 and pcDNA6.2-GW/EmGFP-miR-184 resulted in a similar reduction of cell numbers in both SK-N-AS and Kelly cell lines (Figure 3.7 a-d). These findings suggest that up-regulation of miR-184 through transfection of pcDNA6.2-GW/EmGFP-miR-184, which displayed up-regulation comparable to physiological levels, had an equivalent effect on cell viability when compared to over-expression using the mature mimic.

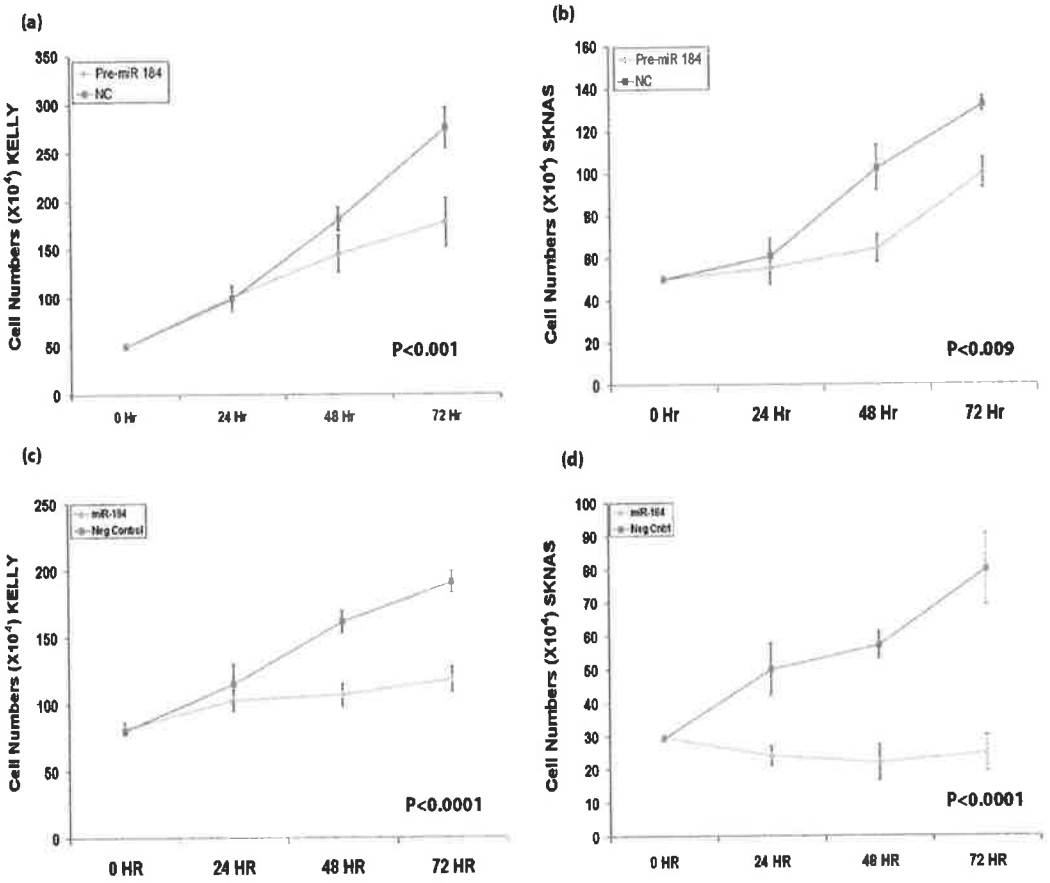

Figure 3.7. Ectopic up-regulation using the miR-184 plasmid had a similar effect on cell viability to the mature synthetic mimic. MiR-184 up-regulation, through transfection of the mature synthetic mimic, resulted in a significant reduction in cell numbers following transfection of both (a) Kelly cells and (b) SK-N-AS cells relative to a scrambled oligonucleotide negative control. Up-regulation by means of pcDNA6.2-GW/EmGFP-miR-184 showed a significant decrease in cell numbers relative to cells transfected with the empty plasmid in both (c) Kellyand (d) SK-N-AS.

3.1.5 Effect of down regulation of miR-184 on cell numbers

The down-regulation of miR-184 expression was achieved in both Kelly and SK-N-AS cell lines using the anti-miR to miR-184 (as discussed in Section 3.1.3). Down-regulation of miR-184 had an inverse effect on cell numbers compared to the scrambled oligonucleotide control, resulting in a significant increase in cell numbers (Figure 3.8).

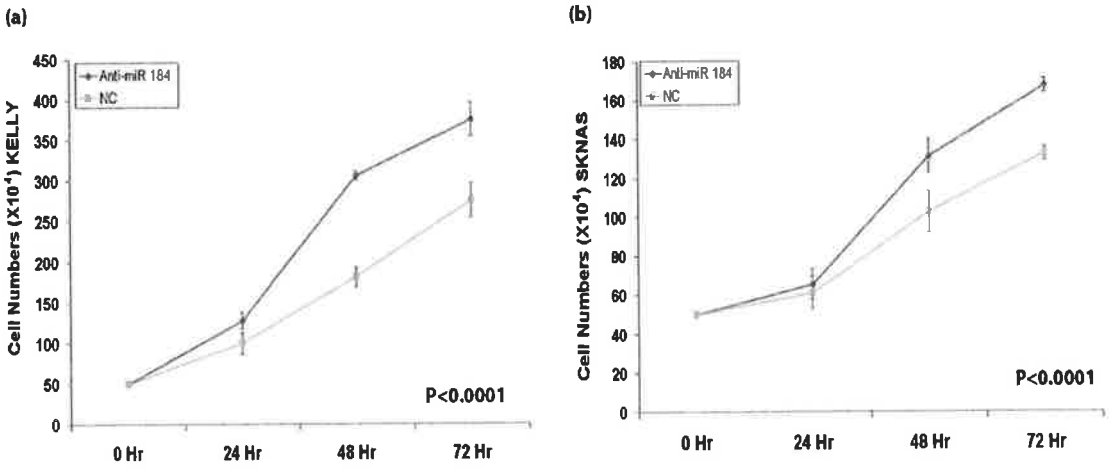

Figure 3.8. Down-regulation of miR-184 using the anti-miR results in an increase in cell numbers. MiR-184 down-regulation using the anti-miR showed a significant increase in cell numbers following transfection in both (a) Kelly cells and (b) SK-N-AS cells relative to a scrambled oligonucleotide control over a 72h period.

3.1.6 Over expression of miR-184 induces apoptosis in Kelly cells

MiR-184 induces apoptosis when delivered as a mature mimics mimic and when expressed from the pcDNA6.2-GW/EmGFP-miR-184 plasmid. FACs analysis for annexin V and propidium iodide staining was used to measure apoptosis. This was carried out with the mature mimics, relative to untreated cells and cells treated with the scrambled oligonucleotide control. Ectopic up-regulation of miR-184 resulted in a 4-fold increase in apoptosis compared to control samples (Figure 3.9 a-c). A caspase 3/7 assay was used to determine if apoptosis was caspase mediated. A significant increase in caspase 3/7 activity ($P<0.001$) was detected following transfection with either the miR-184 expressing mature mimic or pcDNA6.2-GW/EmGFP-miR-184 into Kelly Cells (Figure 3.10 a and b respectively) confirming that the induction of apoptosis was induced caspase mediated.

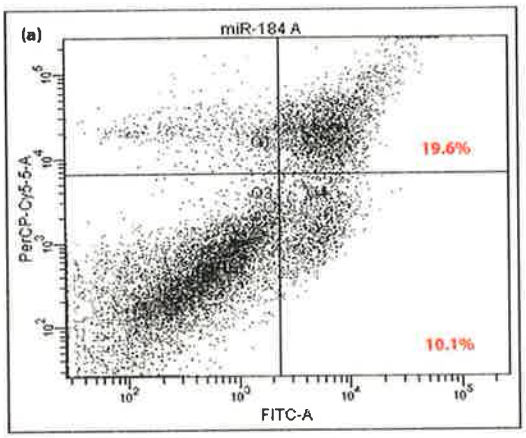

Experiment Name: Niamh-Annexin Kelly
Specimen Name: 15th Dec 2009
Tube Name: miR-184 A
Record Date: Dec 15, 2009 4:20:49 PM

Population	#Events	%Parent	FITC-A Mean	PerCP-Cy5-... Mean
All Events	10,000	###	2,621	8,605
Q1	479	4.8	913	23,666
Q2	1,964	19.6	8,731	35,248
Q3	6,550	65.5	507	521
Q4	1,007	10.1	5,265	2,066

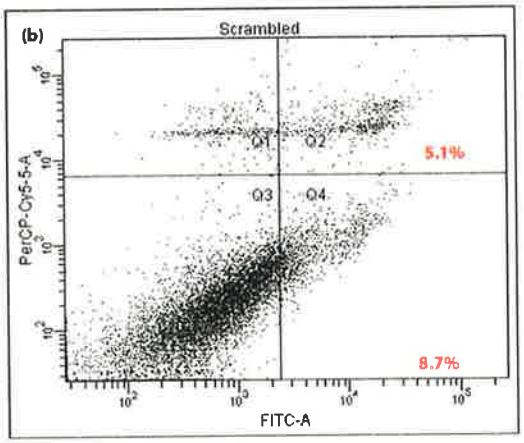

Experiment Name: Niamh-Annexin Kelly
Specimen Name: 15th Dec 2009
Tube Name: Scrambled
Record Date: Dec 15, 2009 4:16:14 PM

Population	#Events	%Parent	FITC-A Mean	PerCP-Cy5-... Mean
All Events	10,000	###	1,839	2,752
Q1	328	3.3	978	24,818
Q2	509	5.1	14,552	32,724
Q3	8,295	83.0	658	215
Q4	868	8.7	5,996	1,085

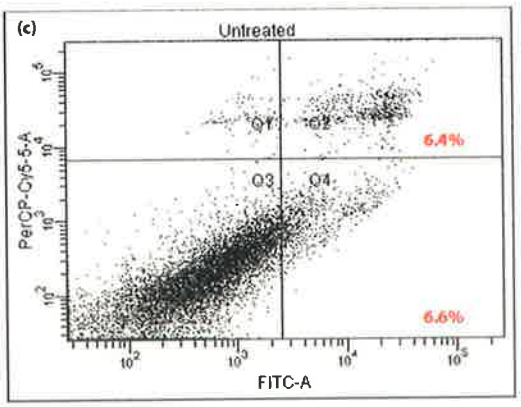

Experiment Name: Niamh-Annexin Kelly
Specimen Name: 15th Dec 2009
Tube Name: Untreated
Record Date: Dec 15, 2009 4:01:17 PM

Population	#Events	%Parent	FITC-A Mean	PerCP-Cy5-... Mean
Q1	361	1.2	1,303	27,364
Q2	1,911	6.4	18,592	34,888
Q3	25,754	85.8	555	214
Q4	1,974	6.6	6,848	1,288

Figure 3.9. MiR-184 induces apoptosis in the Kelly NB cells. Flow cytometry analysis was performed using Annexin V staining of cells transfected with (a) the mature mimic to miR-184, (b) the scrambled control and (c) non treated cells.

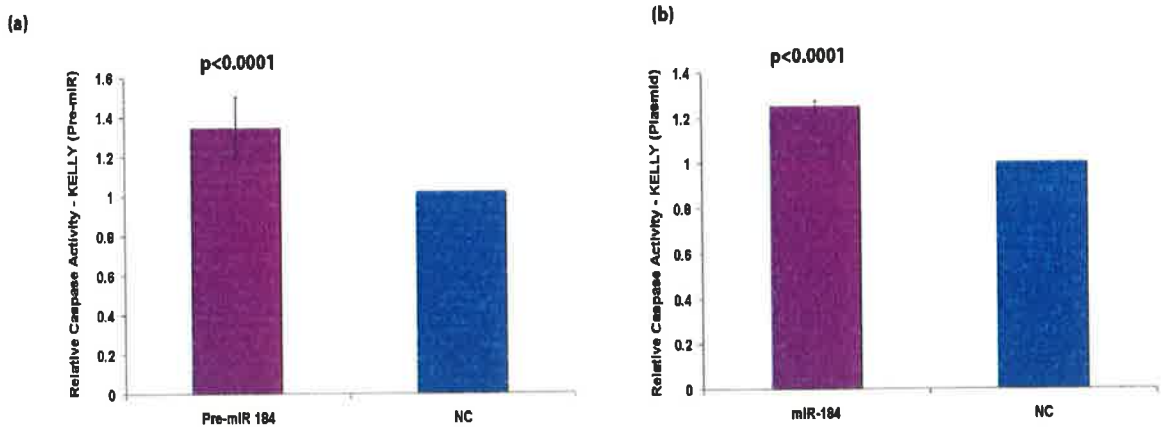

Figure 3.10. Over-expression of miR-184 activates caspase 3/7 in the Kelly NB cell line. MiR-184 up-regulation using the (a) the Pre-miR 184 and (b) pcDNA6.2-GW/EmGFP-miR-184 resulted in an increase in caspase 3/7 relative to the negative controls (NC) in Kelly cells.

3.1.7 Over-expression of miR-184 induces apoptosis in SK-N-AS cells

SK-N-AS cells transfected with either the miR-184 expressing mature mimic or the pcDNA6.2-GW/EmGFP-miR-184 expression plasmid both resulted in a significant increase in caspase 3/7 (Figure 3.11).

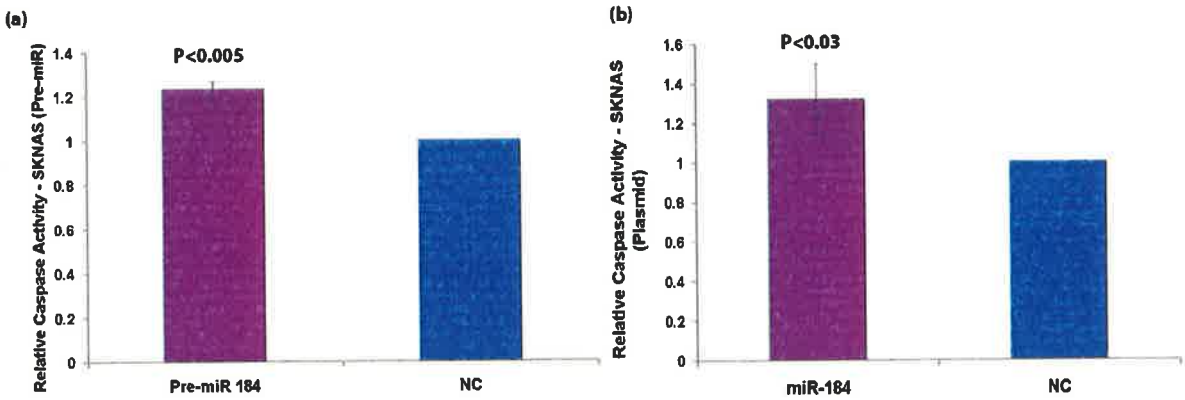

Figure 3.11 MiR-184 mature mimics and plasmid can induce apoptosis in SK-N-AS neuroblastoma cells. MiR-184 up-regulation using (a) the mature mimics 184 resulted in an increase in caspase activity relative to the NC in SK-N-AS cells, a similar result was seen using (b) pcDNA6.2-GW/EmGFP-miR-184 relative to empty plasmid.

3.1.8 Ectopic over-expression of miR-184 reduces the invasive potential of NB cell lines

Treatment with the mature miR-184 mimic resulted in a significant reduction in the number of cells which invaded across a matrigel-membrane in both Kelly and SK-N-AS cells relative to the scrambled oligonucleotide NC (Figures 3.12-3.14). The anti-miR also had a profound affect on invasion, which was very evident in SK-N-AS cells, a naturally invasive cell line. Down regulation of miR-184 in SK-N-AS, (which has highest endogenous levels of miR-184 (Figure 3.1), demonstrated a greater than 2-fold increase in invasion when compared to a scrambled NC (Figure 3.13 a).

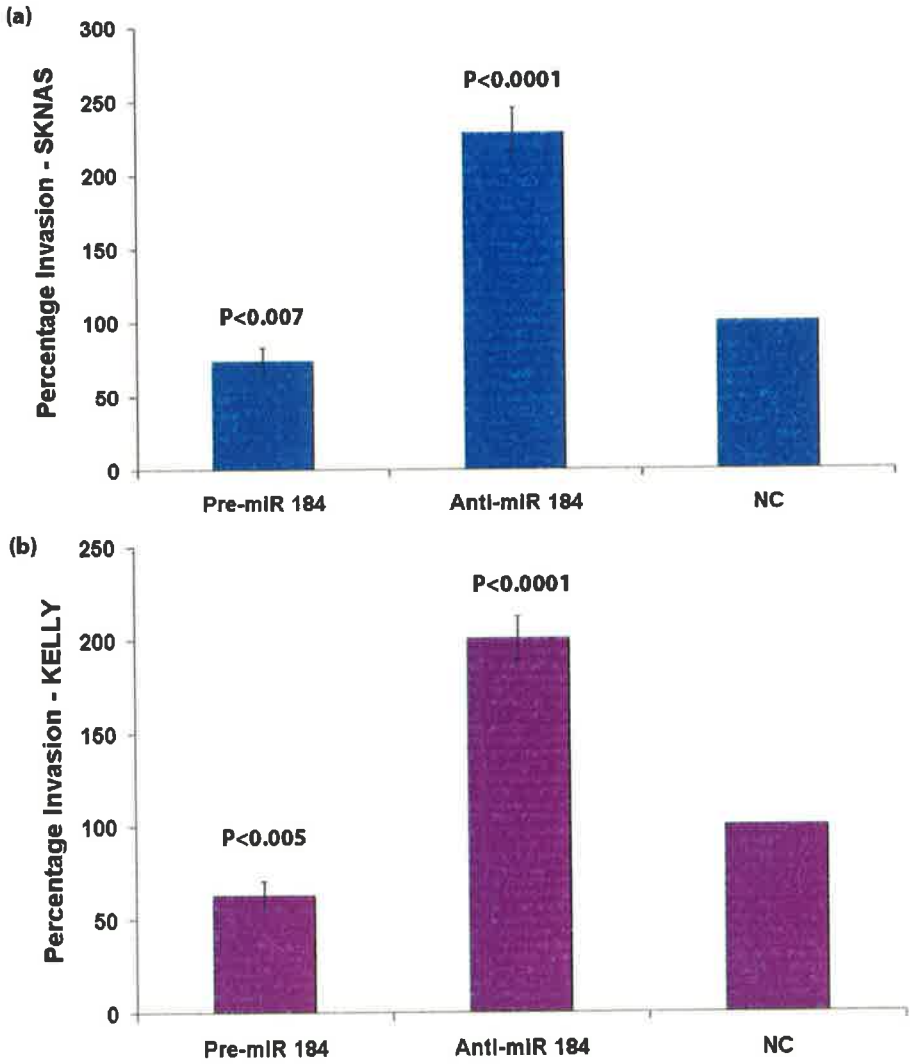

Figure 3.12. Effects of miR-184 expression on neuroblastoma cell invasion. Graphs show the effect of miR-184 over expression using the mature mimics and miR-184 knockdown using the anti-miR on percentage cell invasion, relative to scrambled NC set as 100% in (a) SK-N-AS and (b) Kelly neuroblastoma cells.

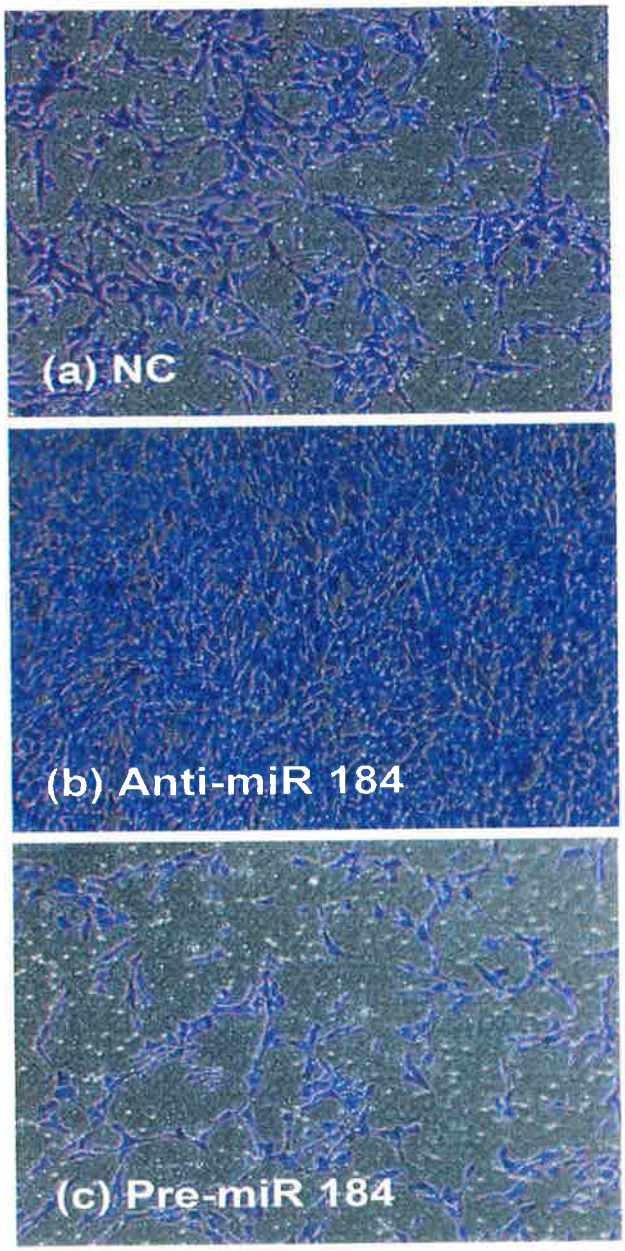

Figure 3.13 Images of invading SK-N-AS cells transfected with mature miR-184 mimic and anti-miR to miR 184. Cells stained with crystal violet (purple) have invaded through the matrigel structure. The scrambled oligonucleotide control (NC) is representative of normal ability of SK-N-AS cells to invade.

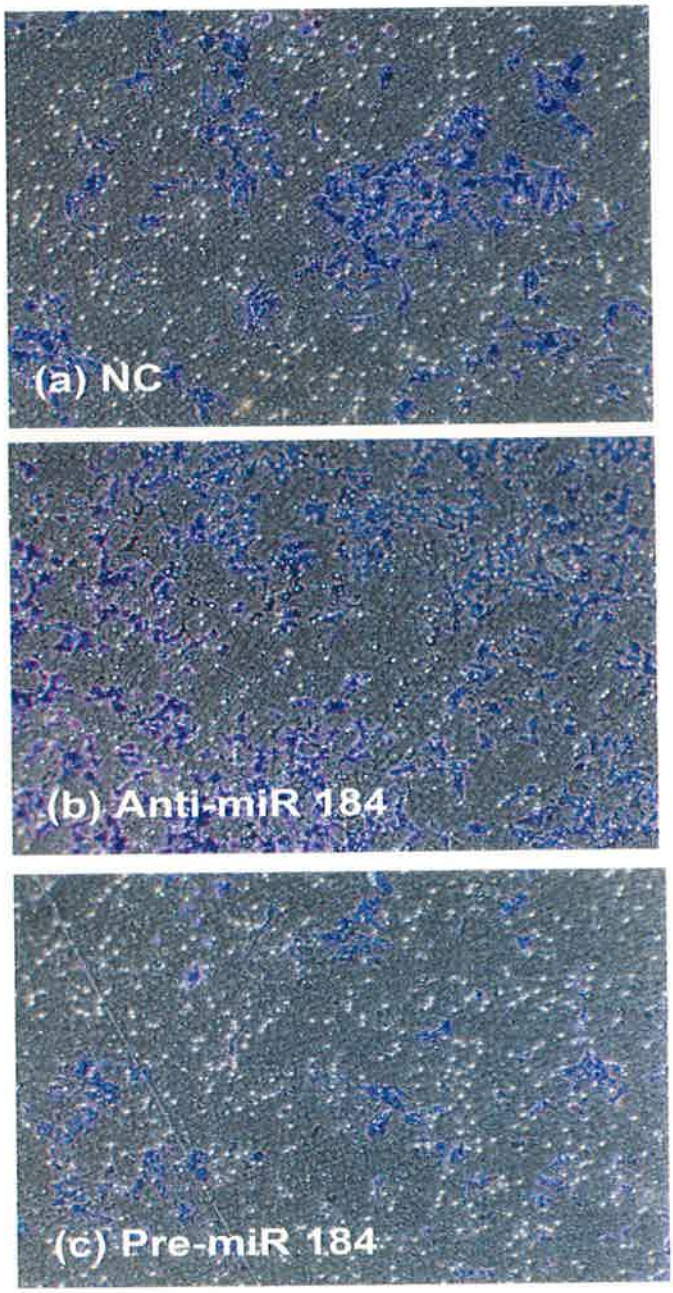

Figure 3.14. Images of invading Kelly cells transfected with the mature miR-184 mimic and anti-miR to miR 184. Cells stained with crystal violet (purple) have invaded through the matrigel structure. The scrambled oligonucleotide NC is representative of normal ability of Kelly cells to invade.

3.1.9 *AKT2* is a predicted target of miR-184

The Sanger miR Registry Database (http://microrna.sanger.ac.uk/sequences/ was used to identify potential targets of miR-184. A region in the 3'UTR of *AKT2*, a well documented oncogenic, pro-survival protein was among the top 3% (n=30) of miR-184 predicted targets and showed a very high complementarity (13 base-pair match) to the miR-184 seed region (Figure 3.15).

Figure 3.15. MiR-184 predicted alignment with *AKT2*. *AKT2* was among the top 3% (n = 30) of miR-184 predicted targets, and had a high level of sequence complementarity with the miR-184 seed region (a 13 base pair match).

3.1.10 The expression levels of miR-184 and *AKT2* are inversely correlated

RTqPCR analysis of miR-184 (Figure 3.1) and *AKT2* mRNA (Figure 3.16 a) levels demonstrated that the expression of these transcripts were inversely correlated, indicating that miR-184 could be causing degradation of the *AKT2* mRNA sequence. AKT2 protein levels were also lower in cell lines with higher levels of miR-184 (Figure 3.16 a). To investigate this further, 19 tumours samples were selected from the cohort previously described (209); 10 with low miR-184 levels (MNA tumours) and 9 with high levels (non MNA). This analysis confirmed, that *AKT2* was significantly repressed ($p < 0.002$) in tumours with high miR-184 levels when compared to tumours with low miR-184 expression (Figure 3.16 b). Interestingly, *AKT2* levels were lower in *MYCN* single copy compared to MNA tumours ($P<0.035$) (Figure 3.16 c), confirming that the relationship between miR-184 and *MYCN* has an impact on *AKT2* levels.

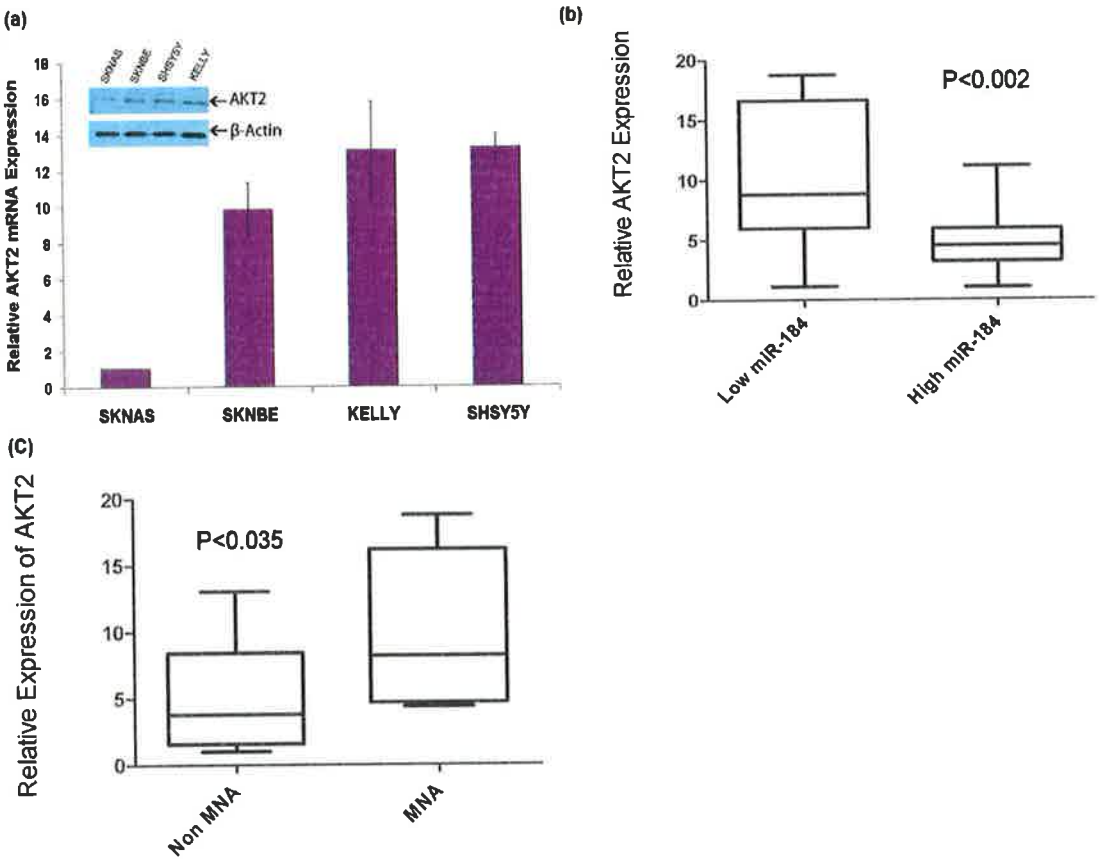

Figure 3.16. MiR-184 expression is inversely correlated with *AKT2* in NB cell lines and primary tumours. (a) *AKT2* mRNA and protein levels are inversely correlated with miR-184 levels (Figure 3.1) in NB cell lines. This inverse relationship was also observed in (b) clinical samples. Tumours with low miR-184 (n=9) had higher levels of *AKT2* than tumours with higher levels of miR-184 (n=10). Higher levels of *AKT2* were also seen in (c) MNA tumours versus non MNA tumours.

3.1.11 Ectopic over expression of miR-184 results in down regulation of *AKT2*

To confirm that *AKT2* was indeed regulated by miR-184 in neuroblastoma, the miR-184 mature mimic and the anti-miR to miR-184 were individually transfected into Kelly and SK-N-AS NB cell lines. Cells were harvested for total RNA and protein at 24, 48 and 72 h. A large decrease of *AKT2* mRNA was observed over all three time points in Kelly (Figure 3.17 a) and SK-N-AS (Figure 3.17 b) relative to the scrambled NC. Conversely, the suppression of miR-184 using the anti-mir-184 caused an increase in mRNA for *AKT2* across all time points in both cell lines, which was also confirmed at protein level (Figure 3.17 a inset). These results strengthen the argument that miR-184 reduces NB cell proliferation by degrading the mRNA of *AKT2*, thus preventing the translation of this pro-survival protein.

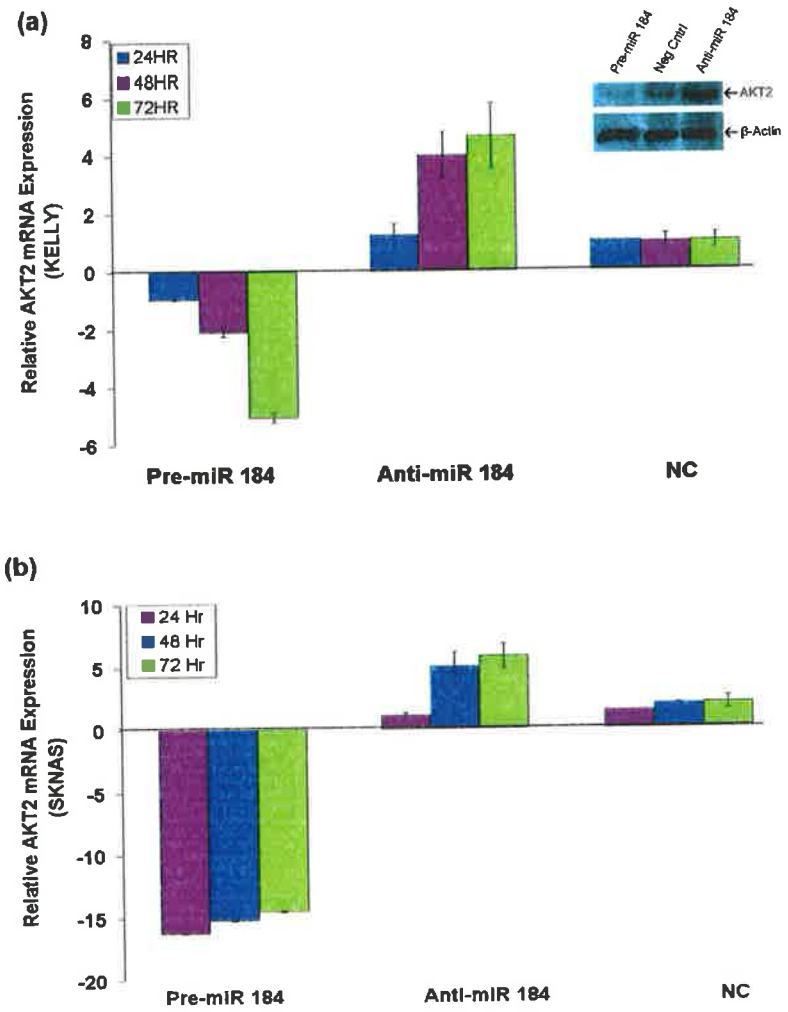

Figure 3.17. Expression of miR-184 negatively affects AKT2 mRNA and protein levels. The miR-184 mature mimic and anti-miR to miR-184 resulted in the down-regulation and up-regulation of *AKT2* in (a) Kelly (mRNA and protein) and (b) SK-N-AS mRNA relative to the scrambled oligonucleotide NC.

3.1.12 *AKT2* is a direct target of miR-184

To validate *AKT2* as a direct target of miR-184 a luciferase reporter vector containing the miR-184 target site of the *AKT2* 3'UTR was constructed. Co-transfection of the mature mimic to miR-184 with this plasmid resulted in 44% reduction in luciferase expression relative to the plasmid transfected with the scrambled negative control (Figure 3.18). A control vector was also constructed with a 3 base pair mutation in the seed region of the miR-184 binding site. This mutated plasmid showed no reduction in luciferase activity when transfected with miR-184 compared to the mutated plasmid co-transfected with the scrambled negative control, confirming that *AKT2* is a direct target of miR-184 and that seed region binding by miR-184 is essential for RNA degradation.

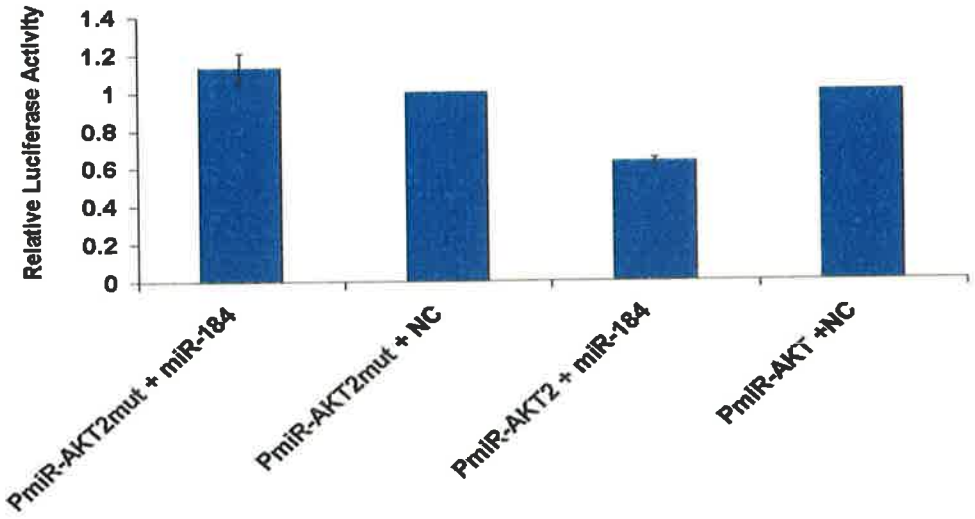

Figure 3.18. *AKT2* is a direct target of miR-184. Kelly cells were co-transfected with miR-184 and the PmiR-REPORT™ luciferase vector containing the miR-184 target site of *AKT2* or miR-184 and the PmiR Report luciferase vector containing the mutated target site. Overall decrease in luciferase activity was measured relative to each vector (PmiR-AKT2 and PmiR-AKT2mut) co-transfected with a scrambled oligonucleotide NC.

3.1.13 *AKT2* depletion in neuroblastoma cells using three different small interfering RNAs (siRNAs)

MiR-184 has many computationally predicted targets, so in order to confirm that the reduction in cell numbers by miR-184 occurs primarily through targeting *AKT2,* we transfected both Kelly and SK-N-AS NB cell lines with three different siRNAs to *AKT2* and examined the effects of cell proliferation. The efficiency of *AKT2* knockdown ranged from 60 to 98% (Figure 3.19).

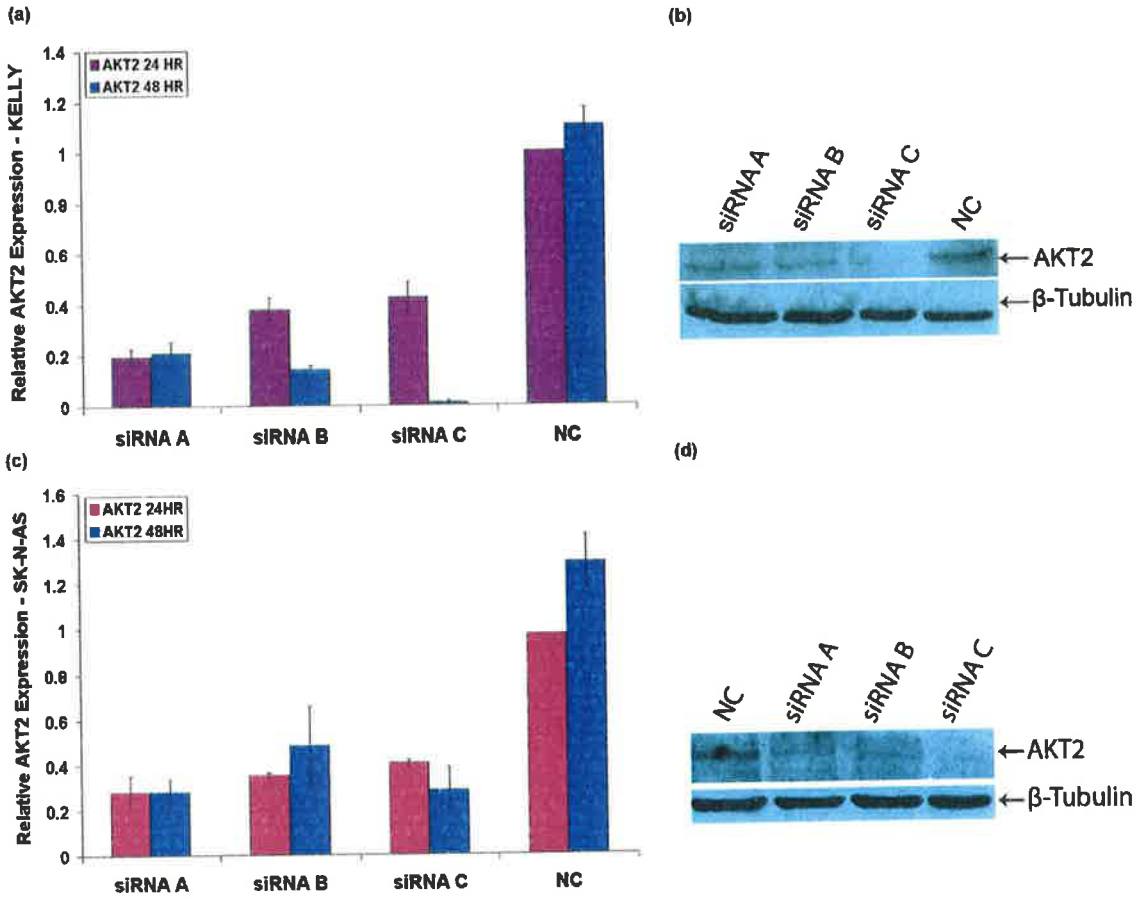

Figure 3.19. SiRNA down-regulation of *AKT2*. Three different siRNAs to AKT2 were used to knock down *AKT2* levels. Knock down of both RNA and protein was seen in (a and b) Kelly cells and (c and d) SK-N-AS cells relative to the scrambled oligonucleotide NC.

3.1.14 Effects of *AKT2* depletion on neuroblastoma cell numbers

As it has previously been demonstrated that miR-184 up-regulation causes a decrease in cell numbers (Section 3.1.4), here using siRNAs to *AKT2* we show that knockout of *AKT2* causes a similar effect on cell numbers. Both Kelly and SK-N-AS cell lines exhibited a marked inhibition in cell growth compared to the scrambled NC (Figure 3.20 a and b).

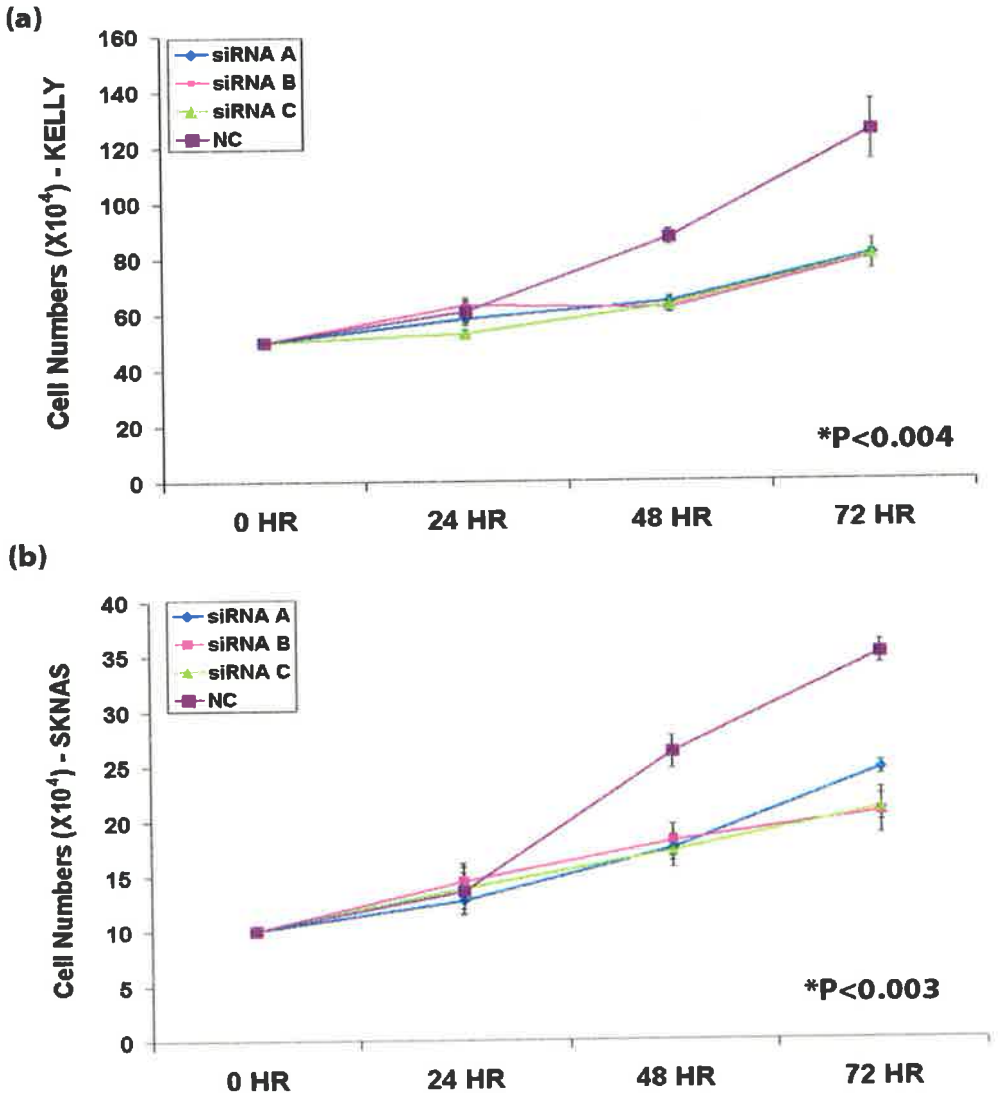

Figure 3.20. SiRNA knock-down of *AKT2* using three different siRNAs results in a reduction in cell numbers. 3 siRNAs which target *AKT2* resulted in a significant reduction in cell numbers in (a) Kelly and (b) SK-N-AS, after 72 h when compared to a scrambled oligonucleotide NC. *P-value displayed on graph was the least significant of the 3 siRNAs tested.

3.1.15 *AKT2* knock-down induces apoptosis in NB cell lines

Both Kelly and SK-N-AS cell lines exhibited a marked increase in levels of apoptosis as measured by caspase 3/7 activity, following transfection with three different siRNAs to *AKT2* (Figure 3.21a). Apoptosis was also noted using siRNA C in Kelly cells, when analyzed using Annexin V and PI staining with FACs analysis (Figure 3.21 b and c).

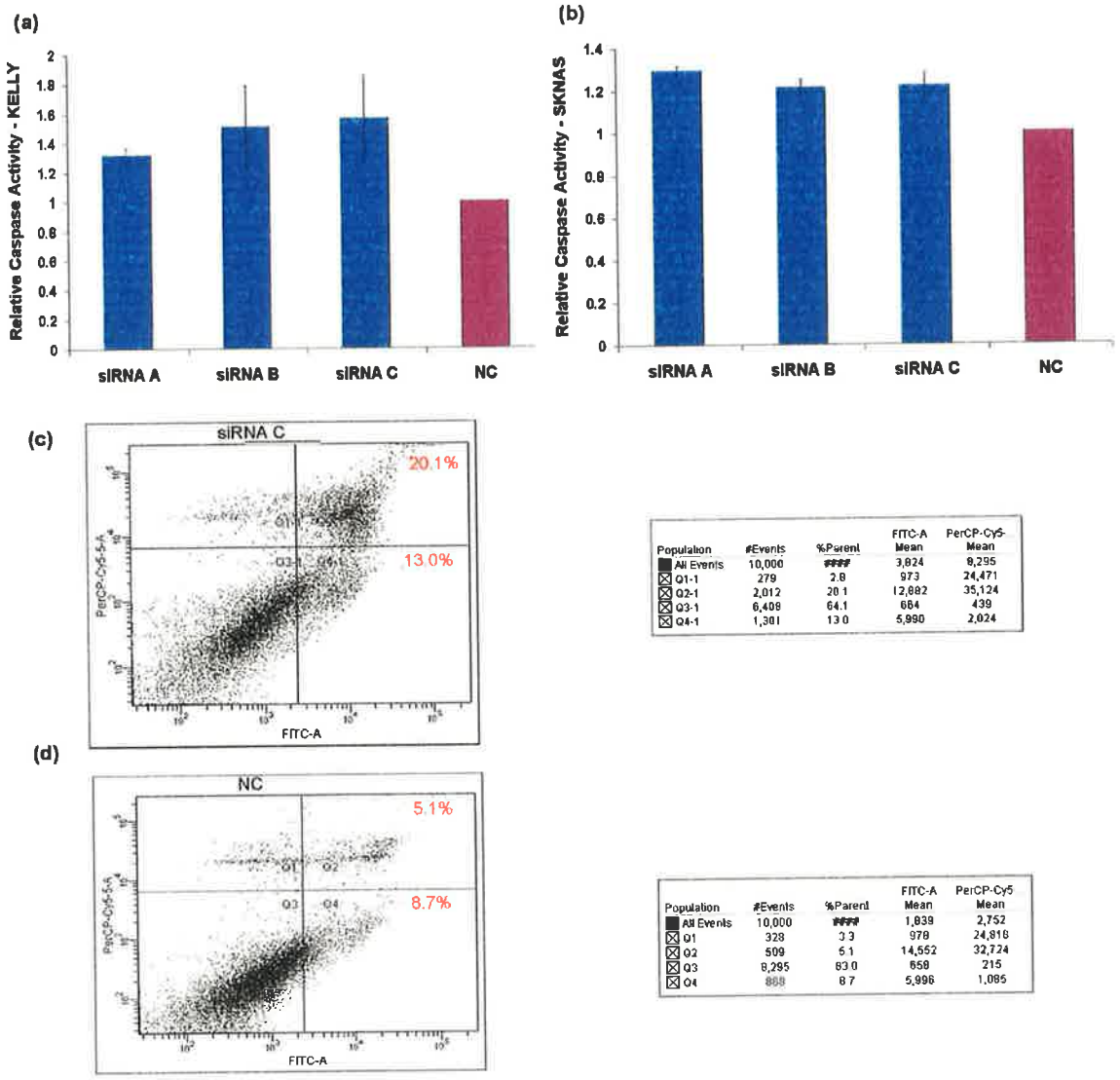

Figure 3.21. SiRNA knock-down of *AKT2* results in an increase in apoptosis. SiRNA knockdown resulted in an increase in apoptosis in (a) Kelly and (b) SK-N-AS cell lines as measured by caspase 3/7 activity relative to scrambled oligonucleotide NC. Validation was carried out with (c) siRNA C, in Kelly cells using annexin V and PI staining, compared to (d) cells treated with the scrambled oligonucleotide NC.

3.1.16 *AKT2* over expression on increase NB cell numbers

To demonstrate that the increase in cell number which was demonstrated following miR-184 down-regulation resulted specifically from *AKT2* up-regulation, the pcDNA3-AKT2 plasmid was transfected into Kelly cells. This resulted in a 5 to 22-fold increase in *AKT2* mRNA levels (Figure 3.22 a) and a 30% increase in cell numbers 72h post transfection relative to the NC (Figure 3.22 b; $P = 0.006$).

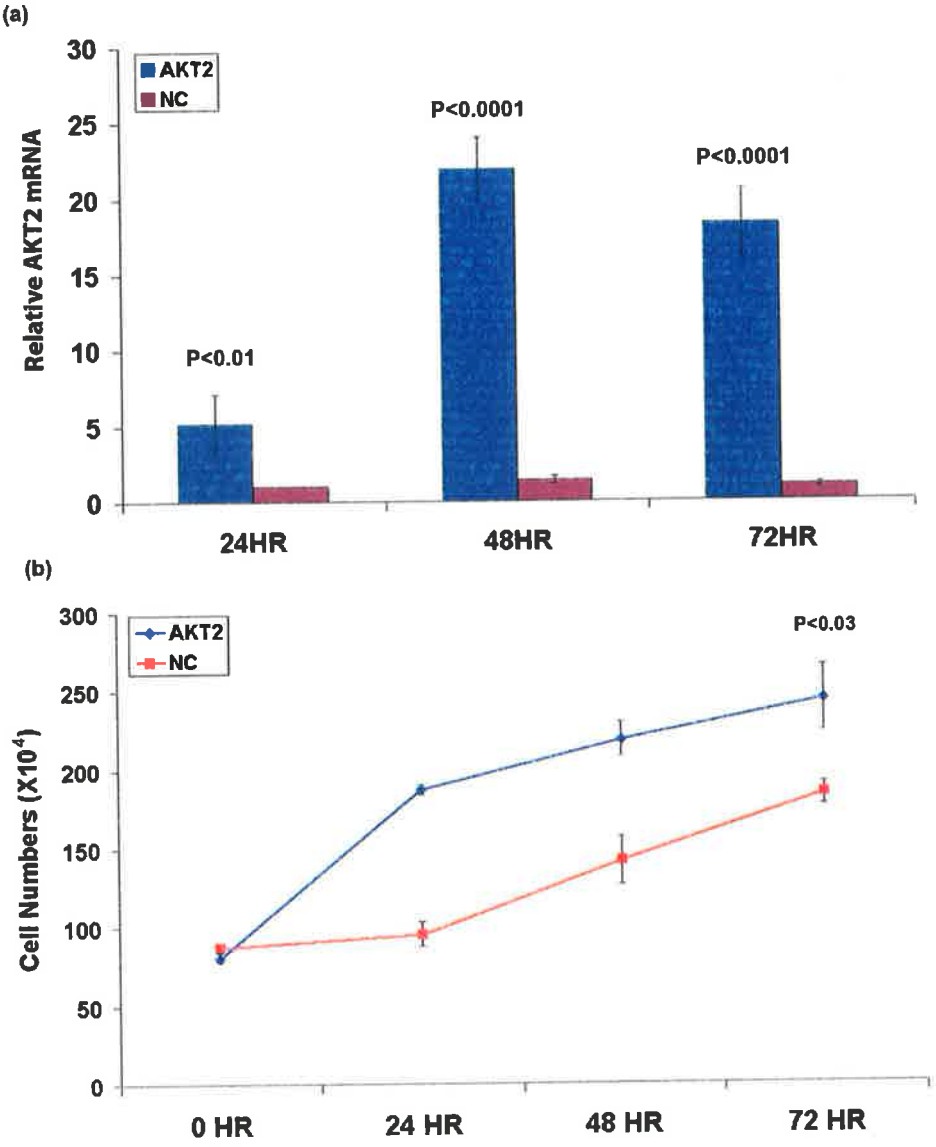

Figure 3.22. *AKT2* up-regulation results in an increase in cell numbers. (a) Up-regulation of *AKT2* using the pcDNA3-AKT2 plasmid transfection results in a significant up-regulation of *AKT2* mRNA, this up-regulation resulted (b) in an increase in cell numbers relative to Kelly cells transfected with the empty pcDNA3 vector (NC).

3.1.17 *AKT2* over-expression can rescue the miR-184 induced phenotype

The pcDNA3-AKT2 construct lacks the miR-184 binding site in the 3' UTR, therefore pcDNA3-AKT2 was co-transfected with the miR-184 mimic to determine if ectopic up-regulation of *AKT2* could rescue Kelly cells from the phenotypic effects of miR-184. As illustrated in Figure 3.23 a, RT-qPCR analysis of *AKT2* mRNA indicated that there were statistically significant ($p < 0.01$) differences in *AKT2* mRNA levels in each of the transfected cell populations for each time point, consistent with expectations. As illustrated in Figure 3.23 b, the number of cells accumulated over 72h for Kelly cells co-transfected with pcDNA3-AKT2 and miR-184 was not statistically different to that of Kelly cells transfected with a negative control oligonucleotide and the pcDNA3 empty vector. However, co-transfection with pcDNA3-AKT2 and miR-184 mimics yielded a cell accumulation rate that was significantly higher then cells transfected with miR-184 mimics ($p<0.003$) or miR-184 mimics and pc-DNA3.1 empty vector ($p <0.003$). This indicates that ectopic *AKT2* lacking a miR-184 binding site can rescue the cells from ectopic miR-184 up-regulation (Figure 3.23 b). From all of the above experiments, we conclude that the phenotypic effects of miR-184 expression, at least to a large extent, can be attributed to the targeting and reduction of *AKT2*.

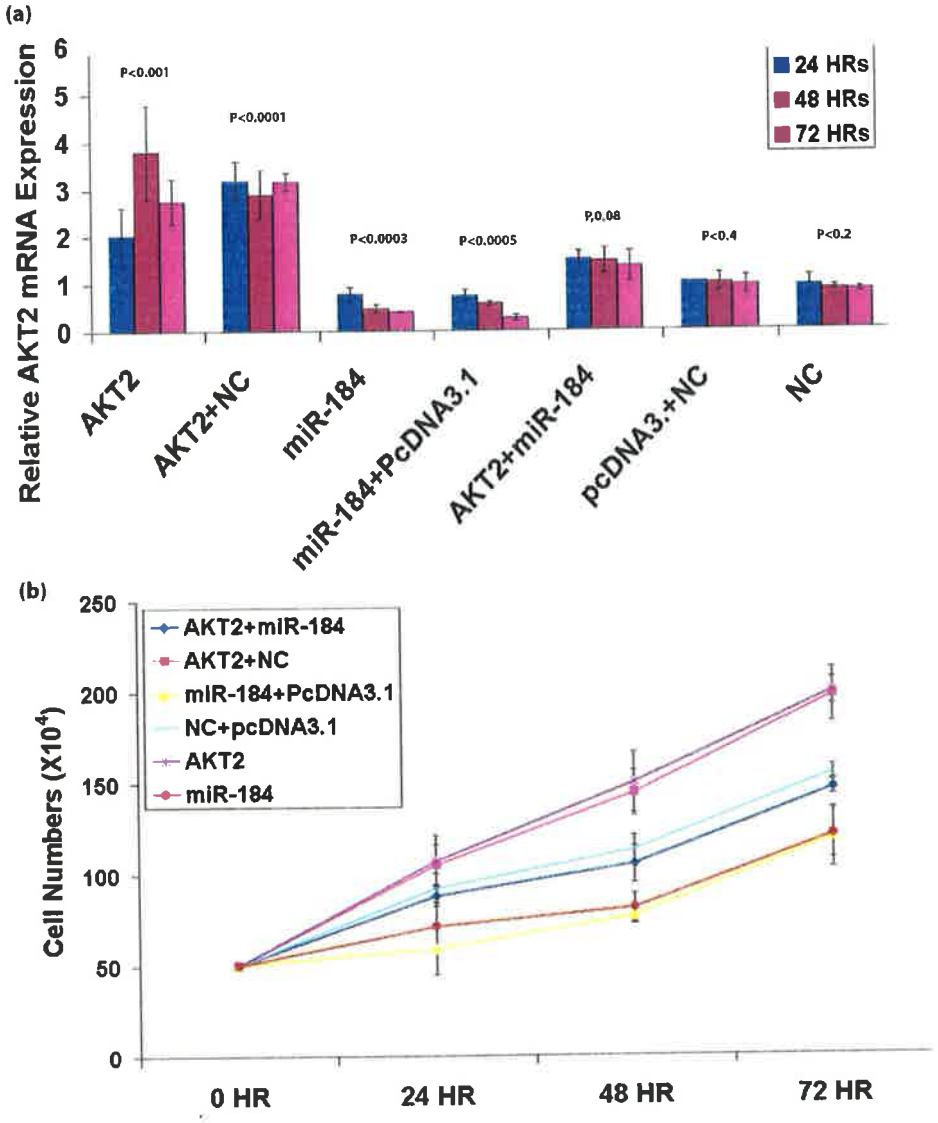

Figure 3.23. *AKT2* rescue of the miR-184 induced phenotype. (a) *AKT2* expression in Kelly cells is demonstrated using RTqPCR at 24, 48 and 72h post transfection with different combinations of the *AKT2* or NC plasmid and miR-184 or NC oligonucleotides. In the *AKT2* rescue experiment (*AKT2* plasmid + miR-184 mimics); *AKT2* levels are not significantly different from the negative controls (pDNA3.1 empty vector + negative control oligo or negative control oligo). (b) Co-transfection of AKT2 with miR-184 can rescue the miR-184 phenotypic effects on cell numbers.

3.1.18 *AKT1* and *AKT3* in NB cell lines

Levels of *AKT1* and *AKT3* were examined in NB cell lines through RTqPCR. *AKT3* was expressed at very low levels, (CT values of 35+) or was not expressed at all. As *AKT1* was expressed we examined the effects of transfection with miR-184 on *AKT1* to determine if this miR also affects the other members of the *AKT* family. Consistent with the fact that *AKT1* does not contain a predicted binding site for miR-184 the mRNA levels remained constant after transfection with miR-184 (Figure 3.24 a). We also carried out RTqPCR to ensure that the siRNAs to *AKT2* did not result in unspecific targeting of *AKT1* levels. All three siRNAs in this study had no effect on the mRNA levels of *AKT1* (Figure 3.24 b).

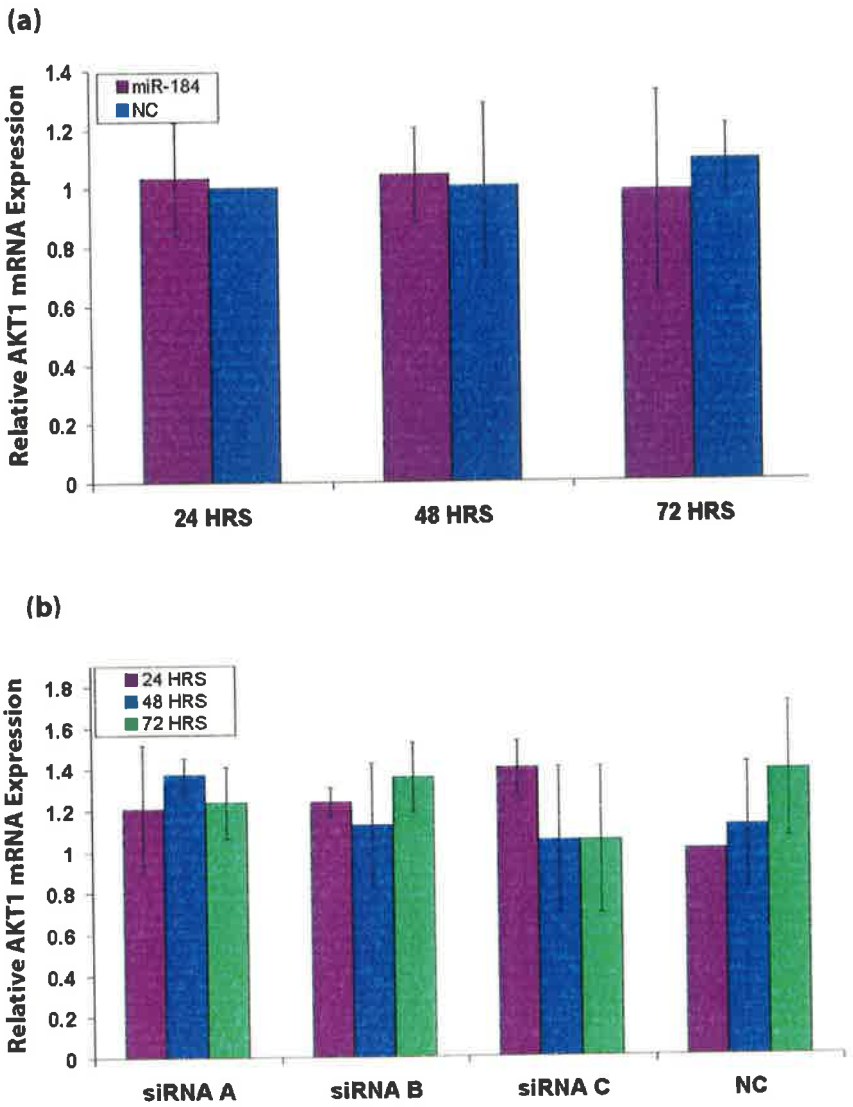

Figure 3.24. *AKT1* levels in Kelly cells transfected with miR-184 and siRNAs to *AKT2*. (a) *AKT1* levels were measured in Kelly cells transfected with miR-184 compared to cells transfected with the scrambled oligonucleotide control. There was no significant alterations in *AKT1* following miR-184 transfection. (b) *AKT1* levels were also quantified in Kelly cells transfected with the three siRNAs to *AKT2* there was no significant change in *AKT1* with these siRNAs.

3.1.19 *AKT* isoforms and their association with survival in neuroblastoma tumours

R2 database, http://hgserver1.amc.nl, is a microarray analysis and visualization platform, developed and run by The Department of Human Genetics Academic and Medical Centre, University of Amsterdam. A data set of 88 NB tumours was used to examine the association of each *AKT* isoform with patient survival. Kaplan Meier analysis demonstrated that high *AKT2* mRNA expression was predictive of poor overall survival and relapse free survival before correction for multiple comparisons. After correction this data did not remain significant however a trend towards significance in both cases was noted (Figure 3.25 a and b). *AKT2* was also shown to have the highest expression in poor prognosis stage 4 tumours, compared to other tumour stages $p<0.003$ (Figure 3.25 c). This *AKT1* had no association with overall (Figure 3.26 a) or event free survival (Figure 3.26 b) in neuroblastoma. However, low *AKT3* mRNA expression values were associated with poor overall (Figure 3.26 c) and event free survival (Figure 3.26 d). Interestingly, *AKT3* transcripts were undetectable in cell lines that were derived from poor prognosis tumours.

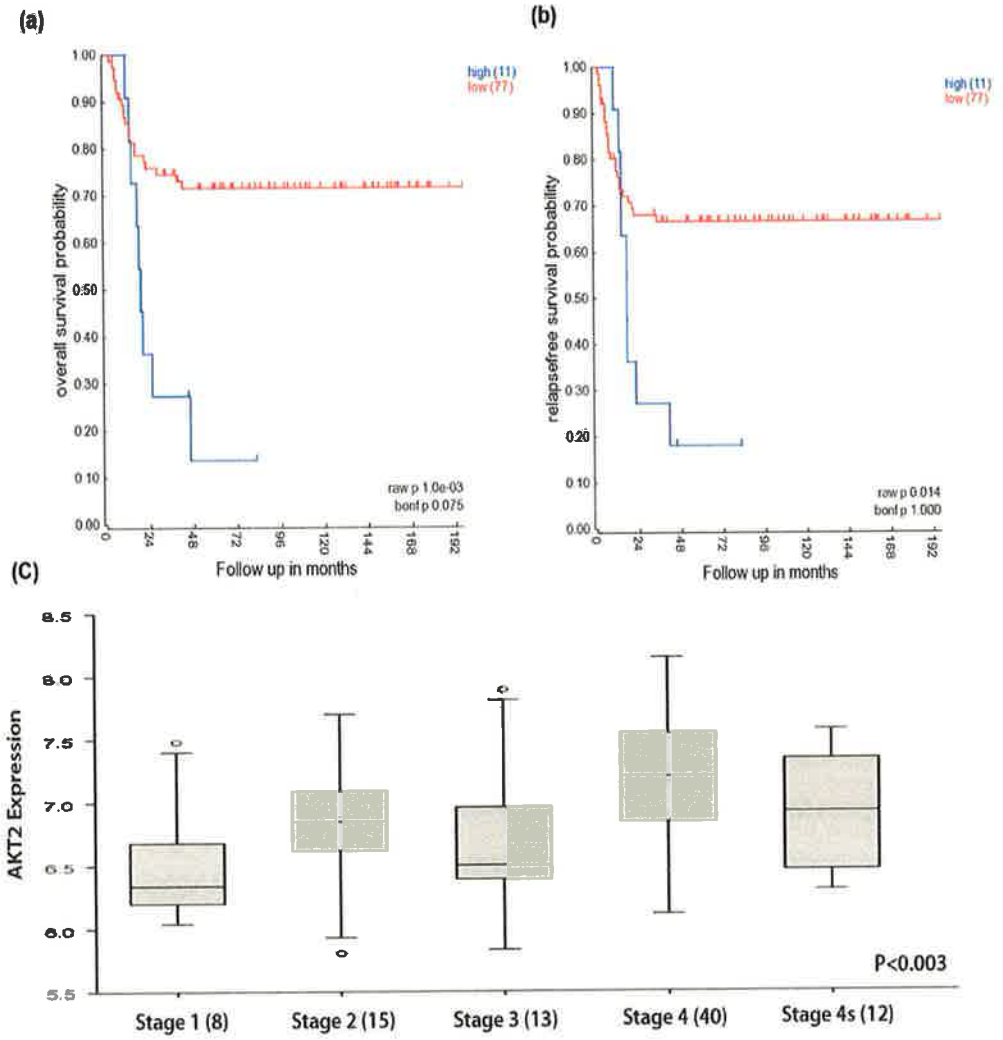

Figure 3.25. *AKT2* is associated with overall survival, relapse free survival and stage in neuroblastoma tumours. (a) Low levels of *AKT2* are associated with a good prognosis before correction for multiple comparisons in a NB patient cohort; (b) low *AKT2* levels are also positively associated with relapse free survival before correction for multiple comparisons. (c) *AKT2* is expressed at highest levels in stage 4 tumours (P<0.003).

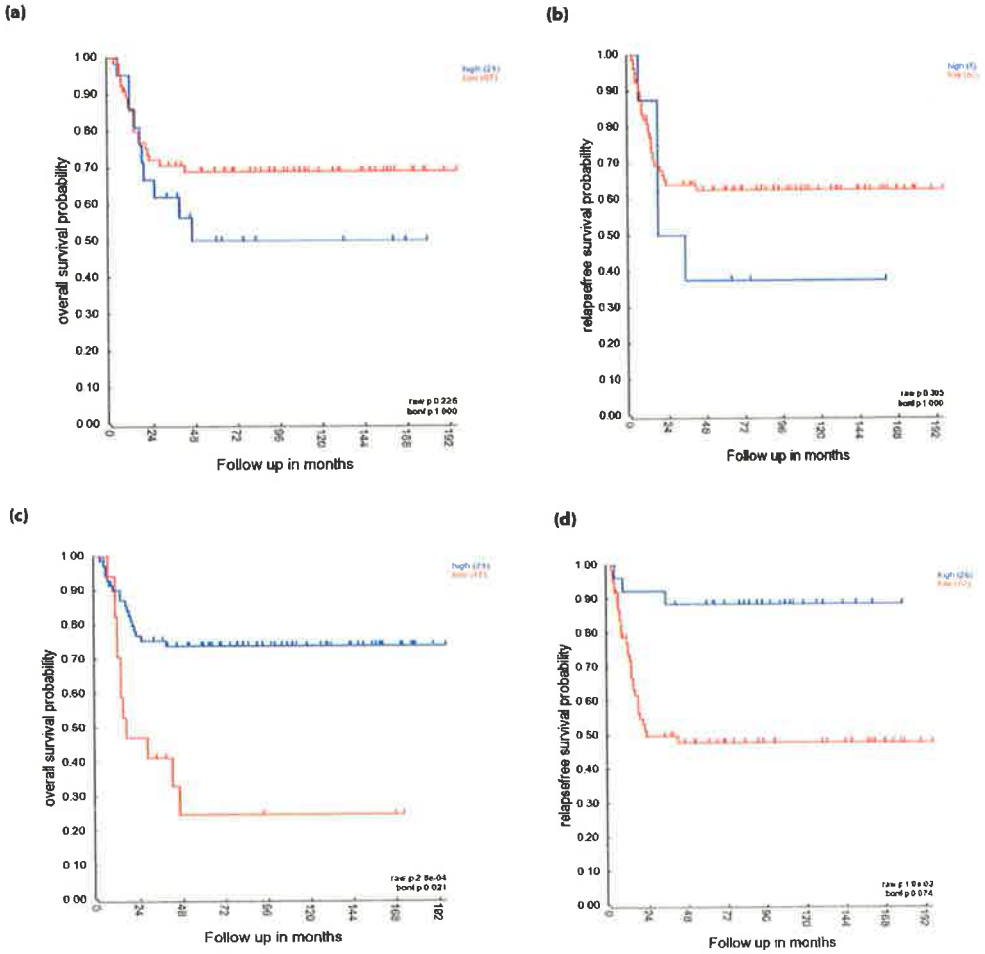

Figure 3.26. Survival analysis for *AKT1* and *AKT3* in neuroblastoma patients. Kaplan meier curve for *AKT1* displayed no association with (a) overall or (b) event free survival in neuroblastoma. High levels of *AKT3* are positively associated better with (c) overall survival probability, high *AKT3* levels are also positively associated with (d) relapse free survival.

3.2 Discussion

3.2.1 MiR-184: a tumour suppressor in neuroblastoma

Amplification of *MYCN* is a key prognostic factor in neuroblastoma (46). Understanding the mechanisms by which *MYCN* amplification exerts its effects on neuroblastoma disease initiation and progression is paramount to understanding this aggressive subtype of neuroblastoma. As previously discussed, a number of studies have demonstrated that MYCN can exert regulatory control over a large number of microRNAs in neuroblastoma (208-210, 229). It is evident from this study that MYCN is the driving force, whether direct or in-direct, behind the suppression of miR-184 in MNA tumours. We have demonstrated *MYCN* binding occurs approximately 2.7kb up-stream of the miR-184 gene on chromosome 15 (212). This finding cannot however be fully elucidated as the definitive mechanism for control of miR-184 expression, until the promoter region of miR-184 is functionally annotated.

An initial aim of this study was to address the controversy surrounding the use of mature microRNA mimics in ectopic over-expression experiments, which result in supra-physiological changes in mature microRNA levels. We set out to determine if the use of mature microRNA mimics has a different functional effect when compared to more physiological miR levels, through the use of a miRNA expression vector producing the pre-microRNA stem-loop for miR-184. The resulting pre-microRNA stem loop must be processed by Dicer and therefore results in more physiological levels of up-regulation. The functional effects of over-expression of miR-184 at physiological levels were comparable to those induced by the mature microRNA mimics to miR-184, confirming the findings

previously report by Chen and Stallings (2007) (208). This suggests that microRNA levels may be saturated and massive supra-physiological levels versus physiological levels do not differ in their functional effects. Based upon this result, it was deemed un-necessary to design microRNA stem-loop plasmids for functional analysis of all microRNAs in this study.

Here we validate miR-184 as a potent tumour-suppressor microRNA in NB cells. Over-expression of miR-184 induced caspase-mediated apoptosis resulting in reduced cell numbers. We also demonstrate a substantial reduction in cell invasiveness; however the primary conclusion that can be drawn from these results is that the reduction in cellular invasiveness is most likely to be due to a reduction in viable cells as a result of the increase in apoptosis levels induced by miR-184. To understand the mechanism by which miR-184 induces apoptosis in neuroblastoma it was necessary to identify mRNA targets. Here we identify and validate *AKT2,* a member of the potent pro-survival PI3K pathway as a direct mRNA target of miR-184 and conclude that MYCN can either directly or indirectly regulate the effects of *AKT2* through suppression of miR-184.

Although miR-184 is predicted to target a large number of genes, we have established that the induction of apoptosis following miR-184 up-regulation is predominantly due to knockdown of *AKT2.* SiRNA down-regulation of *AKT2* induced a level of apoptosis comparable to that demonstrated by miR-184 ectopic over expression. Furthermore, a rescue experiment demonstrated that an *AKT2* expressing plasmid lacking the 3'UTR of *AKT2* could rescue the effects of miR-184 ectopic over-expression on cell viability.

AKT2 is a homolog of the v-akt oncogene; it encodes a serine-threonine kinase protein, a member of the AKT family of proteins which are down-stream effectors of the potent pro-survival PI3K pathway (260, 261). The PI3K-AKT pathway is a cell signalling pathway which is well established to play roles in cellular functions such as cell survival, cell growth and angiogenesis. Aberrant activation of this pathway is a characteristic feature of human cancers and has been associated with poor survival in numerous cancers including glioblastoma, breast , prostate and lung (Reviewed in (259)). Furthermore, activation of the AKT pathway has been associated with poor survival (262) and resistance to therapy (263) in neuroblastoma.

Although there are three different isoforms of AKT (*AKT1, AKT2* and *AKT3*) which are structurally similar (264), there is little known about the precise role of each different isoform. Moro *et al.*, (2009) (265) demonstrated that AKT2 and not AKT1 or AKT3 is activated in prostate cancer cells in response to oxidative stress, resulting in enhanced cell migration and survival. It has also been established that although AKT1 may play a role in breast cancer induction, it is the *AKT2* isoform which plays a more oncogenic role in cell survival and metastasis (266). Other reported incidence of AKT2 involvement in cancer include over-expression in ovarian cancer (267), activation in breast and ovarian cancer (268) and over-expression in approximately 32% of pancreatic tumours (269). It has become evident that the AKT2 isoform may also play an important role in drug resistance, reducing sensitivity to the chemotherapeutic agent cisplatin (270) and when down regulated sensitises ovarian cancer cells to pacilitaxel-induced apoptosis (271). Biologically distinct roles for the AKT isoform have also been established in a number of

other diseases including diabetes, heart disease and schizophrenia (Reviewed in Franke, 2008 (264)).

Consistent with these results, AKT2 is perhaps the most important isoform in neuroblastoma, and targeting of *AKT2* mRNA rather than all three isoforms may be a more effective pathway for therapeutic development. Results from the R2 database verify that *AKT1* has no association with survival in neuroblastoma. This is consistent with a recent paper reporting that *AKT1,* although targeted by tumour suppressor microRNA miR-149* in neuroblastoma cell line experiments, has no inverse relationship with miR-149* expression in NB tumours and is not associated with outcome or clinical staging (272). Of greater interest were the R2 results that demonstrate that *AKT3* is under-expressed in neuroblastoma cell lines and when highly expressed in neuroblastoma tumours is associated with good overall survival. A number of groups are currently evaluating the use of small molecule inhibitors which prevent activation of this pathway as a therapeutic target for neuroblastoma and other cancers (273, 274). Results from the present study suggest that complete inactivation of all isoforms of this pathway is unnecessary and may be counterproductive. Further study is required to define the exact role of AKT3 in neuroblastoma. One of the higher scoring microRNAs predicted to target *AKT3* in TargetScan is miR-17-5p. This microRNA has been reported to act in an oncogenic manner in neuroblastoma (224) and numerous other cancers (190, 250) , suggesting a possible mechanism for the suppression of *AKT3* in neuroblastoma.

To date there is little known about miR-184 and the role it plays in development and disease. There have been contradictory reports about miR-184 and its role in the squamous cell carcinoma (SCC) of the tongue. One group reported an oncogenic anti-

apoptotic role for miR-184 (275). This group established that suppression of miR-184 in cell lines derived from this cancer resulted in a reduction in cell numbers and an increase in apoptosis. This result was however contradictory to data published by Wong *et al.,* (2008) (275) in which miR-184 was demonstrated to have a tumour suppressive effect in SCC cell lines. Wong *et al.,* (2008) showed that miR-205 targets *SHIP2*, a protein that causes a reduction in activated, phosphorylated AKT, but not in total *AKT* mRNA amounts. Thus, miR-205, which is elevated in aggressive SCC, acts in an oncogenic manner by targeting *SHIP2* and allowing AKT activation. They further established that miR-184 antagonizes miR-205, so in this sense, miR-184 acts as a tumour suppressor. This was the first report of a microRNA regulating the action of another miRNA. Another study from this group demonstrated that suppression of miR-184 resulted in enhanced AKT signaling and an increase in cellular migration (276). This enhancement was due to an increase in miR-205, as it was released from miR-184 suppression. MiR-205 subsequently down regulated *SHIP2* which dephosphorylates phosphatidylinositol 3,4,5-triphosphate (PIP3) causing an increase in phosphorylated AKT (276). However, the effects of ectopic miR-184 over-expression on total *AKT* mRNA or protein levels was not examined by Yu *et al.*, (2008),

In adult neural progenitor cells miR-184 is regulated by the methyl binding protein1 (*MBD1*) and ectopic over-expression promotes proliferation and inhibits differentiation by targeting *NUMBL*, a brain derived protein (277). It has also been demonstrated that miR-184 was reduced in highly aggressive glioblastomas, and ectopic up-regulation resulted in a reduction in cell viability (278). The same study identified *AKT2* as a potential target of miR-184 and showed evidence that over-expression of miR-

184 causes a reduction in both mRNA and protein levels of *AKT2*. They did not however validate *AKT2* as a direct miR-184 target (278).

Although we determine miR-184 to be a pro-apoptotic, tumour suppressor microRNA in neuroblastoma (208, 279), as described above there have been some other contradictory reports. Interestingly, miR-184 has an established tumour suppressor effect on phosphorylated levels of AKT in SCC, through down-regulation of miR-205. This displays an alternative indirect-effect of miR-184 on the pro-survival AKT pathway and warrants further investigation to determine if it also has this effect in neuroblastoma. The identification of miR-184 as a tumour suppressor in glioblastoma through down-regulation of *AKT2* further validates *AKT2* as a direct target of miR-184. Although miR-184 targets *AKT2* in neuroblastoma cells resulting in apoptosis, we cannot rule out the possibility that miR-184 could be targeting other genes with other phenotypic effects on the cells. It is also possible the miR-184/*AKT2* relationship demonstrated here may not translate to other tissues or cell types, as it is well established that microRNA have highly diverse functions and that their expression and function can be dependant on the cell context (280).

In conclusion, we demonstrate a miRNA mediated degradation of *AKT2* mRNA, a major downstream effector of the phosphatidylinositol 3-kinase (PI3K) pathway and one of the most potent pro-survival pathways in cancer. We identify *MYCN* as the driving force, whether direct or in-direct, behind the repression of miR-184 in MNA tumours, leading to an increase in the levels of the pro-survival protein *AKT2* and resultant tumourigenic effects. MiR-184 has potential as a therapeutic as a direct inhibitor of *AKT2* in both neuroblastoma and other cancers which display aberrant *AKT2* activities. As discussed previously the use of microRNAs as therapeutic regimens is still in early discovery stages,

however preliminary results here suggest that miR-184 could be an interesting potential therapeutic microRNA in NB. Further *in-vivo* studies with this microRNA are on-going using a NB cancer mouse model.

Chapter 4

Effects of ATRA-induced differentiation on microRNA profiles

Chapter 4

Effects of ATRA-induced differentiation on microRNA profiles

4.1 Differential expression of miRNAs in response to All Trans Retinoic Acid (ATRA) induced neuroblastoma differentiation

ATRA treatment of SK-N-BE NB cells leads to the outgrowth of neurities, the up-regulation of markers of neural differentiation such as TUBB3 and GAP43, and a decrease in the rate of cell proliferation. Most notably, ATRA treatment leads to the immediate transcriptional down-regulation of the neuroblastoma oncogene *MYCN* before the onset of cellular morphological differentiation (237), which further contributes to the remodeling of the transcriptome. *MYCN* is amplified and expressed at high levels in this cell line, and it is notable that *MYCN* amplification is one of the most potent genetic predictors of poor clinical outcome for neuroblastoma patients (44, 46). Recently, it has been demonstrated that some of the miRNAs which undergo expressional changes following ATRA treatment appear to functionally contribute to the differentiation phenotype of neuroblastoma. The first such microRNA profiling study on ATRA-induced microRNAs carried out by Chen and Stallings, 2007 (208) determined that ATRA-induced differentiation of the neuroblastoma cell line SK-N-BE resulted in profound alterations of microRNA expression. Since this earlier study was limited to the study of 32 miRNAs, an expanded set of 364 microRNAs were analysed in this differentiation model. In addition, a detailed functional analysis of selected microRNAs, most significantly altered in response to ATRA treatment was carried out.

4.1.1 Effects of ATRA treatment on SK-N-BE neuroblastoma cells

ATRA treatment of neuroblastoma SK-N-BE cells induces neuronal differentiation. Differentiation was determined by neurite outgrowth (Figure 4.1 a), a decrease in cell growth (Figure 4.1 b), up-regulation of neuronal markers GAP43 (Figure 4.1 c) and βIII Tubulin (Figure 4.1 d) at both mRNA and protein level, and a large decrease in MYCN mRNA and protein (Figure 4.1 e and f). All these factors play a well established role in neuroblastoma cell differentiation.

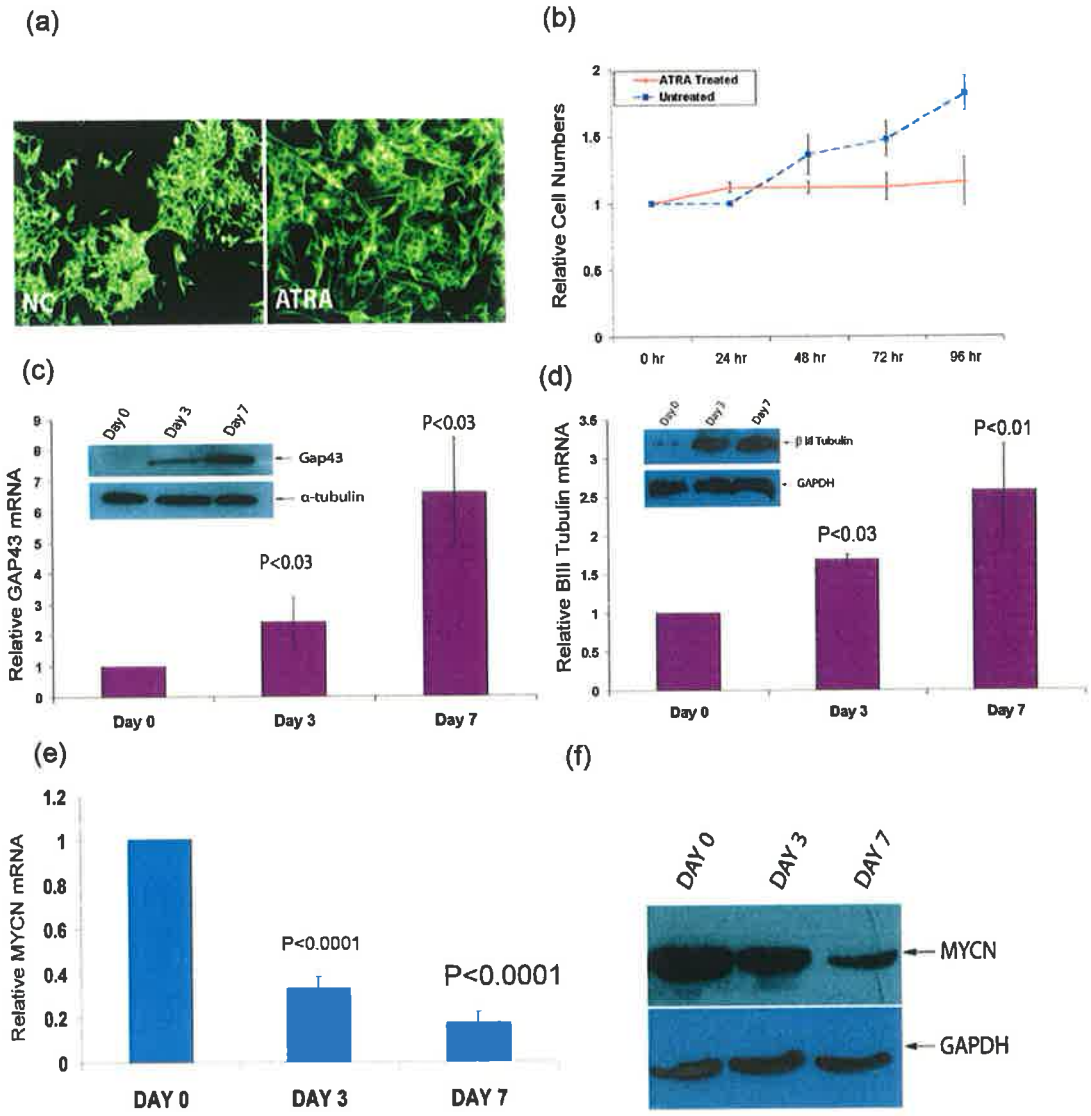

Figure 4.1. Phenotypic and molecular alterations in the SK-N-BE cell lines following ATRA treatment. ATRA induces (a) neurite outgrowth, reduces (b) cell viability relative, increases the mRNA and protein levels of neuronal markers (c) GAP43 and (d) βIII Tubulin and reduces MYCN (e) mRNA and (f) protein levels relative to non treated control.

4.1.2 Altered expression of microRNAs in response to ATRA

MicroRNA expression levels were measured for all 364 miRs in biological repeat at Day 0, Day 3 and Day 7 after treatment with ATRA using the Taqman low density arrays (TLDA). For miR analysis a fold change of ≥ 2.0 was selected as significant change in miRNA expression. Using this stringent cut off, 17 microRNAs were down regulated in response to ATRA treatment (Figure 4.2), while 17 miRs were up-regulated by ATRA.

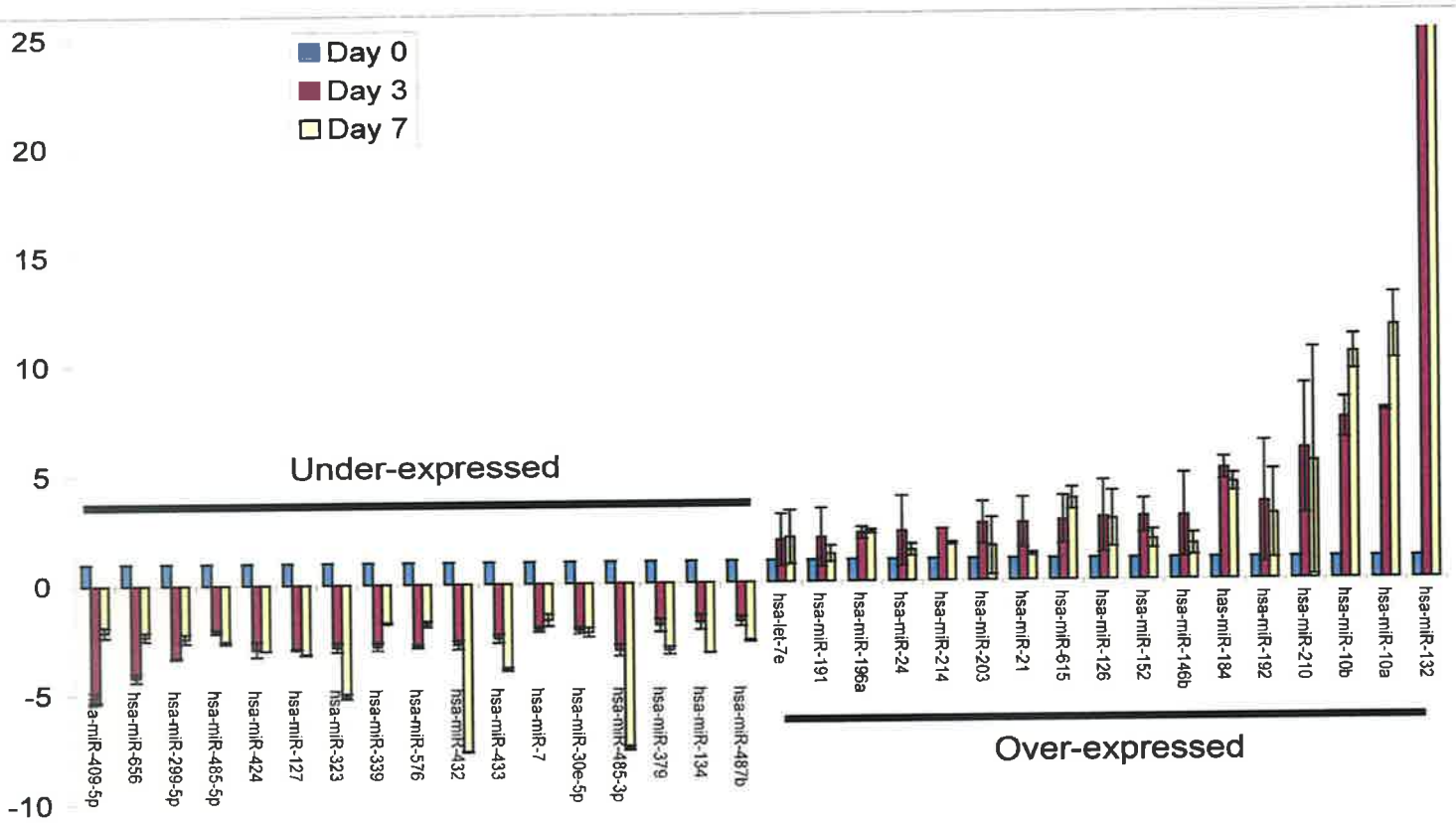

Figure 4.2. MicroRNAs differentially expressed in response to ATRA. This graph illustrates the relative quantification (RQ) of over and under expressed microRNAs post ATRA treatment at Day 3 and Day 7, relative to non-treated control (Day 0).

4.1.3 MicroRNAs "switched on" in response to ATRA treatment

In total were 7 microRNAs which were not expressed at Day 0 (a Cycle Threshold value of 40), that were significantly activated by Day 3 and Day 7 or by Day 7. It is not possible to calculate the relative quantification (RQ) of these microRNAs due to the fact that they are not expressed at day 0. The microRNAs in question are summarized in Table 4.1, with the CT change over the time course. Theoretically when a PCR is 100% efficient a 1 CT change is approximately a doubling in the quantity of DNA. This indicates that these microRNAs are indeed highly significant. The levels of these microRNAs were also examined in the tumour subset used in Bray *et al*, 2009 (209). MiR-579 was not profiled in this study so data was not available. MiR-34b was shown to be of greatest significance, and was not expressed in 58.94% of the tumours. In addition, miR-548d, miR-449 and miR-505 were also not expressed in a large number of tumours.

Table 4.1. MicroRNAs that are "switched on" by ATRA. This table lists the microRNAs that are not expressed in non treated SK-N-BE cells (Day 0), but which increase over time as indicated by decreasing CT values. Percentage tumour expression is the percentage of a subset of 145 tumours that do not express the microRNA.

microRNA	CT Day 0	CT Day 3	CT Day 7	Percentage tumours with no expression
miR-548d	40	40	33.12	24.736
miR-128b	40	40	32.50	19.47
miR-579	40	39	34.24	NA
miR-449	40	36.56	34.54	29.474
miR-34b	40	34.30	33.59	58.947
miR-146a	40	31.58	32.55	6.25
miR-505	40	36.99	32.34	38.947

4.1.4 Up-regulation of miR-184 in response to ATRA coincides with a down-regulation of *MYCN*

Interestingly, miR-184 our microRNA of interest from Chapter 3 was up regulated 5.06 and 4.4-fold at Day 3 and Day 7 respectively after ATRA treatment relative to Day 0 untreated SK-N-BE Cells (Day 0 is set at 1; Figure 4.3). The levels of miR-184 expression following ATRA treatment inversely correlated with *MYCN* expression levels (Figure 4.1).

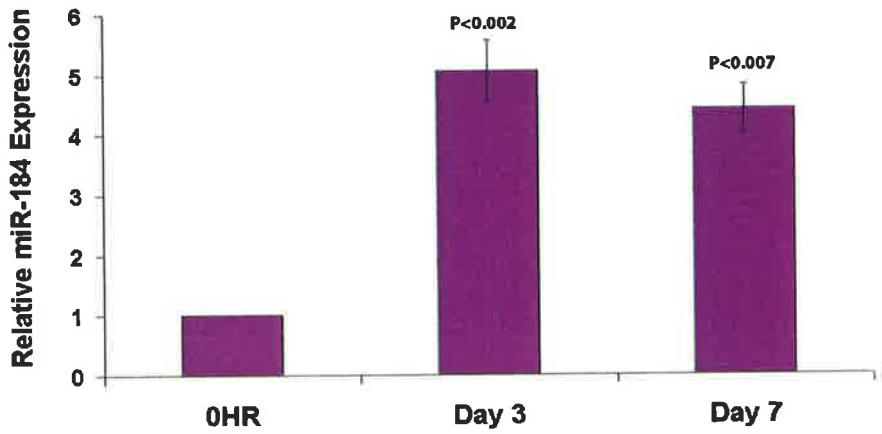

Figure 4.3. MiR-184 is up-regulated in SK-N-BE neuroblastoma cells in response to ATRA. MiR-184 mRNA was up 5.06-fold at Day 3 and 4.4-fold at Day 7 relative to untreated cells (Day 0).

4.1.5 Down-regulation of miR-184 can partially counteract the physiological effects induced by ATRA

To investigate if knock-down of miR-184 could abrogate the effects of ATRA, SK-N-BE cells were transfected with an anti-miR to miR-184 before treatment with ATRA. This down regulation resulted in a reduction in the ability of ATRA to decrease cell viability (Figure 4.4 a). Although ectopic up-regulation of miR-184 cannot induce differentiation in SK-N-BE cells, results indicated that knockdown of miR-184 decreased cell sensitivity to ATRA-induced differentiation (Figure 4.4 b).

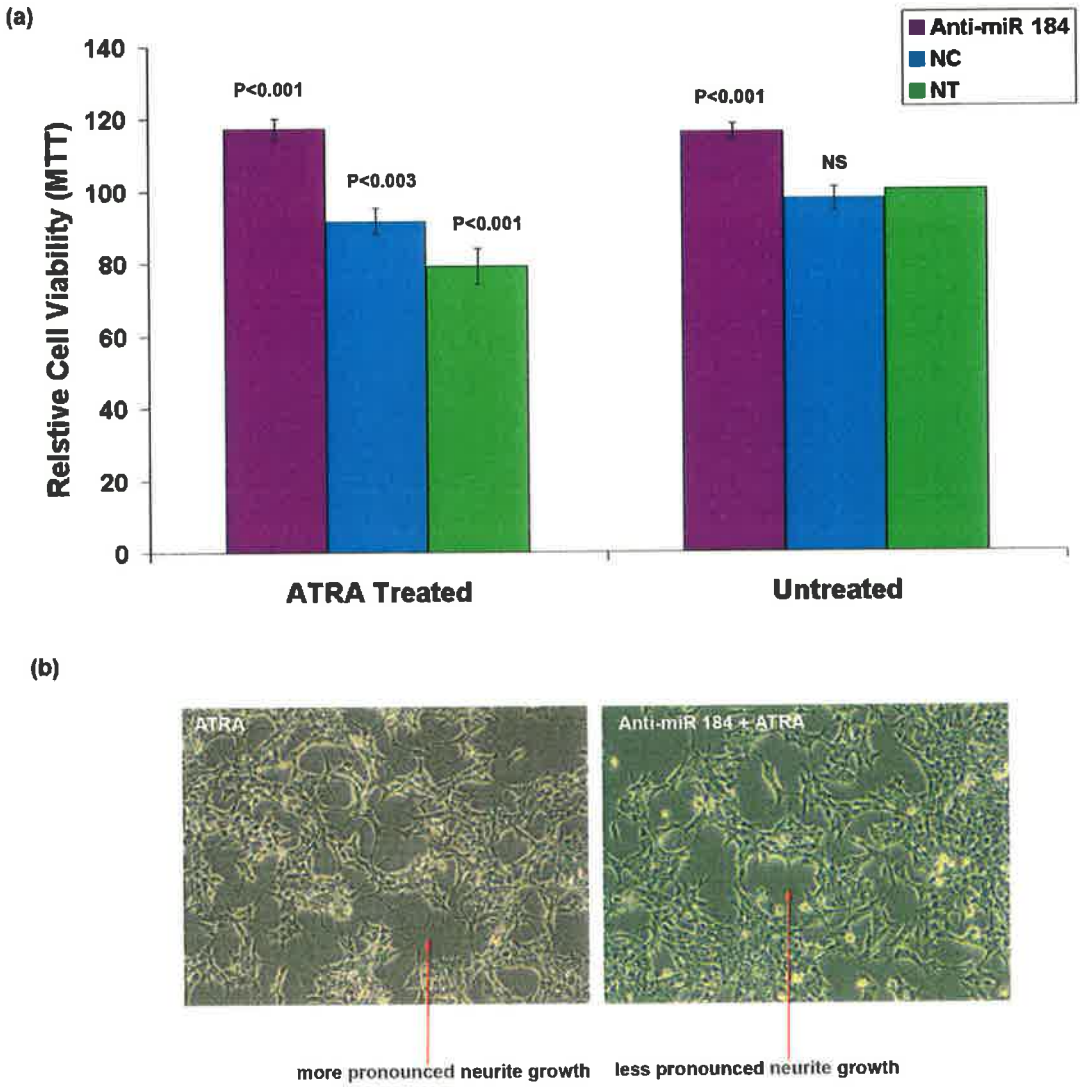

Figure 4.4 Effects of ATRA on SK-N-BE cells transfected with the miR-184 anti-miR. (a) This graph shows cell viability of SK-NB-E cells 96h post ATRA treatment and the effects of SK-N-BE cells transfected with anti-miR or scrambled oligonucleotide prior to ATRA treatment. The anti-miR results in increased viability following ATRA treatment. (b) Images of cells treated with the anti-miR to miR-184 display a reduction in neurite outgrowth versus treated cells at the same time point.

4.2 Discussion

4.2.1 The effects of ATRA-induced differentiation on the microRNA profile of SK-N-BE cells

The aim of this study was to identify novel microRNAs involved in ATRA-induced differentiation. The ability to induce differentiation is of major importance in neuroblastoma as it would result in the recapitulation of a more mature neuronal cell type (123). Tumours which exhibit a more differentiated phenotype have been associated with positive clinical parameters such as single copy *MYCN* (49), young age, lower stage and better OS and EFS (26, 124).

ATRA is a retinoid relative of 13-Cis-retinoic acid which is currently used as part of the NB therapeutic regime in high risk disease. This retinoid can induce a differentiated phenotype in numerous cell lines including SK-N-BE cells. ATRA-treatment of SK-N-BE cells is a well established model of neuroblastoma cell differentiation. Features of differentiation include neurite outgrowth, down-regulation of *MYCN*, slow-down in cell growth and the induction of markers of mature neuronal cells. To further clarify the mechanism by which ATRA induces neuroblastoma cells differentiation we examined the expression of 364 microRNAs in response to treatment. This profiling study identified a large number of microRNAs both activated and repressed following ATRA treatment, which will be discussed in further detail. Furthermore, in this chapter and the proceeding chapter, functional experiments were carried out for a subset of these microRNAs to

examine their effects on cell characteristics such as cell viability, differentiation and colony forming efficiency.

Two prior studies established that microRNAs are dysregulated in neuroblastoma in response to ATRA-induced differentiation (208, 223). However, both reports were limited with respect to the number of microRNA examined. In the present study we profiled a much larger group of microRNAs. This study also employed a strict cut-off of fold change >2, with the aim of identifying novel microRNAs involved in this process. In total, 41 microRNAs showed altered expression after ATRA treatment, 17 microRNAs were up-regulated, 17 microRNAs were down regulated and 7 microRNAs were "switched on" with a fold change which is technically un-quantifiable. It is not at all surprising that such a large number of microRNAs exhibited altered expression after treatment, given it is well established that a large number of microRNAs are subject to regulation by *MYCN* (208-210, 229) and that an early event in ATRA-induced differentiation of NB cells is the down regulation of *MYCN* (237). Of the 41 dysregulated microRNAs identified here, 9 had previously been demonstrated to be under the control of *MYCN* (208-210, 229).

A large number of microRNAs identified as significantly differentially expressed in our study had prior associations with various other types of cancers; validating our method of analysis. Examples included miR-10a and miR-10b (281-285) and miR-152 which has been reported to be down-regulated in *MYCN* amplified tumours (209). These three microRNAs were chosen for functional follow-up which is summarized in Chapter 5. Other examples of cancer-associated microRNAs include miR-24 which can induce apoptosis in a number of different cancer cell lines (184) and has also been shown to have tumour suppressor activities by regulating p53-independent cellular proliferation through

targeting of an S-phase enzyme, dihydrofolate reductase, DHFR (286). Low levels of miR-191, which was up-regulated in response to ATRA, has been reported to be associated with poor survival in malignant melanoma (287). A significant validation of the results obtained in this study was the report by Chen *et al*, which demonstrated that miR-7 and miR-214 which were up- and down-regulated respectively in our study were involved in differentiation of SH-SY5Y NB cells (242). Ectopic up-regulation of miR-214 and conversely knockdown of miR-7 resulted in profound neurite outgrowth in these cells.

It was also evident that the microRNAs "switched on" in response to ATRA could be extremely important in the pathogenesis of neuroblastoma. A number of these microRNAs were not expressed in a large portion of the tumour cohort previously described (209). MiR-34b was the most significant microRNA from this group, with SK-N-BE cells and 58.94% of the tumor cohort lacking expression of this microRNA. The miR-34 family of microRNA are well established as anti-apoptotic, tumour suppressor microRNAs in a number of cancers including neuroblastoma (230-233, 288). Interestingly miR-34b is located on chromosome 11q, a region frequently deleted in NB tumours. MiR-34a is recognized as a potent pro-survival microRNA in neuroblastoma and is expressed at low levels in tumours harboring a 1p deletion. Ectopic over-expression of this microRNA induces apoptosis in neuroblastoma cells by targeting a number of genes including *E2F3* and MYCN transcription factors (230-232). MiR-34c also exhibits anti-proliferative effects when up-regulated in neuroblastoma cells (231) and similar to miR-34b, miR-34c also maps to chromosome 11q. Although there are currently no publications on miR-34b in neuroblastoma, provisional results reported here suggest it may play a role in the pathogenesis of neuroblastoma. Also of interest, was miR-128b which is transcribed from

chromosome 3p22 a region also commonly deleted in neuroblastoma (Section 1.1.12). Although not reported in neuroblastoma to date, this microRNA has been shown to be down-regulated in undifferentiated gastric cancer tissue compared to the normal differentiated paired tissue (288).

Identification of microRNAs altered in response to the differentiation phenotype of the cell by high-through put profiling is extremely important, however, it is also of extreme importance to functionally validate the effects, if any, that these microRNAs have *in-vitro*. This involves carrying out detailed functional analysis of individual dysregulated microRNAs. Functional follow up of a selection of microRNAs identified in a profiling study was demonstrated by Laneve *et al.* (223). This study identify 14 microRNAs as being up-regulated following ATRA-induced differentiation in neuroblastoma. The authors further demonstrated the functional importance of three up-regulated microRNAs, namely miR-125a, miR-125b and miR-9. Ectopic over-expression of these microRNAs in SH-SY5Y NB cells resulted in a down regulation of *MYCN* and reduced cellular proliferation. All 3 microRNAs directly target the 3'UTR of *TrkC* and siRNA knockout of this mRNA mimicked the effects of ectopic over-expression of the microRNAs (223). Furthermore, this group demonstrated the mechanism controlling miR-9 expression during the differentiation process by characterising the promoter of miR-9. They demonstrated that this promoter is repressed in the undifferentiated state by REST, a protein involved in transcriptional regulation. Activation of the promoter after induction of differentiation occurs by the phosphorylation of CREB and REST dismissal (241). Although these three microRNAs were up-regulated in our study they did not fall into our stringent threshold of 2-fold change in expression.

To further investigate the functional role of ATRA-induced microRNAs we choose to initially evaluate miR-184. We had already established that this microRNA had a profound pro-apoptotic effect in neuroblastoma. This ATRA study aimed to elucidate the functional role of miR-184 during the onset of differentiation. Knock-down of miR-184 prior to ATRA treatment resulted in an abrogation of the decreased cell viability that occurs post-ATRA treatment. This suggests that miR-184 up-regulation during ATRA treatment is an event necessary for the reduction of cell viability. Images taken 96h post transfection of miR-184 and treatment with ATRA demonstrated a slight reduction in neurite outgrowth relative to that of ATRA control treated cells.

In conclusion we identify an ATRA-induced microRNA profile containing microRNAs with both previous and novel association with differentiation. Furthermore, we demonstrate for the first time a functional role for miR-184 induction during neuroblastoma differentiation.

Chapter 5

HOX Cluster microRNAs induced by ATRA

Chapter 5

HOX cluster microRNAs induced by ATRA

5.1 The Role of the HOX microRNAs in neuroblastoma

Four of the microRNAs (miR-10a, miR-10b, miR-152 and miR-196a) up-regulated as a result of ATRA treatment in this study are imbedded within the Homeobox (HOX) gene cluster. HOX genes are transcription factors that play an essential role in development and disease (289-291). They are precisely regulated and expressed during embryogenesis in distinct regions of the head-tail body axis of mammalian embryos (290). This cluster of genes is highly important in development, as precise regulation is necessary for efficient differentiation to occur (291). In addition to being embedded within *HOX* gene clusters, these miRNAs are also known to directly inhibit some of the *HOX* genes, with miR-10a targeting *HOXA1* (292), miR-10b targeting *HOXD10* (284) and miR-196 targeting *HOXD8/C8/A7/A8* (293). Tsang *et al.*, (294) have previously shown neuronal enriched miRNAs tend to be co-expressed with their target genes, suggesting a role for these miRNAs in neuronal homeostasis. This portion of the study examines the effects of HOX cluster microRNAs on neuroblastoma pathogenesis, and further attempts to identify targets and elucidate mechanisms of action of these microRNAs.

Detailed functional analysis of all four of these microRNAs miR-10a, 10b, miR152 and miR-196a, all of which are highly up-regulated in SK-N-BE cells in response to ATRA, was carried out. We investigated the importance of these miRNAs in ATRA-induced neuroblastoma cell differentiation, including the identification of a direct target gene of miR-10a and miR-10b, nuclear receptor co-repressor 2 (*NCOR2*; also known as

SMRT), whose silencing recapitulates an ATRA-induced differentiated phenotype and miR-152 which was identified as an essential regulator of the epigenome through targeting of the methyltransferase *DNMT1*. We demonstrate that ATRA treatment results in global DNA demethylation and conclude that this is, in part a result of miR-152 inhibition of *DNMT1*. Ectopic over-expression of miR-152, targeting *DNMT1*, also negatively impacted cell invasiveness and anchorage independent growth, contributing in part to the differentiated phenotype. These results demonstrate that functionally important, miRNA-mediated DNA de-methylation changes contribute to the process of ATRA-induced differentiation.

We also investigate a novel mechanism of action for miR-196a, a potential tumour suppressor microRNA which might be transported into the nucleus, and activating transcription of the neuroblastoma RAS gene *NRAS*.

5.1.1 Over-expression of the HOX miRs in ATRA-treated neuroblastoma SK-N-BE cells

A group of microRNAs shown to be up-regulated in response to ATRA and located within the highly conserved HOX gene clusters were chosen for further examination. These four miRs were shown to be significantly up regulated initially using the TLDA cards (Figure 4.2), which was further validated using individual microRNA Taqman assays (Figure 5.1).

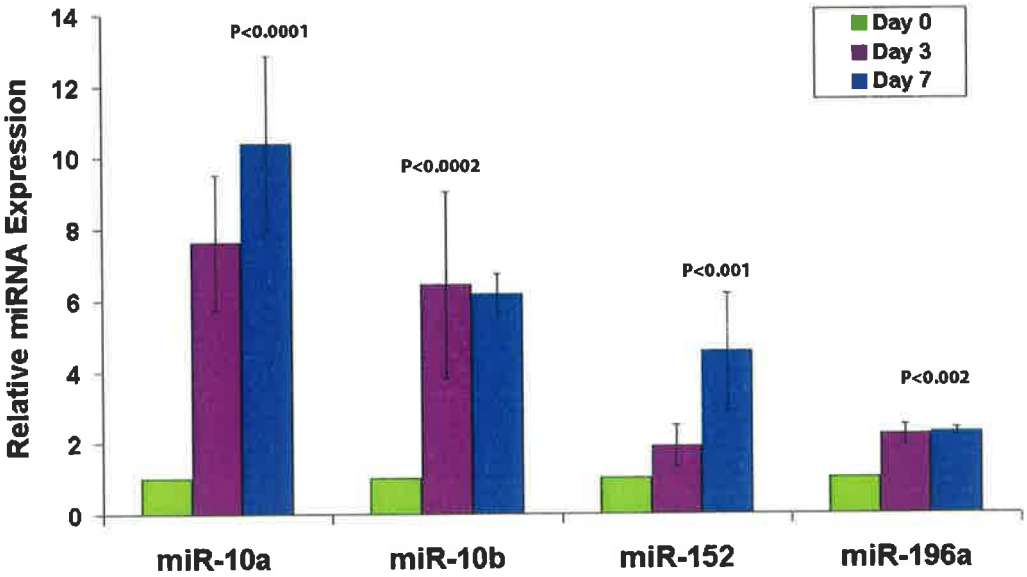

Figure 5.1 Four microRNAs located in the HOX gene cluster are significantly over expressed in response to ATRA. QRTPCR validation of miR-10a, miR-10b, miR-152 and miR-196a which are all up regulated after ATRA treatment relative to untreated cells at Day 0.

5.1.2 Ectopic up-regulation of HOX cluster miRs

To identify and define functional roles for these microRNAs in neuroblastoma, miR-196a, miR-152, miR-10a and miR-10b, mature mimics were transfected both individually and in pools in to SK-N-BE cells. Fold change increases from 1,000-10,000 was observed across all experiments (Figure 5.2).

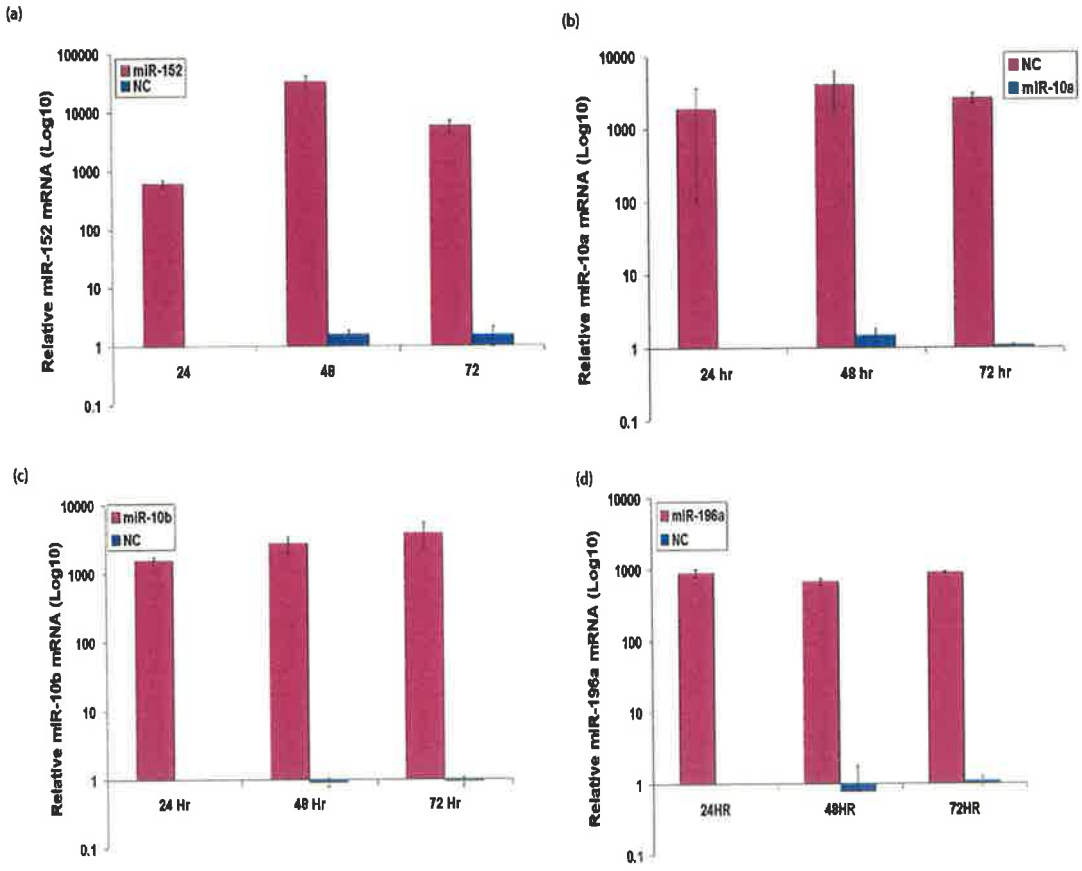

Figure 5.2. Fold change of HOX cluster microRNAs following transfection with the miRNA mature mimics. Significant increases in levels of each of the microRNAs was determined following transfection relative to SK-N-BE cells transfected with scrambled oligonucleotide control (NC).

5.1.3 Effect of ectopic up-regulation of HOX cluster miRs on SK-N-BE cell numbers

Ectopic up-regulation of miR-10a, miR-10b, miR-196a, miR-10a/miR-10b, and all four HOX cluster microRNAs in combination showed a significant negative effect on cell numbers using a cell counting technique when compared to cells transfected with the negative control (Figure 5.3 a), this result was validated using an acid phosphatase assay (Figure 5.3 b). MiR-152 over-expression by itself had no effect on cell numbers.

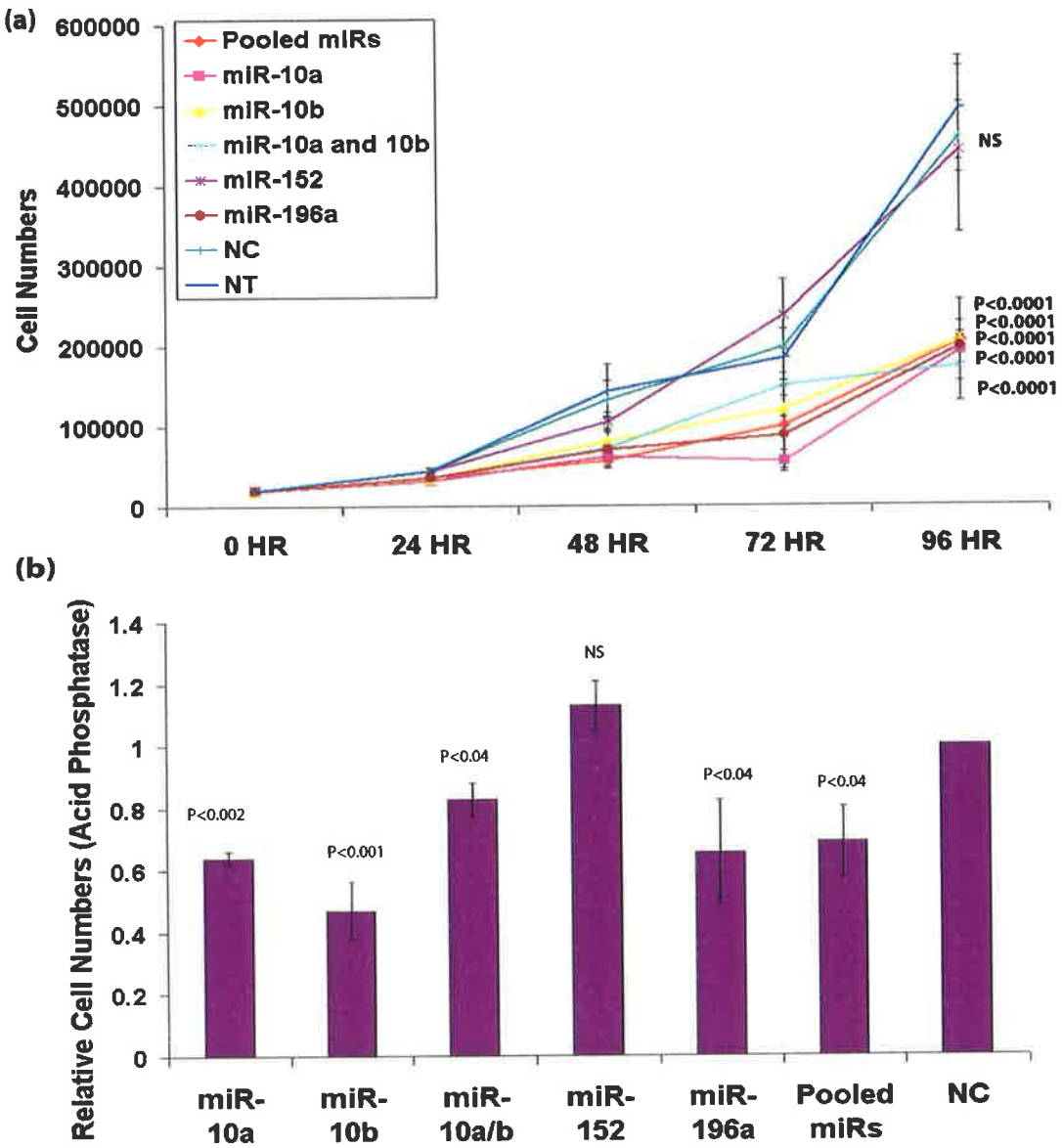

Figure 5.3. Effects of HOX cluster miRs on SK-N-BE cell numbers. (a) MiR-196a, miR-10a, miR10b, miR-10a and miR-10b co-transfected, miR-10a, 10b, 196a and miR-152 all combined reduced cell numbers in SK-N-BE cells. MiR-152 did not have any significant effect on cell numbers. (b) Results were validated using an acid phosphatase assay. Experiments were normalized to cells transfected with the scrambled oligonucleotide control (NC).

5.1.4 Effects of HOX cluster miRs on cell invasion

The effects of over-expression of each of the microRNAs of interest, both individually and pooled, on cell invasion was measured. The ability of cells to move through a matrigel matrix was quantified relative to the scrambled oligonucleotide control. All transfections decreased the invasive ability of neuroblastoma cells (Figure 5.4 and Figure 5.5).

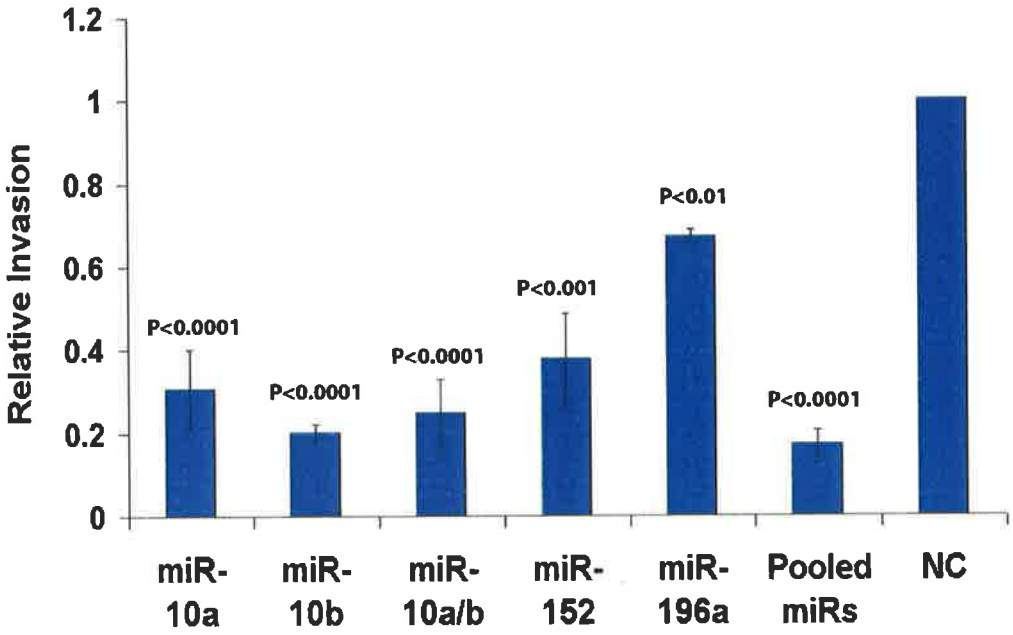

Figure 5.4. Relative invasion following transfection with HOX cluster microRNAs. All the HOX cluster microRNAs up regulated with ATRA reduce SK-N-BE cell invasion *in-vitro*, compared to SK-N-BE cells transfected with the scrambled oligonucleotide control (NC).

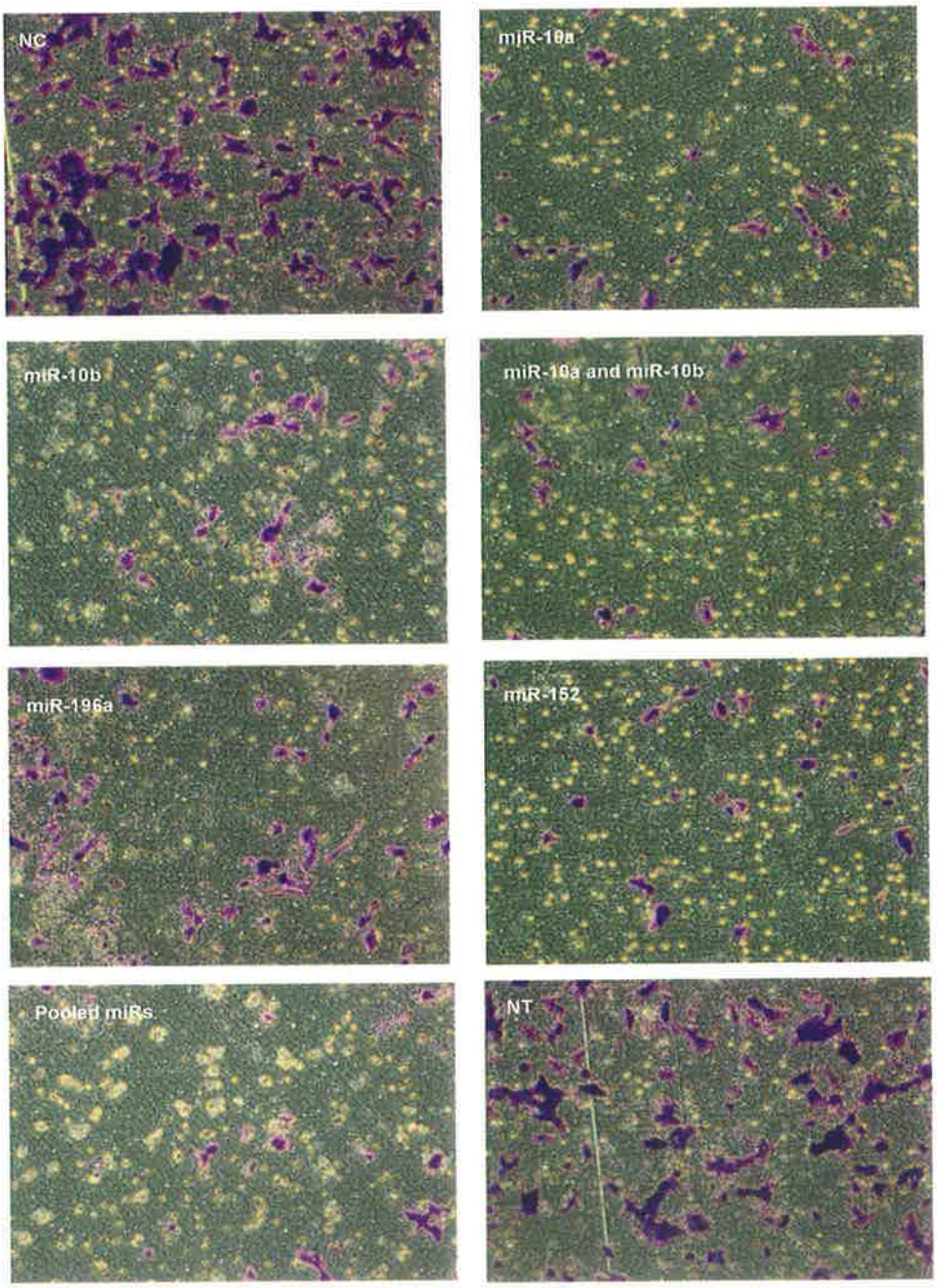

Figure 5.5. Images of invading SK-N-BE cells transfected with individual and pooled mature mimics for each of the HOX cluster microRNAs. Images show each microRNA transfected individually, miR-10a and miR-10b pooled, all four microRNAs pooled, a scrambled oligonucleotide control (NC) and a non transfected control (NT)

5.1.5 Effects of the HOX cluster miRs on colony forming qability

The soft agar assay was preformed to determine if cells are capable of anchorage-independent growth, which is assumed to be closely related to the processes of *in-vivo* tumourogenesis. All HOX cluster microRNAs significantly reduced the ability of SK-N-BE neuroblastoma cells to form colonies in soft agar compared to negative control transfected cells (Figure 5.6), indicating that each one of these microRNAs is potentially a tumour suppressor microRNA.

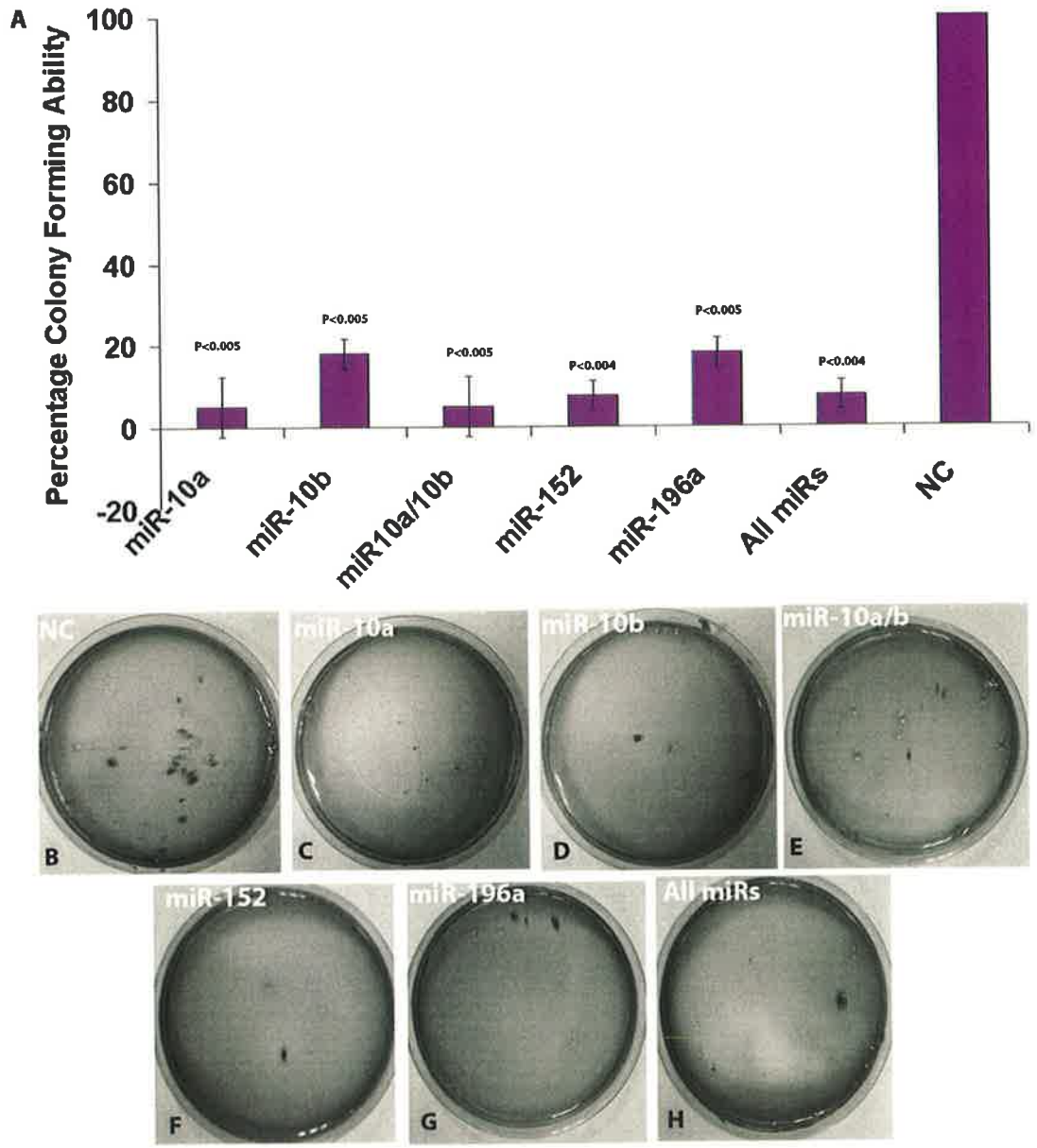

Figure 5.6. Effects of HOX cluster microRNAs on colony forming efficiency. (a) Colony forming efficiency of the SK-N-BE cells in soft agar was significantly reduced with each of the HOX cluster microRNAs. Values were obtained relative to the ability of SK-N-BE cells treated with the scrambled oligonucleotide control to produce colonies. (b-h) Images of one plate from each treatment.

5.1.6 MiR-10a and miR-10b increase neurite outgrowth

Ectopic over-expression of both miR-10a and miR-10b resulted in pronounced neurite outgrowth in SK-N-BE NB cells when compared to the negative control scrambled oligonucleotide (Figure 5.7 a). Neurite measurement using the Cellomics ArrayScan VTi instrument showed ATRA treatment increased neurite length ~75% after 5 days, up regulation of miR-10a increased neurite length by ~50%, miR-10b ~35% and miR-10a and miR-10b co-transfected ~28%. The anti-miRs to miR-10a/miR-10b reduced but did not abrogate the effect of ATRA on neurite outgrowth (Figure 5.7 b).

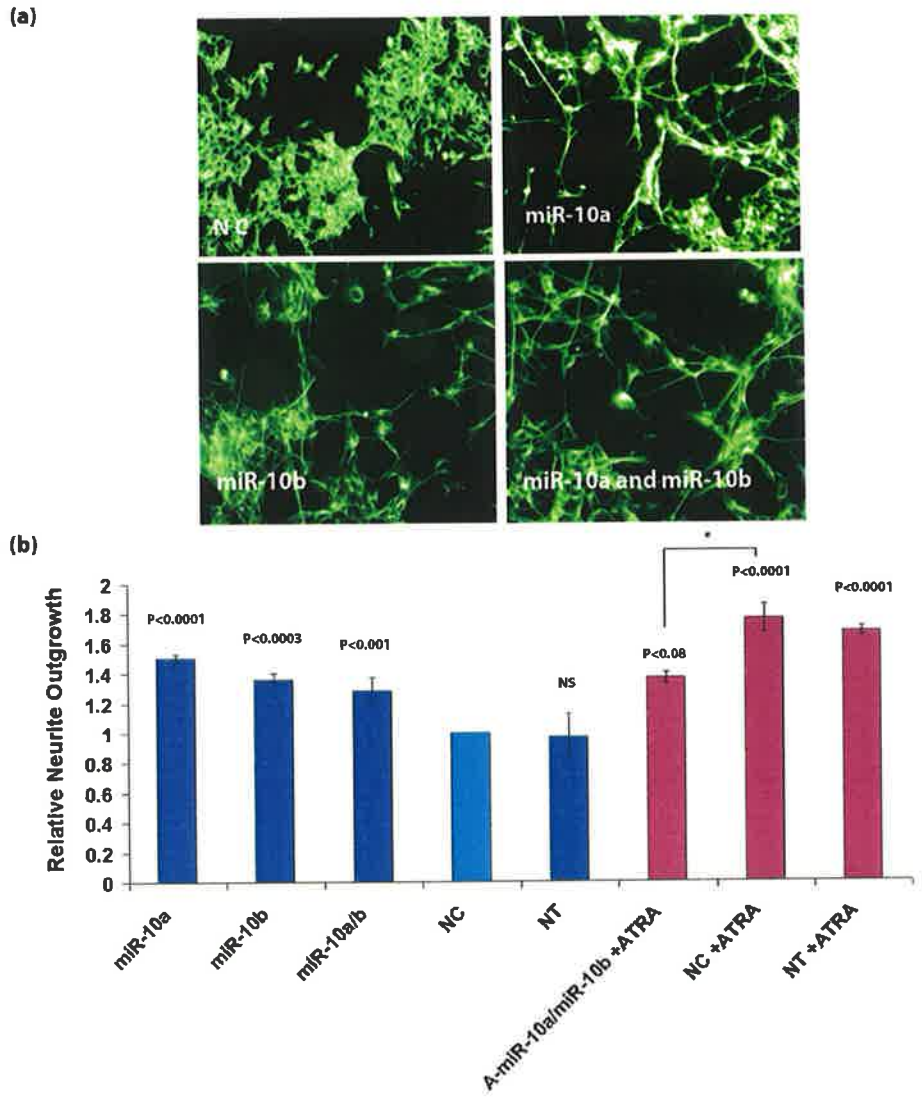

Figure 5.7. MiR-10a and miR-10b induce neurite outgrowth in SK-N-BE neuroblastoma cells. (a) Extensive neurite outgrowth was observed in SK-N-BE cells 96h after ectopic over-expression of miR-10a, miR-10b and miR-10a/b when compared to cells transfected with scrambled oligonucleotide control. This neurite outgrowth was quantified using Cellomics ArrayScan VTi instrument. The total neurite length from cell body (per cell) was used to estimate neurite outgrowth. The length was normalized to the respective value for the cells treated with the scrambled oligonucleotide control except for the anti-miR 10a/10b transfected cells, which is normalized to the ATRA-treated cells* (b). In all experiments n=2, Error bars represent standard deviation.

5.1.7 Ectopic over-expression of miR-10a and miR-10b induces neuronal specific markers.

Ectopic over expression of miR-10a and miR-10b in SK-N-BE cells, using the mature miR-10a and 10b mimics both individually and in combination resulted in an increase in the neuronal differentiation markers *GAP43* and *βIII Tubulin*. Increases were observed for mRNA (Figure 5.8 a and c) and protein (Figure 5.8 b and d) levels after transfection with the mature mimics to these microRNAs. A similar increase in these markers was reported in Section 4.1 following ATRA treatment of SK-N-BE cells.

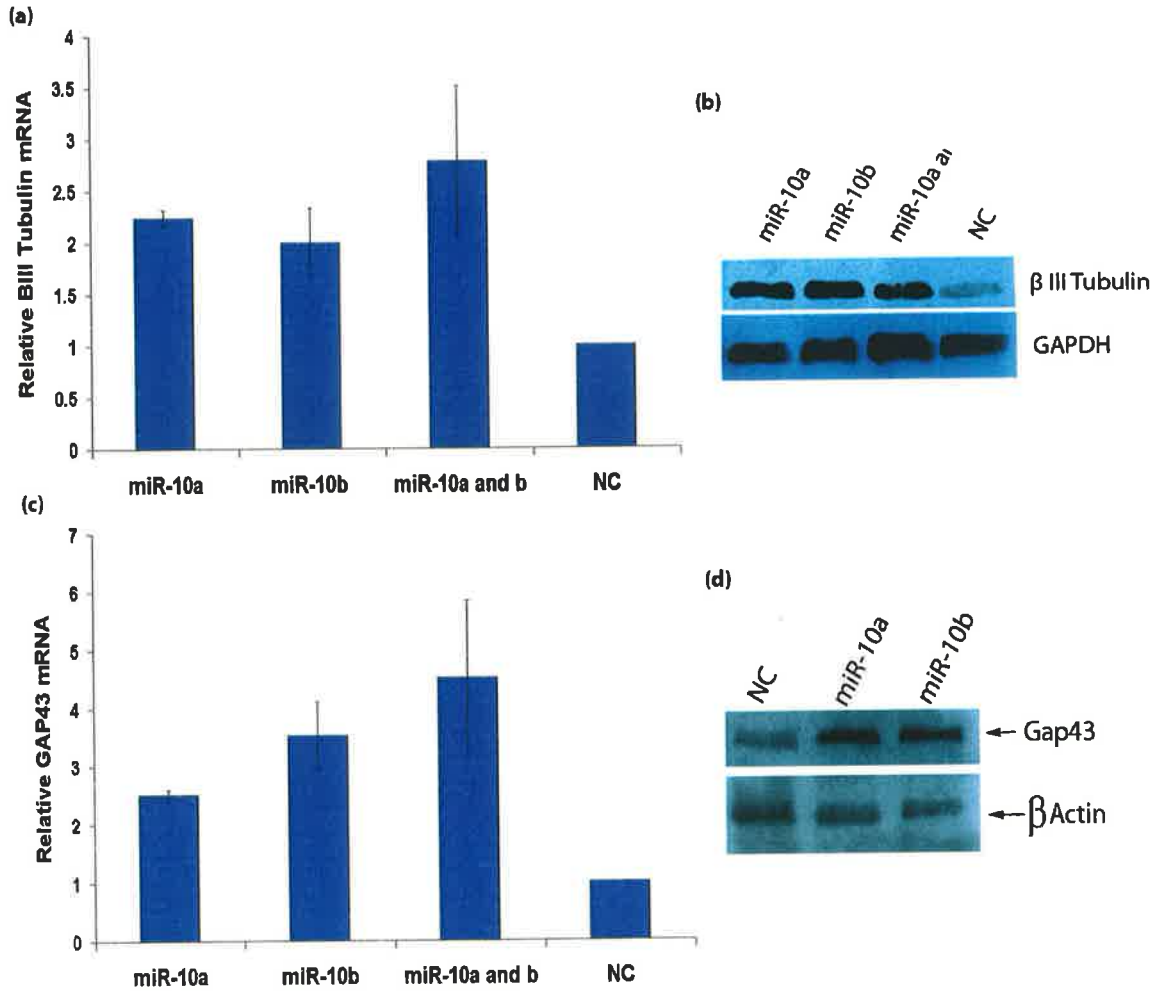

Figure 5.8. MiR-10a and miR-10b induce neuronal cell markers when ectopically over-expressed in SK-N-BE cells. Induction of neuronal marker ßIII Tubulin at (a) mRNA and (b) protein level and GAP43 at (c) mRNA and (d) protein level occurred following transfection with miR-10a and miR-10b when compared to cells transfected with the scrambled oligonucleotide control (NC).

5.1.8 Ectopic over-expression of miR-10a and miR-10b reduces *MYCN* levels in SK-N-BE cells

Ectopic over-expression of miR-10a and miR-10b showed a significant down regulation in the levels of *MYCN* both at mRNA and protein level (Figure 5.9 a and b). Neither microRNA is predicated to target the 3'UTR of *MYCN*, indicating that this could be an indirect effect of up-regulation.

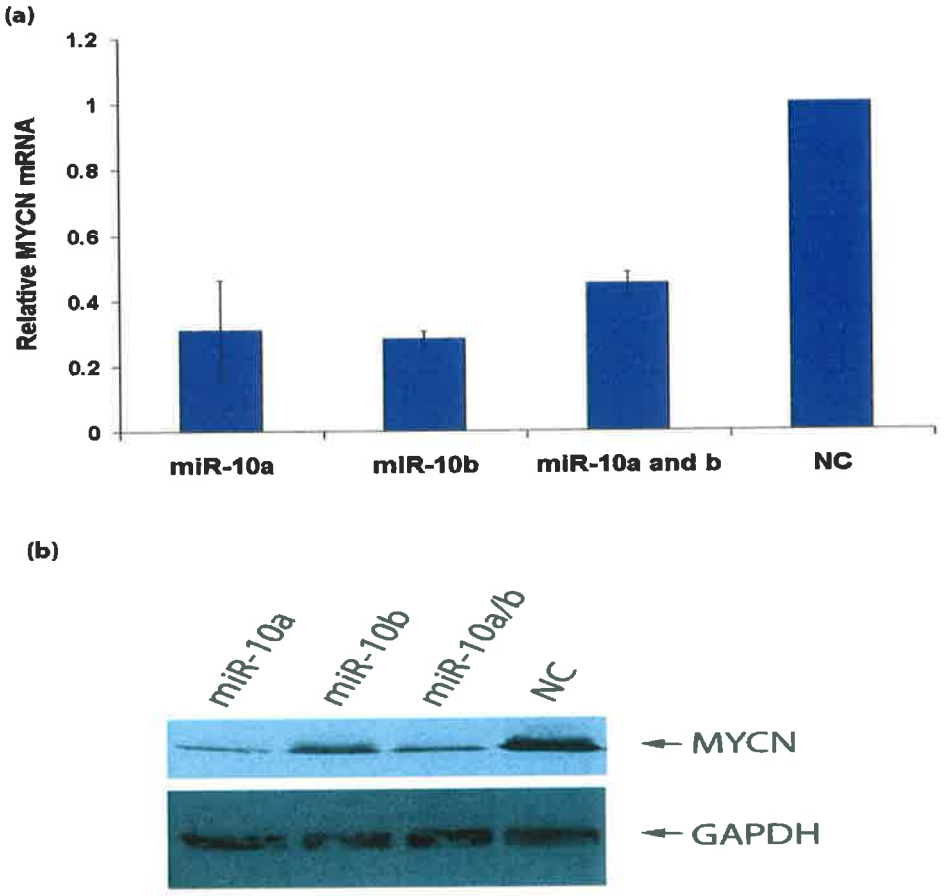

Figure 5.9. MiR-10a and miR-10b down regulate the neuroblastoma oncogene MYCN. MiR-10a and miR-10b ectopic over expression reduces the levels of neuroblastoma oncogene MYCN in SK-N-BE cells, relative to the scrambled oligonucleotide control (NC) at both (a) mRNA and (b) protein levels.

5.1.9 MRNA expression profiling and gene ontology analysis following miR-10 transfection of SK-N-BE cells.

To experimentally identify down regulated targets of miR-10a/b mRNA microarray expression profiling was performed on SK-N-BE cells using microarrays representing 24,000 protein coding genes. Microarray analysis was performed on SK-N-BE cells 5 days post-transfection with either miR-10a, miR-10b or a combination of miR10a and 10b. The results of each profiling experiment indicated that the numbers of genes that were up or down regulated by > 1.5-fold in these experiments ranged from 5352 for down-regulated genes and 4525 for the up-regulated. There is an overlap of 3910 loci up and 2642 down regulated genes between miR-10a and miR-10b transfections. Given that there are only 233 predicted targets (conserved and non-conserved) for miR-10a/10b in TargetScan, it is highly likely that the majority of differentially expressed genes were due to secondary effects. As illustrated in Figure 5.10 mRNA sequences which decreased by 1.5-fold or greater following miR-10 transfections were placed into three subgroups based on their fold change: 1.5 to 3-fold, 3 to 6-fold and >3-fold. Genes showing expressional decreases exceeding 3-fold contained more predicted target sites in their 3' UTRs than what can be accounted for by random chance (expected number of binding sites generated by simulation studies based on 10^6 iterations of similar numbers of randomly selected mRNAs). Co-transfection of miR-10a and 10b (Figure 5.10 c) together may have had greater efficacy than when individually transfected, as p-values were more significant and the group of genes down-regulated 1.5 to 3-fold also had an enrichment of target sites. As expected, mRNAs increased between 1.5 to 3-fold, 3-fold to 6-fold and > 6-fold exhibited statistically significant inverse correlations with miR-10a/10b target sites. Microarray

expression results were used to carry out gene ontology (GO) analysis on the most significantly up-regulated and down-regulated mRNAs (top 20%). There was statistically significant enrichment for GO categories that were common to 10a and 10b, as well as unique catagories to either 10a and 10b. The up-regulated genes were predominantly enriched for cell surface receptor linked signal transduction ($P<0.0001$), epidermal cell differentiation ($P<0.001$) and ectoderm development ($P<0.004$). The down-regulated genes demonstrated enrichment for the categories of protein transport ($P<0.001$) and establishment of protein localization ($P<0.004$) following correction for multiple comparisons (Figure 5.11). Thus, although miR10a and 10b differ by only a single nucleotide and have the same phenotypic effect when over-expressed in SK-N-BE cells, these miRNAs result in overlapping, but non-identical alterations of mRNA transcript levels.

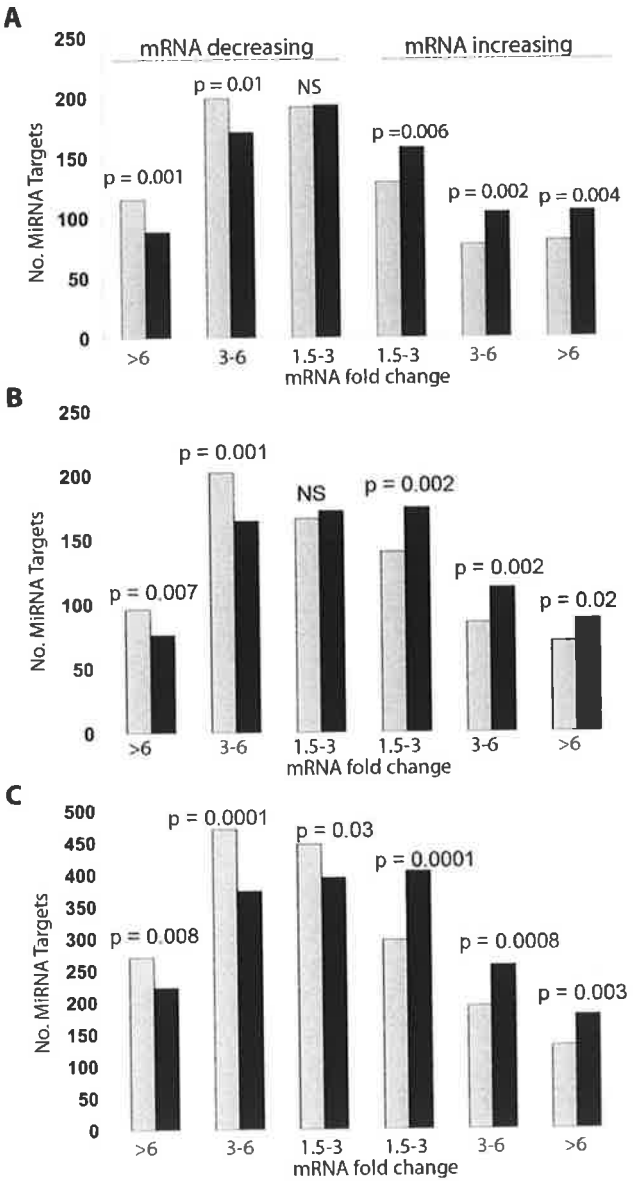

Figure 5.10. MiR-10a/b target enrichment. MRNA sequences which decreased by 1.5-fold or greater following (a) miR-10a, (b) miR-10b and (c) miR-10/b transfections were placed into three subgroups based on their fold change. Genes showing expressional decreases exceeding 3-fold were enriched for predicted target sites in their 3' UTRs. Co-transfection of miR-10a and 10b (c) also showed enrichment for the group of genes down-regulated 1.5 to 3-fold. In all experiments n=2.

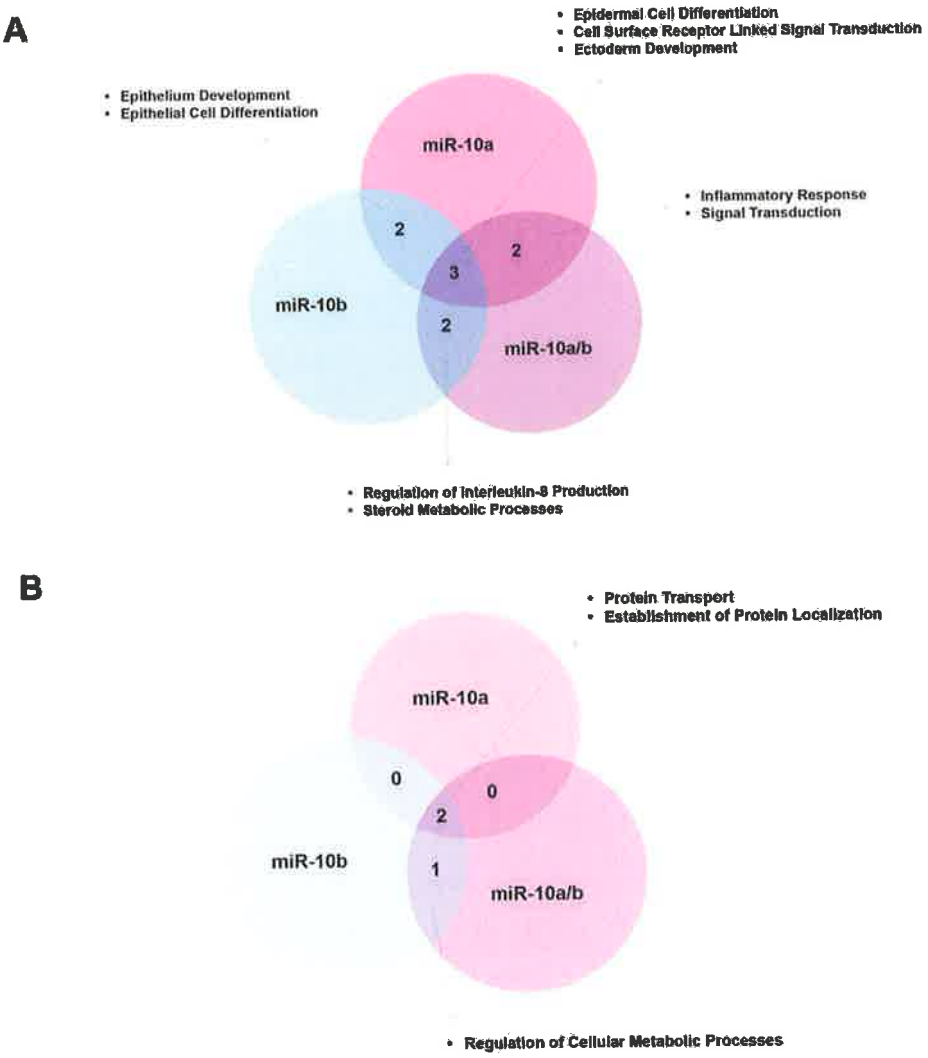

Figure 5.11. Overlap between miR-10a and miR-10b altered mRNAs. Venn diagram represents the overlap in GO terms in the most significantly (a) up-regulated mRNAs (top 20%) following transfection of SK-N-BE cells with 10a, 10b and 10a/10b and the most (b) down-regulated mRNA (20%).

5.1.10 The nuclear co-repressor protein NCOR2 is down regulated in response to ATRA

With the resultant effect of miR-10 on cell viability and neurite outgrowth, *NCOR2*, a down-regulated miR-10 predicted target was of immediate interest. A previous study showed that neural stem cells derived from *NCOR2* homozygous knockout mice exhibit extensive neurite outgrowth and reduction in cell proliferation following 5 days in culture (295). *NCOR2* mRNA was down regulated ~50% and ~60% following ATRA treatment at Day 3 and Day 7 respectively (Figure 5.12 a) when validated by RTqPCR. This down-regulation of NCOR2 was also demonstrated at protein level (Figure 5.12 b).

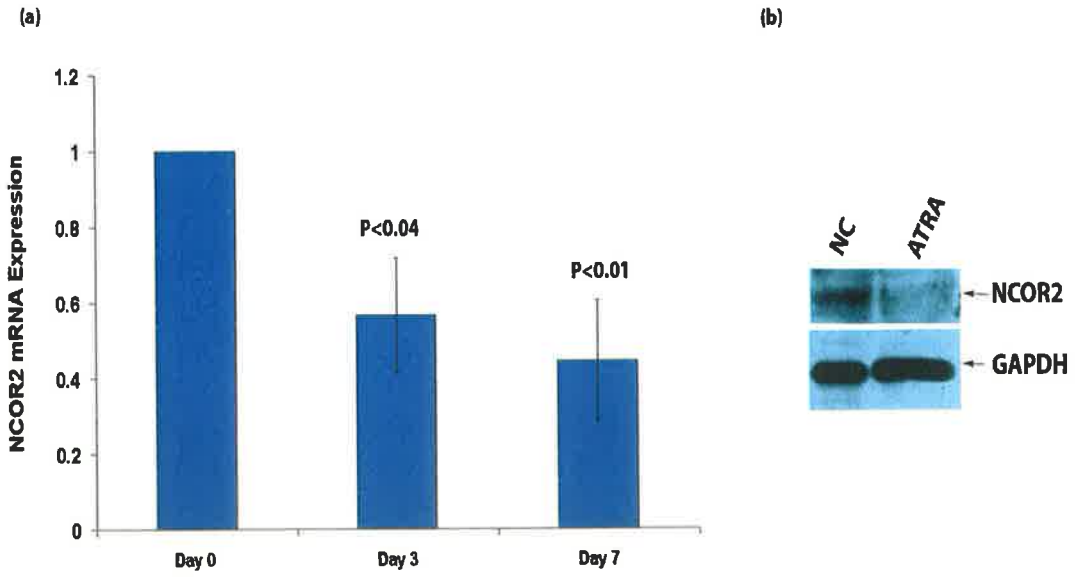

Figure 5.12 ATRA causes the down regulation of miR-10a/10b predicted target *NCOR2*. ATRA results in down regulation of *NCOR2*; this down-regulation was seen at (a) mRNA and (b) protein level.

5.1.11 *NCOR2* is a predicted target of miR-10a and miR-10b

MiR-10a/10b was predicted to bind *NCOR2* by Target Scan V5.1. The miR-10a/10b predicted target site in the 3' UTR of *NCOR2* is broadly conserved and contains an 8 nucleotide match in the seed region of miR-10a/b.

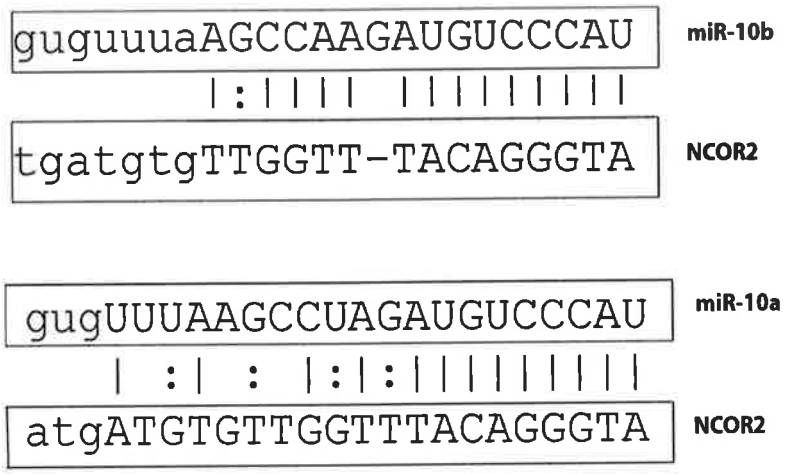

Figure 5.13. MiR-10 *NCOR2* predicted alignments. Graph displays the predicted alignment between miR-10a and miR-10b to the 3'UTR of *NCOR2.* Alignment was predicted using Target Scan version 5.1 http://www.targetscan.org.

5.1.12 MiR-10a and miR-10b ectopic over-expression causes down-regulation of *NCOR2*

To demonstrate if the over-expression of miR-10a and miR-10b causes the down-regulation of their predicted target *NCOR2,* miR-10a, miR-10b and miR-10a/10b in combination were transfected into SK-N-BE cells. Cells were harvested for mRNA and protein 72hpost transfection. *NCOR2* was significantly down-regulated after ectopic over-expression of miR-10a and miR-10b individually and in combination. The down-regulation of *NCOR2* mRNA following miR-10 over-expression was shown at mRNA and protein level (Figure 5.14a/b).

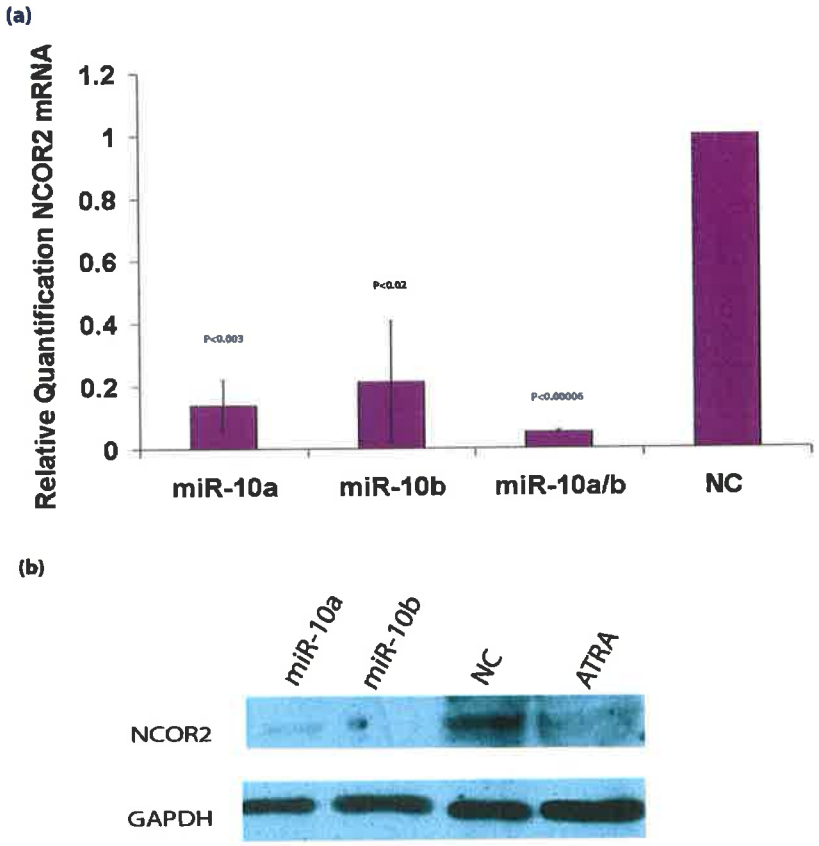

Figure 5.14. MiR-10a and miR-10b caused down-regulation of *NCOR2*. Significant down regulation of *NCOR2* (a) mRNA was displayed 72h post transfection with the Pre-miR to 10a or 10b and 10a/b combined. This high level of down regulation was also seen at (b) protein level after 72 h, the level of down regulation of NCOR2 at protein level was similar to the down regulation demonstrated in ATRA treatment of SK-N-BE cells.

5.1.13 MiR-10a and miR-10b ectopic over expression directly down regulates *NCOR2*

A luciferase reporter vector containing a 500 nucleotide region of the 3'UTR of *NCOR2* with the miR-10a and miR-10b target sequence was co-transfected with the miR-10a, miR-10b or miR-10a and 10b mature miRNA. This resulted in a reduction in luciferase activity of 65% ($P<0.0001$), 66% ($P<0.0001$) and 63% ($P<0.0001$) respectively, relative to the luciferase reporter vector co-transfected with the scrambled oligonucleotide negative control (Figure 5.15). The same luciferase reporter vector with a 3 base pair mutation in the seed region of miR-10 target sequence resulted in no significant change in luciferase activity when transfected with miR-10a, miR-10b or miR-10a and 10b relative to control. This indicates that seed region binding is essential for the mechanism of down regulation.

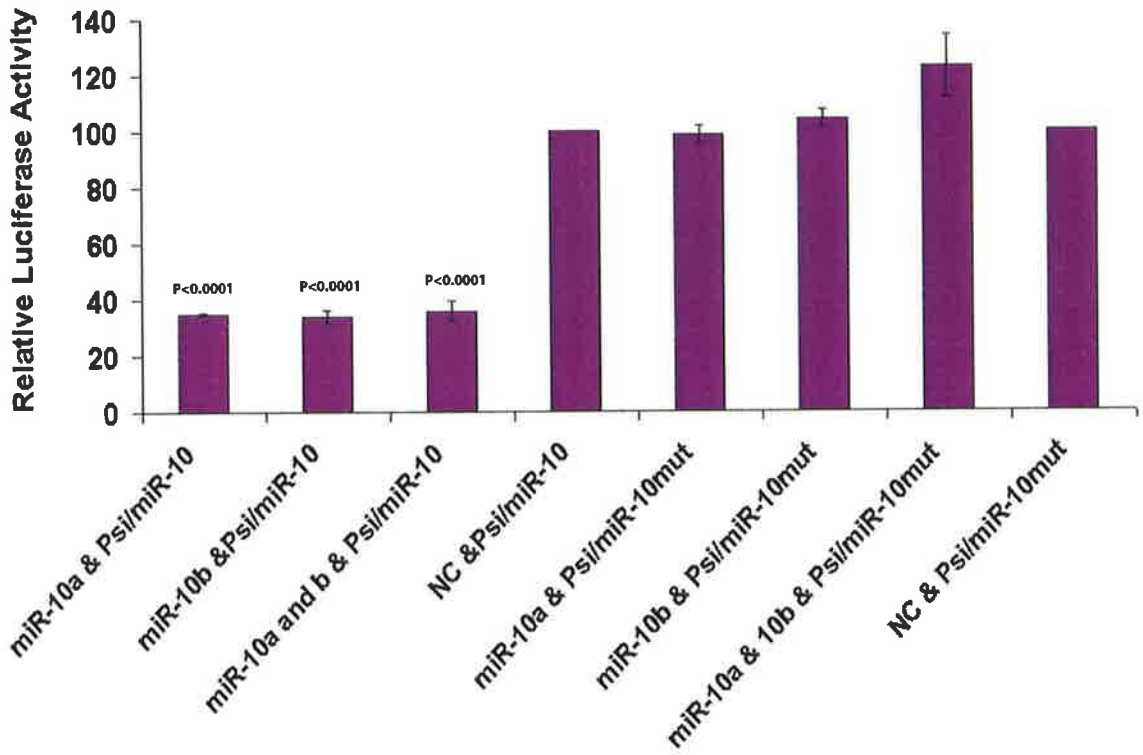

Figure 5.15. MiR-10a and miR-10b directly targets *NCOR2* resulting in reduced luciferase activity. MiR-10a, miR-10b and miR-10a and b in combination resulted in a reduction in luciferase activity when co-transfected with the luciferase vector containing a 500nt region of the 3'UTR of *NCOR2* with the miR-10 binding site (Psi/miR-10). This was normalised to the same Psi/miR-10 vector co-transfected with the scrambled oligonucleotide control. A 3bp mutation was made in the seed region binding site and this was co-transfected with miR-10a, miR-10b, miR-10a and b in combination and the negative control, there was no significant change in luciferase activity.

5.1.14 *NCOR2* is associated with poor survival in neuroblastoma tumours

The R2 tumour database (Section 3.1.19) was again utilised to examine *NCOR2* levels in neuroblastoma tumours. High *NCOR2* levels were predictive of poor overall and event free survival (Figure 5.16 a and b). *NCOR2* was more highly expressed in MNA tumours when compared to non-MNA tumours (Figure 5.16 c).

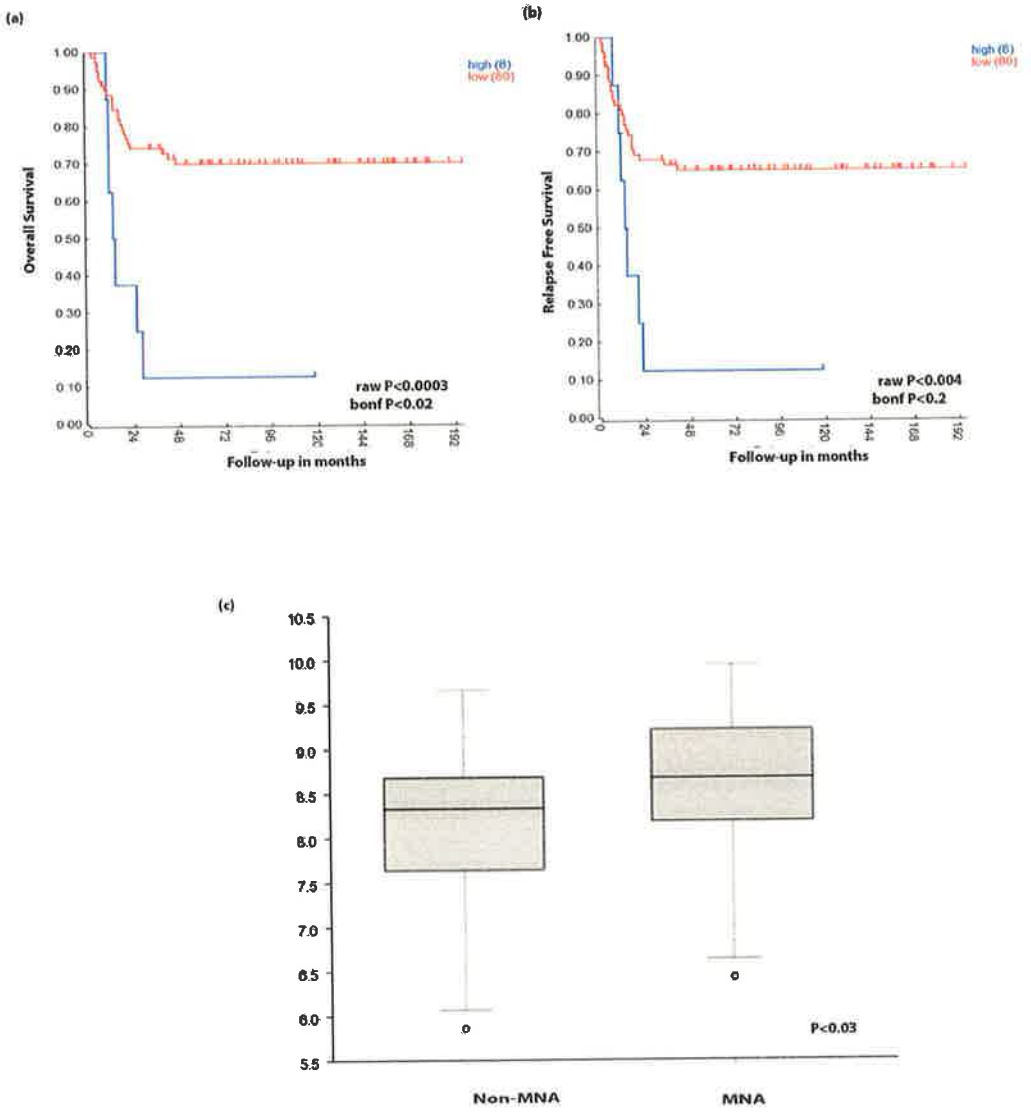

Figure 5.16. *NCOR2* is associated with overall survival, relapse free survival, MYCN status and can divide stage four neuroblastoma tumours from stage 4s tumours. High levels of *NCOR2* were associated with (a) poor overall survival probability after correction for multiple comparison. High *NCOR2* levels were associated with (b) poor relapse free survival, but only before correction for multiple comparisons. (c) *NCOR2* is expressed at a higher level in MNA tumours versus the non-MNA subset.

5.1.15 SiRNA knockout of *NCOR2*

To further examine if *NCOR2* down regulation could mimic the phenotypic effects of miR-10a/b transfections. *NCOR2* knock-down experiments were carried out. Three different siRNAs were chosen to use for the NCOR2 knockout experiments. Two of these siRNAs had approximately a 60% knockdown of *NCOR2* mRNA relative to the control scrambled siRNA (Figure 5.17 a). Western blot confirmed NCOR2 knock down at protein level (Figure 5.17 b).

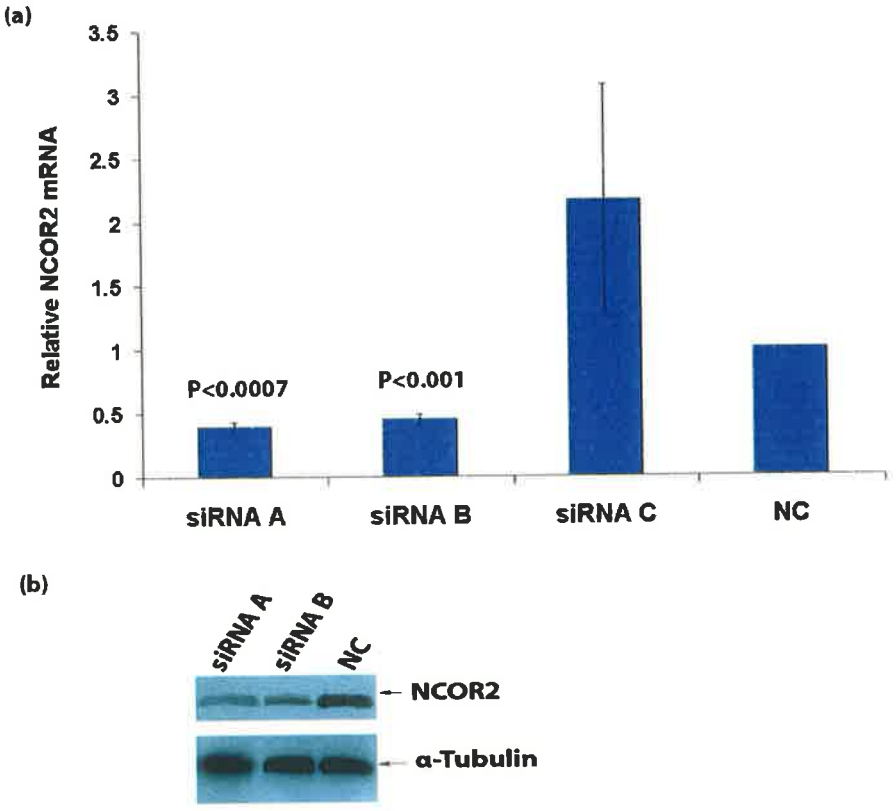

Figure 5.17. SiRNA knock-down of *NCOR2*. (a) Three different siRNAs to *NCOR2* were used, only two of these siRNAs were deemed suitable after RTqPCR was carried out to determine down-regulation. (b) Transfection with siRNA A and siRNA B were then followed up with western blot analysis to confirm down regulation at protein level.

5.1.16 SiRNA down-regulation of *NCOR2* results in a slow down in cell proliferation

SiRNA mediated down-regulation of *NCOR2* resulted in a slow down in cell growth relative to cells transfected with a negative control siRNA (Figure 5.18). This mimics the effect of a reduction in cell viability as seen in the same cells transfected with miR-10a/b.

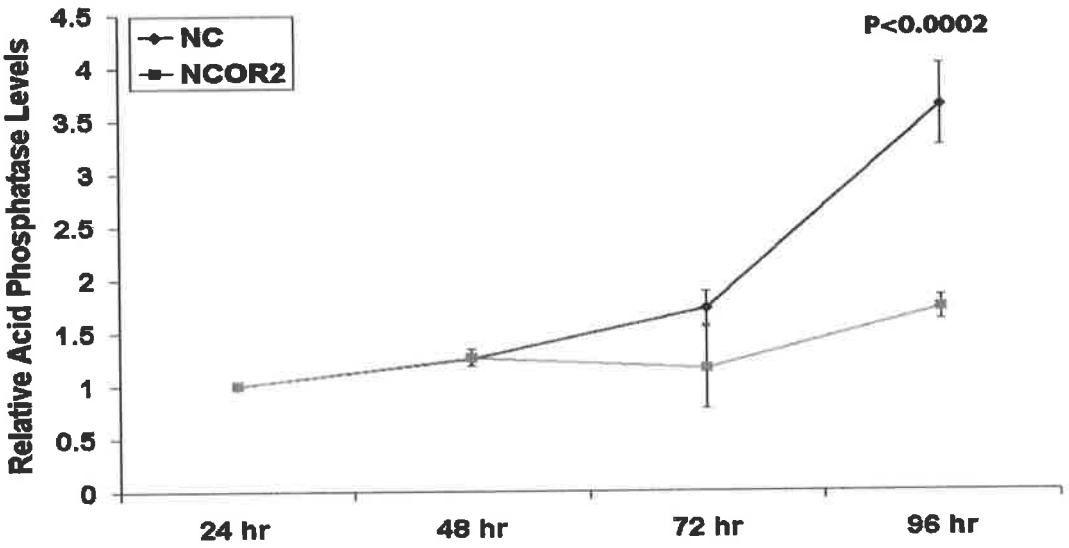

Figure 5.18. SiRNA down-regulation of *NCOR2* results in a slow down in cell proliferation. SiRNA knock-down of *NCOR2* reduced cell numbers in SK-N-BE cells, when compared to the scrambled oligonucleotide control (NC).

5.1.17 SiRNA down-regulation of *NCOR2* induces SK-N-BE differentiation

Down-regulation of *NCOR2* using silencer select siRNA A resulted in prominent neurite outgrowth (Figure 5.19 a). Neurite lengths were measured relative to the negative control scrambled oligonucleotide using. Down-regulation by the *NCOR2* siRNA resulted in ~49% increase in outgrowth compared to control (Figure 5.19 b). In comparison ATRA treatment as seen previously in Section 4.1.1, resulted in a ~75% increase in neurite outgrowth.

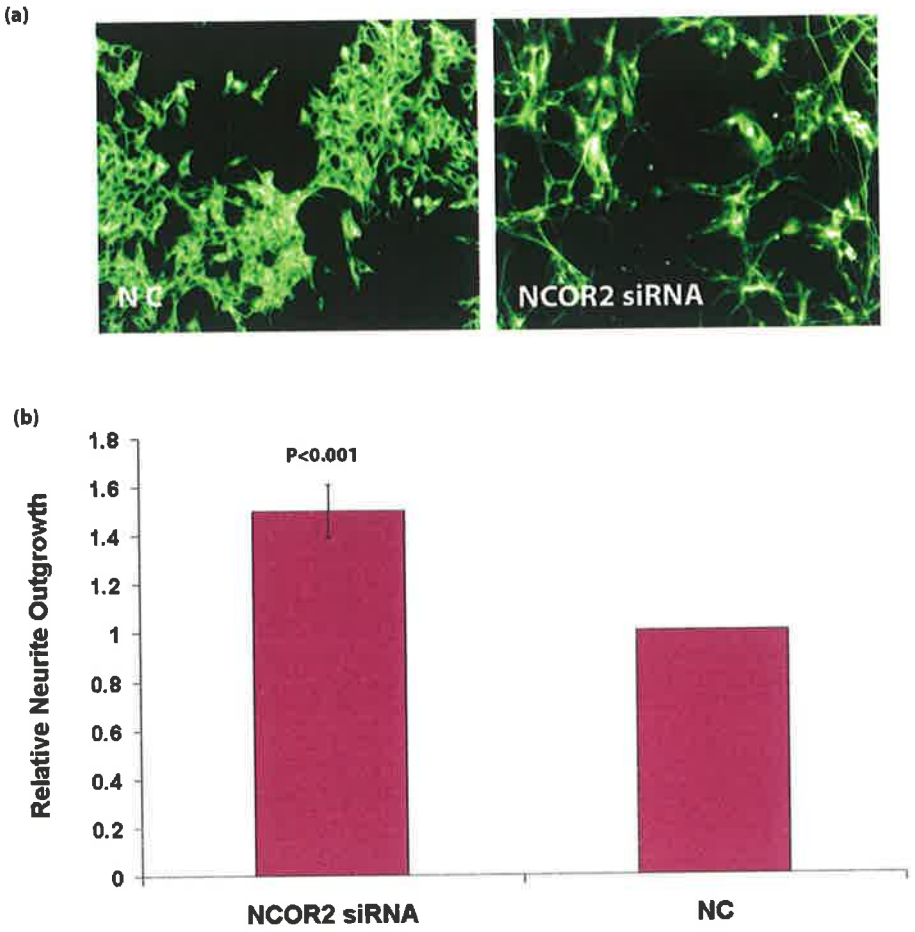

Figure 5.19. SiRNA knock-down of *NCOR2* induces neurite outgrowth in SK-N-BE neuroblastoma cells. (a) Extensive neurite outgrowth was observed in SK-N-BE cells 96h after down-regulation of *NCOR2* when compared to cells transfected with scrambled oligonucleotide control (NC). (a) Neurite length was quantified using the total neurite length from cell body (per cell) to estimate neurite outgrowth. The length was normalized to the respective value for the cells treated with the scrambled oligonucleotide control (NC)

5.1.18 *NCOR2* down-regulation results in an increase in the level of neuronal markers, GAP43 and βIII tubulin

Similarly to miR-10 ectopic up-regulation siRNA knockdown of *NCOR2* showed an increase in both markers of mature neuronal cells GAP43 (Figure 5.20 a) and βIII Tubulin (Figure 5.20 b).

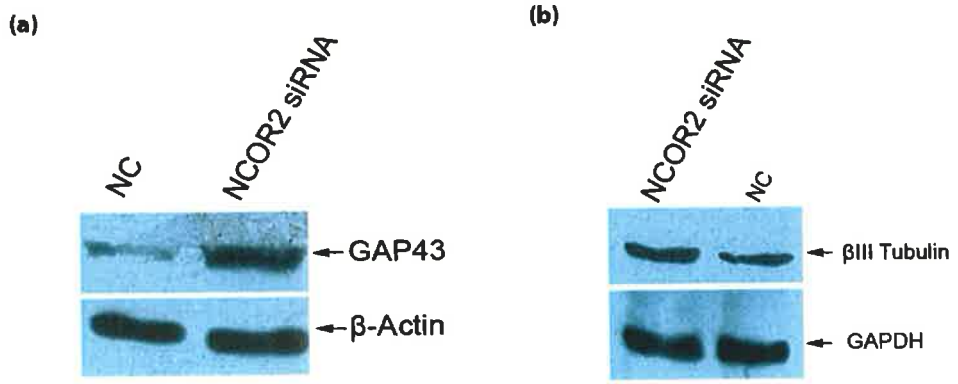

Figure 5.20. SiRNA knock-down of *NCOR2* results in up-regulation of neuronal markers GAP43 and βIII Tubulin. Using siRNA A (Section 5.16), down regulation of *NCOR2* resulted in a substantial increase in the levels of (a) GAP43 and (b) βIII Tubulin, when compared to the scrambled oligonucleotide control (NC).

5.1.19 *NCOR2* down-regulation reduces *MYCN* levels

Similar to miR-10a/miR-10b ectopic over-expression, *NCOR2* siRNA mediated knock-down resulted in a down regulation in *MYCN*, suggesting that this pathway may be the mechanism by which *MYCN* is reduced in ATRA-induced differentiation. This down regulation of *MYCN* occurs at both mRNA (Figure 2.21 a) and protein (Figure 5.21 b) levels.

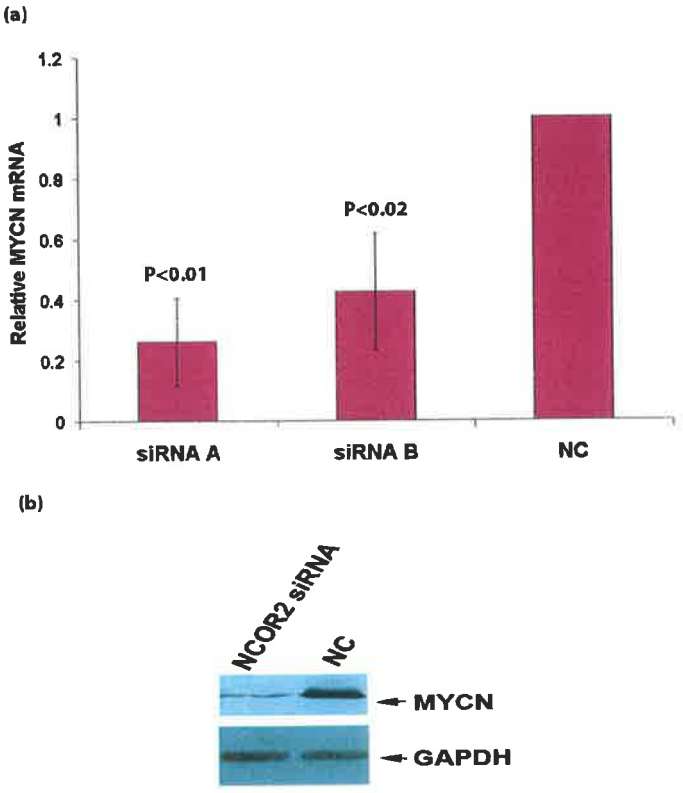

Figure 5.21. *NCOR2* down-regulation results in a reduction of *MYCN*. (a) Two different siRNAs to *NCOR2* showed down-regulation of *MYCN* at mRNA level compared to the scrambled siRNA control. SiRNA A which showed the greater level of down regulation (~74%) was used for further analysis of *MYCN* protein levels following transfection; this also displayed a large down regulation of MYCN at (b) protein level.

5.1.20 *NCOR2* knock-down results in an up-regulation of miR-10a levels

SiRNA knock-down of *NCOR2* resulted in up-regulation of miR-10a, when compared to a negative control siRNA (Figure 5.22), this result suggests that a putative feed-back loop exists for the regulation of *NCOR2* and miR-10.

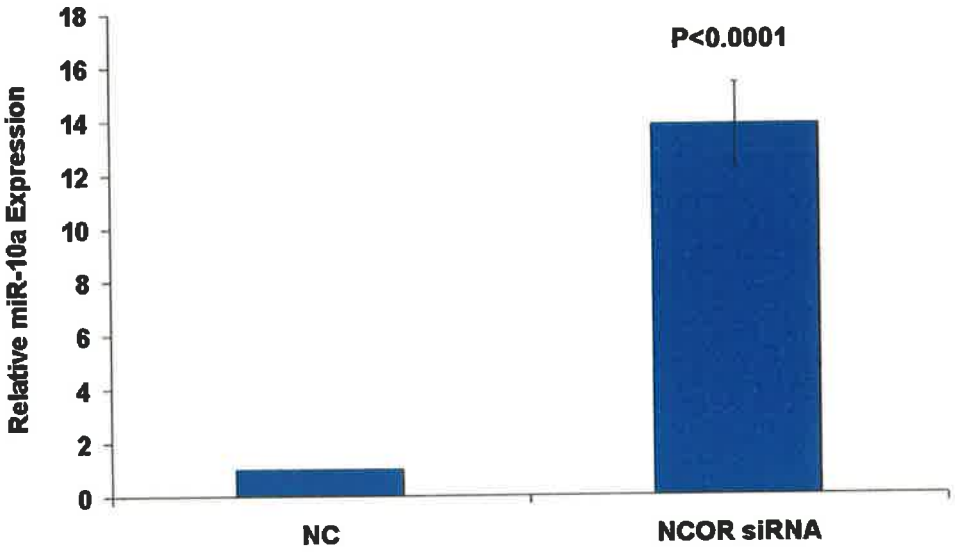

Figure 5.22. Down-regulation of *NCOR2* results in miR-10a up-regulation. SiRNA knock-down of *NCOR2* resulted a ~12-15-fold increase in miR-10a levels relative to a siRNA negative control (NC).

5.1.21 MiR-10 levels in the NB tumour cohort

The levels of miR-10a and b were examined the cohort of 145 tumours previously described in this study. Analysis of the expression of miR-10a and 10b in primary neuroblastoma tumours, along with patient survival, indicated that these miRNAs differ in both their patterns of expression in genetic subtypes and in their associations with clinical outcome. Patients with tumours exhibiting lower than median miR-10a expression, although not significant, displayed a trend towards poorer overall survival (P=0.08), and poorer chance of an event free survival (EFS) (P=0.15). Kaplan-Meier plots for the 11q- tumour cohort (n = 30), displayed a statistically significant association between lower miR-10a expression and lower OS with a trend towards lower EFS (P = 0.057; Figure 5.23 a and b) No association between miR-10b expression and survival was established. MiR-10a was significantly under-expressed in high grade stage 4 tumours with MNA (n=20) or loss of 11q (n=30), relative to other stage 4 tumours (n=22) and relative to low stage disease (stage 1,2,3 and 4s; n=45; P<0.0001; Figure 5.23 c). Interestingly miR-10b displayed an inverse pattern of expression in the same set of tumours, with MNA and 11q- tumours having slightly higher expression (Figure 5.23 d).

Although miR-10a maps to a region on chromosome 17q that commonly undergoes increased copy-number in most high-risk neuroblastomas, we show here that miR-10a expression is significantly lower in tumours with 17q gain relative to tumours with diploid 17q copy number status, indicating that a mechanism exists to counteract the gain in DNA dosage (Figure 5.23 e). This suggests that it may be vital for unfavorable tumours, particularly of the 11q- subtype, to have low miR-10a expression levels, presumably because of the positive effects on differentiation. In contrast, miR-10b is expressed at

higher levels in less favorable neuroblastoma tumours and is not associated with lower patient survival even though this miRNA causes *in vitro* biological effects that are indistinguishable from miR-10a. However, there are differing secondary effects of these miRNAs on the transcriptome of NB cells, that might account for the observed differences in patient survival.

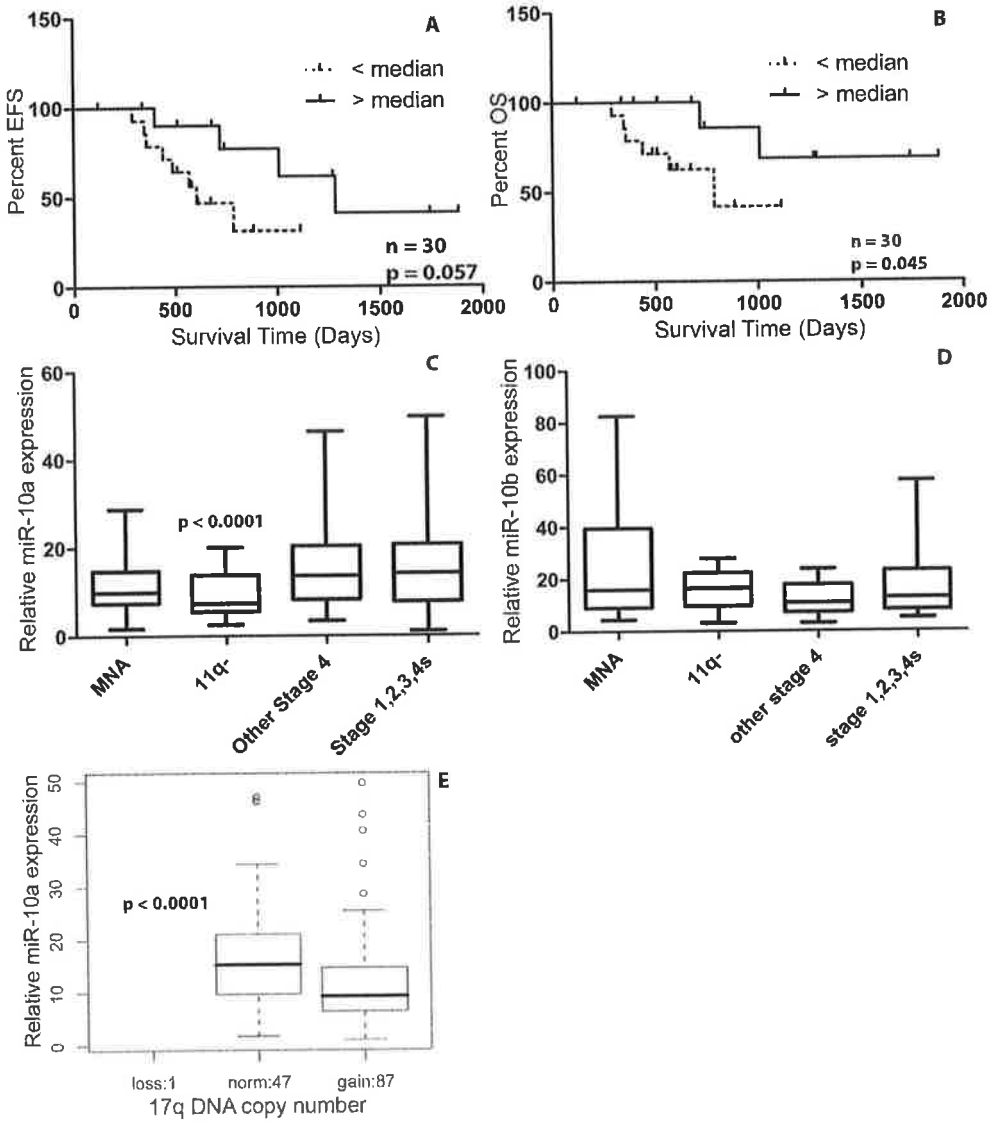

Figure 5.23. Association of miR-10 in neuroblastoma tumours. Tumours expressing lower than median miR-10a a trends towards significance for (a) EFS and are significant for (b) OS. (c) MiR-10a was significantly under-expressed in high grade stage 4 tumours with MNA (n=20) or loss of 11q (n=30), relative to other stage 4 tumours (n=22) and relative to low stage disease (stage 1,2,3 and 4s). (d) MiR-10b displayed an inverse pattern of expression in the same set of tumours, with MNA and 11q- tumours having slightly higher expression. (e) MiR-10a expression is significantly lower in tumours with 17q gain relative to tumours with diploid 17q copy number status.

5.2 MiR-152 a microRNA involved in the epigenetic regulation of NB cells

5.2.1 Alterations in levels of DNA methyltransferases following ATRA

Given that miR-152 ectopic over-expression had interesting biological effects, namely a reduction in cell invasiveness, it was of interest to identify mRNA targets for this miRNA. An examination of computationally predicted targets for miR-152 in TargetScan V5.1 indicated the DNA methyltransferase, *DNMT1*, as a potential target (Figure 5.24). As previously mentioned, ATRA treatment of SK-N-BE cells leads to miR-152 up-regulation (Section 4.1.2). DNA methyltransferase genes *DNMT1*, *DNMT3a* and *DNMT3b* are involved in the initiation and maintenance of methylation in the genome. As aberration alterations in methylation are widely reported to play a role in cancer progression, the miR-152 target *DNMT1* was of great interest. Initially mRNA microarray profiling of ATRA-treated SK-N-BE cells was carried out. This analysis identified a large number of genes, which were altered in response to ATRA. Interestingly two of the DNA methyltransferases, namely *DNMT1* and *DNMT3b,* were significantly reduced after ATRA treatment (Figure 5.25).The expression of *DNMT3a* was not altered in response to ATRA.

Figure 5.24. MiR-152 predicted alignment with *DNMT1*. *DNMT1* was predicted by Target Scan V5.1 as a potential target of miR-152. A high level of sequence complementarity was identified within the miR-152 seed region (a 10 base pair match).

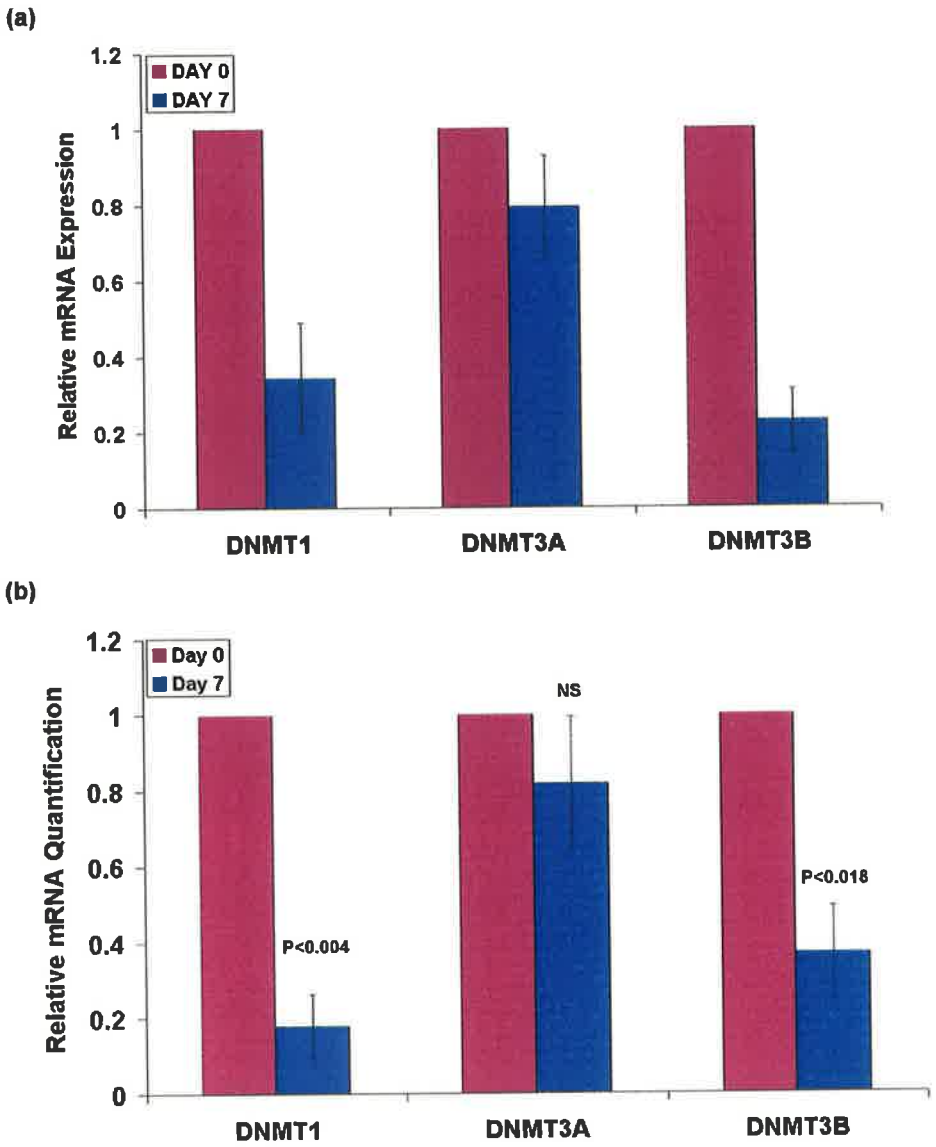

Figure 5.25. *DNMT* levels after ATRA treatment. (a) ATRA causes down regulation of *DNMT1* and *DNMT3b* but not *DNMT3a* as shown by microarray gene expression profiling. (b) Differential expression was validated using qPCR.

5.2.2 *DNMT1* is down regulated by miR-152

In order to validate *DNMT1* as a target of miR-152, using a mature mimic miR-152 was ectopically over-expressed in SK-N-BE cells. Cells were harvested for total RNA and protein at 24, 48 and 72 h. A large decrease of *DNMT1* mRNA was observed over all three time points (Figure 5.26 a). These results were confirmed at the protein level after 72 h (Figure 5.26 b) and suggest that miR-152 over-expression after ATRA treatment contributes to the down-regulation of *DNMT1*.

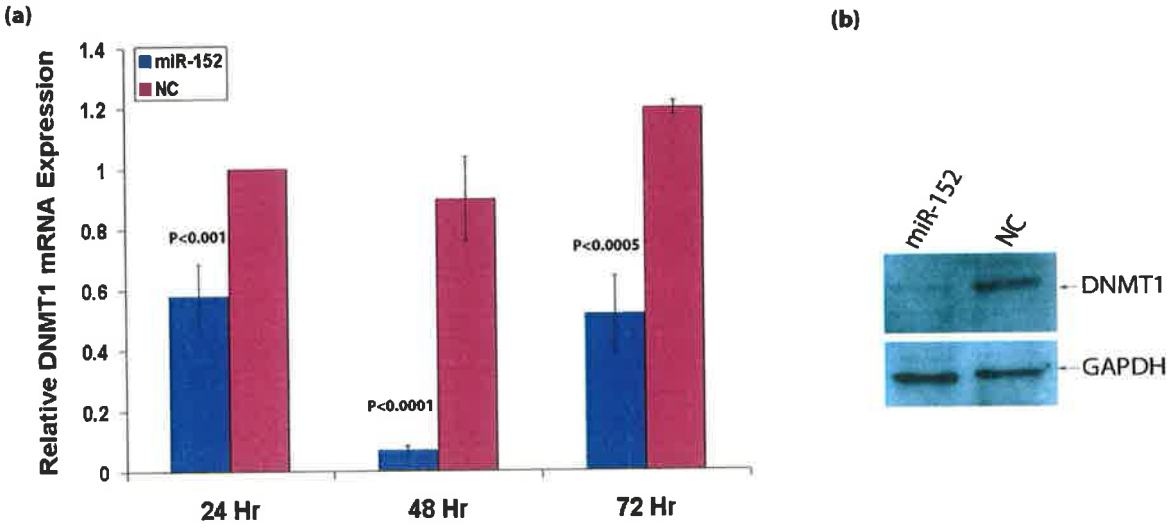

Figure 5.26. MiR-152 causes down-regulation of *DNMT1*. MiR-152 up-regulation in SK-N-BE cells using mature mimics cause the down regulation of *DNMT1* at both (a) mRNA and (b) protein level when compared to SK-N-BE cells transfected with a scrambled oligonucleotide control.

5.2.3 *DNMT1* a target of miR-152

The PsiCHECK2™ Luciferase reporter vector containing a 321 nucleotide section of the *DNMT1* 3'UTR including the miR-152 binding site, was co-transfected with the mature mimic for miR-152. Luciferase activity was measured and compared to the *DNMT1* 3'UTR plasmid co-transfected with the scrambled control oligonucleotide. A reduction of 42% in luciferase activity ($P<0.02$) after transfection with the mature mimic was detected. As a control, the mature mimic was co-transfected with the PsiCHECK2™ vector containing a 3 base pair mutation in the seed region of the binding site (Appendix 2.3). This experiment showed no reduction in luciferase activity versus the mutated vector co-transfected with the scrambled negative control. This result validates *DNMT1* as a miR-152 target (Figure 5.27) and confirms the requirement of seed region binding for degradation of the transcript.

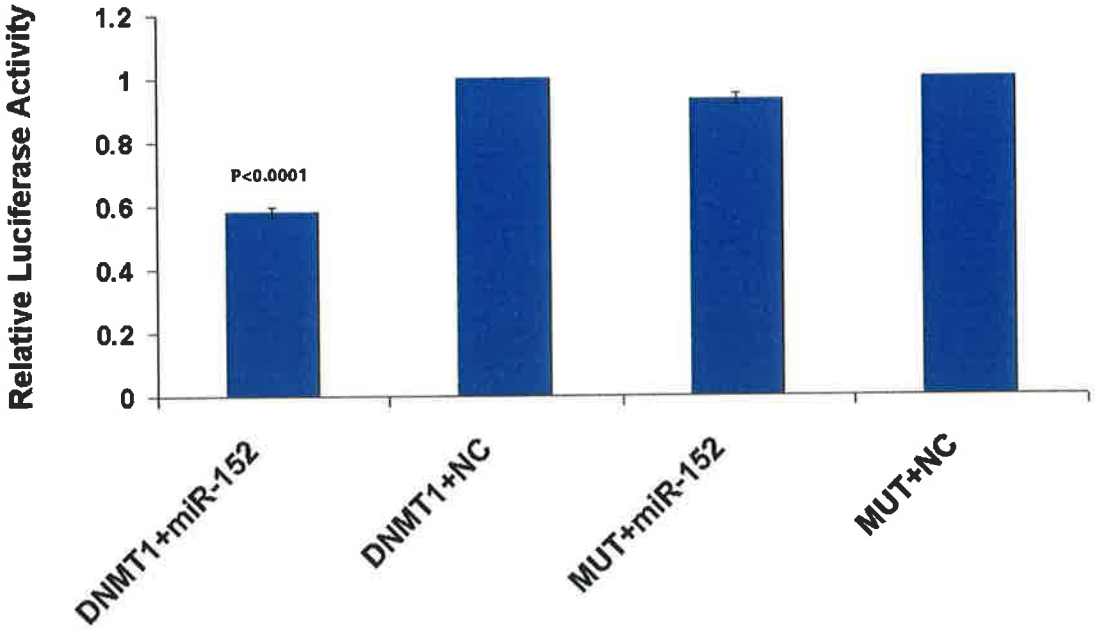

Figure 5.27. MiR-152 binds to *DNMT1* reducing luciferase activity. This figure shows a substantial reduction in luciferase activity when the mature miR-152 mimic is co-transfected with the luciferase expressing plasmid containing the miR-152 binding site of *DNMT1*. This was normalised to the plasmid co-transfected with the scrambled oligonucleotide control (NC). Three point mutations were made in the seed region binding site of the *DNMT1* sequence (MUT), there was no reduction in luciferase activity when this mutant was co-transfected with the mature mimics or the scrambled control (NC).

5.2.4 Global De-methylation of the NB genome following ATRA

In order to determine if down-regulation of DNMTs following ATRA treatment led to alterations in DNA methylation patterns, DNA methylation profiling on neuroblastoma SK-N-BE cells treated with ATRA was carried out. ATRA-treated samples were hybridised after immunprecipitation with an anti-methyl-cytidine antibody versus non-immunoprecipitated samples. These were then analysed using an array containing all known promoter and CpG island regions. This analysis showed that ATRA causes a global decrease in methylation levels in SK-N-BE neuroblastoma cells. In total, 2499 promoter regions and 1721 non promoter CpG island sites were hypermethylated in untreated SK-N-BE cells. In total, 402 gene promoters (excluding non-promoter CpG island sites) were de-methylated following ATRA treatment, with eighty-two of these genes being over-expressed greater than 2-fold in the ATRA-treated cells (7 days post ATRA) relative to untreated, as ascertained by mRNA expression microarrays. Thus, down-regulation of the DNMTs had a significant impact on the epigenome (Figure 5.28). In contrast 88 genes become hypermethylated post ATRA, 13 of which were under-expressed >2-fold.

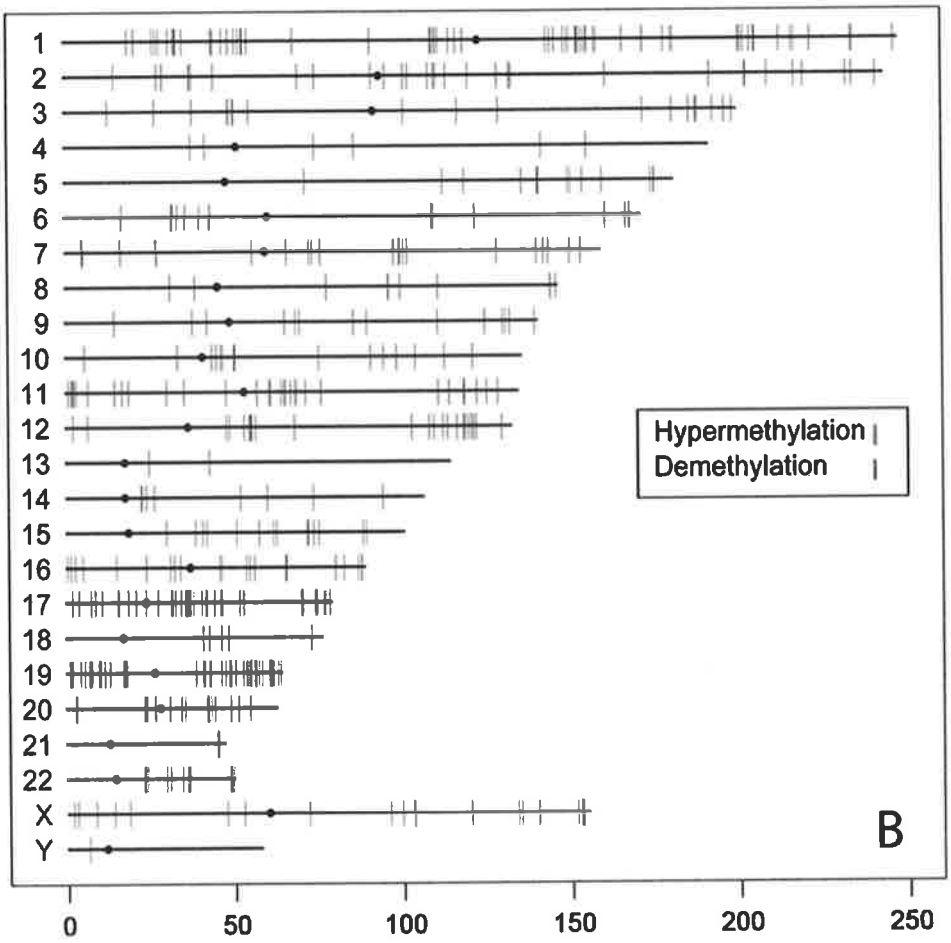

Figure 5.28. Chromosomal gene promoter de-methylation following ATRA treatment. 402 gene promoters were de-methylated (blue-lines) and 88 gene promoters methylated (re-lines) through-out the genome after ATRA treatment of SK-N-BE cells.

5.2.5 MiR-152 and *MYCN* status

Tumour data from Bray *et al.* (2009) indicated a relationship between *MYCN* status and miR-152 in neuroblastoma tumours (209). We demonstrate here using the same tumour set that miR-152 is under-expressed in MNA tumours (n=35) versus non-MNA (n=111; Figure 5.29 a). A MYCN repressible system (as previously described in Section 3.1.2) was then used to examine miR-152 and *DNMT1* levels when *MYCN* is over-expressed. This SH-EP21N *MYCN* repressible model showed an increase in miR-152 of ~3-fold within 48 h after *MYCN* depletion (Figure 5.29 b), while *DNMT1* mRNA levels are decreased by ~5-fold, (Figure 5.29 c) confirming the inverse relationship between *MYCN* and miR-152 expression, which has a subsequent effect on *DNMT1*.

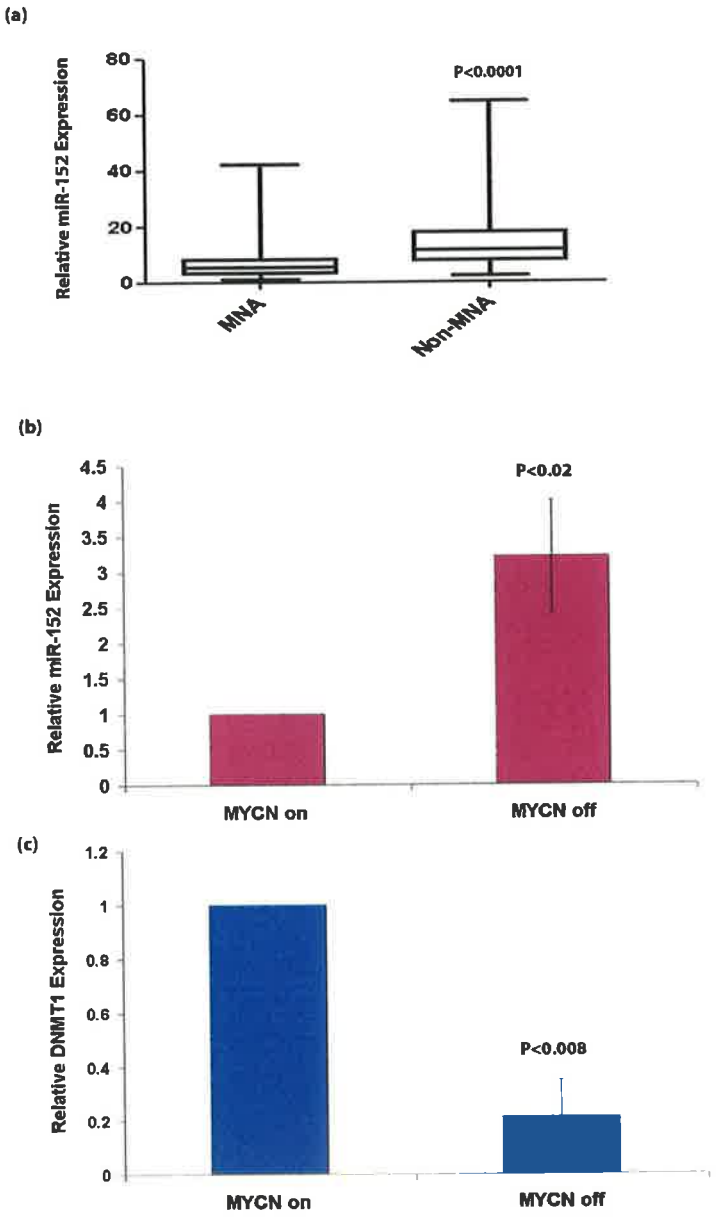

Figure 5.29. Relationship between *MYCN*, miR-152 and *DNMT1*. (a) MiR-152 is significantly under-expressed in MNA tumours versus non-MNA. (b) MiR-152 is up-regulated ~3-fold in the *MYCN* off state this result was reflective of a subsequent down regulation of (c) *DNMT1* in the same condition.

5.2.6 *DNMT1*, survival and *MYCN* association in tumours

The R2 tumour database as described in Section 3.1.19 was again utilised to examine *DNMT1* levels in neuroblastoma tumours. High *DNMT1* levels were predictive of poor OS and EFS (Figure 5.30 a and b), this is in keeping with numerous reports demonstrating that hypermethylation is associated with cancer. In keeping with results seen in this study, *DNMT1* was more highly expressed in MNA tumours when compared to non-MNA tumours (Figure 5.31 c). *DNMT1* was also significantly highly expressed in poor outcome, stage 4 tumours, compared to all other stages (Figure 5.30 d).

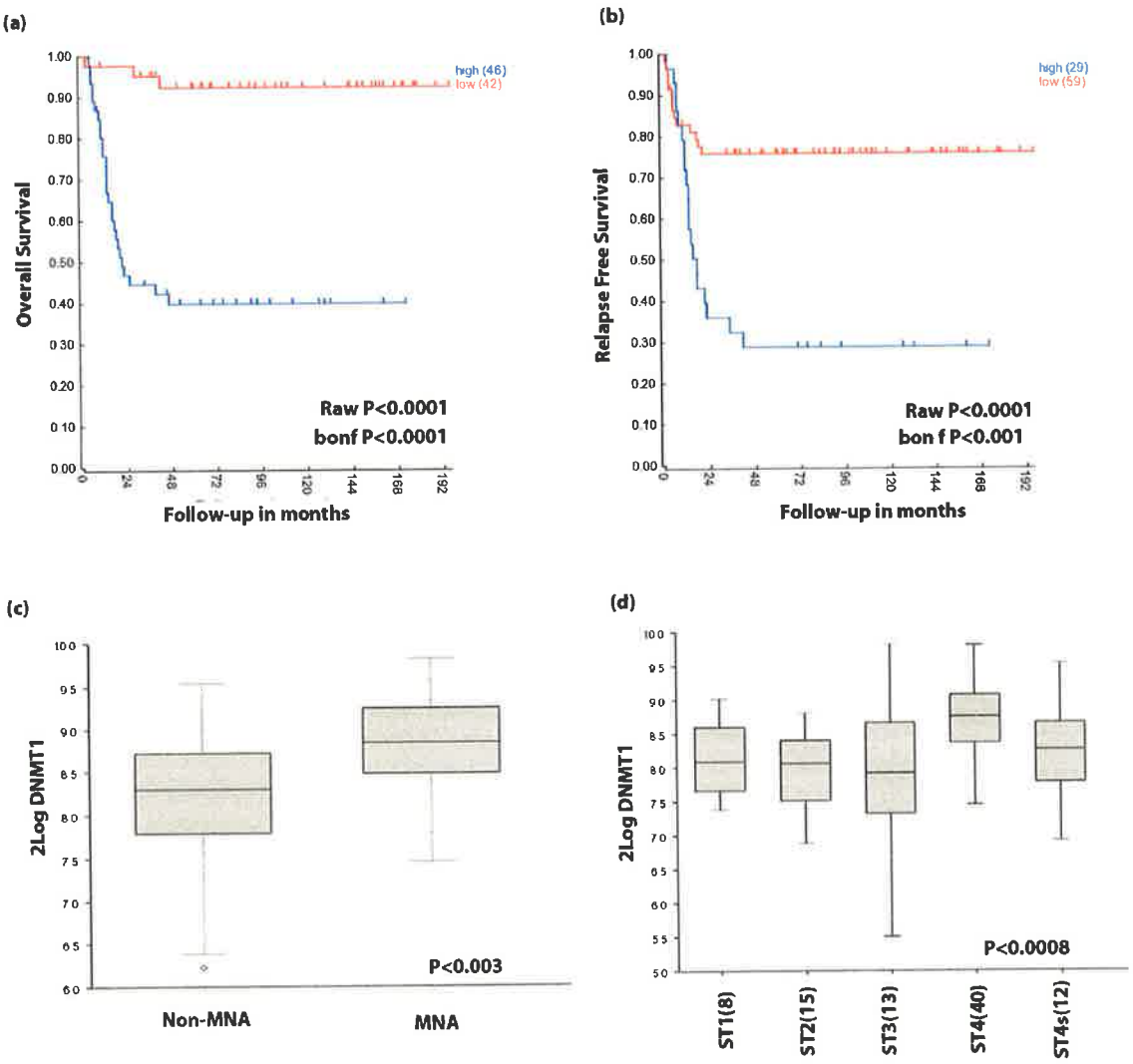

Figure 5.30. *DNMT1* is associated with overall survival, relapse free survival, MYCN status and stage in neuroblastoma tumours. High levels of *DNMT1* are positively associated with poor (a) overall survival after correction for multiple comparison, high *DNMT1* levels are also positively associated with (b) poor relapse free survival after correction for multiple comparisons. *DNMT1* is expressed at a higher level in (c) MNA tumours versus the non-MNA subset. *DNMT1* is expressed at highest levels in (d) stage 4 tumours.

5.3 MiR-196a a potential tumour suppressor in neuroblastoma

5.3.1 The miR-196a predicted target *NRAS* is down-regulated on ATRA mRNA arrays

MRNA expression profiling was performed using whole genome cDNA microarrays for SK-N-BE cells at 7 days post treatment with ATRA. MiR-196a was up-regulated in response to ATRA-induced differentiation of SK-N-BE cells (Section 3.1.2) and a high scoring Target Scan predicted target of miR-196a, *NRAS* (Figure 5.31) was of immediate interest as it was significantly down regulated after ATRA treatment (Figure 5.32).

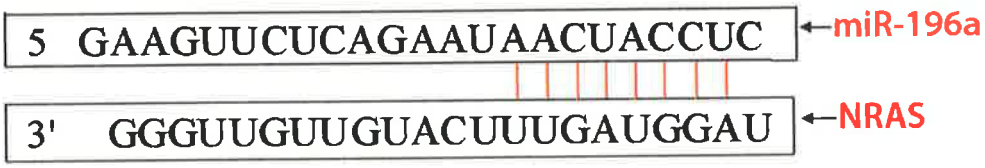

Figure 5.31. Predicted alignment of miR-196a and *NRAS*. *NRAS* was predicted by Target Scan V5.1 as a potential target of miR-196a. There is a high level of sequence complementarity with the miR-196a seed region (an 8 base pair match).

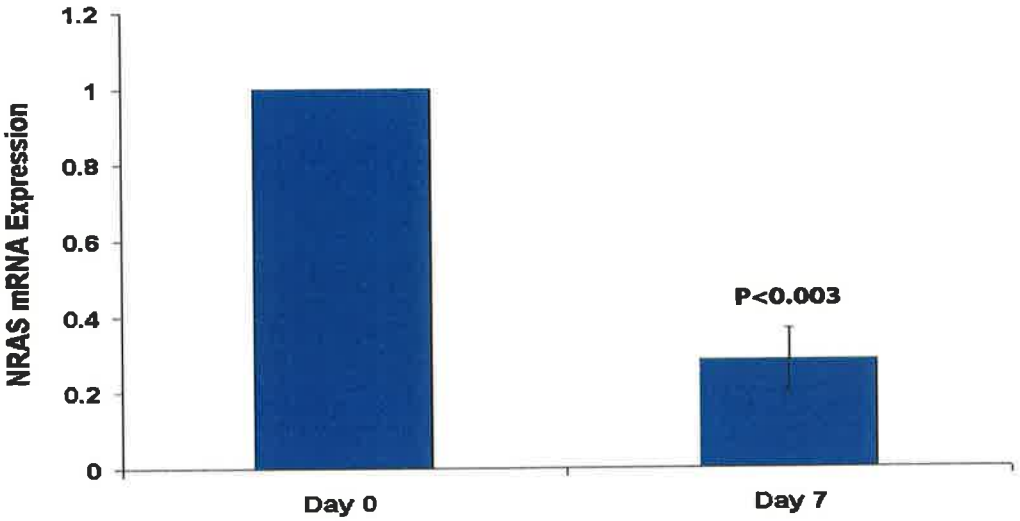

Figure 5.32. *NRAS* is down regulated after ATRA treatment. *NRAS* mRNA levels were down-regulated post ATRA treatment of SK-N-BE neuroblastoma cells relative to non-treated control cells.

5.3.2 Ectopic up-regulation of miR-196a results in an increase in *NRAS*

To examine if miR-196a targets *NRAS in vitro*, miR-196a was ectopically over-expressed in SK-N-BE cells. Contrary to what was expected, ectopic up-regulation of miR-196a using the mature mimics (as demonstrated in Section 5.1.2) resulted in an up-regulation of NRAS at both mRNA (Figure 5.33 a) and protein level (Figure 5.33 b).

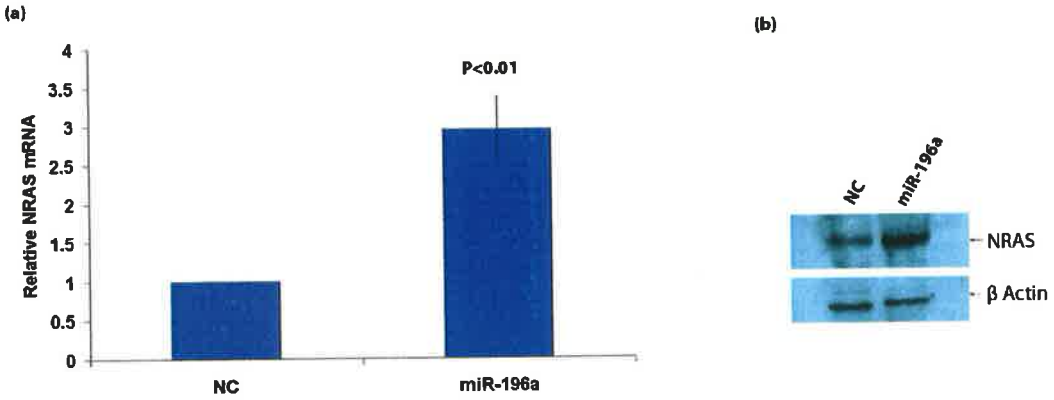

Figure 5.33. MiR-196a causes up regulation of *NRAS*. MiR-196a ectopic over expression increases the levels of NRAS in SK-N-BE cells, relative to the scrambled oligonucleotide control at both (a) mRNA and (b) protein levels.

5.3.3 MiR-196a does not bind to the predict target site in the 3'UTR of *NRAS*.

MiR-196a was predicted by Target Scan V5.1 to bind to a region in the 3'UTR of *NRAS*. The PsiCHECK2™ Luciferase reporter vector containing a 500 nucleotide section of the *NRAS* 3'UTR including the miR-196a binding site, was co-transfected with the mature miR-196a mimics. Luciferase activity was measured and compared to the *NRAS* 3'UTR plasmid co-transfected with the scrambled control oligonucleotide. There was no reduction in luciferase activity after transfection with the mature mimic to miR-196a. As a control, the mature mimic was co-transfected with the PsiCHECK2™ vector containing a 3 base pair mutation in the seed region of the binding site. This experiment also showed no reduction in luciferase activity versus the mutated vector co-transfected with the scrambled negative control. These results indicate that miR-196a is not binding to the 3'UTR of *NRAS* (Figure 5.34).

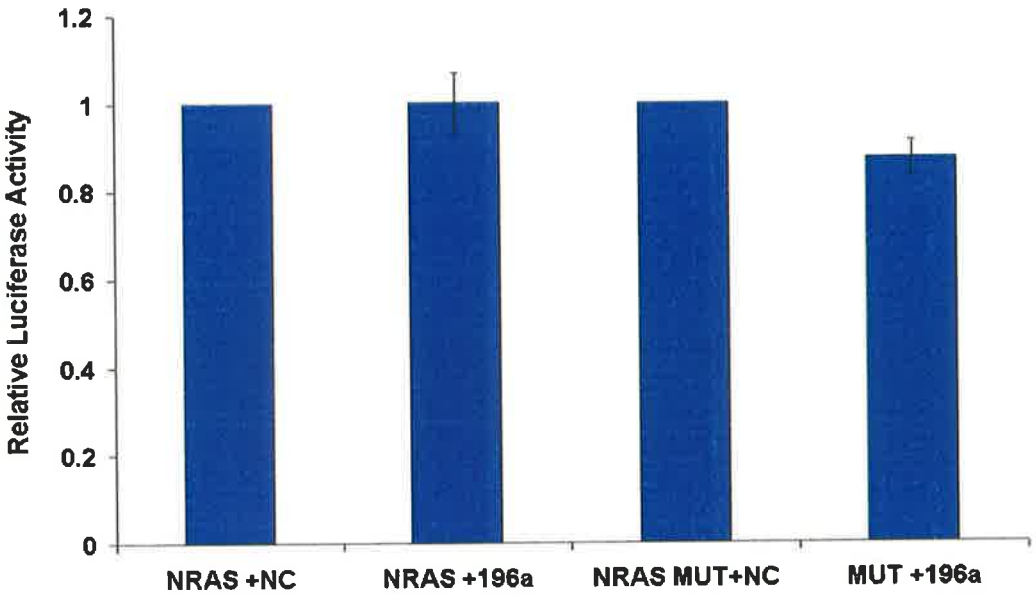

Figure 5.34 MiR-196a does not bind to the 3'UTR of *NRAS*. This figure displays no significant reduction in luciferase activity when the mature mimics 196a is co-transfected with the luciferase expressing plasmid containing the miR-196a binding site of *NRAS*. This was normalised to the plasmid co-transfected with the scrambled oligonucleotide control (NC). Three point mutations were made in the seed region binding site of the *NRAS* sequence (MUT), there was no reduction in luciferase activity when this mutant was co-transfected with the mature mimics or the scrambled control (NC).

5.3.4 High levels of miR-196a and *NRAS* are both positively associated with overall and event free survival in neuroblastoma

High levels of miR-196a was statistically associated with OS ($P<0.05$) and EFS ($P<0.05$) in the subset of 145 neuroblastoma tumours previously described (Figure 5.35 a and b). MiR-196a was expressed at lower levels in 11q- tumours vs. non-11q- tumours ($P<0.0006$; Figure 5.35 c). The R2 tumour database (Section 3.1.19) was again utilised to examine *NRAS* levels in neuroblastoma tumours. High *NRAS* levels were predictive of positive OS and EFS (Figure 5.36 a and b) both before and after correction for multiple comparisons. We have demonstrated that miR-196a is associated with good survival in neuroblastoma, suggesting that up-regulation of miR-196a may up-regulate *NRAS*, resulting in good overall survival predictions.

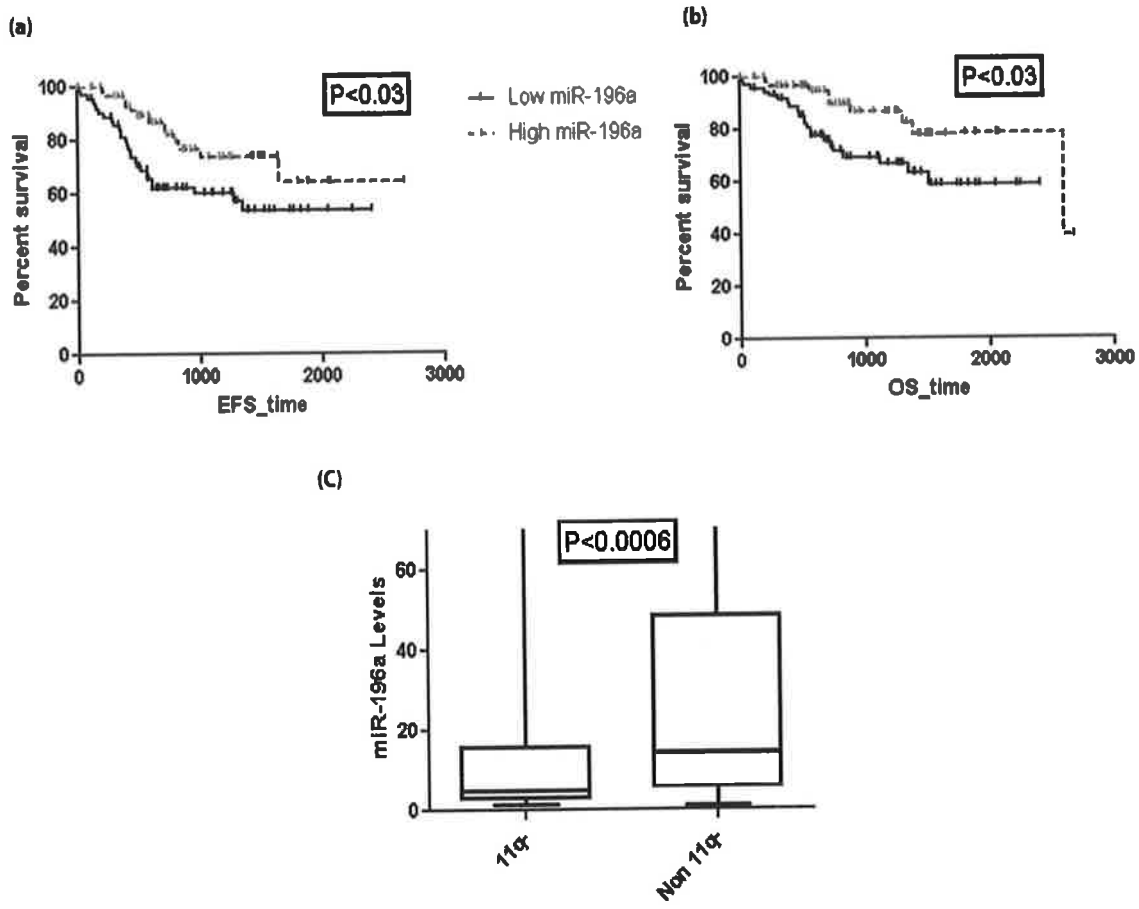

Figure 5.35. MiR-196a is down-regulated in 11q- tumours and high miR-196a is associated with good EFS and OS. A greater than median levels of miR-196a are positively associated with (a) OS and (b) EFS. (c) MiR-196a is expressed at lower levels in 11q- tumours.

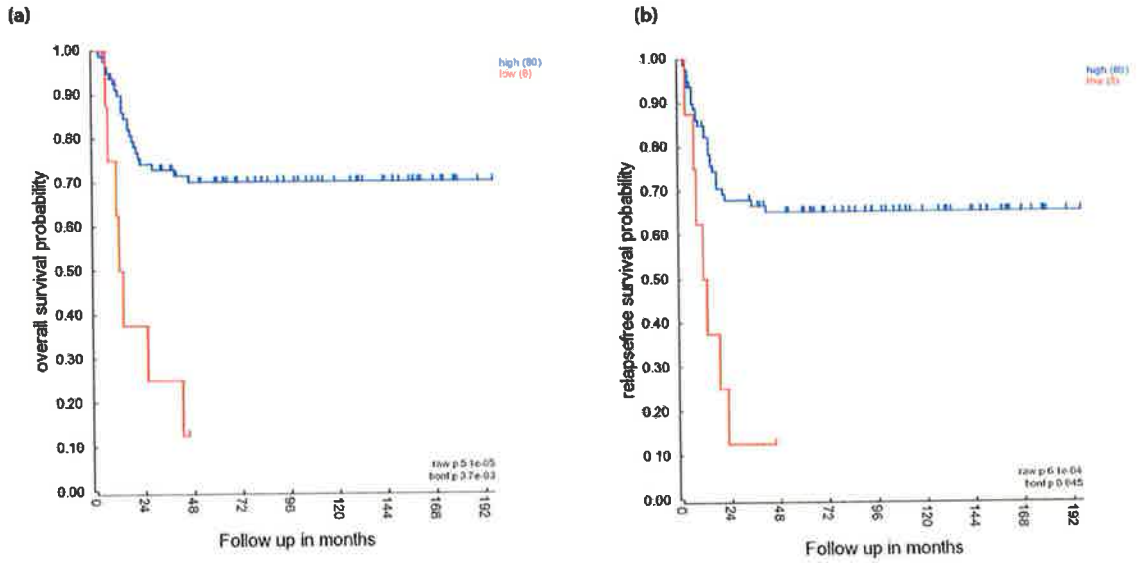

Figure 5.36. *NRAS* is associated with good overall survival, relapse free survival and stage in neuroblastoma tumours. (a) High levels of *NRAS* are positively associated with overall survival probability before and after correction for multiple comparison. (b) High *NRAS* levels are also positively associated with relapse free survival before and after correction for multiple comparisons.

5.3.5 Mature miR-196a is expressed in the nucleus of the cell

We hypothesized that it is possible that miR-196a maybe up-regulating *NRAS*, by some unknown method at a transcriptional level. To further investigate this both nuclear and cytoplasmic levels of miR-196a were quantified samples by separating cytoplasmic and nuclear fractions of the cell, and performing RTqPCR. This result demonstrates that the mature miR-196a was expressed in both the nucleus and the cytoplasm (both coming up at a CT value of ~22) suggesting that the mature microRNA is being transported back into the nucleus after maturation by some un-known mechanism, possibly to act in a transcriptional control role.

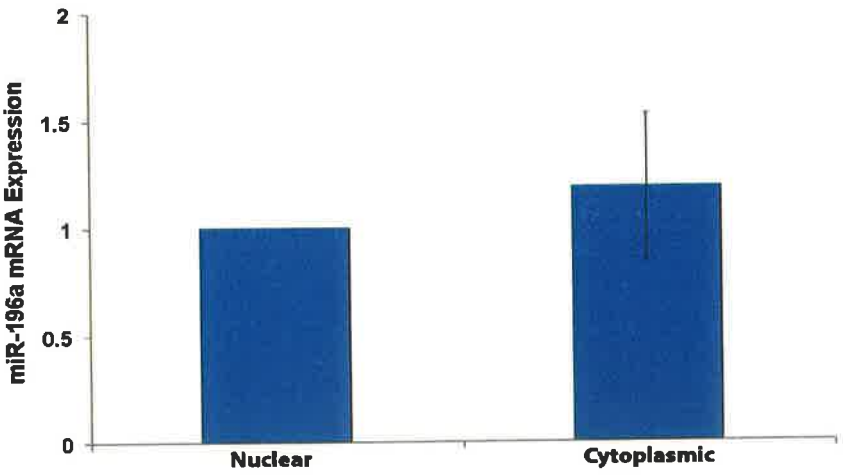

Figure 5.37. Mature miR-196a is expressed in both the nucleus and the cytoplasm of SK-N-BE neuroblastoma cells. MiR-196a levels were expressed in both the nucleus and the cytoplasm at similar levels.

5.4 Discussion

5.4.1 HOX cluster microRNAs functional roles in neuroblastoma

A comprehensive map of the miRNA network involved in neural differentiation is poorly charcterised. Here we delve deeper into the processes of differentiation by examining the contribution of individual microRNAs.

Of the microRNAs identified in the profiling study, miR-132 was the most highly up-regulated microRNA in response to the ATRA treatment. This microRNA had however already been reported to have no functional effect in neuroblastoma (242) and was not chosen for further investigation. The next most highly up-regulated microRNAs were those of the miR-10 family; miR-10a and miR-10b. These two microRNAs along with miR-152 and miR-196a were chosen for functional analysis. MiR-152 and miR-196a were also selected for study due to that they are also embedded within the *HOX* gene cluster (see Figure 5.38).

The *HOX* family are highly conserved genes controlling many essential processes during development including growth, differentiation and cell fate (289, 290, 296). Aberrant expression of these genes have been associated with a large number of cancers (291). Not only are the miRNAs located within this cluster they are also known to directly inhibit some of the *HOX* genes, with miR-10a targeting *HOXA1* (292), and miR-10b targeting *HOXD10* (284), miR-196a targeting *HOXA7, HOXB8, HOXC8, HOXD8* (297) and *HOXB7* (298).

Taking into account the fact that neuroblastoma is a developmental cancer and that the regions of the genome containing the HOX clusters are highly conserved across species and play an important role in development processes, it was considered that HOX-embedded microRNAs would be interesting candidates for further study. Ectopic over-expression of each microRNA was carried out both individually and in pools. Results from pooled experiments were not visibly more effective than individual transfections *in vitro*, for experiments carried out here.

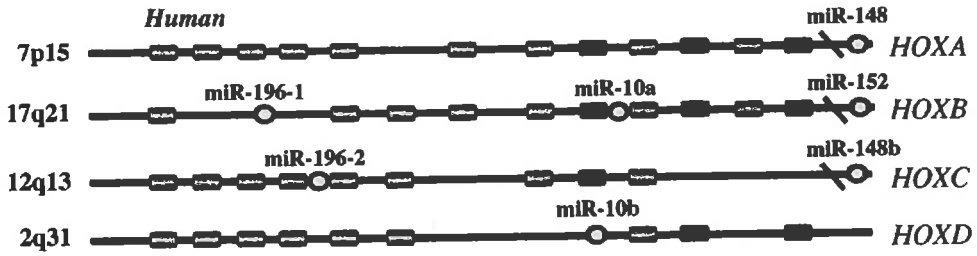

Calin *et al.*, (2004) (199)

Figure 5.38. MicroRNAs located within the HOX cluster of genes. This diagram represents the four chromosomal clusters of HOX genes, with the locations of the microRNA transcripts.

5.4.2 MiR-10a and miR-10b an essential role in differentiation

We demonstrate here that ectopic over-expression of miR-10a or miR-10b and miR-10a/b combined lead to a significant increase in neurite out-growth, the up-regulation of markers of mature neuronal cell type *GAP43* and *TUBB3*, the down-regulation of *MYCN* and a reduction in the rate of cell growth. All these changes mimic the effects associated with ATRA-induced differentiation in this cell line. MiR-10a and 10b differ by a single nucleotide which occurs outside of the "seed" region, thus, it is not surprising that

the *in vitro* biological effects of these miRNAs are indistinguishable following ectopic up-regulation in SK-N-BE cells.

In order to experimentally identify direct targets down-regulated by miR-10a/b, mRNA expression profiling was performed using microarrays representing 24,000 protein coding genes for SK-N-BE cells. Of immediate interest was the down-regulation of *NCOR2,* a gene previously demonstrated to induce profound neurite outgrowth when down regulate in cultured neuronal stem cells (295). Over-expression of miR-10a and miR-10b both individually and in combination resulted in a significant down regulation of *NCOR2* mRNA and protein. This result was validated using a luciferase reporter vector which determined that the "seed region" of miR-10a/b was essential for *NCOR2* down regulation. As both microRNAs have identical seed regions, it is not surprising that either can function in the transcriptional down-regulation of *NCOR2*. Further to this analysis of *NCOR2,* we showed that this gene is of major prognostic significance in neuroblastoma, with high expression associated with MNA tumours, poor OS and EFS.

In addition to *NCOR2* down-regulation, microarray studies demonstrate that miR-10a and 10b over-expression launches a cascade of changes at transcriptional and post-transcriptional levels through a complex series of primary and secondary mechanisms. Despite vast re-programming of the SK-N-BE cell transcriptome following miR-10a/10b transfections, siRNA-mediated inhibition of this single direct target, *NCOR2*, can recapitulate differentiating phenotypic effects including; increased neurite outgrowth, the up-regulation of markers of mature neuronal cell type GAP43 and TUBB3, the down-regulation of *MYCN* and a reduction in the rate of cell growth.

NCOR2 has the ability to bind to hormone receptors, recruit co-repressor proteins and silence primary response genes (reviewed by Jepsen (299)). NCOR2 exerts its functions as a co-repressor through recruitment of a complex of proteins to DNA promoter region, including SIN3A/B, histone deacetylases HDAC1, HDAC2 and HDAC3 to hormone receptor complexes such as the retinoic acid receptor complexes and the steroid receptor complexes (300). SiRNA/miR-10a/b mediated inhibition of *NCOR2* would therefore be expected to result in the increased acetylation and transcriptional activation of numerous genes caused by the disruption of an NCOR2/HDAC repressor protein complex. Indeed, increased expression of large numbers of genes was observed following miR-10a/10b mediated inhibition of *NCOR2*. We observed decreased expression of a large numbers of genes that are significantly enriched for miR-10a/b predicted target sites, along with other genes that do not contain target sites. The later category of genes clearly results from secondary events, with a notable example being *MYCN*. Jaboin *et al.* (301) and Ruijiter *et al.* (302) showed that HDAC inhibitors can also result in a down regulation of *MYCN* through an unknown secondary mechanism. As both *HDAC* inhibition and *NCOR2* inhibition cause down regulation of *MYCN* we postulate that destabilising the NCOR2 /HDAC complex may have a role in the regulation of *MYCN*.

It is suggested that neuroblastoma has its origins in developing neural crest cells that have been blocked in their ability to differentiate, resulting in unchecked proliferation and progression to tumour development and disease. Maintenance of this de-differentiated state may be due to a lack of response to normal developmental signals; either signals are not sent to the cells or the cells do not respond. Histopathological analysis of *MYCN* amplified tumours by the Childrens Cancer Group (2001) demonstrated that the vast

majority of these tumours (93.9%) did not show any form of differentiation and were classified into either undifferentiated or poorly differentiated subgroups (49). It is possible that the decrease in *MYCN* levels, via a secondary mechanism initiated by miR-10 down-regulation of *NCOR2,* could be one of the pathways by which these microRNAs induce neuroblastoma cell differentiation.

Le *et al.* (240) recently demonstrated that miR-125b promotes neuronal differentiation when ectopically over-expressed in neuroblastoma SH-SY5Y cells through directly repressing 10 key target genes, which further regulate many other key neurogenesis pathways. MiR-125b was up-regulated ~1.6-fold in this ATRA study but did not fall under the 2-fold cut off employed. From this analysis, there appears to be some level of redundancy in function of miR-125b with miR-10a/b as three of these key target genes (*ITCH*, *GAB2*, and *MKNK2*) have miR-10 seed sites in their 3' UTRs and are down-regulated following ectopic up-regulation of miR-10a/b in our studies. Remarkably, miR-125b has a 7-mer conserved seed match in the 3' UTR of *NCOR2* (TargetScan). Based on the overlap of key targets, it is perhaps not surprising that ectopic up-regulation of both of these miRNA families leads to neuronal differentiation. We demonstrated that anti-sense knock-down of both miR-10a and -10b, 24 h prior to ATRA treatment led to a highly significant, but incomplete, reduction in the outgrowth of neurites. It is possible that miR-10a/b knockdown was insufficient to completely reverse the effects of ATRA, given that other ATRA-induced miRNAs (such as 125b) would still have been over-expressed.

The discovery that down-regulation of *NCOR2* resulted in ~14-fold increase in miR-10a added a greater degree of complexity to the process. As knock-down of the retinoic acid receptor in a pancreatic cancer cell line resulted in complete inhibition of

miR-10a expression it was concluded that miR-10a, located on chromosome 17q within the *HOXB3* gene, is a retinoic acid receptor target (51). Thus, miR-10a up-regulation in response to ATRA is a direct consequence of ATRA causing displacement of the co-repressor complex with a co-activator complex, leading to chromatin acetylation and concurrent miR-10a transcription. MiR-10a can then post-transcriptionally down-regulate *NCOR2*, maintaining the disruption of the co-repressor complex in the absence of ATRA. SiRNA or miR-10a/b mediated inhibition of *NCOR2* therefore results in the same differentiated phenotype that is caused by ATRA treatment. The involvement of NCOR2 in a co-repressor complex that down-regulates miR-10a expression indicates that a regulatory feed-back loop exists (see Figure 5.39 for a putative model for this feedback loop).

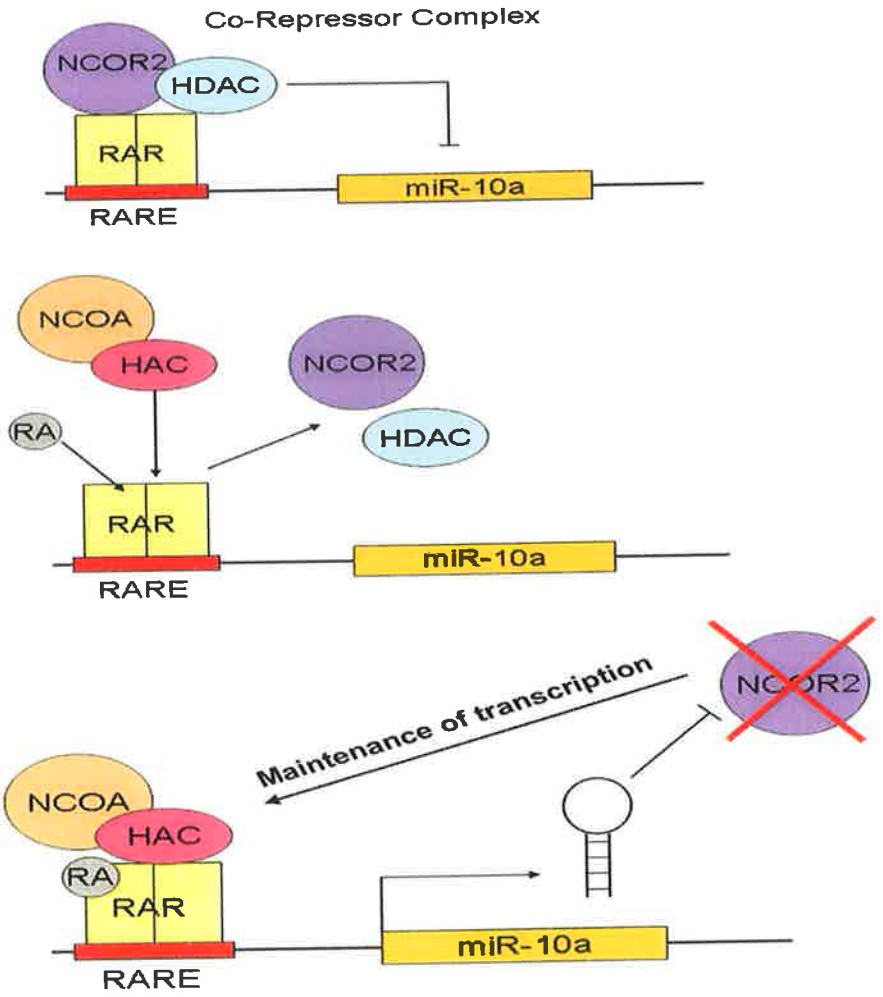

Figure 5.39. MiR-10a and *NCOR2* a regulatory loop. In this model, a very early step is the disruption of an *NCOR2*/retinoic acid receptor (RAR)/histone deacetylase (HDAC) co-repressor complex bound to a retinoic acid receptor element (RARE) upstream of miR-10a. In the presence of retinoic acid (RA) this complex is displaced and replaced by a co-activator complex leading to transcriptional activation of miR-10a. MiR-10a directly targets and represses *NCOR2*, allowing continued expression of miR-10a.

Analysis of the expression of miR-10a and 10b in a cohort of 145 primary neuroblastoma tumours showed they differ not only in their pattern of expression in genetic subtypes, but also in their associations with clinical outcome. MiR-10b expression does not correlate with patient survival, whereas low-expression of miR-10a shows a trend towards poor OS and EFS, particularly for patients with 11q- tumours. Although miR-10a maps to a region on chromosome 17q that commonly undergoes copy-number gain in high-risk neuroblastomas, miR-10a expression is significantly lower in tumours with 17q gain relative to tumours with diploid 17q copy number status. This suggests that a mechanism exists to counteract the gain in dosage due to copy number alteration. Thus, it appears to be vital for unfavorable tumours, particularly of the 11q- subtype, to have low miR-10a expression levels, presumably because of the positive effects on differentiation. Exactly why this is not the case for miR-10b, which produces *in vitro* biological effects that are indistinguishable from miR-10a, is unknown. The role of miR-10a/b in cancer appears to be tumour and cell context dependent, as miR-10a has been reported to be under-expressed in haematological malignancies such as CML (281), while both miRNAs have been reported to be over-expressed in a variety of solid tumours (see (283) for review). Over-expression of miR-10b has been associated with breast cancer metastasis (285), although this view has been challenged (282). In this regard it is interesting that miR-10b is marginally over-expressed in tumours with either MNA or 11q LOH from patients with metastatic disease, relative to loco-regional tumours lacking these unfavorable genetic alterations.

In conclusion we have identified two novel microRNAs which induce differentiation and inhibit cell proliferation in SK-N-BE NB cells, and validate *NCOR2* as

a direct target of miR-10a and miR-10b. Interestingly *NCOR2* down regulation leads to the indirect suppression of *MYCN,* a potent oncoprotein in neuroblastoma. MiR-10a/b could be of potential therapeutic benefit if targeted delivery of these miRNAs is achievable, given their pro-differentiation and anti-proliferative effects.

5.4.3 MiR-152 a methylation controlling microRNA

Functionally miR-152 it did not have any effect on the morphology or viability of cells after transfection, however ectopic over-expression resulted in reduced colony forming efficiency and a highly significant reduction in cell invasion across a matrigel structure. Investigation of potential mRNA targets was carried out to determine further mechanisms which could potentially cause these functional effects. The highest scoring predicted mRNA target for miR-152 in Target Scan was the DNA methyltransferase *DNMT1*, which is responsible for the maintenance of the methylated state in the genome (303).

Methylation is the addition of a methyl group to a cysteine residue results in the conversion of cytosine to 5-methylcytosine. Methylation typically occurs at CpG sites (cytosine-phosphate-guanine sites) and has a major impact on gene expression (304, 305). This process is catalysed by enzymes and known to be involved in gene expression and regulation, genomic stability and chromatin structure (306). Aberrant DNA methylation is an important epigenetic event resulting in gene silencing and playing a role in the initiation and progression of cancer (214, 215). The key DNA methyltransferases involved in epigenetic modulation are *DNMT1*, *DNMT3A* and *DNMT3B*. Diminished expression of

DNA methyltransferase *DNMT1*, *DNMT3A* and *DNMT3B* in mouse embryonic stem cells leads to complete abolishment of genome-wide methylation (307).

In the present study, mRNA microarray analyses of ATRA-treated cells was carried out and results indicated that both *DNMT1* and *DNMT3B* but not *DNMT3A* were significantly down-regulated in SK-N-BE cells. This result was validated using qPCR analysis. The exact mechanism which leads to diminished *DNMT1* and *DNMT3B* in ATRA-treated cells, however, is unknown. We hypothesize that up-regulation of microRNAs predicted to target the *DNMT*s is a potential mechanism leading to their reduced mRNA levels. Due to the highly published relationship between methylation levels in the genome and cancer, and the hypothesis that ATRA-induced microRNAs may play a role in the control of epigenetics, we wished to further classify the global epigenetic effects of ATRA treatment in neuroblastoma. To examine if ATRA affects methylation levels in neuroblastoma cells, methylated DNA immunoprecipitation (MeDIP) was carried out. DNA from untreated and ATRA-treated SK-N-BE cells was examined using microarrays representative of all known promoter and CpG island regions. Significantly large reductions in methylation levels were observed. In total, 402 gene promoters (excluding non-promoter CpG island sites) were de-methylated following ATRA treatment (across two biological replicates).

MiR-152, which has an 8-mer conserved seed match with *DNMT1*, had a 2.5-fold increase in expression in SK-N-BE cells following ATRA treatment, and therefore could potentially account for the reduction in *DNMT1* levels observed. MiR-152 ectopic over-expression in SK-N-BE cell resulted in down-regulation of DNMT1 at both mRNA level and at protein level, confirming that endogenous up-regulation of miR-152 in ATRA-

treated cells is the likely cause for reduction in *DNMT1*. In addition, luciferase reporter constructs containing both the wild-type and mutated target sequence of *DNMT1* were used to confirm miR-152 directly targets *DNMT1* in SK-N-BE neuroblastoma cells. This is consistent with a recent report by Branconi *et al.* who confirmed miR-152 targeting of *DNMT1* in the metastatic gallbladder cancer cell line Mz-ChA-1 (308).

As described in Chapter 4, ATRA treatment of SK-N-BE cells results in a massive reduction in the levels of *MYCN* expression (237). We have previously reported, and validated here, that miR-152 is expressed at significantly lower levels in MNA tumours relative to those lacking MNA (209), indicating that MYCN either directly or indirectly represses this miRNA. To further validate the suppression of miR-152 by MYCN, we used the SH-EPN21 repressible system to demonstrate that the down-regulation of *MYCN* results in ~3-fold increase in miR-152 within 48 h. Conversely, the up-regulation of miR-152 resulted in a ~5-fold decrease of *DNMT1* mRNA levels, confirming experimentally an inverse relationship between *MYCN* and miR-152 expression. What is also interesting is that *MYCN* is a predicted target of miR-152, so it is possible that *MYCN* suppresses miR-152 as a mechanism of protecting itself against degradation. This theory however needs further functional analysis and validation.

The fact that there was no change in *DNMT3A* levels following ATRA exposure could explain why we do not see a complete reduction in methylation after treatment. It is also possible that the decrease in one or both down-regulated DNA methyltransferases can account for the observed demethylation. A study in 2002 by Rhee *et al.* (309) demonstrated that *DNMT1* and *DNMT3B* but not *DNMT3A* function co-operatively during epigenetic gene silencing of cancer cells. The methods leading to decreased *DNMT3B*

mRNA levels following ATRA is uncertain, although this may also be miRNA driven. For example, miR-125a/b and miR-26a/b are predicted to target DNMT3B and both of these miRNA families have been published to be up-regulated in ATRA-treated cells (223). These microRNAs were up regulated in our study (~1.5-fold up-regulation) however they did not fall within the stringent cut off employed. MiRNA 26a and b are also repressed by MYCN (229) and may also be over-expressed in ATRA-treated cells due to the reduction in *MYCN* levels.

All the evidence presented here suggests that *MYCN* plays an essential role in the control of microRNAs with tumour-suppressor properties. This also adds a layer of complexity to out model of differentiation proposed in Section 5.4.2. This is the proposal that down-regulation of *MYCN* induced by the onset of differentiation may be modulated by microRNAs and *NCOR2.* This in turn, results in an increase in the *MYCN* regulated microRNAs involved in reducing the levels of methylation (Figure 5.40).

Epigentic therapy as a means of treatment for cancer is currently focusing on mechanisms of switching off DNA methlytransferases (DNMTs) and histone deacetylases (HDAC). Here we have identified a microRNA which can target one such protein, *DNMT1* and act in a tumour suppressing manor.

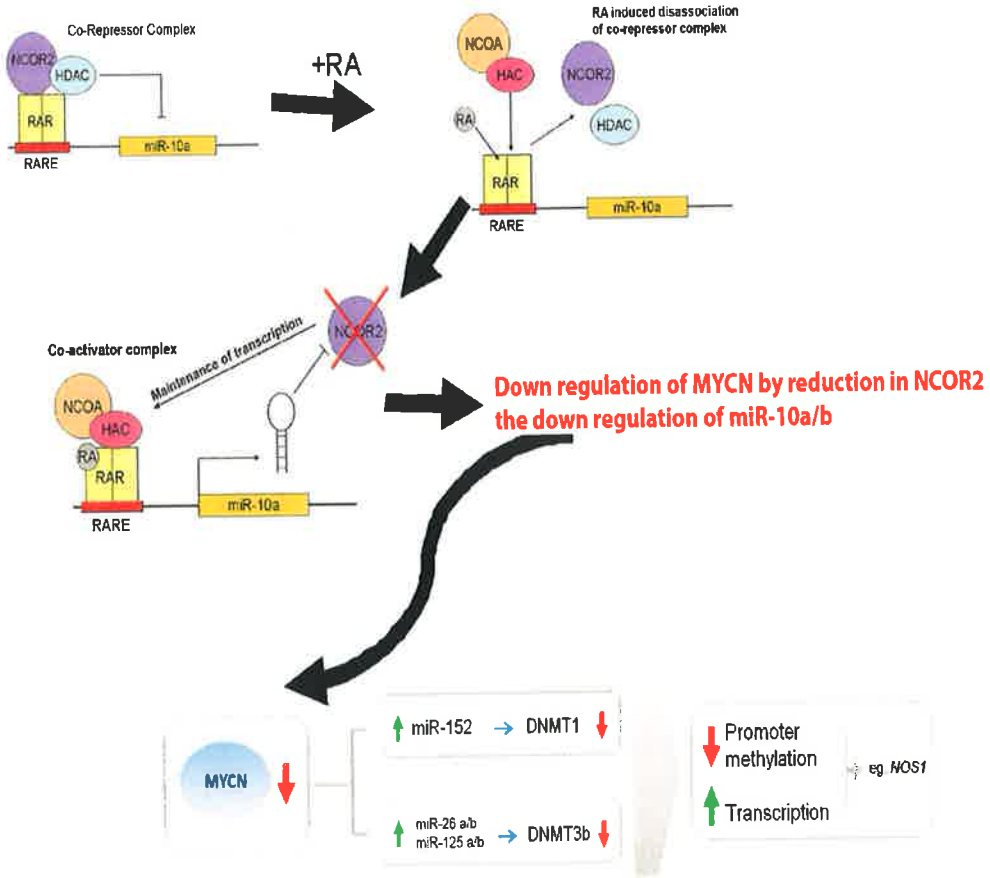

Figure 5.40. Proposed model of ATRA-induced differentiation. In this model, a very early step is the disruption of an NCOR2/retinoic acid receptor (RAR)/histone deacetylase (HDAC) co-repressor complex bound to a retinoic acid receptor element (RARE) upstream of miR-10a. In the presence of RA this complex is displaced with a co-activator complex binding and leading to transcriptional activation of miR-10a. MiR-10a directly targets and represses *NCOR2*, allowing continued expression of miR-10a. The down-regulation of *MYCN* as a result of the miR-10-*NCOR2* down regulation may contribute to the increase in DNMT targeting microRNAs which are suppressed by *MYCN*, resulting in a reduction in global methylation levels.

5.4.4 MiR-196a: a role in the regulation of *N-RAS*?

There are currently no publications on the involvement of miR-196a in neuroblastoma, but there are however a substantial number of studies examining this microRNA in other cancers. MiR-196a is established as a having a major role to play in the regulation of the HOX genes. It has so far been validated to target *HOXA7, HOXB8, HOXC8, HOXD8* (36, 297) and *HOXB7* (298). However reports in different cancers are contradictory as to whether this is an oncogenic or tumour suppressor microRNA. Oncogenic roles assigned to miR-196a include over-expression in breast cancer compared to normal tissue (310), elevated levels in esophageal adenocarcinoma (311), ectopic-over expression resulted in increased cell detachment and invasion of colon cancer cells *in vitro* (297) and high levels of miR-196a in the blood serum of patients with colon cancer when compared to normal controls (312).

There have also been reports of miR-196a being associated with good prognosis and tumour suppressor activities in cancers. Kim *et al.* (2009) (313) demonstrated that over-expression of miR-196a in human adipose derived mesenchymal stem cells (hASCs) could induce an increase in osteogenic differentiation and a reduction in cell proliferation. They went on to identify *HOXC8* as a direct target, and demonstrated that siRNA silencing of *HOXC8* induced the same phenotypic effects as miR-196a over-expression. MiR-196a displays reduced expression levels in melanoma cells versus healthy melanocytes and this low level of miR-196a corresponded with a high level of *HOXB7* (298). The contradiction in these reports may possibly be attributed to cell type specificity, resulting in different subsequent targets, and alternative functional outcomes.

Microarray results showed *N-RAS*, a highly predicated mRNA targets of miR-196a in TargetScan, was significantly down-regulated after ATRA treatment. *NRAS* is a member of the family of RAS genes, of which there are three primary members, H-, K- and N-RAS. These closely related family members function as GTP binding proteins and are involved in signal transduction. Activating oncogenic mutations in the RAS gene family are observed in ~30% of human cancer (314), with the majority of the *N-RAS* mutations occurring in cancers of myeloid origin (315). Transformation of N-RAS into an activated oncogenic protein occurs by a missense mutation at codon 61 (316). Oncogenic activation protects cells from apoptosis through activation of the PI3K/AKT pathway (315) and by the down regulation of FAS receptor expression resulting in a resistance to FAS mediated cell death (317).

To demonstrate if miR-196a was responsible for this down-regulation in *N-RAS* levels in ATRA-treated cells, ectopic up-regulation using the mature mimic to miR-196a was carried out. Contrary to our hypothesis, miR-196a over-expression resulted in an increase in *N-RAS* mRNA and protein levels. A luciferase reporter vector containing the predicted 3'UTR *N-RAS* target site resulted in no change in luciferase activity, confirming that miR-196a does not bind to this region of the *N-RAS*. This suggested N-RAS down-regulation post-ATRA treatment was due to a different mechanism.

It appeared therefore that miR-196a was causing the transcriptional up-regulation of *N-RAS* by some un-known mechanism. Using the tumour cohort previously described for microRNA analysis and the R2 database for mRNA analysis, we demonstrated that high levels of miR-196a and high levels of N-RAS were both associated with EFS and OS.

This clinical data allowed us to further validate a positive correlation between miR-196a and N-RAS in neuroblastoma.

Mutations of the N-RAS gene are extremely infrequent in neuroblastoma (318-320), suggesting that activated RAS-mediated signal transduction is not a mechanism of oncogenic activity in neuroblastoma. Although there has been one report which demonstrated that expression of normal *H-RAS* can suppress the tumourgenic phenotype induced by the activated oncogenic isoform of *H-RAS* (321), there is nothing in the literature describing a functional role for normal *N-RAS* in cancer. This suggests our findings are novel not only in the context of neuroblastoma, but cancer in general.

These results are interesting and novel in a number of ways. Not only have we provided evidence for the first time that the normal *N-RAS* gene and microRNA-196a may be acting in a tumour suppressor manner in neuroblastoma, but we also present preliminary data suggesting that miR-196a is entering the nucleus. A previous study by Place *et al.* (179) demonstrated that miR-373 could induce expression of two different genes by binding to their promoter region. This study lead us to hypothesis that miR-196a, may cause up-regulation of *N-RAS* through some transcriptional mechanism, possibly promoter binding carried out within the nucleus of the cell.

Chapter 6

Concluding remarks and future work

6.1 Concluding remarks

Cancer is a multistep process that can be attributed to many genetic and environmental factors. Although we know genetic aberrations of oncogenes and tumor suppressors play a fundamental role in the onset and progression of cancer, the contributing factors involved in initiation and progression of carcinogenesis are still widely unknown. The discovery of microRNAs has added a new layer of complexity to the already multifaceted and poorly understood processes involved in carcinogenesis. Dysregulation of these post-transcriptionally regulative, small, non-coding RNAs can greatly impact on cell behaviour due to their large number of target genes.

Neuroblastoma is a paediatric cancer which displays profound heterogeneity of clinical behaviour, ranging from rapid disease progression and death, to spontaneous regression. Despite the use of multimodal therapy, there has been an inability to make a significant impact on high risk tumours. This highlights the need for more accurate categorisation, which in turn could lead to better refined, more optimal treatment.

Despite recent developments in genetic subgroup discovery, the transcription factor MYCN remains the most significant marker in neuroblastoma. As part of this work functional analysis was carried out on miR-184 and miR-152, both of which are regulated by the MYCN oncogene. As a result of this, the direct target of miR-184, *AKT2* was identified and validated as an apoptosis-inducing tumor suppressor gene in NB cells.

Understanding differentiation is paramount to elucidating the process involved in the pathogenesis of neuroblastoma. This thesis has examined the roles of microRNAs in ATRA-induced differentiating neuroblastoma cells. This study identified 41 microRNAs that display altered expression during the process of differentiation, and further validated the functional roles of five of these microRNAs. This study also demonstrates novel roles for each of these microRNAs in ATRA-induced differentiation.

Two microRNAs which induce neuronal cell differentiation when ectopically over-expressed *in vitro* were identified, and a means by which these microRNAs induce differentiation through the direct down regulation of their target mRNA the nuclear co-repressor protein *NCOR2,* was demonstrated. Furthermore we have identified the existence of a positive feedback mechanism whereby miR-10a can positively enhance its own transcription, by the down regulation of one of its functionally validated targets *NCOR2* and hence contributes to the maintenance of differentiation in NB cells.

Little is known about the contribution of promoter methylation to neuroblastoma pathogenesis and differentiation. Down-regulation of the methyltransferases DNMT1 and DNMT3B, along with the up-regulation of endogenous microRNAs targeting them is demonstrated and proposed as a mechanism for DNA methylation. Ectopic over-expression of miR-152, which targets *DNMT1*, also negatively impacted cell invasiveness and anchorage independent growth, contributing in part to the differentiated phenotype.

Our proposed model of microRNAs involvement in neuroblastoma cell differentiation is shown in Figure 6.1. The work presented here emphasises the need for integration of all genomic, biological and clinical data in understanding the pathogenesis of

neuroblastoma. These factors must in turn be considered in an individualised approach to diagnosis and treatment of this complex and highly diversified disease.

This thesis tested the hypothesis that microRNAs play a role in the poorly understood mechanism of NB differentiation. Using the ATRA induced model of NB cell differentiation, a number of microRNAs with critical roles in this phenomenon were identified. This thesis demonstrated that the NB oncogene MYCN exerts its tumorgenic effects in part by suppression of miR-184 and miR-152. Both of these microRNAs in turn were confirmed to play major roles as tumor suppressors in NB cells in vitro. MiR-184 exerts a pro-apoptotic effect by the direct targeting of the pro-survival gene *AKT2*. MiR-152 causes the down regulation of DNMT1, a protein essential in the maintenance of DNA methylation in the genome. Two other microRNAs, miR-10a and 10b, were identified which can induce NB cell differentiation, through the targeted down regulation of *NCOR2*. Notably, these two microRNAs can also suppress MYCN transcription through an unknown secondary mechanism, confirming that these microRNAs play critical roles in suppression of tumorgenesis in NB cells. In summary, a number of microRNAs that play tumor suppressor roles in the critical process of NB cell differentiation, a highly critical event in this cancer, have been identified and validated. This novel work highlights the therapeutic potential of differentiation induced microRNAs in neuroblastoma.

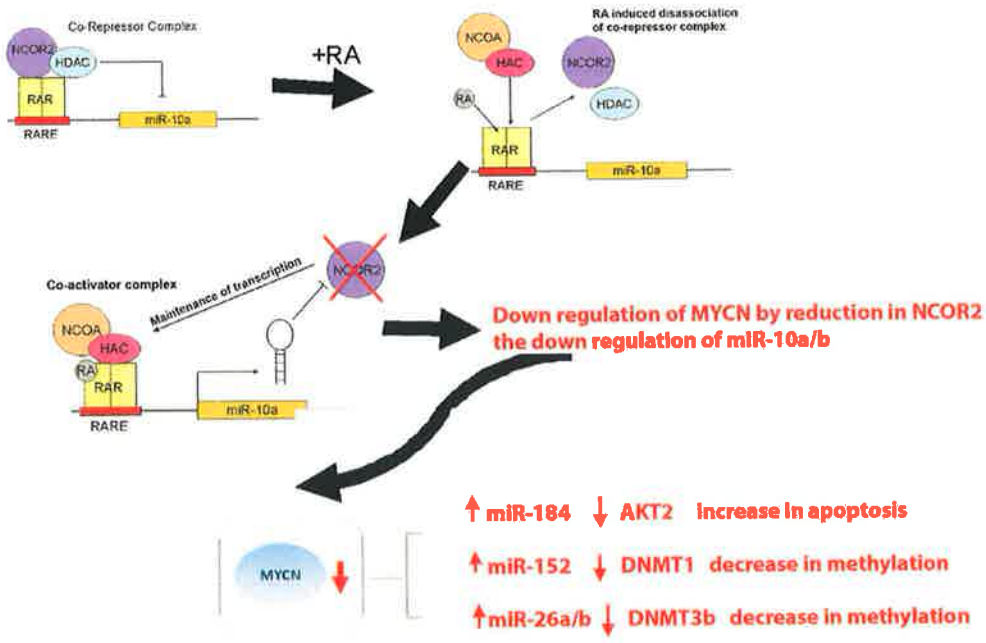

Figure 6.1. Proposed integrated model of ATRA-induced differentiation. This model is based on results described int this thesis, identifing functional roles for ATRA-induced microRNAs in the process of NB cells undergoing differentiation.

6.2 Future work

It is important to remember that there are many aspects of tumor biology which cannot be modelled *in vitro*. *In vivo* validation of all functional work must be carried out in order to establish a true tumor suppressor model for each microRNA. This work is currently underway for miR-184 and miR-10, with the aim of all other microRNAs used here in to be included in the near future.

The relationship between microRNAs and methylation status in neuroblastoma cell differentiation was established at Day 3 and Day 7 post- ATRA treatment. In order to examine the exact means by which these alterations occur, it is necessary to look at shorter time points post-treatment with the aim of pinpointing the exact integrated pattern of events which leads to neuronal cell differentiation.

To date only one publication has concentrated on microRNA binding to the promoter region of a gene resulting in direct transcriptional regulation (179). With the aim of identifying potential promoter targets of microRNAs, we are currently designing an algorithm using all known promoter sequences in the genome and all annotated microRNA, to identify patterns of sequence homology. This project was initially instigated to determine if miR-196a is binding to the *NRAS* promoter resulting in the transcriptional up-regulation of this gene *in vitro*. It will be interesting to determine if this is indeed the case, however the wider scope of this project has potentially massive implications on the regulatory control of the cell.

In order for miRNA promoter regulation to take place, mature miRNA would have to be present in the nucleus. We are currently using mRNA fractioning, to separate and profile levels of mature microRNAs in the nucleus and cytoplasm of neuroblastoma cell

lines. We intend to validate the translocation of mature miRNA back into the nucleus using in situ hybridization. Future plans involve further elucidation of how miR-196a exerts its functional effect, while simultaneously carrying out this large scale study.

Finally, the microRNA regulatory network is highly complex and poorly understood. Additional functional studies of all miRNAs differentially regulated in the process of NB cell differentiation are required along with the identification and experimental validation of their targets.

Bibliography

1. Hoehner JC, Gestblom C, Hedborg F, Sandstedt B, Olsen L, Pahlman S. A developmental model of neuroblastoma: differentiating stroma-poor tumors' progress along an extra-adrenal chromaffin lineage. Lab Invest. 1996 Nov;75(5):659-75.
2. Gurney JG, Severson RK, Davis S, Robison LL. Incidence of cancer in children in the United States. Sex-, race-, and 1-year age-specific rates by histologic type. Cancer. 1995 Apr 15;75(8):2186-95.
3. Spix C, Pastore G, Sankila R, Stiller CA, Steliarova-Foucher E. Neuroblastoma incidence and survival in European children (1978-1997): report from the Automated Childhood Cancer Information System project. Eur J Cancer. 2006 Sep;42(13):2081-91.
4. Brodeur GM. Neuroblastoma: biological insights into a clinical enigma. Nat Rev Cancer. 2003 Mar;3(3):203-16.
5. Abemayor E, Sidell N. Human neuroblastoma cell lines as models for the in vitro study of neoplastic and neuronal cell differentiation. Environ Health Perspect. 1989 Mar;80:3-15.
6. Bronner-Fraser M. Neural crest cell formation and migration in the developing embryo. FASEB J. 1994 Jul;8(10):699-706.
7. Gammill LS, Bronner-Fraser M. Neural crest specification: migrating into genomics. Nat Rev Neurosci. 2003 Oct;4(10):795-805.
8. Weston JA. Neural crest cell development. Prog Clin Biol Res. 1982;85 Pt B:359-79.
9. Cooper MJ, Hutchins GM, Cohen PS, Helman LJ, Mennie RJ, Israel MA. Human neuroblastoma tumor cell lines correspond to the arrested differentiation of chromaffin adrenal medullary neuroblasts. Cell Growth Differ. 1990 Apr;1(4):149-59.
10. Knudson AG, Jr., Strong LC. Mutation and cancer: neuroblastoma and pheochromocytoma. Am J Hum Genet. 1972 Sep;24(5):514-32.
11. Kushner BH, Gilbert F, Helson L. Familial neuroblastoma. Case reports, literature review, and etiologic considerations. Cancer. 1986 May 1;57(9):1887-93.
12. Carlsen NL. Neuroblastomas in Denmark 1943-80. Epidemiological and clinical studies. Acta Paediatr Suppl. 1994 Oct;403:1-27.
13. Claviez A, Lakomek M, Ritter J, Suttorp M, Kremens B, Dickerhoff R, et al. Low occurrence of familial neuroblastomas and ganglioneuromas in five consecutive GPOH neuroblastoma treatment studies. Eur J Cancer. 2004 Dec;40(18):2760-5.
14. Shojaei-Brosseau T, Chompret A, Abel A, de Vathaire F, Raquin MA, Brugieres L, et al. Genetic epidemiology of neuroblastoma: a study of 426 cases at the Institut Gustave-Roussy in France. Pediatr Blood Cancer. 2004 Jan;42(1):99-105.
15. Mosse YP, Laudenslager M, Longo L, Cole KA, Wood A, Attiyeh EF, et al. Identification of ALK as a major familial neuroblastoma predisposition gene. Nature. 2008 Oct 16;455(7215):930-5.
16. Mosse YP, Laudenslager M, Khazi D, Carlisle AJ, Winter CL, Rappaport E, et al. Germline PHOX2B mutation in hereditary neuroblastoma. Am J Hum Genet. 2004 Oct;75(4):727-30.

17. Trochet D, Bourdeaut F, Janoueix-Lerosey I, Deville A, de Pontual L, Schleiermacher G, et al. Germline mutations of the paired-like homeobox 2B (PHOX2B) gene in neuroblastoma. Am J Hum Genet. 2004 Apr;74(4):761-4.
18. Altura RA, Maris JM, Li H, Boyett JM, Brodeur GM, Look AT. Novel regions of chromosomal loss in familial neuroblastoma by comparative genomic hybridization. Genes Chromosomes Cancer. 1997 Jul;19(3):176-84.
19. Moore K. PPVN. The Developing Human: Clinically Orientated Embryology 6th ed.: W.B Saunders Company; 2003.
20. Williams TH, House RF, Jr., Burgert EO, Jr., Lynn HB. Unusual manifestations of neuroblastoma: chronic diarrhea, polymyoclonia-opsoclonus, and erythrocyte abnormalities. Cancer. 1972 Feb;29(2):475-80.
21. Ries L EM, Kosary CL, et al. Seer Cancer Statistics Review, 1975-2002.
. Bethesda, MD, National Cancer Institute. 2002.
22. Brodeur GM, Seeger RC, Barrett A, Berthold F, Castleberry RP, D'Angio G, et al. International criteria for diagnosis, staging, and response to treatment in patients with neuroblastoma. J Clin Oncol. 1988 Dec;6(12):1874-81.
23. Brodeur GM, Pritchard J, Berthold F, Carlsen NL, Castel V, Castelberry RP, et al. Revisions of the international criteria for neuroblastoma diagnosis, staging, and response to treatment. J Clin Oncol. 1993 Aug;11(8):1466-77.
24. Shimada H. The International Neuroblastoma Pathology Classification. Pathologica. 2003 Oct;95(5):240-1.
25. Shimada H, Ambros IM, Dehner LP, Hata J, Joshi VV, Roald B, et al. The International Neuroblastoma Pathology Classification (the Shimada system). Cancer. 1999 Jul 15;86(2):364-72.
26. Shimada H, Chatten J, Newton WA, Jr., Sachs N, Hamoudi AB, Chiba T, et al. Histopathologic prognostic factors in neuroblastic tumors: definition of subtypes of ganglioneuroblastoma and an age-linked classification of neuroblastomas. J Natl Cancer Inst. 1984 Aug;73(2):405-16.
27. Schwab M, Westermann F, Hero B, Berthold F. Neuroblastoma: biology and molecular and chromosomal pathology. Lancet Oncol. 2003 Aug;4(8):472-80.
28. Shimada HN, MD. Pathology of the Peripheral Neuroblastic Tumors: Case Presentation. Laboratory Medicine. 2006;37(11):684-9.
29. Cohn SL, Pearson AD, London WB, Monclair T, Ambros PF, Brodeur GM, et al. The International Neuroblastoma Risk Group (INRG) classification system: an INRG Task Force report. J Clin Oncol. 2009 Jan 10;27(2):289-97.
30. Castleberry RP, Pritchard J, Ambros P, Berthold F, Brodeur GM, Castel V, et al. The International Neuroblastoma Risk Groups (INRG): a preliminary report. Eur J Cancer. 1997 Oct;33(12):2113-6.
31. Schmidt ML, Lal A, Seeger RC, Maris JM, Shimada H, O'Leary M, et al. Favorable prognosis for patients 12 to 18 months of age with stage 4 nonamplified MYCN neuroblastoma: a Children's Cancer Group Study. J Clin Oncol. 2005 Sep 20;23(27):6474-80.
32. London WB, Castleberry RP, Matthay KK, Look AT, Seeger RC, Shimada H, et al. Evidence for an age cutoff greater than 365 days for neuroblastoma risk group stratification in the Children's Oncology Group. J Clin Oncol. 2005 Sep 20;23(27):6459-65.

33. Caren H, Erichsen J, Olsson L, Enerback C, Sjoberg RM, Abrahamsson J, et al. High-resolution array copy number analyses for detection of deletion, gain, amplification and copy-neutral LOH in primary neuroblastoma tumors: four cases of homozygous deletions of the CDKN2A gene. BMC Genomics. 2008;9:353.
34. Chen QR, Bilke S, Wei JS, Whiteford CC, Cenacchi N, Krasnoselsky AL, et al. cDNA array-CGH profiling identifies genomic alterations specific to stage and MYCN-amplification in neuroblastoma. BMC Genomics. 2004 Sep 20;5(1):70.
35. Mosse YP, Greshock J, Margolin A, Naylor T, Cole K, Khazi D, et al. High-resolution detection and mapping of genomic DNA alterations in neuroblastoma. Genes Chromosomes Cancer. 2005 Aug;43(4):390-403.
36. Scaruffi P, Coco S, Cifuentes F, Albino D, Nair M, Defferrari R, et al. Identification and characterization of DNA imbalances in neuroblastoma by high-resolution oligonucleotide array comparative genomic hybridization. Cancer Genet Cytogenet. 2007 Aug;177(1):20-9.
37. Spitz R, Betts DR, Simon T, Boensch M, Oestreich J, Niggli FK, et al. Favorable outcome of triploid neuroblastomas: a contribution to the special oncogenesis of neuroblastoma. Cancer Genet Cytogenet. 2006 May;167(1):51-6.
38. Kaneko Y, Kanda N, Maseki N, Sakurai M, Tsuchida Y, Takeda T, et al. Different karyotypic patterns in early and advanced stage neuroblastomas. Cancer Res. 1987 Jan 1;47(1):311-8.
39. Michels E, Vandesompele J, De Preter K, Hoebeeck J, Vermeulen J, Schramm A, et al. ArrayCGH-based classification of neuroblastoma into genomic subgroups. Genes Chromosomes Cancer. 2007 Dec;46(12):1098-108.
40. Mosse YP, Diskin SJ, Wasserman N, Rinaldi K, Attiyeh EF, Cole K, et al. Neuroblastomas have distinct genomic DNA profiles that predict clinical phenotype and regional gene expression. Genes Chromosomes Cancer. 2007 Oct;46(10):936-49.
41. Attiyeh EF, London WB, Mosse YP, Wang Q, Winter C, Khazi D, et al. Chromosome 1p and 11q deletions and outcome in neuroblastoma. N Engl J Med. 2005 Nov 24;353(21):2243-53.
42. Bown N, Cotterill S, Lastowska M, O'Neill S, Pearson AD, Plantaz D, et al. Gain of chromosome arm 17q and adverse outcome in patients with neuroblastoma. N Engl J Med. 1999 Jun 24;340(25):1954-61.
43. Cohn SL, Rademaker AW, Salwen HR, Franklin WA, Gonzales-Crussi F, Rosen ST, et al. Analysis of DNA ploidy and proliferative activity in relation to histology and N-myc amplification in neuroblastoma. Am J Pathol. 2000 May;136(5):1043-52.
44. Seeger RC, Brodeur GM, Sather H, Dalton A, Siegel SE, Wong KY, et al. Association of multiple copies of the N-myc oncogene with rapid progression of neuroblastomas. N Engl J Med. 1985 Oct 31;313(18):1111-6.
45. Vandesompele J, Van Roy N, Van Gele M, Laureys G, Ambros P, Heimann P, et al. Genetic heterogeneity of neuroblastoma studied by comparative genomic hybridization. Genes Chromosomes Cancer. 1998 Oct;23(2):141-52.
46. Brodeur GM, Seeger RC, Schwab M, Varmus HE, Bishop JM. Amplification of N-myc in untreated human neuroblastomas correlates with advanced disease stage. Science. 1984 Jun 8;224(4653):1121-4.

47. Seeger RC, Wada R, Brodeur GM, Moss TJ, Bjork RL, Sousa L, et al. Expression of N-myc by neuroblastomas with one or multiple copies of the oncogene. Prog Clin Biol Res. 1988;271:41-9.
48. Schmidt ML, Lukens JN, Seeger RC, Brodeur GM, Shimada H, Gerbing RB, et al. Biologic factors determine prognosis in infants with stage IV neuroblastoma: A prospective Children's Cancer Group study. J Clin Oncol. 2000 Mar;18(6):1260-8.
49. Goto S, Umehara S, Gerbing RB, Stram DO, Brodeur GM, Seeger RC, et al. Histopathology (International Neuroblastoma Pathology Classification) and MYCN status in patients with peripheral neuroblastic tumors: a report from the Children's Cancer Group. Cancer. 2001 Nov 15;92(10):2699-708.
50. Shimada H, Stram DO, Chatten J, Joshi VV, Hachitanda Y, Brodeur GM, et al. Identification of subsets of neuroblastomas by combined histopathologic and N-myc analysis. J Natl Cancer Inst. 1995 Oct 4;87(19):1470-6.
51. Weiss WA, Aldape K, Mohapatra G, Feuerstein BG, Bishop JM. Targeted expression of MYCN causes neuroblastoma in transgenic mice. EMBO J. 1997 Jun 2;16(11):2985-95.
52. Caron H, van Sluis P, de Kraker J, Bokkerink J, Egeler M, Laureys G, et al. Allelic loss of chromosome 1p as a predictor of unfavorable outcome in patients with neuroblastoma. N Engl J Med. 1996 Jan 25;334(4):225-30.
53. Fong CT, Dracopoli NC, White PS, Merrill PT, Griffith RC, Housman DE, et al. Loss of heterozygosity for the short arm of chromosome 1 in human neuroblastomas: correlation with N-myc amplification. Proc Natl Acad Sci U S A. 1989 May;86(10):3753-7.
54. Maris JM, White PS, Beltinger CP, Sulman EP, Castleberry RP, Shuster JJ, et al. Significance of chromosome 1p loss of heterozygosity in neuroblastoma. Cancer Res. 1995 Oct 15;55(20):4664-9.
55. Martinsson T, Sjoberg RM, Hedborg F, Kogner P. Deletion of chromosome 1p loci and microsatellite instability in neuroblastomas analyzed with short-tandem repeat polymorphisms. Cancer Res. 1995 Dec 1;55(23):5681-6.
56. White PS, Maris JM, Beltinger C, Sulman E, Marshall HN, Fujimori M, et al. A region of consistent deletion in neuroblastoma maps within human chromosome 1p36.2-36.3. Proc Natl Acad Sci U S A. 1995 Jun 6;92(12):5520-4.
57. Maris JM, Guo C, Blake D, White PS, Hogarty MD, Thompson PM, et al. Comprehensive analysis of chromosome 1p deletions in neuroblastoma. Med Pediatr Oncol. 2001 Jan;36(1):32-6.
58. Caron H, Peter M, van Sluis P, Speleman F, de Kraker J, Laureys G, et al. Evidence for two tumour suppressor loci on chromosomal bands 1p35-36 involved in neuroblastoma: one probably imprinted, another associated with N-myc amplification. Hum Mol Genet. 1995 Apr;4(4):535-9.
59. Caron H, Spieker N, Godfried M, Veenstra M, van Sluis P, de Kraker J, et al. Chromosome bands 1p35-36 contain two distinct neuroblastoma tumor suppressor loci, one of which is imprinted. Genes Chromosomes Cancer. 2001 Feb;30(2):168-74.
60. Thompson PM, Gotoh T, Kok M, White PS, Brodeur GM. CHD5, a new member of the chromodomain gene family, is preferentially expressed in the nervous system. Oncogene. 2003 Feb 20;22(7):1002-11.

61. Okawa ER, Gotoh T, Manne J, Igarashi J, Fujita T, Silverman KA, et al. Expression and sequence analysis of candidates for the 1p36.31 tumor suppressor gene deleted in neuroblastomas. Oncogene. 2008 Jan 31;27(6):803-10.
62. Fujita T, Igarashi J, Okawa ER, Gotoh T, Manne J, Kolla V, et al. CHD5, a tumor suppressor gene deleted from 1p36.31 in neuroblastomas. J Natl Cancer Inst. 2008 Jul 2;100(13):940-9.
63. Munirajan AK, Ando K, Mukai A, Takahashi M, Suenaga Y, Ohira M, et al. KIF1Bbeta functions as a haploinsufficient tumor suppressor gene mapped to chromosome 1p36.2 by inducing apoptotic cell death. J Biol Chem. 2008 Sep 5;283(36):24426-34.
64. Schlisio S, Kenchappa RS, Vredeveld LC, George RE, Stewart R, Greulich H, et al. The kinesin KIF1Bbeta acts downstream from EglN3 to induce apoptosis and is a potential 1p36 tumor suppressor. Genes Dev. 2008 Apr 1;22(7):884-93.
65. Brodeur GM, Maris JM, Yamashiro DJ, Hogarty MD, White PS. Biology and genetics of human neuroblastomas. J Pediatr Hematol Oncol. 1997 Mar-Apr;19(2):93-101.
66. Spitz R, Hero B, Skowron M, Ernestus K, Berthold F. MYCN-status in neuroblastoma: characteristics of tumours showing amplification, gain, and non-amplification. Eur J Cancer. 2004 Dec;40(18):2753-9.
67. Spitz R, Hero B, Ernestus K, Berthold F. Deletions in chromosome arms 3p and 11q are new prognostic markers in localized and 4s neuroblastoma. Clin Cancer Res. 2003 Jan;9(1):52-8.
68. Maris JM, Matthay KK. Molecular biology of neuroblastoma. J Clin Oncol. 1999 Jul;17(7):2264-79.
69. Srivatsan ES, Murali V, Seeger RC. Loss of heterozygosity for alleles on chromosomes 11q and 14q in neuroblastoma. Prog Clin Biol Res. 1991;366:91-8.
70. Spitz R, Hero B, Simon T, Berthold F. Loss in chromosome 11q identifies tumors with increased risk for metastatic relapses in localized and 4S neuroblastoma. Clin Cancer Res. 2006 Jun 1;12(11 Pt 1):3368-73.
71. Guo C, White PS, Weiss MJ, Hogarty MD, Thompson PM, Stram DO, et al. Allelic deletion at 11q23 is common in MYCN single copy neuroblastomas. Oncogene. 1999 Sep 2;18(35):4948-57.
72. Maris JM. The biologic basis for neuroblastoma heterogeneity and risk stratification. Curr Opin Pediatr. 2005 Feb;17(1):7-13.
73. Plantaz D, Vandesompele J, Van Roy N, Lastowska M, Bown N, Combaret V, et al. Comparative genomic hybridization (CGH) analysis of stage 4 neuroblastoma reveals high frequency of 11q deletion in tumors lacking MYCN amplification. Int J Cancer. 2001 Mar 1;91(5):680-6.
74. Vandesompele J, Baudis M, De Preter K, Van Roy N, Ambros P, Bown N, et al. Unequivocal delineation of clinicogenetic subgroups and development of a new model for improved outcome prediction in neuroblastoma. J Clin Oncol. 2005 Apr 1;23(10):2280-99.
75. Biederer T, Sara Y, Mozhayeva M, Atasoy D, Liu X, Kavalali ET, et al. SynCAM, a synaptic adhesion molecule that drives synapse assembly. Science. 2002 Aug 30;297(5586):1525-31.
76. Nowacki S, Skowron M, Oberthuer A, Fagin A, Voth H, Brors B, et al. Expression of the tumour suppressor gene CADM1 is associated with favourable outcome and inhibits cell survival in neuroblastoma. Oncogene. 2008 May 22;27(23):3329-38.

77. Gilbert F, Feder M, Balaban G, Brangman D, Lurie DK, Podolsky R, et al. Human neuroblastomas and abnormalities of chromosomes 1 and 17. Cancer Res. 1984 Nov;44(11):5444-9.
78. Caron H, van Sluis P, van Roy N, Beks L, Maes P, Pereira do Tanque R, et al. Chromosome 1p allelic loss in neuroblastoma: prognosis, genomic imprinting and 1;17 translocations. Prog Clin Biol Res. 1994;385:35-42.
79. Caron H, van Sluis P, van Roy N, de Kraker J, Speleman F, Voute PA, et al. Recurrent 1;17 translocations in human neuroblastoma reveal nonhomologous mitotic recombination during the S/G2 phase as a novel mechanism for loss of heterozygosity. Am J Hum Genet. 1994 Aug;55(2):341-7.
80. Van Roy N, Laureys G, Cheng NC, Willem P, Opdenakker G, Versteeg R, et al. 1;17 translocations and other chromosome 17 rearrangements in human primary neuroblastoma tumors and cell lines. Genes Chromosomes Cancer. 1994 Jun;10(2):103-14.
81. Savelyeva L, Corvi R, Schwab M. Translocation involving 1p and 17q is a recurrent genetic alteration of human neuroblastoma cells. Am J Hum Genet. 1994 Aug;55(2):334-40.
82. Lastowska M, Roberts P, Pearson AD, Lewis I, Wolstenholme J, Bown N. Promiscuous translocations of chromosome arm 17q in human neuroblastomas. Genes Chromosomes Cancer. 1997 Jul;19(3):143-9.
83. Buckley PG, Alcock L, Bryan K, Bray I, Schulte JH, Schramm A, et al. Chromosomal and microRNA expression patterns reveal biologically distinct subgroups of 11q- neuroblastoma. Clin Cancer Res. 2010 Jun 1;16(11):2971-8.
84. Stallings RL, Howard J, Dunlop A, Mullarkey M, McDermott M, Breatnach F, et al. Are gains of chromosomal regions 7q and 11p important abnormalities in neuroblastoma? Cancer Genet Cytogenet. 2003 Jan 15;140(2):133-7.
85. Caron H. Allelic loss of chromosome 1 and additional chromosome 17 material are both unfavourable prognostic markers in neuroblastoma. Med Pediatr Oncol. 1995 Apr;24(4):215-21.
86. Plantaz D, Mohapatra G, Matthay KK, Pellarin M, Seeger RC, Feuerstein BG. Gain of chromosome 17 is the most frequent abnormality detected in neuroblastoma by comparative genomic hybridization. Am J Pathol. 1997 Jan;150(1):81-9.
87. Bown N. Neuroblastoma tumour genetics: clinical and biological aspects. J Clin Pathol. 2001 Dec;54(12):897-910.
88. Brinkschmidt C, Christiansen H, Terpe HJ, Simon R, Lampert F, Boecker W, et al. Distal chromosome 17 gains in neuroblastomas detected by comparative genomic hybridization (CGH) are associated with a poor clinical outcome. Med Pediatr Oncol. 2001 Jan;36(1):11-3.
89. Spitz R, Hero B, Ernestus K, Berthold F. Gain of distal chromosome arm 17q is not associated with poor prognosis in neuroblastoma. Clin Cancer Res. 2003 Oct 15;9(13):4835-40.
90. Caren H, Kryh H, Nethander M, Sjoberg RM, Trager C, Nilsson S, et al. High-risk neuroblastoma tumors with 11q-deletion display a poor prognostic, chromosome instability phenotype with later onset. Proc Natl Acad Sci U S A. 2010 Mar 2;107(9):4323-8.
91. Hallstensson K, Thulin S, Aburatani H, Hippo Y, Martinsson T. Representational difference analysis and loss of heterozygosity studies detect 3p deletions in neuroblastoma. Eur J Cancer. 1997 Oct;33(12):1966-70.

92. Spitz R, Oberthuer A, Zapatka M, Brors B, Hero B, Ernestus K, et al. Oligonucleotide array-based comparative genomic hybridization (aCGH) of 90 neuroblastomas reveals aberration patterns closely associated with relapse pattern and outcome. Genes Chromosomes Cancer. 2006 Dec;45(12):1130-42.
93. Breen CJ, O'Meara A, McDermott M, Mullarkey M, Stallings RL. Coordinate deletion of chromosome 3p and 11q in neuroblastoma detected by comparative genomic hybridization. Cancer Genet Cytogenet. 2000 Jul 1;120(1):44-9.
94. Schleiermacher G, Michon J, Huon I, d'Enghien CD, Klijanienko J, Brisse H, et al. Chromosomal CGH identifies patients with a higher risk of relapse in neuroblastoma without MYCN amplification. Br J Cancer. 2007 Jul 16;97(2):238-46.
95. Barontini M, Gutierrez MI, Levin G, Mur N, Diez B. N-myc oncogene and urinary catecholamines in children with neuroblastoma. Med Pediatr Oncol. 1993;21(7):499-504.
96. Laug WE, Siegel SE, Shaw KN, Landing B, Baptista J, Gutenstein M. Initial urinary catecholamine metabolite concentrations and prognosis in neuroblastoma. Pediatrics. 1978 Jul;62(1):77-83.
97. Nakagawara A, Ikeda K, Higashi K, Sasazuki T. Inverse correlation between N-myc amplification and catecholamine metabolism in children with advanced neuroblastoma. Surgery. 1990 Jan;107(1):43-9.
98. Strenger V, Kerbl R, Dornbusch HJ, Ladenstein R, Ambros PF, Ambros IM, et al. Diagnostic and prognostic impact of urinary catecholamines in neuroblastoma patients. Pediatr Blood Cancer. 2007 May;48(5):504-9.
99. Nakagawara A, Ikeda K, Tasaka H. Dopaminergic neuroblastoma as a poor prognostic subgroup. J Pediatr Surg. 1988 Apr;23(4):346-9.
100. Nakagawara A, Azar CG, Scavarda NJ, Brodeur GM. Expression and function of TRK-B and BDNF in human neuroblastomas. Mol Cell Biol. 1994 Jan;14(1):759-67.
101. Combaret V, Gross N, Lasset C, Balmas K, Bouvier R, Frappaz D, et al. Clinical relevance of TRKA expression on neuroblastoma: comparison with N-MYC amplification and CD44 expression. Br J Cancer. 1997;75(8):1151-5.
102. Nakagawara A, Arima-Nakagawara M, Scavarda NJ, Azar CG, Cantor AB, Brodeur GM. Association between high levels of expression of the TRK gene and favorable outcome in human neuroblastoma. N Engl J Med. 1993 Mar 25;328(12):847-54.
103. Kramer K, Cheung NK, Gerald WL, LaQuaglia M, Kushner BH, LeClerc JM, et al. Correlation of MYCN amplification, Trk-A and CD44 expression with clinical stage in 250 patients with neuroblastoma. Eur J Cancer. 1997 Oct;33(12):2098-100.
104. Brodeur GM, Minturn JE, Ho R, Simpson AM, Iyer R, Varela CR, et al. Trk receptor expression and inhibition in neuroblastomas. Clin Cancer Res. 2009 May 15;15(10):3244-50.
105. Chen J, Chattopadhyay B, Venkatakrishnan G, Ross AH. Nerve growth factor-induced differentiation of human neuroblastoma and neuroepithelioma cell lines. Cell Growth Differ. 1990 Feb;1(2):79-85.
106. Matsushima H, Bogenmann E. Expression of trkA cDNA in neuroblastomas mediates differentiation in vitro and in vivo. Mol Cell Biol. 1993 Dec;13(12):7447-56.
107. Pomeroy SL, Sutton ME, Goumnerova LC, Segal RA. Neurotrophins in cerebellar granule cell development and medulloblastoma. J Neurooncol. 1997 Dec;35(3):347-52.

108. Lavoie JF, Lesauteur L, Kohn J, Wong J, Furtoss O, Thiele CJ, et al. TrkA induces apoptosis of neuroblastoma cells and does so via a p53-dependent mechanism. J Biol Chem. 2005 Aug 12;280(32):29199-207.
109. Harel L, Costa B, Tcherpakov M, Zapatka M, Oberthuer A, Hansford LM, et al. CCM2 mediates death signaling by the TrkA receptor tyrosine kinase. Neuron. 2009 Sep 10;63(5):585-91.
110. Crane R, Gadea B, Littlepage L, Wu H, Ruderman JV. Aurora A, meiosis and mitosis. Biol Cell. 2004 Apr;96(3):215-29.
111. Carvajal RD, Tse A, Schwartz GK. Aurora kinases: new targets for cancer therapy. Clin Cancer Res. 2006 Dec 1;12(23):6869-75.
112. Berwanger B, Hartmann O, Bergmann E, Bernard S, Nielsen D, Krause M, et al. Loss of a FYN-regulated differentiation and growth arrest pathway in advanced stage neuroblastoma. Cancer Cell. 2002 Nov;2(5):377-86.
113. Otto T, Horn S, Brockmann M, Eilers U, Schuttrumpf L, Popov N, et al. Stabilization of N-Myc is a critical function of Aurora A in human neuroblastoma. Cancer Cell. 2009 Jan 6;15(1):67-78.
114. Maris JM, Morton CL, Gorlick R, Kolb EA, Lock R, Carol H, et al. Initial testing of the aurora kinase A inhibitor MLN8237 by the Pediatric Preclinical Testing Program (PPTP). Pediatr Blood Cancer. 2010 Jul 15;55(1):26-34.
115. Cecchetto G, Mosseri V, De Bernardi B, Helardot P, Monclair T, Costa E, et al. Surgical risk factors in primary surgery for localized neuroblastoma: the LNESG1 study of the European International Society of Pediatric Oncology Neuroblastoma Group. J Clin Oncol. 2005 Nov 20;23(33):8483-9.
116. Matthay KK, Shulkin B, Ladenstein R, Michon J, Giammarile F, Lewington V, et al. Criteria for evaluation of disease extent by (123)I-metaiodobenzylguanidine scans in neuroblastoma: a report for the International Neuroblastoma Risk Group (INRG) Task Force. Br J Cancer. 2010 Apr 27;102(9):1319-26.
117. Simon T, Hero B, Benz-Bohm G, von Schweinitz D, Berthold F. Review of image defined risk factors in localized neuroblastoma patients: Results of the GPOH NB97 trial. Pediatr Blood Cancer. 2008 May;50(5):965-9.
118. Monclair T, Brodeur GM, Ambros PF, Brisse HJ, Cecchetto G, Holmes K, et al. The International Neuroblastoma Risk Group (INRG) staging system: an INRG Task Force report. J Clin Oncol. 2009 Jan 10;27(2):298-303.
119. Fritsch P, Kerbl R, Lackner H, Urban C. "Wait and see" strategy in localized neuroblastoma in infants: an option not only for cases detected by mass screening. Pediatr Blood Cancer. 2004 Nov;43(6):679-82.
120. Cushing H, Wolbach SB. The Transformation of a Malignant Paravertebral Sympathicoblastoma into a Benign Ganglioneuroma. Am J Pathol. 1927 May;3(3):203-16 7.
121. Everson TC. Spontaneous Regression of Cancer. Ann N Y Acad Sci. 1964 Apr 2;114:721-35.
122. Nickerson HJ, Matthay KK, Seeger RC, Brodeur GM, Shimada H, Perez C, et al. Favorable biology and outcome of stage IV-S neuroblastoma with supportive care or minimal therapy: a Children's Cancer Group study. J Clin Oncol. 2000 Feb;18(3):477-86.

123. Edsjo A, Holmquist L, Pahlman S. Neuroblastoma as an experimental model for neuronal differentiation and hypoxia-induced tumor cell dedifferentiation. Semin Cancer Biol. 2007 Jun;17(3):248-56.
124. Shimada H, Umehara S, Monobe Y, Hachitanda Y, Nakagawa A, Goto S, et al. International neuroblastoma pathology classification for prognostic evaluation of patients with peripheral neuroblastic tumors: a report from the Children's Cancer Group. Cancer. 2001 Nov 1;92(9):2451-61.
125. Tsokos M, Scarpa S, Ross RA, Triche TJ. Differentiation of human neuroblastoma recapitulates neural crest development. Study of morphology, neurotransmitter enzymes, and extracellular matrix proteins. Am J Pathol. 1987 Sep;128(3):484-96.
126. Lee RC, Feinbaum RL, Ambros V. The C. elegans heterochronic gene lin-4 encodes small RNAs with antisense complementarity to lin-14. Cell. 1993 Dec 3;75(5):843-54.
127. Reinhart BJ, Slack FJ, Basson M, Pasquinelli AE, Bettinger JC, Rougvie AE, et al. The 21-nucleotide let-7 RNA regulates developmental timing in Caenorhabditis elegans. Nature. 2000 Feb 24;403(6772):901-6.
128. Pasquinelli AE, Reinhart BJ, Slack F, Martindale MQ, Kuroda MI, Maller B, et al. Conservation of the sequence and temporal expression of let-7 heterochronic regulatory RNA. Nature. 2000 Nov 2;408(6808):86-9.
129. Lee RC, Ambros V. An extensive class of small RNAs in Caenorhabditis elegans. Science. 2001 Oct 26;294(5543):862-4.
130. Barbarotto E, Secchiero P, Dasgupta A, Fortina P, Calin GA, Hyslop T. MicroRNAs as new players in the genomic galaxy and disease puzzles. Clin Transl Sci. 2008 May;1(1):50-6.
131. Liu J, Carmell MA, Rivas FV, Marsden CG, Thomson JM, Song JJ, et al. Argonaute2 is the catalytic engine of mammalian RNAi. Science. 2004 Sep 3;305(5689):1437-41.
132. Carrington JC, Ambros V. Role of microRNAs in plant and animal development. Science. 2003 Jul 18;301(5631):336-8.
133. Miska EA. How microRNAs control cell division, differentiation and death. Curr Opin Genet Dev. 2005 Oct;15(5):563-8.
134. Lee Y, Jeon K, Lee JT, Kim S, Kim VN. MicroRNA maturation: stepwise processing and subcellular localization. EMBO J. 2002 Sep 2;21(17):4663-70.
135. Lai EC. Predicting and validating microRNA targets. Genome Biol. 2004;5(9):115.
136. Smalheiser NR. EST analyses predict the existence of a population of chimeric microRNA precursor-mRNA transcripts expressed in normal human and mouse tissues. Genome Biol. 2003;4(7):403.
137. Lee Y, Kim M, Han J, Yeom KH, Lee S, Baek SH, et al. MicroRNA genes are transcribed by RNA polymerase II. EMBO J. 2004 Oct 13;23(20):4051-60.
138. Borchert GM, Lanier W, Davidson BL. RNA polymerase III transcribes human microRNAs. Nat Struct Mol Biol. 2006 Dec;13(12):1097-101.
139. Monteys AM, Spengler RM, Wan J, Tecedor L, Lennox KA, Xing Y, et al. Structure and activity of putative intronic miRNA promoters. RNA. 2010 Mar;16(3):495-505.
140. Lee Y, Ahn C, Han J, Choi H, Kim J, Yim J, et al. The nuclear RNase III Drosha initiates microRNA processing. Nature. 2003 Sep 25;425(6956):415-9.

141. Gregory RI, Yan KP, Amuthan G, Chendrimada T, Doratotaj B, Cooch N, et al. The Microprocessor complex mediates the genesis of microRNAs. Nature. 2004 Nov 11;432(7014):235-40.
142. Wu H, Xu H, Miraglia LJ, Crooke ST. Human RNase III is a 160-kDa protein involved in preribosomal RNA processing. J Biol Chem. 2000 Nov 24;275(47):36957-65.
143. Han J, Lee Y, Yeom KH, Kim YK, Jin H, Kim VN. The Drosha-DGCR8 complex in primary microRNA processing. Genes Dev. 2004 Dec 15;18(24):3016-27.
144. Han J, Lee Y, Yeom KH, Nam JW, Heo I, Rhee JK, et al. Molecular basis for the recognition of primary microRNAs by the Drosha-DGCR8 complex. Cell. 2006 Jun 2;125(5):887-901.
145. Zeng Y, Cullen BR. Efficient processing of primary microRNA hairpins by Drosha requires flanking nonstructured RNA sequences. J Biol Chem. 2005 Jul 29;280(30):27595-603.
146. Okamura K, Hagen JW, Duan H, Tyler DM, Lai EC. The mirtron pathway generates microRNA-class regulatory RNAs in Drosophila. Cell. 2007 Jul 13;130(1):89-100.
147. Ruby JG, Jan CH, Bartel DP. Intronic microRNA precursors that bypass Drosha processing. Nature. 2007 Jul 5;448(7149):83-6.
148. Bohnsack MT, Regener K, Schwappach B, Saffrich R, Paraskeva E, Hartmann E, et al. Exp5 exports eEF1A via tRNA from nuclei and synergizes with other transport pathways to confine translation to the cytoplasm. EMBO J. 2002 Nov 15;21(22):6205-15.
149. Calado A, Treichel N, Muller EC, Otto A, Kutay U. Exportin-5-mediated nuclear export of eukaryotic elongation factor 1A and tRNA. EMBO J. 2002 Nov 15;21(22):6216-24.
150. Yi R, Qin Y, Macara IG, Cullen BR. Exportin-5 mediates the nuclear export of pre-microRNAs and short hairpin RNAs. Genes Dev. 2003 Dec 15;17(24):3011-6.
151. Fornerod M, Ohno M, Yoshida M, Mattaj IW. CRM1 is an export receptor for leucine-rich nuclear export signals. Cell. 1997 Sep 19;90(6):1051-60.
152. Kutay U, Bischoff FR, Kostka S, Kraft R, Gorlich D. Export of importin alpha from the nucleus is mediated by a specific nuclear transport factor. Cell. 1997 Sep 19;90(6):1061-71.
153. Bohnsack MT, Czaplinski K, Gorlich D. Exportin 5 is a RanGTP-dependent dsRNA-binding protein that mediates nuclear export of pre-miRNAs. RNA. 2004 Feb;10(2):185-91.
154. Zeng Y, Cullen BR. Structural requirements for pre-microRNA binding and nuclear export by Exportin 5. Nucleic Acids Res. 2004;32(16):4776-85.
155. Okada C, Yamashita E, Lee SJ, Shibata S, Katahira J, Nakagawa A, et al. A high-resolution structure of the pre-microRNA nuclear export machinery. Science. 2009 Nov 27;326(5957):1275-9.
156. Bernstein E, Caudy AA, Hammond SM, Hannon GJ. Role for a bidentate ribonuclease in the initiation step of RNA interference. Nature. 2001 Jan 18;409(6818):363-6.
157. Grishok A, Pasquinelli AE, Conte D, Li N, Parrish S, Ha I, et al. Genes and mechanisms related to RNA interference regulate expression of the small temporal RNAs that control C. elegans developmental timing. Cell. 2001 Jul 13;106(1):23-34.

158. Lee Y, Hur I, Park SY, Kim YK, Suh MR, Kim VN. The role of PACT in the RNA silencing pathway. EMBO J. 2006 Feb 8;25(3):522-32.
159. Chendrimada TP, Gregory RI, Kumaraswamy E, Norman J, Cooch N, Nishikura K, et al. TRBP recruits the Dicer complex to Ago2 for microRNA processing and gene silencing. Nature. 2005 Aug 4;436(7051):740-4.
160. Bass BL. Double-stranded RNA as a template for gene silencing. Cell. 2000 Apr 28;101(3):235-8.
161. Cerutti L, Mian N, Bateman A. Domains in gene silencing and cell differentiation proteins: the novel PAZ domain and redefinition of the Piwi domain. Trends Biochem Sci. 2000 Oct;25(10):481-2.
162. Okamura K, Ishizuka A, Siomi H, Siomi MC. Distinct roles for Argonaute proteins in small RNA-directed RNA cleavage pathways. Genes Dev. 2004 Jul 15;18(14):1655-66.
163. Kim VN, Han J, Siomi MC. Biogenesis of small RNAs in animals. Nat Rev Mol Cell Biol. 2009 Feb;10(2):126-39.
164. Khvorova A, Reynolds A, Jayasena SD. Functional siRNAs and miRNAs exhibit strand bias. Cell. 2003 Oct 17;115(2):209-16.
165. Schwarz DS, Hutvagner G, Du T, Xu Z, Aronin N, Zamore PD. Asymmetry in the assembly of the RNAi enzyme complex. Cell. 2003 Oct 17;115(2):199-208.
166. Caudy AA, Myers M, Hannon GJ, Hammond SM. Fragile X-related protein and VIG associate with the RNA interference machinery. Genes Dev. 2002 Oct 1;16(19):2491-6.
167. Hutvagner G, Zamore PD. A microRNA in a multiple-turnover RNAi enzyme complex. Science. 2002 Sep 20;297(5589):2056-60.
168. Martinez J, Patkaniowska A, Urlaub H, Luhrmann R, Tuschl T. Single-stranded antisense siRNAs guide target RNA cleavage in RNAi. Cell. 2002 Sep 6;110(5):563-74.
169. Hammond SM, Boettcher S, Caudy AA, Kobayashi R, Hannon GJ. Argonaute2, a link between genetic and biochemical analyses of RNAi. Science. 2001 Aug 10;293(5532):1146-50.
170. Leuschner PJ, Ameres SL, Kueng S, Martinez J. Cleavage of the siRNA passenger strand during RISC assembly in human cells. EMBO Rep. 2006 Mar;7(3):314-20.
171. Bartel DP. MicroRNAs: genomics, biogenesis, mechanism, and function. Cell. 2004 Jan 23;116(2):281-97.
172. Pillai RS, Artus CG, Filipowicz W. Tethering of human Ago proteins to mRNA mimics the miRNA-mediated repression of protein synthesis. RNA. 2004 Oct;10(10):1518-25.
173. Peters L, Meister G. Argonaute proteins: mediators of RNA silencing. Mol Cell. 2007 Jun 8;26(5):611-23.
174. Tolia NH, Joshua-Tor L. Slicer and the argonautes. Nat Chem Biol. 2007 Jan;3(1):36-43.
175. Garzon R, Fabbri M, Cimmino A, Calin GA, Croce CM. MicroRNA expression and function in cancer. Trends Mol Med. 2006 Dec;12(12):580-7.
176. Lee I, Ajay SS, Yook JI, Kim HS, Hong SH, Kim NH, et al. New class of microRNA targets containing simultaneous 5'-UTR and 3'-UTR interaction sites. Genome Res. 2009 Jul;19(7):1175-83.

177. Lytle JR, Yario TA, Steitz JA. Target mRNAs are repressed as efficiently by microRNA-binding sites in the 5' UTR as in the 3' UTR. Proc Natl Acad Sci U S A. 2007 Jun 5;104(23):9667-72.
178. Orom UA, Nielsen FC, Lund AH. MicroRNA-10a binds the 5'UTR of ribosomal protein mRNAs and enhances their translation. Mol Cell. 2008 May 23;30(4):460-71.
179. Place RF, Li LC, Pookot D, Noonan EJ, Dahiya R. MicroRNA-373 induces expression of genes with complementary promoter sequences. Proc Natl Acad Sci U S A. 2008 Feb 5;105(5):1608-13.
180. Faller M, Guo F. MicroRNA biogenesis: there's more than one way to skin a cat. Biochim Biophys Acta. 2008 Nov;1779(11):663-7.
181. Jones-Rhoades MW, Bartel DP. Computational identification of plant microRNAs and their targets, including a stress-induced miRNA. Mol Cell. 2004 Jun 18;14(6):787-99.
182. Calin GA, Croce CM. MicroRNA-cancer connection: the beginning of a new tale. Cancer Res. 2006 Aug 1;66(15):7390-4.
183. Baek D, Villen J, Shin C, Camargo FD, Gygi SP, Bartel DP. The impact of microRNAs on protein output. Nature. 2008 Sep 4;455(7209):64-71.
184. Qin W, Shi Y, Zhao B, Yao C, Jin L, Ma J, et al. miR-24 regulates apoptosis by targeting the open reading frame (ORF) region of FAF1 in cancer cells. PLoS One. 2010;5(2):e9429.
185. Vasudevan S, Tong Y, Steitz JA. Switching from repression to activation: microRNAs can up-regulate translation. Science. 2007 Dec 21;318(5858):1931-4.
186. Ajay SS, Athey BD, Lee I. Unified translation repression mechanism for microRNAs and upstream AUGs. BMC Genomics. 2010;11:155.
187. Forman JJ, Legesse-Miller A, Coller HA. A search for conserved sequences in coding regions reveals that the let-7 microRNA targets Dicer within its coding sequence. Proc Natl Acad Sci U S A. 2008 Sep 30;105(39):14879-84.
188. Castanotto D, Lingeman R, Riggs AD, Rossi JJ. CRM1 mediates nuclear-cytoplasmic shuttling of mature microRNAs. Proc Natl Acad Sci U S A. 2009 Dec 22;106(51):21655-9.
189. Buhler M, Verdel A, Moazed D. Tethering RITS to a nascent transcript initiates RNAi- and heterochromatin-dependent gene silencing. Cell. 2006 Jun 2;125(5):873-86.
190. Gonzalez S, Pisano DG, Serrano M. Mechanistic principles of chromatin remodeling guided by siRNAs and miRNAs. Cell Cycle. 2008 Aug 15;7(16):2601-8.
191. Chiou TJ, Aung K, Lin SI, Wu CC, Chiang SF, Su CL. Regulation of phosphate homeostasis by MicroRNA in Arabidopsis. Plant Cell. 2006 Feb;18(2):412-21.
192. Elia L, Quintavalle M, Zhang J, Contu R, Cossu L, Latronico MV, et al. The knockout of miR-143 and -145 alters smooth muscle cell maintenance and vascular homeostasis in mice: correlates with human disease. Cell Death Differ. 2009 Dec;16(12):1590-8.
193. Kuipers H, Schnorfeil FM, Fehling HJ, Bartels H, Brocker T. Dicer-dependent microRNAs control maturation, function, and maintenance of Langerhans cells in vivo. J Immunol. 2010 Jul 1;185(1):400-9.
194. Fineberg SK, Kosik KS, Davidson BL. MicroRNAs potentiate neural development. Neuron. 2009 Nov 12;64(3):303-9.
195. Ramachandran V, Chen X. Degradation of microRNAs by a family of exoribonucleases in Arabidopsis. Science. 2008 Sep 12;321(5895):1490-2.

196. Heo I, Joo C, Cho J, Ha M, Han J, Kim VN. Lin28 mediates the terminal uridylation of let-7 precursor MicroRNA. Mol Cell. 2008 Oct 24;32(2):276-84.
197. Hagan JP, Piskounova E, Gregory RI. Lin28 recruits the TUTase Zcchc11 to inhibit let-7 maturation in mouse embryonic stem cells. Nat Struct Mol Biol. 2009 Oct;16(10):1021-5.
198. Heo I, Joo C, Kim YK, Ha M, Yoon MJ, Cho J, et al. TUT4 in concert with Lin28 suppresses microRNA biogenesis through pre-microRNA uridylation. Cell. 2009 Aug 21;138(4):696-708.
199. Calin GA, Sevignani C, Dumitru CD, Hyslop T, Noch E, Yendamuri S, et al. Human microRNA genes are frequently located at fragile sites and genomic regions involved in cancers. Proc Natl Acad Sci U S A. 2004 Mar 2;101(9):2999-3004.
200. Calin GA, Dumitru CD, Shimizu M, Bichi R, Zupo S, Noch E, et al. Frequent deletions and down-regulation of micro- RNA genes miR15 and miR16 at 13q14 in chronic lymphocytic leukemia. Proc Natl Acad Sci U S A. 2002 Nov 26;99(24):15524-9.
201. Cimmino A, Calin GA, Fabbri M, Iorio MV, Ferracin M, Shimizu M, et al. miR-15 and miR-16 induce apoptosis by targeting BCL2. Proc Natl Acad Sci U S A. 2005 Sep 27;102(39):13944-9.
202. Lee EJ, Gusev Y, Jiang J, Nuovo GJ, Lerner MR, Frankel WL, et al. Expression profiling identifies microRNA signature in pancreatic cancer. Int J Cancer. 2007 Mar 1;120(5):1046-54.
203. Michael MZ, SM OC, van Holst Pellekaan NG, Young GP, James RJ. Reduced accumulation of specific microRNAs in colorectal neoplasia. Mol Cancer Res. 2003 Oct;1(12):882-91.
204. Pallante P, Visone R, Ferracin M, Ferraro A, Berlingieri MT, Troncone G, et al. MicroRNA deregulation in human thyroid papillary carcinomas. Endocr Relat Cancer. 2006 Jun;13(2):497-508.
205. Yanaihara N, Caplen N, Bowman E, Seike M, Kumamoto K, Yi M, et al. Unique microRNA molecular profiles in lung cancer diagnosis and prognosis. Cancer Cell. 2006 Mar;9(3):189-98.
206. Iorio MV, Ferracin M, Liu CG, Veronese A, Spizzo R, Sabbioni S, et al. MicroRNA gene expression deregulation in human breast cancer. Cancer Res. 2005 Aug 15;65(16):7065-70.
207. Mattie MD, Benz CC, Bowers J, Sensinger K, Wong L, Scott GK, et al. Optimized high-throughput microRNA expression profiling provides novel biomarker assessment of clinical prostate and breast cancer biopsies. Mol Cancer. 2006;5:24.
208. Chen Y, Stallings RL. Differential patterns of microRNA expression in neuroblastoma are correlated with prognosis, differentiation, and apoptosis. Cancer Res. 2007 Feb 1;67(3):976-83.
209. Bray I, Bryan K, Prenter S, Buckley PG, Foley NH, Murphy DM, et al. Widespread dysregulation of MiRNAs by MYCN amplification and chromosomal imbalances in neuroblastoma: association of miRNA expression with survival. PLoS One. 2009;4(11):e7850.
210. Mestdagh P, Fredlund E, Pattyn F, Schulte JH, Muth D, Vermeulen J, et al. MYCN/c-MYC-induced microRNAs repress coding gene networks associated with poor outcome in MYCN/c-MYC-activated tumors. Oncogene. 2010 Mar 4;29(9):1394-404.

211. Schulte JH, Schowe B, Mestdagh P, Kaderali L, Kalaghatgi P, Schlierf S, et al. Accurate prediction of neuroblastoma outcome based on miRNA expression profiles. Int J Cancer. 2010 May 5.
212. Murphy DM, Buckley PG, Bryan K, Das S, Alcock L, Foley NH, et al. Global MYCN transcription factor binding analysis in neuroblastoma reveals association with distinct E-box motifs and regions of DNA hypermethylation. PLoS One. 2009;4(12):e8154.
213. Xu H, Cheung IY, Guo HF, Cheung NK. MicroRNA miR-29 modulates expression of immunoinhibitory molecule B7-H3: potential implications for immune based therapy of human solid tumors. Cancer Res. 2009 Aug 1;69(15):6275-81.
214. Esteller M. Aberrant DNA methylation as a cancer-inducing mechanism. Annu Rev Pharmacol Toxicol. 2005;45:629-56.
215. Feinberg AP, Tycko B. The history of cancer epigenetics. Nat Rev Cancer. 2004 Feb;4(2):143-53.
216. Herman JG, Baylin SB. Gene silencing in cancer in association with promoter hypermethylation. N Engl J Med. 2003 Nov 20;349(21):2042-54.
217. Jones PA, Baylin SB. The epigenomics of cancer. Cell. 2007 Feb 23;128(4):683-92.
218. Banelli B, Casciano I, Croce M, Di Vinci A, Gelvi I, Pagnan G, et al. Expression and methylation of CASP8 in neuroblastoma: identification of a promoter region. Nat Med. 2002 Dec;8(12):1333-5; author reply 5.
219. Casciano I, Banelli B, Croce M, Allemanni G, Ferrini S, Tonini GP, et al. Role of methylation in the control of DeltaNp73 expression in neuroblastoma. Cell Death Differ. 2002 Mar;9(3):343-5.
220. Gonzalez-Gomez P, Bello MJ, Alonso ME, Arjona D, Lomas J, de Campos JM, et al. CpG island methylation status and mutation analysis of the RB1 gene essential promoter region and protein-binding pocket domain in nervous system tumours. Br J Cancer. 2003 Jan 13;88(1):109-14.
221. Gonzalez-Gomez P, Bello MJ, Alonso ME, Lomas J, Arjona D, Campos JM, et al. CpG island methylation in sporadic and neurofibromatis type 2-associated schwannomas. Clin Cancer Res. 2003 Nov 15;9(15):5601-6.
222. Ting AH, Jair KW, Schuebel KE, Baylin SB. Differential requirement for DNA methyltransferase 1 in maintaining human cancer cell gene promoter hypermethylation. Cancer Res. 2006 Jan 15;66(2):729-35.
223. Laneve P, Di Marcotullio L, Gioia U, Fiori ME, Ferretti E, Gulino A, et al. The interplay between microRNAs and the neurotrophin receptor tropomyosin-related kinase C controls proliferation of human neuroblastoma cells. Proc Natl Acad Sci U S A. 2007 May 8;104(19):7957-62.
224. Fontana L, Fiori ME, Albini S, Cifaldi L, Giovinazzi S, Forloni M, et al. Antagomir-17-5p abolishes the growth of therapy-resistant neuroblastoma through p21 and BIM. PLoS One. 2008;3(5):e2236.
225. Wei JS, Johansson P, Chen QR, Song YK, Durinck S, Wen X, et al. microRNA profiling identifies cancer-specific and prognostic signatures in pediatric malignancies. Clin Cancer Res. 2009 Sep 1;15(17):5560-8.

226. Westermann F, Muth D, Benner A, Bauer T, Henrich KO, Oberthuer A, et al. Distinct transcriptional MYCN/c-MYC activities are associated with spontaneous regression or malignant progression in neuroblastomas. Genome Biol. 2008;9(10):R150.
227. Chayka O, Corvetta D, Dews M, Caccamo AE, Piotrowska I, Santilli G, et al. Clusterin, a haploinsufficient tumor suppressor gene in neuroblastomas. J Natl Cancer Inst. 2009 May 6;101(9):663-77.
228. Hu H, Du L, Nagabayashi G, Seeger RC, Gatti RA. ATM is down-regulated by N-Myc-regulated microRNA-421. Proc Natl Acad Sci U S A. 2010 Jan 26;107(4):1506-11.
229. Schulte JH, Horn S, Otto T, Samans B, Heukamp LC, Eilers UC, et al. MYCN regulates oncogenic MicroRNAs in neuroblastoma. Int J Cancer. 2008 Feb 1;122(3):699-704.
230. Welch C, Chen Y, Stallings RL. MicroRNA-34a functions as a potential tumor suppressor by inducing apoptosis in neuroblastoma cells. Oncogene. 2007 Jul 26;26(34):5017-22.
231. Cole KA, Attiyeh EF, Mosse YP, Laquaglia MJ, Diskin SJ, Brodeur GM, et al. A functional screen identifies miR-34a as a candidate neuroblastoma tumor suppressor gene. Mol Cancer Res. 2008 May;6(5):735-42.
232. Wei JS, Song YK, Durinck S, Chen QR, Cheuk AT, Tsang P, et al. The MYCN oncogene is a direct target of miR-34a. Oncogene. 2008 Sep 4;27(39):5204-13.
233. Sun F, Fu H, Liu Q, Tie Y, Zhu J, Xing R, et al. Downregulation of CCND1 and CDK6 by miR-34a induces cell cycle arrest. FEBS Lett. 2008 Apr 30;582(10):1564-8.
234. Sjostrom SK, Finn G, Hahn WC, Rowitch DH, Kenney AM. The Cdk1 complex plays a prime role in regulating N-myc phosphorylation and turnover in neural precursors. Dev Cell. 2005 Sep;9(3):327-38.
235. Qu Q, Shi Y. Neural stem cells in the developing and adult brains. J Cell Physiol. 2009 Oct;221(1):5-9.
236. Li X, Jin P. Roles of small regulatory RNAs in determining neuronal identity. Nat Rev Neurosci. 2010 May;11(5):329-38.
237. Thiele CJ, Reynolds CP, Israel MA. Decreased expression of N-myc precedes retinoic acid-induced morphological differentiation of human neuroblastoma. Nature. 1985 Jan 31-Feb 6;313(6001):404-6.
238. Loven J, Zinin N, Wahlstrom T, Muller I, Brodin P, Fredlund E, et al. MYCN-regulated microRNAs repress estrogen receptor-alpha (ESR1) expression and neuronal differentiation in human neuroblastoma. Proc Natl Acad Sci U S A. 2010 Jan 26;107(4):1553-8.
239. Beveridge NJ, Tooney PA, Carroll AP, Tran N, Cairns MJ. Down-regulation of miR-17 family expression in response to retinoic acid induced neuronal differentiation. Cell Signal. 2009 Dec;21(12):1837-45.
240. Le MT, Xie H, Zhou B, Chia PH, Rizk P, Um M, et al. MicroRNA-125b promotes neuronal differentiation in human cells by repressing multiple targets. Mol Cell Biol. 2009 Oct;29(19):5290-305.
241. Laneve P, Gioia U, Andriotto A, Moretti F, Bozzoni I, Caffarelli E. A minicircuitry involving REST and CREB controls miR-9-2 expression during human neuronal differentiation. Nucleic Acids Res. 2010 Jul 12.
242. Chen H, Shalom-Feuerstein R, Riley J, Zhang SD, Tucci P, Agostini M, et al. miR-7 and miR-214 are specifically expressed during neuroblastoma differentiation, cortical

development and embryonic stem cells differentiation, and control neurite outgrowth in vitro. Biochem Biophys Res Commun. 2010 Apr 16;394(4):921-7.
243. Lee ST, Chu K, Oh HJ, Im WS, Lim JY, Kim SK, et al. Let-7 microRNA inhibits the proliferation of human glioblastoma cells. J Neurooncol. 2010 Jul 7.
244. Liu W, Liu C, Zhu J, Shu P, Yin B, Gong Y, et al. MicroRNA-16 targets amyloid precursor protein to potentially modulate Alzheimer's-associated pathogenesis in SAMP8 mice. Neurobiol Aging. 2010 Jul 7.
245. Zhao W, Yu S, Lu Z, Ma Y, Gu Y, Chen J. The miR-217 microRNA functions as a potential tumor suppressor in pancreatic ductal adenocarcinoma by targeting KRAS. Carcinogenesis. 2010 Jul 30.
246. Sharland A, Logan GJ, Bishop A, Alexander IE. Liver-directed gene expression using recombinant AAV 2/8 vectors--a tolerogenic strategy for gene delivery? Discov Med. 2010 Jun;9(49):519-27.
247. Serda RE, Godin B, Blanco E, Chiappini C, Ferrari M. Multi-stage delivery nano-particle systems for therapeutic applications. Biochim Biophys Acta. 2010 May 21.
248. Lanford RE, Hildebrandt-Eriksen ES, Petri A, Persson R, Lindow M, Munk ME, et al. Therapeutic silencing of microRNA-122 in primates with chronic hepatitis C virus infection. Science. 2010 Jan 8;327(5962):198-201.
249. Mitchell PS, Parkin RK, Kroh EM, Fritz BR, Wyman SK, Pogosova-Agadjanyan EL, et al. Circulating microRNAs as stable blood-based markers for cancer detection. Proc Natl Acad Sci U S A. 2008 Jul 29;105(30):10513-8.
250. Motoyama K, Inoue H, Takatsuno Y, Tanaka F, Mimori K, Uetake H, et al. Over- and under-expressed microRNAs in human colorectal cancer. Int J Oncol. 2009 Apr;34(4):1069-75.
251. Schetter AJ, Leung SY, Sohn JJ, Zanetti KA, Bowman ED, Yanaihara N, et al. MicroRNA expression profiles associated with prognosis and therapeutic outcome in colon adenocarcinoma. JAMA. 2008 Jan 30;299(4):425-36.
252. Ng EK, Chong WW, Jin H, Lam EK, Shin VY, Yu J, et al. Differential expression of microRNAs in plasma of patients with colorectal cancer: a potential marker for colorectal cancer screening. Gut. 2009 Oct;58(10):1375-81.
253. Fischer M, Bauer T, Oberthur A, Hero B, Theissen J, Ehrich M, et al. Integrated genomic profiling identifies two distinct molecular subtypes with divergent outcome in neuroblastoma with loss of chromosome 11q. Oncogene. 2010 Feb 11;29(6):865-75.
254. Janoueix-Lerosey I, Schleiermacher G, Michels E, Mosseri V, Ribeiro A, Lequin D, et al. Overall genomic pattern is a predictor of outcome in neuroblastoma. J Clin Oncol. 2009 Mar 1;27(7):1026-33.
255. Gossen M, Bujard H. Studying gene function in eukaryotes by conditional gene inactivation. Annu Rev Genet. 2002;36:153-73.
256. Gupta A, Williams BR, Hanash SM, Rawwas J. Cellular retinoic acid-binding protein II is a direct transcriptional target of MycN in neuroblastoma. Cancer Res. 2006 Aug 15;66(16):8100-8.
257. Bolstad BM, Irizarry RA, Astrand M, Speed TP. A comparison of normalization methods for high density oligonucleotide array data based on variance and bias. Bioinformatics. 2003 Jan 22;19(2):185-93.

258. Irizarry RA, Hobbs B, Collin F, Beazer-Barclay YD, Antonellis KJ, Scherf U, et al. Exploration, normalization, and summaries of high density oligonucleotide array probe level data. Biostatistics. 2003 Apr;4(2):249-64.
259. Vivanco I, Sawyers CL. The phosphatidylinositol 3-Kinase AKT pathway in human cancer. Nat Rev Cancer. 2002 Jul;2(7):489-501.
260. Franke TF, Kaplan DR, Cantley LC, Toker A. Direct regulation of the Akt proto-oncogene product by phosphatidylinositol-3,4-bisphosphate. Science. 1997 Jan 31;275(5300):665-8.
261. Franke TF, Yang SI, Chan TO, Datta K, Kazlauskas A, Morrison DK, et al. The protein kinase encoded by the Akt proto-oncogene is a target of the PDGF-activated phosphatidylinositol 3-kinase. Cell. 1995 Jun 2;81(5):727-36.
262. Opel D, Poremba C, Simon T, Debatin KM, Fulda S. Activation of Akt predicts poor outcome in neuroblastoma. Cancer Res. 2007 Jan 15;67(2):735-45.
263. Li Z, Jaboin J, Dennis PA, Thiele CJ. Genetic and pharmacologic identification of Akt as a mediator of brain-derived neurotrophic factor/TrkB rescue of neuroblastoma cells from chemotherapy-induced cell death. Cancer Res. 2005 Mar 15;65(6):2070-5.
264. Franke TF. PI3K/Akt: getting it right matters. Oncogene. 2008 Oct 27;27(50):6473-88.
265. Moro L, Arbini AA, Yao JL, di Sant'Agnese PA, Marra E, Greco M. Mitochondrial DNA depletion in prostate epithelial cells promotes anoikis resistance and invasion through activation of PI3K/Akt2. Cell Death Differ. 2009 Apr;16(4):571-83.
266. Dillon RL, Muller WJ. Distinct biological roles for the akt family in mammary tumor progression. Cancer Res. 2010 Jun 1;70(11):4260-4.
267. Yuan ZQ, Sun M, Feldman RI, Wang G, Ma X, Jiang C, et al. Frequent activation of AKT2 and induction of apoptosis by inhibition of phosphoinositide-3-OH kinase/Akt pathway in human ovarian cancer. Oncogene. 2000 May 4;19(19):2324-30.
268. Bellacosa A, de Feo D, Godwin AK, Bell DW, Cheng JQ, Altomare DA, et al. Molecular alterations of the AKT2 oncogene in ovarian and breast carcinomas. Int J Cancer. 1995 Aug 22;64(4):280-5.
269. Altomare DA, Tanno S, De Rienzo A, Klein-Szanto AJ, Skele KL, Hoffman JP, et al. Frequent activation of AKT2 kinase in human pancreatic carcinomas. J Cell Biochem. 2002;87(4):470-6.
270. Fraser M, Leung BM, Yan X, Dan HC, Cheng JQ, Tsang BK. p53 is a determinant of X-linked inhibitor of apoptosis protein/Akt-mediated chemoresistance in human ovarian cancer cells. Cancer Res. 2003 Nov 1;63(21):7081-8.
271. Weng D, Song X, Xing H, Ma X, Xia X, Weng Y, et al. Implication of the Akt2/survivin pathway as a critical target in paclitaxel treatment in human ovarian cancer cells. Cancer Lett. 2009 Jan 18;273(2):257-65.
272. Lin RJ, Lin YC, Yu AL. miR-149* induces apoptosis by inhibiting Akt1 and E2F1 in human cancer cells. Mol Carcinog. 2010 Aug;49(8):719-27.
273. Castillo SS, Brognard J, Petukhov PA, Zhang C, Tsurutani J, Granville CA, et al. Preferential inhibition of Akt and killing of Akt-dependent cancer cells by rationally designed phosphatidylinositol ether lipid analogues. Cancer Res. 2004 Apr 15;64(8):2782-92.
274. Fulda S. The PI3K/Akt/mTOR pathway as therapeutic target in neuroblastoma. Curr Cancer Drug Targets. 2009 Sep;9(6):729-37.

275. Wong TS, Liu XB, Wong BY, Ng RW, Yuen AP, Wei WI. Mature miR-184 as Potential Oncogenic microRNA of Squamous Cell Carcinoma of Tongue. Clin Cancer Res. 2008 May 1;14(9):2588-92.
276. Yu J, Peng H, Ruan Q, Fatima A, Getsios S, Lavker RM. MicroRNA-205 promotes keratinocyte migration via the lipid phosphatase SHIP2. FASEB J. 2010 Jun 9.
277. Liu C, Teng ZQ, Santistevan NJ, Szulwach KE, Guo W, Jin P, et al. Epigenetic regulation of miR-184 by MBD1 governs neural stem cell proliferation and differentiation. Cell Stem Cell. 2010 May 7;6(5):433-44.
278. Malzkorn B, Wolter M, Liesenberg F, Grzendowski M, Stuhler K, Meyer HE, et al. Identification and functional characterization of microRNAs involved in the malignant progression of gliomas. Brain Pathol. 2010 May;20(3):539-50.
279. Foley NH, Bray IM, Tivnan A, Bryan K, Murphy DM, Buckley PG, et al. MicroRNA-184 inhibits neuroblastoma cell survival through targeting the serine/threonine kinase AKT2. Mol Cancer. 2010;9:83.
280. Liu CG, Calin GA, Meloon B, Gamliel N, Sevignani C, Ferracin M, et al. An oligonucleotide microchip for genome-wide microRNA profiling in human and mouse tissues. Proc Natl Acad Sci U S A. 2004 Jun 29;101(26):9740-4.
281. Agirre X, Jimenez-Velasco A, San Jose-Eneriz E, Garate L, Bandres E, Cordeu L, et al. Down-regulation of hsa-miR-10a in chronic myeloid leukemia CD34+ cells increases USF2-mediated cell growth. Mol Cancer Res. 2008 Dec;6(12):1830-40.
282. Gee HE, Camps C, Buffa FM, Colella S, Sheldon H, Gleadle JM, et al. MicroRNA-10b and breast cancer metastasis. Nature. 2008 Oct 23;455(7216):E8-9; author reply E.
283. Lund AH. miR-10 in development and cancer. Cell Death Differ. 2010 Feb;17(2):209-14.
284. Ma L, Reinhardt F, Pan E, Soutschek J, Bhat B, Marcusson EG, et al. Therapeutic silencing of miR-10b inhibits metastasis in a mouse mammary tumor model. Nat Biotechnol. 2010 Apr;28(4):341-7.
285. Ma L, Teruya-Feldstein J, Weinberg RA. Tumour invasion and metastasis initiated by microRNA-10b in breast cancer. Nature. 2007 Oct 11;449(7163):682-8.
286. Mishra PJ, Song B, Wang Y, Humeniuk R, Banerjee D, Merlino G, et al. MiR-24 tumor suppressor activity is regulated independent of p53 and through a target site polymorphism. PLoS One. 2009;4(12):e8445.
287. Caramuta S, Egyhazi S, Rodolfo M, Witten D, Hansson J, Larsson C, et al. MicroRNA expression profiles associated with mutational status and survival in malignant melanoma. J Invest Dermatol. 2010 Aug;130(8):2062-70.
288. Katada T, Ishiguro H, Kuwabara Y, Kimura M, Mitui A, Mori Y, et al. microRNA expression profile in undifferentiated gastric cancer. Int J Oncol. 2009 Feb;34(2):537-42.
289. Morgan BA. Hox genes and embryonic development. Poult Sci. 1997 Jan;76(1):96-104.
290. Pearson JC, Lemons D, McGinnis W. Modulating Hox gene functions during animal body patterning. Nat Rev Genet. 2005 Dec;6(12):893-904.
291. Shah N, Sukumar S. The Hox genes and their roles in oncogenesis. Nat Rev Cancer. 2010 May;10(5):361-71.
292. Garzon R, Pichiorri F, Palumbo T, Iuliano R, Cimmino A, Aqeilan R, et al. MicroRNA fingerprints during human megakaryocytopoiesis. Proc Natl Acad Sci U S A. 2006 Mar 28;103(13):5078-83.

293. Yekta S, Shih IH, Bartel DP. MicroRNA-directed cleavage of HOXB8 mRNA. Science. 2004 Apr 23;304(5670):594-6.
294. Tsang J, Zhu J, van Oudenaarden A. MicroRNA-mediated feedback and feedforward loops are recurrent network motifs in mammals. Mol Cell. 2007 Jun 8;26(5):753-67.
295. Jepsen K, Solum D, Zhou T, McEvilly RJ, Kim HJ, Glass CK, et al. SMRT-mediated repression of an H3K27 demethylase in progression from neural stem cell to neuron. Nature. 2007 Nov 15;450(7168):415-9.
296. Scotting PJ, Rex M. Transcription factors in early development of the central nervous system. Neuropathol Appl Neurobiol. 1996 Dec;22(6):469-81.
297. Schimanski CC, Frerichs K, Rahman F, Berger M, Lang H, Galle PR, et al. High miR-196a levels promote the oncogenic phenotype of colorectal cancer cells. World J Gastroenterol. 2009 May 7;15(17):2089-96.
298. Braig S, Mueller DW, Rothhammer T, Bosserhoff AK. MicroRNA miR-196a is a central regulator of HOX-B7 and BMP4 expression in malignant melanoma. Cell Mol Life Sci. 2010 May 18.
299. Jepsen K, Rosenfeld MG. Biological roles and mechanistic actions of co-repressor complexes. J Cell Sci. 2002 Feb 15;115(Pt 4):689-98.
300. Nagy L, Kao HY, Chakravarti D, Lin RJ, Hassig CA, Ayer DE, et al. Nuclear receptor repression mediated by a complex containing SMRT, mSin3A, and histone deacetylase. Cell. 1997 May 2;89(3):373-80.
301. Jaboin J, Wild J, Hamidi H, Khanna C, Kim CJ, Robey R, et al. MS-27-275, an inhibitor of histone deacetylase, has marked in vitro and in vivo antitumor activity against pediatric solid tumors. Cancer Res. 2002 Nov 1;62(21):6108-15.
302. de Ruijter AJ, Kemp S, Kramer G, Meinsma RJ, Kaufmann JO, Caron HN, et al. The novel histone deacetylase inhibitor BL1521 inhibits proliferation and induces apoptosis in neuroblastoma cells. Biochem Pharmacol. 2004 Oct 1;68(7):1279-88.
303. Robert MF, Morin S, Beaulieu N, Gauthier F, Chute IC, Barsalou A, et al. DNMT1 is required to maintain CpG methylation and aberrant gene silencing in human cancer cells. Nat Genet. 2003 Jan;33(1):61-5.
304. Esteller M, Fraga MF, Paz MF, Campo E, Colomer D, Novo FJ, et al. Cancer epigenetics and methylation. Science. 2002 Sep 13;297(5588):1807-8; discussion -8.
305. Esteller M, Herman JG. Cancer as an epigenetic disease: DNA methylation and chromatin alterations in human tumours. J Pathol. 2002 Jan;196(1):1-7.
306. Bird A. DNA methylation patterns and epigenetic memory. Genes Dev. 2002 Jan 1;16(1):6-21.
307. Tsumura A, Hayakawa T, Kumaki Y, Takebayashi S, Sakaue M, Matsuoka C, et al. Maintenance of self-renewal ability of mouse embryonic stem cells in the absence of DNA methyltransferases Dnmt1, Dnmt3a and Dnmt3b. Genes Cells. 2006 Jul;11(7):805-14.
308. Braconi C, Huang N, Patel T. MicroRNA-dependent regulation of DNA methyltransferase-1 and tumor suppressor gene expression by interleukin-6 in human malignant cholangiocytes. Hepatology. 2010 Mar;51(3):881-90.
309. Rhee I, Bachman KE, Park BH, Jair KW, Yen RW, Schuebel KE, et al. DNMT1 and DNMT3b cooperate to silence genes in human cancer cells. Nature. 2002 Apr 4;416(6880):552-6.

310. Hui AB, Shi W, Boutros PC, Miller N, Pintilie M, Fyles T, et al. Robust global micro-RNA profiling with formalin-fixed paraffin-embedded breast cancer tissues. Lab Invest. 2009 May;89(5):597-606.
311. Luthra R, Singh RR, Luthra MG, Li YX, Hannah C, Romans AM, et al. MicroRNA-196a targets annexin A1: a microRNA-mediated mechanism of annexin A1 downregulation in cancers. Oncogene. 2008 Nov 6;27(52):6667-78.
312. Kong X, Du Y, Wang G, Gao J, Gong Y, Li L, et al. Detection of Differentially Expressed microRNAs in Serum of Pancreatic Ductal Adenocarcinoma Patients: miR-196a Could Be a Potential Marker for Poor Prognosis. Dig Dis Sci. 2010 Jul 8.
313. Kim YJ, Bae SW, Yu SS, Bae YC, Jung JS. miR-196a regulates proliferation and osteogenic differentiation in mesenchymal stem cells derived from human adipose tissue. J Bone Miner Res. 2009 May;24(5):816-25.
314. Bos JL. ras oncogenes in human cancer: a review. Cancer Res. 1989 Sep 1;49(17):4682-9.
315. Eskandarpour M, Kiaii S, Zhu C, Castro J, Sakko AJ, Hansson J. Suppression of oncogenic NRAS by RNA interference induces apoptosis of human melanoma cells. Int J Cancer. 2005 May 20;115(1):65-73.
316. Barbacid M. ras genes. Annu Rev Biochem. 1987;56:779-827.
317. Urquhart JL, Meech SJ, Marr DG, Shellman YG, Duke RC, Norris DA. Regulation of Fas-mediated apoptosis by N-ras in melanoma. J Invest Dermatol. 2002 Sep;119(3):556-61.
318. Ballas K, Lyons J, Janssen JW, Bartram CR. Incidence of ras gene mutations in neuroblastoma. Eur J Pediatr. 1988 Apr;147(3):313-4.
319. Ireland CM. Activated N-ras oncogenes in human neuroblastoma. Cancer Res. 1989 Oct 15;49(20):5530-3.
320. Dam V, Morgan BT, Mazanek P, Hogarty MD. Mutations in PIK3CA are infrequent in neuroblastoma. BMC Cancer. 2006;6:177.
321. Spandidos DA, Frame M, Wilkie NM. Expression of the normal H-ras1 gene can suppress the transformed and tumorigenic phenotypes induced by mutant ras genes. Anticancer Res. 1990 Nov-Dec;10(6):1543-54.

Appendices

Appendix 1

Vector maps for all plasmid used in this thesis

Appendix 1.1 pMIR-REPORT™ miRNA Expression Vector

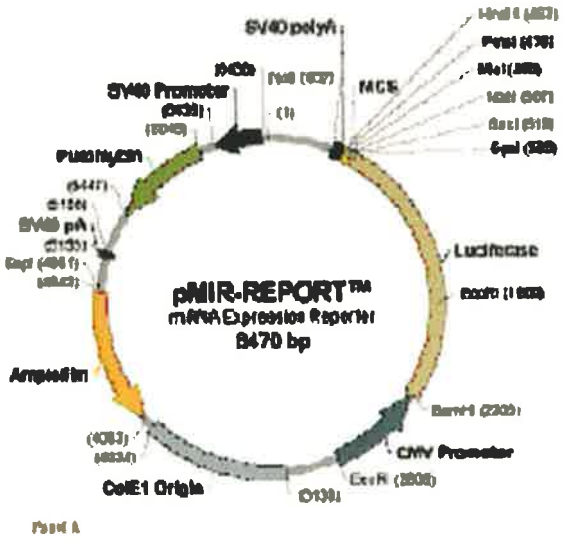

Appendix 1.2 pMIR-REPORT™ miRNA β-Gal Control Vector

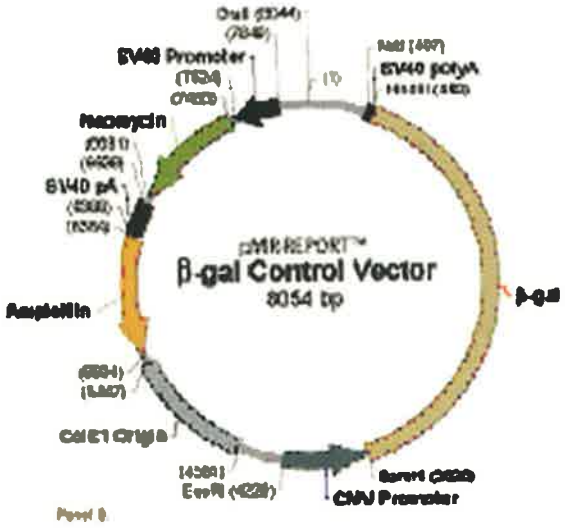

Appendix 1.3 psiCHECK™-2 Vector

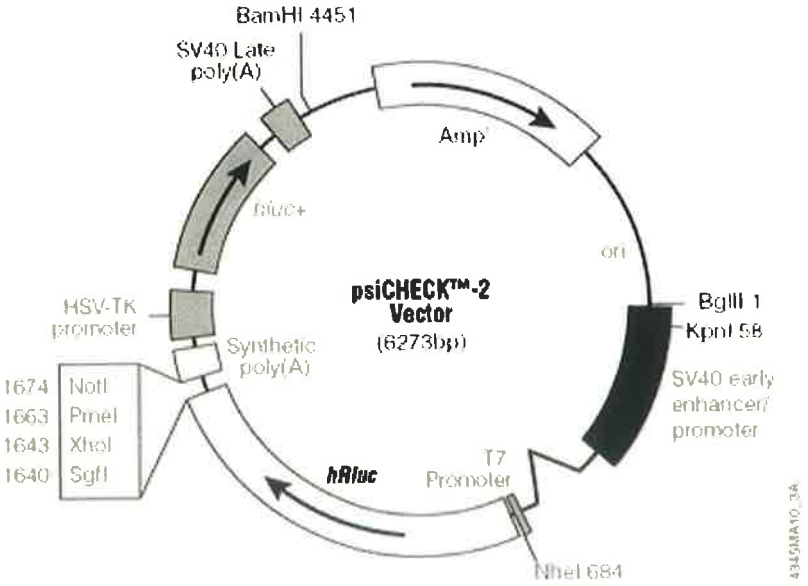

Appendix 1.4 pcDNA6.2–GW/EmGFP Vector

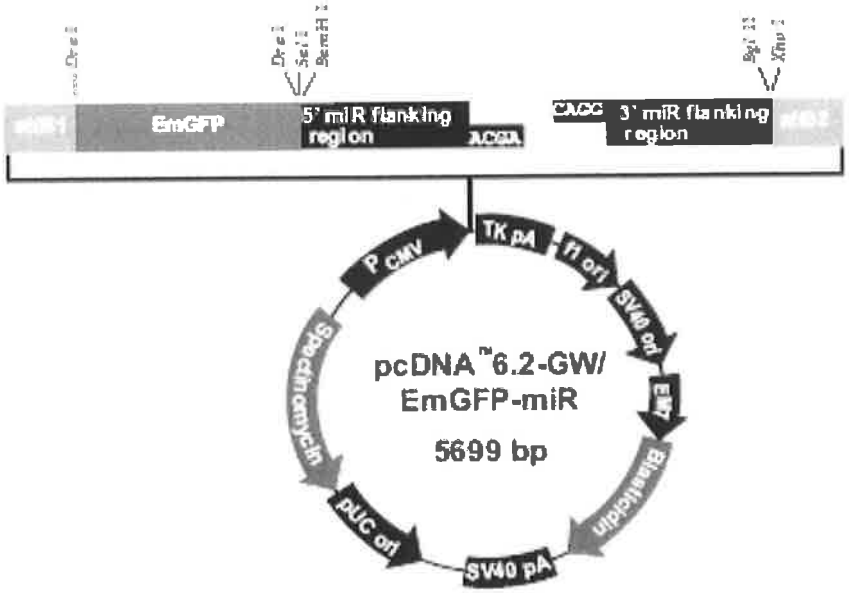

Appendix 1.5 pcDNA3 (used for AKT2 expression vector)

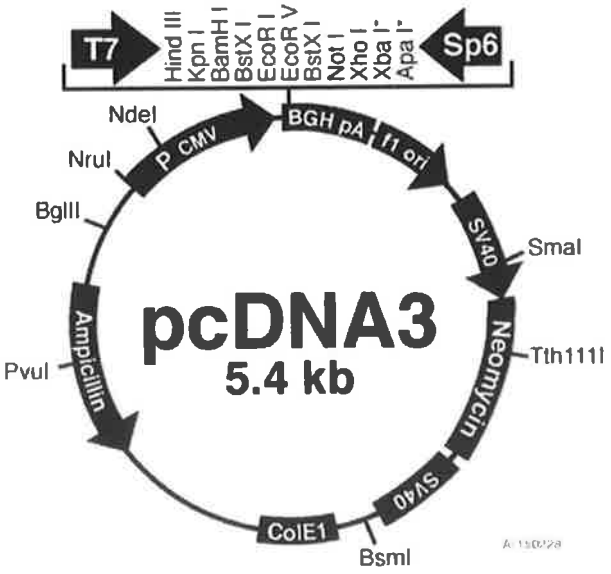

Appendix 2

Oligo inserts designed for microRNA binding regions in genes of interest.

Appendix 2.1 NCOR2 3'UTR (480 NT in length), with miR-10 binding site (Yellow)

5'GCTCGTTCCGGTCCCCACAGACTGCCCCAGCCAACGAGATTGCTGGAAACCA
AGTCAGGCCAGGTGGGCGGACAAAAGGGCCAGGTGCGGCCTGGGGGGAACGG
ATGCTCCGAGGACTGGACTGTTTTTTTCACACATCGTTGCCGCAGCGGTGGGA
AGGAAAGGCAGATGTAAATGATGTGTTGGTTTACAGGGTATATTTTTGATACC
TTCAATGAATTAATTCAGATGTTTTACGCAAGGAAGGACTTACCCAGTATTACT
GCTGCTGTGCTTTTGATCTCTGCTTACCGTTCAAGAGGCGTGTGCAGGCCGACA
GTCGGTGACCCCATCACTCGCAGGACCAAGGGGGCGGGGACTGCTGGCTCACG
CCCCGCTGTGTCCTCCCTCCCTCCCTTCCTTGGGCAGAATGATTCGATGCGTAT
TCTGTGGCCGCCATCTGCGCAGGGTGGTGGTATTCTGTCATTTACACACGTCGT
3'

3'CGAGCAAGGCCAGGGGTGTCTGACGGGGTCGGTTGCTCTAACGACCTTTGGT
TCAGTCCGGTCCACCCGCCTGTTTTCCCGGTCCACGCCGGACCCCCCTTGCCTA
CGAGGCTCCTGACCTGACAAAAAAAGTGTGTAGCAACGGCGTCGCCACCCTTC
CTTTCCGTCTACATTTACTACACAACCAAATGTCCCATATAAAAACTATGGAAG
TTACTTAATTAAGTCTACAAAATGCGTTCCTTCCTGAATGGGTCATAATGACGA
CGACACGAAAACTAGAGACGAATGGCAAGTTCTCCGCACACGTCCGGCTGTCA

GCCACTGGGGTAGTGAGCGTCCTGGTTCCCCCGCCCCTGACGACCGAGTGCGG
GGCGACACAGGAGGGAGGGAGGGAAGGAACCCGTCTTACTTAAGCTACGCAT
AAGACACCGGCGGTAGACGCGTCCCACCACCATAAGACAGTAAATGTGTGCA
GCA 5'

Appendix 2.2 NCOR2 3'UTR (480 NT in length), with miR-10 binding site (Yellow). MUT -muations in red.

5'GCTCGTTCCGGTCCCCACAGACTGCCCCAGCCAACGAGATTGCTGGAAACCA
AGTCAGGCCAGGTGGGCGGACAAAAGGGCCAGGTGCGGCCTGGGGGGAACGG
ATGCTCCGAGGACTGGACTGTTTTTTTCACACATCGTTGCCGCAGCGGTGGGA
AGGAAAGGCAGATGTAAATGATGTGTTGGTTTACCGGTGATATTTTTGATACC
TTCAATGAATTAATTCAGATGTTTTACGCAAGGAAGGACTTACCCAGTATTACT
GCTGCTGTGCTTTTGATCTCTGCTTACCGTTCAAGAGGCGTGTGCAGGCCGACA
GTCGGTGACCCCATCACTCGCAGGACCAAGGGGGCGGGGACTGCTGGCTCACG
CCCCGCTGTGTCCTCCCTCCCTCCCTTCCTTGGGCAGAATGAATTCGATGCGTA
TTCTGTGGCCGCCATCTGCGCAGGGTGGTGGTATTCTGTCATTTACACACGTCG
T 3'

3'CGAGCAAGGCCAGGGGTGTCTGACGGGGTCGGTTGCTCTAACGACCTTTGGT
TCAGTCCGGTCCACCCGCCTGTTTTCCCGGTCCACGCCGGACCCCCCTTGCCTA
CGAGGCTCCTGACCTGACAAAAAAAGTGTGTAGCAACGGCGTCGCCACCCTTC
CTTTCCGTCTACATTTACTACACAACCAAATGGCCACTATAAAAACTATGGAA

GTTACTTAATTAAGTCTACAAAATGCGTTCCTTCCTGAATGGGTCATAATGACG
ACGACACGAAAACTAGAGACGAATGGCAAGTTCTCCGCACACGTCCGGCTGTC
AGCCACTGGGGTAGTGAGCGTCCTGGTTCCCCCGCCCCTGACGACCGAGTGCG
GGGCGACACAGGAGGGAGGGAGGGAAGGAACCCGTCTTACTTAAGCTACGCA
TAAGACACCGGCGGTAGACGCGTCCCACCACCATAAGACAGTAAATGTGTGCA
GCA 5'

Appendix 2.3 DNMT1 3'UTR (321 NT in length), with miR-152 binding site (Yellow)

5'TTCTGCCCTCCCGTCACCCCTGTTTCTGGCACCAGGAATCCCCAACATGCACT
GATGTTGTGTTTTTAACATGTCAATCTGTCCGTTCACATGTGTGGTACATGGTG
TTTGTGGCCTTGGCTGACATGAAGCTGTTGTGTGAGGTTCGCTTATCAACTAAT
GATTTAGTGATCAAATTGTGCAGTACTTTGTGCATTCTGGATTTTAAAAGTTTT
TTATTATGCATTATATCAAATCTACCACTGTATGAGTGGAAATTAAGACTTTAT
GTAGTTTTTATATGTTGTAATATTTCTTCAAATAAATCTCTCCTATAAACCA 3'

3'AAGACGGGAGGGCAGTGGGGACAAAGACCGTGGTCCTTAGGGGTTGTACGT
GACTACAACACAAAAATTGTACAGTTAGACAGGCAAGTGTACACACCATGTAC
CACAAACACCGGAACCGACTGTACTTCGACAACACACTCCAAGCGAATAGTTG
ATTACTAAATCACTAGTTTAACACGTCATGAAACACGTAAGACCTAAAATTTT
CAAAAAATAATACGTAATATAGTTTAGATGGTGACATACTCACCTTTAATTCTG
AAATACATCAAAAATATACAACATTATAAAGAAGTTTATTTAGAGAGGATATT
TGGT 5'

Appendix 2.4 DNMT1 3'UTR (321 NT in length), with miR-152 binding site (Yellow), MUT-mutations in red

5'TTCTGCCCTCCCGTCACCCCTGTTTCTGGCACCAGGAATCCCCAACATGCGCG
TATGTTGTGTTTTTAACATGTCAATCTGTCCGTTCACATGTGTGGTACATGGTG
TTTGTGGCCTTGGCTGACATGAAGCTGTTGTGTGAGGTTCGCTTATCAACTAAT
GATTTAGTGATCAAATTGTGCAGTACTTTGTGCATTCTGGATTTTAAAAGTTTT
TTATTATGCATTATATCAAATCTACCACTGTATGAGTGGAAATTAAGACTTTAT
GTAGTTTTTATATGTTGTAATATTTCTTCAAATAAATCTCTCCTATAAACCA 3'

3'AAGACGGGAGGGCAGTGGGGACAAAGACCGTGGTCCTTAGGGGTTGTACGC
GCATACAACACAAAAATTGTACAGTTAGACAGGCAAGTGTACACACCATGTAC
CACAAACACCGGAACCGACTGTACTTCGACAACACACTCCAAGCGAATAGTTG
ATTACTAAATCACTAGTTTAACACGTCATGAAACACGTAAGACCTAAAATTTT
CAAAAAATAATACGTAATATAGTTTAGATGGTGACATACTCACCTTTAATTCTG
AAATACATCAAAAATATACAACATTATAAAGAAGTTTATTTAGAGAGGATATT
TGGT 5'

Appendix 2.5 NRAS 3'UTR (421 NT in length), with miR-196a binding site (Yellow)

5'CAAGATACTTTTAAAGTTTTGTCAGAAAAGAGCCACTTTCAAGGCTGCACTG
ACACCCTGGTCCTGACTTCCCTGGAGGAGAAGTATTCCTGTTGCTGTCTTCAGT
CTCACAGAGAAGCTCCTGCTACTTCCCCAGCTCTCAGTAGTTTAGTACAATAAT
CTCTATTTGAGAAGTTCTCAGAATAACTACCTCCTCACTTGGCTGTCTGACCAG
AGAATGCACCTCTTGTTACTCCCTGTTATTTTTCTGCCCTGGGTTCTTCCACAGC
ACAAACACACCTCTGCCACCCCAGGTTTTTCATCTGAAAAGCAGTTCATGTCTG
AAACAGAGAACCAAACCGCAAACGTGAAATTCTATTGAAAACAGTGTCTTGA
GCTCTAAAGTAGCAACTGCTGGTGATTTTTTTTTTCTTTTTACTGT '3

3'GTTCTATGAAAATTTCAAAACAGTCTTTTCTCGGTGAAAGTTCCGACGTGACT
GTGGGACCAGGACTGAAGGGACCTCCTCTTCATAAGGACAACGACAGAAGTC
AGAGTGTCTCTTCGAGGACGATGAAGGGGTCGAGAGTCATCAAATCATGTTAT
TAGAGATAAACTCTTCAAGAGTCTTATTGATGGAGGAGTGAACCGACAGACTG
GTCTCTTACGTGGAGAACAATGAGGGACAATAAAAAGACGGGACCCAAGAAG
GTGTCGTGTTTGTGTGGAGACGGTGGGGTCCAAAAAGTAGACTTTTCGTCAAG
TACAGACTTTGTCTCTTGGTTTGGCGTTTGCACTTTAAGATAACTTTTGTCACA
GAACTCGAGATTTCATCGTTGACGACCACTAAAAAAAAAAAGAAAAATGACA 5'

Appendix 2.6 NRAS 3'UTR (421 NT in length), with miR-196a binding site (Yellow). MUT-mutations in red

5'CAAGATACTTTTAAAGTTTTGTCAGAAAAGAGCCACTTTCAAGGCTGCACTG
ACACCCTGGTCCTGACTTCCCTGGAGGAGAAGTATTCCTGTTGCTGTCTTCAGT
CTCACAGAGAAGCTCCTGCTACTTCCCCAGCTCTCAGTAGTTTAGTACAATAAT
CTCTATTTGAGAAGTTCTCAGAATAACTATTTACTCACTTGGCTGTCTGACCAG
AGAATGCACCTCTTGTTACTCCCTGTTATTTTTCTGCCCTGGGTTCTTCCACAGC
ACAAACACACCTCTGCCACCCCAGGTTTTTCATCTGAAAAGCAGTTCATGTCTG
AAACAGAGAACCAAACCGCAAACGTGAAATTCTATTGAAAACAGTGTCTTGA
GCTCTAAAGTAGCAACTGCTGGTGATTTTTTTTTTCTTTTTACTGT 3'

3'GTTCTATGAAAATTTCAAAACAGTCTTTTCTCGGTGAAAGTTCCGACGTGACT
GTGGGACCAGGACTGAAGGGACCTCCTCTTCATAAGGACAACGACAGAAGTC
AGAGTGTCTCTTCGAGGACGATGAAGGGGTCGAGAGTCATCAAATCATGTTAT
TAGAGATAAACTCTTCAAGAGTCTTATTGATAAATGAGTGAACCGACAGACTG
GTCTCTTACGTGGAGAACAATGAGGGACAATAAAAAGACGGGACCCAAGAAG
GTGTCGTGTTTGTGTGGAGACGGTGGGGTCCAAAAAGTAGACTTTTCGTCAAG
TACAGACTTTGTCTCTTGGTTTGGCGTTTGCACTTTAAGATAACTTTTGTCACA
GAACTCGAGATTTCATCGTTGACGACCACTAAAAAAAAAAGAAAAATGACA 5'

Appendix 3

Appendix 3.1 Relative quantification values for microRNAs in TILDA ATRA experiment

microRNA	Day 0	Day 3	Day 7	STD Day 0	STD Day 3	STD Day 7
hsa-miR-409-5p	1	-5.34444	-2.12619	0	0.037973	0.240507
hsa-miR-656	1	-4.22098	-2.33883	0	0.191525	0.190636
hsa-miR-299-5p	1	-3.32845	-2.43513	0	0.038262	0.210554
hsa-miR-485-5p	1	-2.12102	-2.63068	0	0.087957	0.058429
hsa-miR-424	1	-2.9426	-3.01477	0	0.340338	0.006683
hsa-miR-127	1	-2.93518	-3.20118	0	0.030693	0.018449
hsa-miR-323	1	-2.87228	-5.11801	0	0.206906	0.120986
hsa-miR-339	1	-2.84665	-1.78796	0	0.175648	0.031015
hsa-miR-576	1	-2.83639	-1.83928	0	0.076322	0.125364
hsa-miR-432	1	-2.78025	-7.67864	0	0.186243	0.013425
hsa-miR-433	1	-2.51222	-3.91579	0	0.189273	0.077754
hsa-miR-7	1	-2.10351	-1.6834	0	0.114953	0.277138
hsa-miR-30e-5p	1	-2.16772	-2.25634	0	0.140984	0.208429
hsa-miR-485-3p	1	-3.08284	-7.54997	0	0.255822	0.093778
hsa-miR-379	1	-1.95972	-3.09542	0	0.287822	0.171928

hsa-miR-134	1	-1.83202	-3.21833	0	0.332817	0.010242
hsa-miR-487b	1	-1.79937	-2.69342	0	0.22084	0.040713
hsa-let-7e	1	1.915747	2.038823	0	1.215662	1.231117
hsa-miR-191	1	2.020386	1.261885	0	1.354951	0.366772
hsa-miR-196a	1	2.21	2.28	0	0.282843	0.098995
hsa-miR-24	1	2.278695	1.407813	0	1.608701	0.27084
hsa-miR-214	1	2.372894	1.689547	0	0.000841	0.067092
hsa-miR-203	1	2.62442	1.574596	0	0.982913	1.3178
hsa-miR-21	1	2.632988	1.181841	0	1.144831	0.080467
hsa-miR-615	1	2.743228	3.719387	0	1.094409	0.495444
hsa-miR-126	1	2.889312	2.781442	0	1.659215	1.276493
hsa-miR-152	1	2.908098	1.844745	0	0.785343	0.426994
hsa-miR-146b	1	2.921442	1.612441	0	1.922525	0.505666
has-miR-184	1	5.062014	4.415415	0	0.513738	0.400692
hsa-miR-192	1	3.522762	2.983281	0	2.79038	2.035137
hsa-miR-210	1	5.942055	5.36085	0	2.966063	5.197861
hsa-miR-10b	1	7.321366	10.32927	0	0.931788	0.806645
hsa-miR-10a	1	7.676483	11.53043	0	0.08939	1.513708
hsa-miR-132	1	136.6253	219.0474	0	110.5395	173.3614

Appendix 4

Conferences attended and awards received

Appendix 4.1 Oral Presentations

MicroRNA 184 Inhibits Neuroblastoma Cell Proliferation and Promotes Apoptosis by Targeting the Serine/Threonine Kinase AKT2 Foley N, Brai I, Murphy M, Buckley P, Tivnan A, Stallings RL. *ANR, Advances in Neuroblastoma Research, Stolkholm Sweden, June 2010*

Appendix 4.2 Poster Presentation

MicroRNA 184 Inhibits Neuroblastoma Cell Proliferation and Promotes Apoptosis by Targeting the Serine/Threonine Kinase AKT2 Foley N, Bray I, Murphy M, Buckley P, Tivnan A, Stallings RL. *The Keystone Symposia on microRNA and Cancer, Keystone Denver, June 2009.*

All-trans Retinoic Acid Induced Differentiation of SK-N-BE cells Results in Extensive DNA Methylation Alterations of Gene Promoter Regions Niamh Foley*, Sudipto Das*, Kenneth Bryan, Karen M Watters, Isabella Bray, Derek M Murphy, Patrick G. Buckley and Raymond L.Stallings *ANR, Advances in Neuroblastoma Research, Stolkholm Sweden, June 2010*
*both authors contributed equally to this work

Appendix 4.3 Awards

Recipient of the Irish Cancer Society Oncology Scholar Travel Award 2008

Appendix 5

Journal articles published and under-review, produced during the course of this research

Appendix 5.1 Published articles

Stallings RL, **Foley NH**, Bryan K, Buckley PG, Bray I. Therapeutic targeting of miRNAs in neuroblastoma. *Expert Opin Ther Targets* 2010 Jul 27

Foley NH, Bray IM, Tivnan A, Bryan K, Murphy DM, Buckley PG, *et al.*MicroRNA184 inhibits neuroblastoma cell survival through targeting the serine/threonine kinase AKT2. *Mol Cancer* 2010; **9:** 83.

Murphy DM, Buckley PG, Bryan K, Das S, Alcock L, **Foley NH**, *et al.* Global MYCN transcription factor binding analysis in neuroblastoma reveals association with distinct E-box motifs and regions of DNA hypermethylation. *PLoS One* 2009; **4** (12): e8154.

Bray I, Bryan K, Prenter S, Buckley PG, **Foley NH**, Murphy DM, *et al.* Widespread dysregulation of MiRNAs by MYCN amplification and chromosomal imbalances in neuroblastoma: association of miRNA expression with survival. *PLoS One* 2009; **4** (11): e7850.

Appendix 5.2 Articles under-review

Niamh H. Foley[1,2*], Isabella Bray[1,2*], Karen M Watters[1,2], Kenneth Bryan[1,2], Tytus Bernas[3], Jochen H.M. Prehn[3], Raymond L. Stalling. MicroRNAs 10a and 10b Are Potent Inducers of Neuroblastoma Cell Differentiation Through Targeting of Nuclear Receptor Co-repressor 2 **Submitted to Cell Death and Differentiation**

Sudipto Das[1,2*], **Niamh Foley**[1,2*],Kenneth Bryan[1,2], Karen M Watters[1,2], Isabella Bray[1,2], Derek M Murphy[1,2] , Patrick G Buckley[1,2§], Raymond L Stallings[1,2,‡ §].

Functionally Significant MicroRNA Mediated DNA Methylation Alterations in Retinoic Acid Induced Neuroblastoma Cell Differentiation **Submitted to Cancer Research**

***both authors contributed equally to this work**